

Distribution Agreement

In presenting this thesis or dissertation as a partial fulfillment of the requirements for an advanced degree from Emory University, I hereby grant to Emory University and its agents the non-exclusive license to archive, make accessible, and display my thesis or dissertation in whole or in part in all forms of media, now or hereafter known, including display on the world wide web. I understand that I may select some access restrictions as part of the online submission of this thesis or dissertation. I retain all ownership rights to the copyright of the thesis or dissertation. I also retain the right to use in future works (such as articles or books) all or part of this thesis or dissertation.

Signature:

Anthony R. Prosser

Date

Discovery and Synthesis of Next Generation Chemokine Modulators with or without
Concurrent HIV Reverse Transcriptase Inhibitory Activity

By

Anthony R. Prosser
Doctor of Philosophy

Chemistry

Dr. Dennis C. Liotta
Advisor

Dr. Huw Davies
Committee Member

Dr. Khalid Salaita
Committee Member

Accepted:

Lisa A. Tedesco, PhD. Dean of the James T. Laney School of Graduate Studies

_____Date

Discovery and Synthesis of Next Generation Chemokine Modulators with or without
Concurrent HIV Reverse Transcriptase Inhibitory Activity

By

Anthony R. Prosser
B.S., University of Kansas

Advisor: Dr. Dennis C. Liotta, Ph. D.

An abstract of
A dissertation submitted to the Faculty of the
James T. Laney School of Graduate Studies of Emory University
in partial fulfillment of the requirements for the degree of
Doctor of Philosophy
in Chemistry
2015

Abstract

Discovery and Synthesis of Next Generation Chemokine Modulators with or without Concurrent HIV Reverse Transcriptase Inhibitory Activity

By Anthony Prosser

Current HIV regimens require multiple antiviral drugs to arrest ongoing viral replication and restore immune function. These so-called “drug cocktails” work by utilizing several mechanisms of action to disrupt HIV replication. The drugs typically employed in this strategy include entry/fusion inhibitors, non-nucleoside and nucleoside reverse transcriptase inhibitors (NNRTIs/NRTIs), integrase inhibitors, and protease inhibitors. Unfortunately, these so-called “drug cocktails” come with significant financial burden, a continually emerging set of long term side effects, and the potential for resistance if not taken as prescribed, because addressing these problems is key to the eventual eradication of HIV herein disclosed are series of small molecule anti-virals with potential advantages in terms of resistance, cost, and side effects. More specifically, in Chapter 1 CXCR4 antagonists were pursued to potentially produce compounds with robust resistance profiles, by not allowing the virulent X4 tropic HIV viral strain to enter the cell. In Chapter 2 single agents that bind to combinations of CXCR4, CCR5 and HIV reverse transcriptase were also discovered and pursued to potentially decrease the cost and side effects of HIV treatment by combining multiple mechanisms of action in a single agent.

Discovery and Synthesis of Next Generation Chemokine Modulators with or without
Concurrent HIV Reverse Transcriptase Inhibitory Activity

By

Anthony R. Prosser
B.S., University of Kansas

Advisor: Dr. Dennis C. Liotta, Ph. D.

A dissertation submitted to the Faculty of the
James T. Laney School of Graduate Studies of Emory University
in partial fulfillment of the requirements for the degree of
Doctor of Philosophy
in Chemistry
2015

Table of Contents

Introduction: The Need to Develop More Anti-HIV Therapeutics	1
Chapter 1: CXCR4 Antagonists	10
1.1 CXCR4 as a Therapeutic Target	10
1.2 TIQ Modeling Targets – Chemistry	15
1.3 TIQ Modeling Targets – Results	28
1.4 TIQ Selectivity – Chemistry	30
1.5 TIQ Selectivity – Results	33
1.6 PIP SAR Targets – Chemistry	37
1.7 PIP SAR targets – Results	44
1.8 CXCR4 Experimentals	51
Chapter 2: Dual X4/R5 Modulators	130
2.1 CXCR4/CCR5 as a Therapeutic Target	130
2.2 Design of “Stitched” Dual X4/R5 Antagonists	135
2.3 “Stitched” Dual X4/R5 Antagonists – Results	140
2.4 Second Generation “Stitched” Dual X4/R5 Antagonists	141
2.5 Second Generation “Stitched” Dual X4/R5 Antagonists – Results	143
2.6 Virtual Screening and Discovery of Pyrazole Dual X4/R5 Series	145
2.7 Design of One-pot Methodology for the Conversion of Esters to Ketones	152
2.8 Initial Synthetic Studies on Dual-tropic Pyrazoles (D-Ring SAR)	159
2.9 Additional Synthetic Studies on Dual-tropic Pyrazoles (A, B, C-ring SAR)	171
2.10 Dual-tropic Pyrazole Series Conclusions	178
2.11 Dual-Tropic Experimental	186

Figures

Figure 0.1: Startling HIV statistics	1
Figure 0.2: Rate of AIDS diagnosis per year	2
Figure 0.3: The HIV life cycle	3
Figure 0.4: Mechanistic details of HIV entry	4
Figure 0.5: Additional mechanistic details of HIV entry	6
Figure 0.6: The Multinuclear Activation of Galactosidase Indicator (MAGI) assay	7
Figure 1.1: Potent CXCR4 antagonists and their activity against T-tropic HIV and signaling efficacy	12
Figure 1.2: Mutational data for AMD compounds in CXCR4	13
Figure 1.3: Synthetic targets based on first generation molecular modeling	15
Figure 1.4: Early modeling hypothesis for 2-naphthyl 1	16
Figure 1.5: Early modeling hypothesis for di-butyl amine 4	17
Figure 1.6: Compounds designed with medicinal chemistry rationale to	31

probe the CXCR4 selectivity profile.	
Figure 1.7: Initial modeling rationale for compound 45	32
Figure 1.8: Improved modeling rationale for compound 45 's selectivity	37
Figure 1.9: Synthetic targets based on SAR principals on the PIP series.	38
Figure 1.10: Structural similarity of substitution at either piperazine.	39
Figure 1.11: Structural comparison of GSK compound to butyl-amine isosters 52 and 53	39
Figure 1.12: Crystal structure and chiral assignment of 66	42
Figure 2.1: Tropism independent small molecule entry inhibitors	130
Figure 2.2: Potent CCR5 antagonists	132
Figure 2.3: Anti-inflammatory effects of AMD3100 in mouse model	133
Figure 2.4: Compound stitching strategy in the pursuit of dual-active CCR5/CXCR4 antagonists	136
Figure 2.5: Design of "stitched"-compounds 4-7	137
Figure 2.6: Design of "stitched"-compounds 24-29	144
Figure 2.7: Example of Bayesian statistics	149
Figure 2.8: Virtual screening work flow and active hits	151
Figure 2.9: Retrosynthetic analysis and ring designation for screening hit 38	155
Figure 2.10: Correlation between hydrophobicity and toxicity	166
Figure 2.11: Binding of pyrazolo-piperidines to CCR5 (A/B) and CXCR4 (C/D) predicted by molecular modeling	170
Figure 2.12: Binding of pyrazolo-piperidines to HIV-RT predicted by molecular modeling.	173
Figure 2.13: Potency gains from virtual screening hit to compound 92	179

Tables

Table 1.1: CYP450 and hERG Measurements	14
Table 1.2: Screening of Reaction Conditions	20
Table 1.3: Biological Testing of TIQ Modeling Compounds	28
Table 1.4: Biological Testing of TIQ Selectivity Targets	33
Table 1.5: Biological Testing of PIP R ₁ SAR Targets	44
Table 1.6: Biological Testing of PIP R ₂ SAR Targets	46
Table 2.1: Normal CXCR4 Expressing Cells and Analogous CXCR4 Expressing Tumor	134
Table 2.2: Anti-HIV and Antagonist Activity of "Stitched" Series	140
Table 2.3: Anti-HIV Activity of Second Generation "Stitched" Series	143
Table 2.4: Anti-HIV Activity of Pyrazole Screening Hits	149
Table 2.5: Screen of Reaction Conditions	154
Table 2.6: Reaction Scope Versus Piperidine Moiety	156
Table 2.7: Anti-HIV Data for D Ring Analogs	162
Table 2.8: Anti-HIV (% Inhibition) Data for D Ring Analogs	164
Table 2.9: Profiling of Lead D Ring Compounds	165
Table 2.10: R5 vs X4 vs RT activity for D Ring Analogs	168
Table 2.11: SAR of the A, B, and C rings	176
Table 2.12: Profiling of Two Sub-Series	178

Schemes

Scheme 1.1: Initial synthesis of TIQ compounds	18
Scheme 1.2: Synthesis of chiral building blocks 5 and 13	19
Scheme 1.3: Improved synthesis of TIQ series	21
Scheme 1.4: Synthesis of compounds 20 and 21	22
Scheme 1.5: Retrosynthetic design of target 3 and 4	23
Scheme 1.6: Synthesis of intermediate 31 in route to compounds 3 and 4	23
Scheme 1.7: Synthesis of target 3 and attempted synthesis of target 4 from intermediate 31	25
Scheme 1.8: Proposed mechanism for side chain cleavage of compound 32 to form 9	26
Scheme 1.9: Successful synthesis of target 4 from pyrrolidone 37	27
Scheme 1.10: Synthesis of target 43 and 44	31
Scheme 1.11: Synthesis of compound 45	31
Scheme 1.12: Synthesis and resolution of diastereomers 59 and 60	40
Scheme 1.13: Synthesis of Boc-protected advanced intermediates 63-70	41
Scheme 1.14: Synthesis of final products 71-78	43
Scheme 1.15: Synthesis of final products 93-102	44
Scheme 2.1: Synthesis and resolution of diastereomers 14 and 15	138
Scheme 2.2: Synthesis of final products 2-7	139
Scheme 2.3: Synthesis of final products 24 to 29	142
Scheme 2.4: Synthesis of screening hit 37	150
Scheme 2.5: Merck's synthesis of common intermediate 54 and an alternative retrosynthetic analysis of precursor 57	153
Scheme 2.6: Conversion of intermediate 57 to target 54	157
Scheme 2.7: General route to D ring SAR	159
Scheme 2.8: Synthesis of modular intermediate 74	160
Scheme 2.9: Synthesis of compounds with various D rings	161
Scheme 2.10: Synthesis of compound 78	161
Scheme 2.11: Synthesis of C ring analogs	171
Scheme 2.12: Synthesis of compounds 116 and 117	172
Scheme 2.13: Synthesis of compound 121	173
Scheme 2.14: Synthesis of compounds 123 and 124	174
Scheme 2.15: Synthesis of compound 125	175
Scheme 2.16: Synthesis of compound 126	175

Introduction: The Need to Develop More Anti-HIV Therapeutics

Despite commercial access to over two dozen FDA approved antiviral compounds for combating HIV, over 1.2 million Americans have the virus. Worse only 42% of diagnosed patients are on HAART (Highly Active Anti-Retroviral Therapy).¹ These statistics are even more dismal in the developing world, and suggest that the war on HIV is far from over.²

Startling HIV statistics from 2012 CDC report

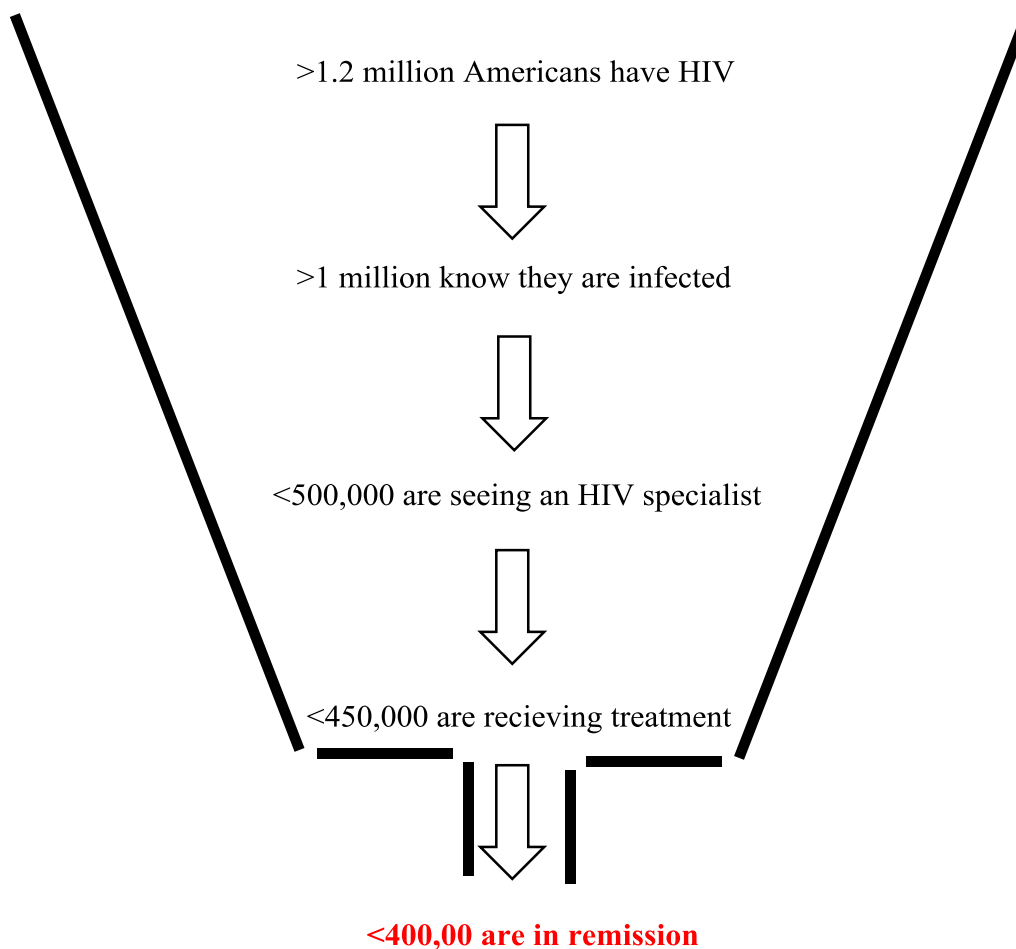


Figure 0.1: Startling HIV statistics¹

Research by the Center for Disease Control (CDC) estimates that over 1.2 million Americans are infected with HIV.¹ This number is disturbingly high number considering the access to healthcare and effectiveness of HIV drugs. In fact despite the transmission rate being significantly decreased by the advent of antiretroviral treatment (Figure 0.2), the rate of infection and the approximate morbidity of the virus has been holding steady since. The ongoing struggles with patient compliance for HIV treatment are often attributed to both the cost of therapy, the side-effects related to therapy, and education about therapy. Herein we postulate small molecule treatments for HIV that may prove advantageous over traditional therapies in terms of cost or side-effects both of which should increase patient compliance.

Current HIV regimens require multiple antiviral drugs to arrest ongoing viral replication and restore immune function.^{2,3} These so-called “drug cocktails” work by utilizing several mechanisms of action to disrupt HIV replication. The drugs typically employed in this strategy include entry/fusion inhibitors, non-nucleoside and nucleoside reverse transcriptase inhibitors (NNRTIs/NRTIs), integrase inhibitors, and protease inhibitors. The complexity of HIV treatment stems from the inherent complexity of the HIV life cycle (Figure 0.3)⁴.

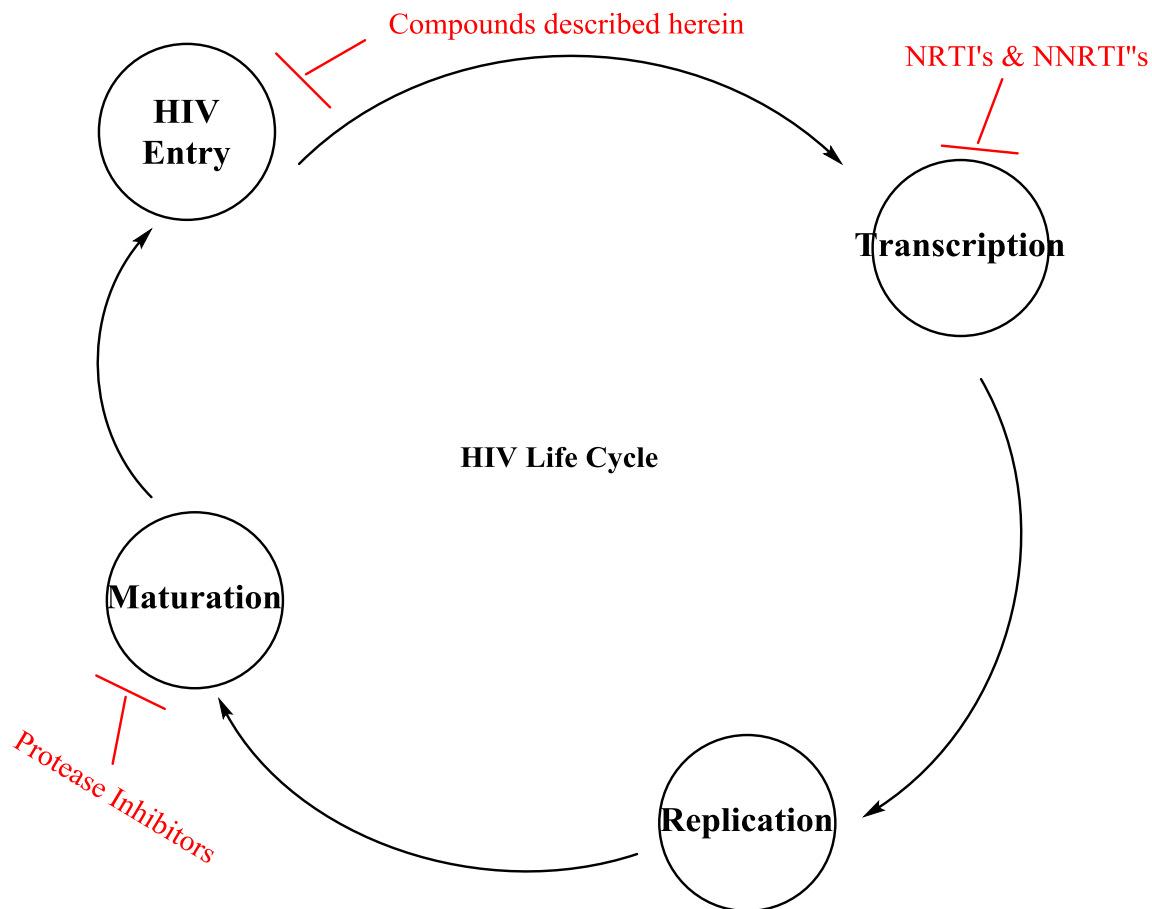


Figure 0.3: HIV life cycle⁴

The HIV virion initially interacts with CD4⁺ cells via a protein-protein interaction of HIV glycoproteins and the host CD4 surface receptor. If a co-receptor is present in close proximity to the interacting CD4 receptor HIV is able to enter the cell. Upon cellular entry HIV must convert its viral RNA to cDNA before being able to hijack the cellular machinery. This process requires HIV reverse transcriptase which is the most prevalent point of therapeutic intervention. Non-nucleoside and nucleoside reverse transcriptase inhibitors (NNRTIs/NRTIs) can disrupt HIV reverse transcriptase in two major ways. First antiviral agents can covalently bind to the growing strand of cDNA essentially terminating its progression, this activity primarily stems from NRTIs. Alternatively, antiviral agents

can bind to the reverse transcriptase activity either blocking the active site of replication or causing a conformational defect that terminates progression, this activity primarily stems from NNRTIs. After conversion of viral DNA to cDNA the HIV integrase enzyme integrates the viral genome into the host DNA. Upon activation, the integrated viral information is transcribed using host transcriptase enzymes causing rapid proliferation. Next a viral enzyme called protease cuts the HIV structural proteins to the correct size to allow manufacturing of new virions. Protease activity is also a major point of therapeutic intervention and several molecules have been developed that deactivate the enzyme by either conformational binding or binding to the active site. If the virus successfully manufactures new virions it finally uses part of the host's membrane to bud out of the cell and begin the life cycle anew.

Due to the focus of this Thesis on HIV entry, a more detailed inspection of the mechanism of HIV entry is warranted. The current understanding of HIV cellular entry. Initially the HIV viron approaches the CD4⁺ cell and glycoprotein (gp) 120 makes a protein-protein interaction with CD4. CD4 is highly flexible and if a chemokine co-receptor (CXCR4 or CCR5) is in close vicinity the CD4 protein will eventually move gp120 into contact with the co-receptor. Co-receptor recognition occurs primarily through the V3 loop of GP120. Also important for receptor recognition but not nearly as variable is gp120 bridging sheet structure as well as the V1/V2 loop (Figure 0.4) The V3 loop is highly variable between strains and determines the specificity of the virus for CXCR4 receptors, CCR5 receptors, or both receptors. Upon recognition and binding the HIV glycoproteins are parted and GP41 mediated fusion occurs, the exact mechanism of this process is not fully understood and some believe a dimer of trimers is responsible.⁶

The potency of HIV viral entry inhibitors is still difficult to assess with entry specific assays. For this reason, potential HIV inhibitors regardless of their class are often screened with cellular assays and live virus. An obvious limitation of this strategy is that even though accurate antiviral potencies can be determined they completely lack mechanistic details. Often “lead” molecules are followed up with more specific mechanistic assays to ensure the series is maintaining the desired mechanistic properties.

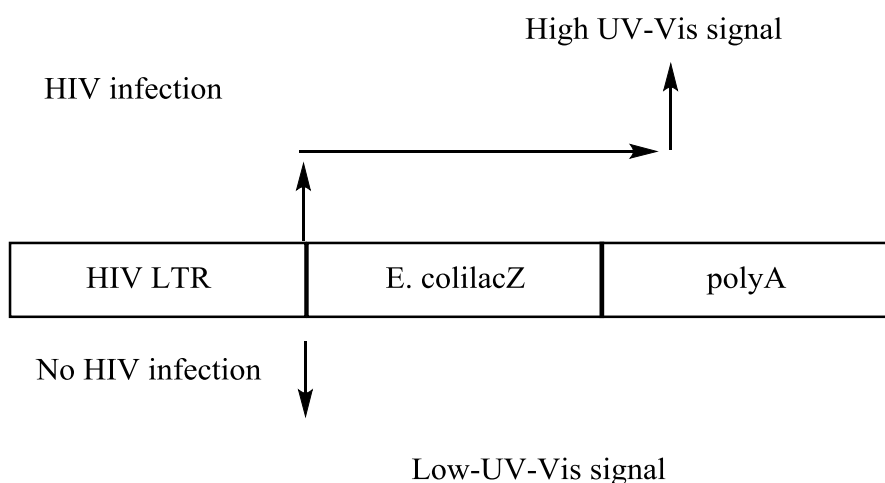


Figure 0.4: The Multinuclear Activation of Galactosidase Indicator (MAGI) assay⁷

One of the most frequently used assays for total anti-HIV activity is the Multinuclear Activation of Galactosidase Indicator (MAGI) assay. The assay was developed in the early 90s in the Emerman lab utilizing a HeLa cell line that has been engineered to express CD4 and high levels of the chemokine receptors CXCR4 and CCR5.⁷ The cells are also transfected with a plasmid containing a long terminal repeat (LTR) that is responsible for viral replication. The LTR is engineered upstream from the gene coding for β -galactosidase release (E. coli lacZ in Figure 0.4). Essentially this assay is engineered in such a way that infected cells will produce β -galactosidase which can be quantified using

a chromogenic substrate called X-gal. A typical workflow with the MAGI assay involves pre-incubating the cells with compound to allow sufficient time to bind, and subsequent addition of the HIV virus. After a set period of time the amount of viral replication is quantified by spectroscopy of the resultant β -galactosidase which has been stained blue by X-gal.

In the present document all MAGI results were collected by the Southern Research Instituted (SRI) on contract. The control compounds used for these studies are well known in the literature to not be active against either X4 or R5 tropic HIV. For all reported experiments AMD3100 had to have an IC₅₀ of greater than 10 μ M (the testing limit) against the R5 using virus and an IC₅₀ of less than .01 μ M against the X4 using virus. Any data sets that did not comply with this requirement were reran as the HIV viral strain was most likely compromised. Similarly, either TAK779 or Maraviroc was ran as a control for ever compound tested herein in the MAGI assay. Both TAK779 and Maraviroc had to have IC₅₀'s of greater than 10 μ M (the testing limit) against the X4 using virus and of less than .01 μ M against the R5 using virus. Except when explicitly noted otherwise, the R tropic HIV virus used for the following studies is Ba-L, and the X tropic HIV virus used is IIIB.

Date	11-15-12	7-26-12	8-24-12	10-8-12	9-24-13	average	Standard Deviation
IC ₅₀ in nM	1	4	4	20	2	6.2	7.8
IC ₉₀ in nM	8	40	40	24	10	24	16

The average error of the MAGI assay is tracked in (Table 0.1) and shows that prior to 2014 that the IC₅₀'s varied by around 1-4 fold on average and a 20 fold variance in

October that significantly increased the variance on the batch to a very high standard deviation of 7.8 nM. After review of the data we determined that the high variance made it incredibly hard to interpret results. Data starting in 2014 is significantly less noisy because SRI agreed to enforce an under 10 nM IC50 requirement for AMD3100 (Table 0.2). Data collected in 2014 was significantly tighter and had an average standard deviation of just 1.5 nM. In terms of interpretation compounds with at least 5 fold difference in potency are considered significantly different, this data supports this interpretation.

Date	3-5-14	5-2-14	5-30-14	6-13-14	7-2-14	7-28-14	12-5-14	12-19-14	average	Standard Deviation
IC50 in nM	3	1	3	3	3	1	4	5	3.2	1.5
IC90 in nM	30	9	30	10	10	8	30	40	20	15

One of the most frequently used follow up assays for chemokine ligands being pursued for antiviral potency is the calcium-flux assay (Ca²⁺ flux). The calcium flux assay can quantify either antagonism (increased calcium) or agonism (decreased calcium) via fluorescent dyes. A commonly used dye is FluoForte which only fluoresces when bound to calcium. In the case of antagonism calcium is released from the endoplasmic reticulum and the overall amount of fluorescence subsequently increases as well. In the case of agonism calcium is stored in the endoplasmic reticulum and fluorescence subsequently decreases.

All of the calcium-flux assay results of this report were collected under contract by Millipore. Unless otherwise noted the %saturation of SDF-1 used is 80%. The calcium flux assay is notoriously variable because it uses's a surrogate signaling pathway instead of the

g-alpha path that is actually occurring. For this reason, the compounds reported herein were tested head to head when comparisons of selectivity factors were made.

References:

1. Centers for Disease Control and Prevention (CDC). *Today's HIV/AIDS Epidemic*.
2. Fauci, A. S., et al. (2013). "HIV-AIDS: much accomplished, much to do." Nat Immunol **14**(11): 1104-1107.
3. Moss, J. A. (2013). "HIV/AIDS Review." Radiol Technol **84**(3): 247-267; quiz p.268-270.
4. Monini, P., et al. (2004). "Antitumour effects of antiretroviral therapy." Nat Rev Cancer **4**(11): 861-875.
5. Connell, B. J. and H. Lortat-Jacob (2013). "Human Immunodeficiency Virus and Heparan Sulfate: from attachment to entry inhibition." Frontiers in Immunology **4**.
6. De Clercq, E. (2003). "The bicyclam AMD3100 story." Nat Rev Drug Discov **2**(7): 581-587.
7. Kimpton, J. and M. Emerman (1992). "Detection of replication-competent and pseudotyped human immunodeficiency virus with a sensitive cell line on the basis of activation of an integrated beta-galactosidase gene." J Virol **66**(4): 2232-2239.

1.1 CXCR4 as a Therapeutic Target

G-protein coupled receptors (GPCRs) represent the largest family of mammalian proteins, with well over 1,000 members. Due to their massive number and large range of diverse structures GPCR's are responsible for a plethora of physiological functions. Modulating GPCR's is a robust area of pharmaceutical research as they play at least a minor role in nearly every disease. Of particular interest is the C-X-C chemokine receptor type 4 (CXCR4) which is expressed on a broad set of cell types including dendritic cells, neutrophils, monocytes, macrophages, T and B-lymphocytes, neurons, and endothelial progenitor cells. Due to CXCR4's broad representation in hematopoietic cell types it is a useful target for potential viral entry.

C-X-C chemokine receptor type 4 (CXCR4) is an alpha-chemokine receptor belonging to the G-protein coupled receptors with only one natural ligand (stromal-derived-factor-1 (SDF-1)). SDF-1 is a small cytokine characterized by 2 disulfide bridges formed from 4 cysteines that are conserved across the cytokine family. SDF-1 is essential to proper development, demonstrated by the fact that CXCL12 (the gene that codes for SDF-1) knock out mice died before or within 1 hour of birth. This developmental necessity is often attributed to SDF-1's role in chemotaxis of hematopoietic cells. Even though adults need the chemotaxis of lymphocytes far less than the developing embryo, this still serves as the major use of SDF-1 as a therapeutic target to this day.

The CXCR4/SDF-1 signaling axis is incredibly complex, and is involved in numerous pathways important for proper cell function. Of note is downstream signaling effect on survival, proliferation, chemotaxis, and transcription gene expression.¹ These activities are often attributed to the biological basis for why tumors must increase CXCR4

expression to effectively survive and eventually metastasis. In the Liotta lab we are particularly interested in CXCR4's role in chemotaxis, as AMD3100 demonstrated that antagonists can have a profound effect on this signaling event. Due to the high cost and low throughput associated with measuring chemotaxis directly, the Ca flux assay is often used as a surrogate for chemotaxis. By measuring the release of intracellular calcium stores a strong approximation for a compounds ability to cause chemotaxis can be determined.

Kaplan Meier curves for the clinical progression to AIDS show that patients whose viral pool can access the CXCR4 receptor progressed to AIDS at a much quicker rate than their CCR5 pure counterparts.² In fact even with treatment more than half of patients in the CCR5/CXCR4 mixed population progressed to AIDS within 4 years' time. A significant criticism of this study is that the compounds used were standard of care in the 90s, whereas current therapies are superior and may not exhibit as pronounced of a difference between R5 and X4 virulence.

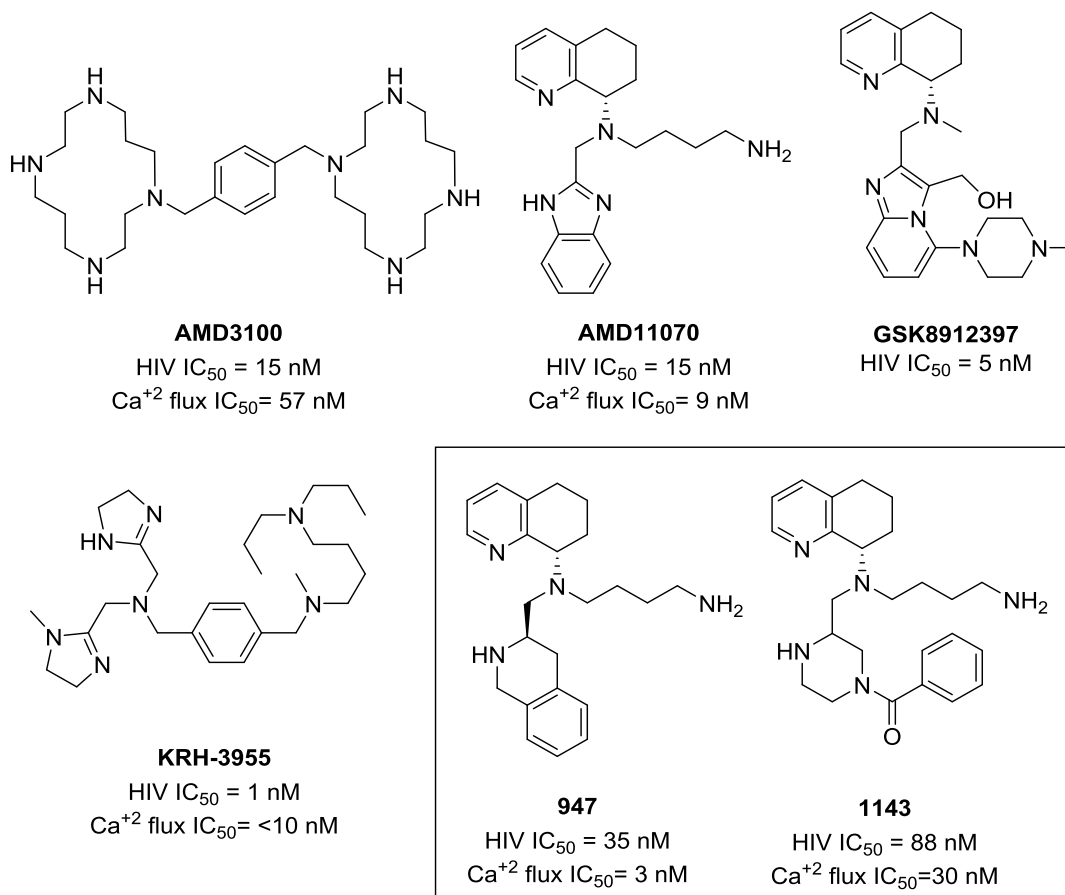


Figure 1.1 Potent CXCR4 antagonists and their activity against T-tropic HIV and signaling efficacy.

Due to the higher virulence and poor treatment outcomes associated with the T-tropic HIV virus, our initial interest in HIV-entry inhibitors centered on CXCR4. **AMD3100** (Figure 1.1) is largely regarded as the initial proof of concept that CXCR4 antagonists can effectively block T-tropic HIV viral entry.³ **AMD3100** successfully met viral load endpoints in a phase II clinical trial, but failed a phase III clinical study due to observed toxicity. During the course of the study, the surprising observation was made that single doses of **AMD3100** effectively mobilized stem cells.⁴ With our increased understanding of the CXCR4 signaling pathway, we now know that stem cell mobilization is an expected result of CXCR4 antagonism. **AMD3100** is now approved for use in stem

cell therapy, and ongoing trials suggest it may be an effective chemotherapy agent.⁵⁻⁷ **AMD3100**'s toxicity was initially attributed to the cyclam structural motif leading to development of **AMD11070** (Figure 1.3) an orally bioavailable CXCR4 antagonist that advanced to phase II clinical trials.⁸ **AMD11070** was pulled from development due to cytochrome P450 (CYP450) activity (specifically 3A4 and 2D6 inhibition).⁹ Despite the continued lack of success for CXCR4 antagonists in treatment of HIV, several similar scaffolds entered preclinical developed based on the **AMD11070** core: such as **GSK8912397** which maintained the chiral tetrahydroquinolin and used an isostere of the bottom benzimidazole.¹⁰ Significantly disparate scaffolds such as the very potent **KRH-3955** are also being pursued.¹¹

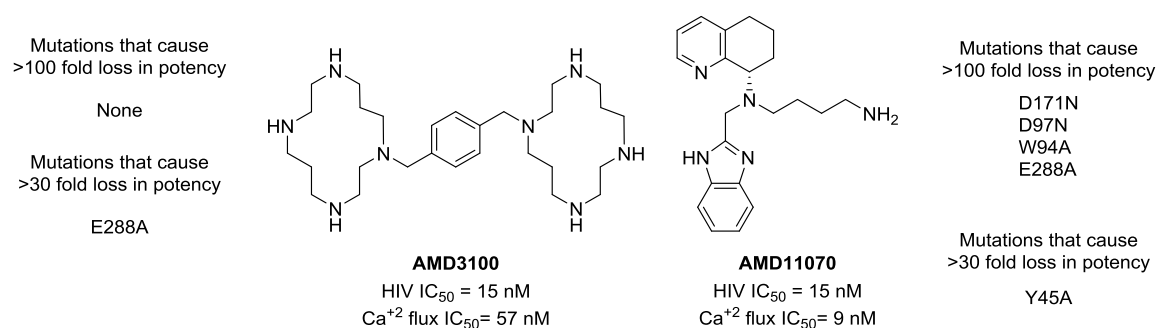


Figure 1.2: Mutational data for AMD compounds in CXCR4

Despite very potent lead molecules being developed, further development of CXCR4 antagonists was further warranted by recent selectivity data published by the Fricker and Huang group.^{13,14}

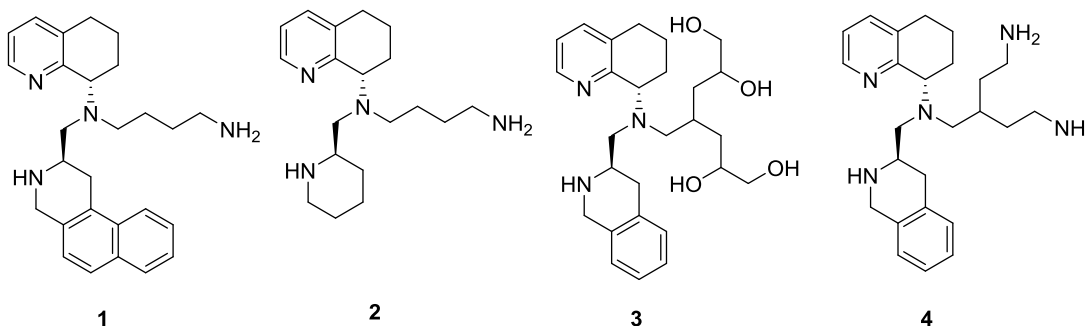
Table 1.1 CYP450 and hERG Measurements					
Compound	CYP450 (inhibition @ 1 μ M) ^a			hERG (inhibition) ^b	
	3A4	2D6	2C19	1 μ M	10 μ M
AMD11070	35%	100%	20%	—	—
947	6%	8%	0%	50%	93%
1143	0%	19%	2%	18%	55%

a. Isolated human enzymes and fluorometric substrates

b. Displacement of 3*H*-dofetilide in HEK293 cells.

The Liotta Lab was interested in maintaining the good potency and bioavailability of **AMD11070** whilst avoiding the CYP450 inhibition liability. It was suspected that the benzimidazole was responsible for the CYP450 activity and that replacement may attenuate the activity. In this pursuit a scaffold hop was conducted that maintained the chiral tetrahydroquinolin and butylamine side chain as two strong anchor points and screened various aryl replacements for the benzimidazole ring.¹⁴ The scaffold hop successfully identified two very potent hit compounds: **947** a tetrahydroisoquinolin replacement and **1143** an acylated piperazine replacement (Figure 1.5).^{14,15} Gratifyingly both compounds were in fact resistant towards CYP450 inhibition with under 20% inhibition against every isotype tested (Table 1.1). Unfortunately, in the screening process a hERG inhibition liability was identified, this coupled with a desire for more anti-viral potency prompted a hit-to-lead structure activity relationship (SAR) study.

1.2 TIQ Modeling Targets -- Chemistry



Early Modeling Hypothesis:

1. Correctly positioned naphthyl picks up enhanced pi-stacking.
2. Lack of aryl group will significantly decrease potency due to no pi-stacking interaction.
3. Correctly positioned alcohols accept hydrogen bonds from various residues.
4. Correctly positioned bis-butyl amine picks up an extra interaction with a aspartic acid.

Figure 1.3: Synthetic targets based on first generation molecular modeling.

Due to the high initial potency of the **947** hit we suspected that any potency improvements we found would have to be rationally designed. In this pursuit we modeled a handful of difficult synthetic targets with our first generation of CXCR4 grid technology with maestro (compounds shown in Figure 1.3).

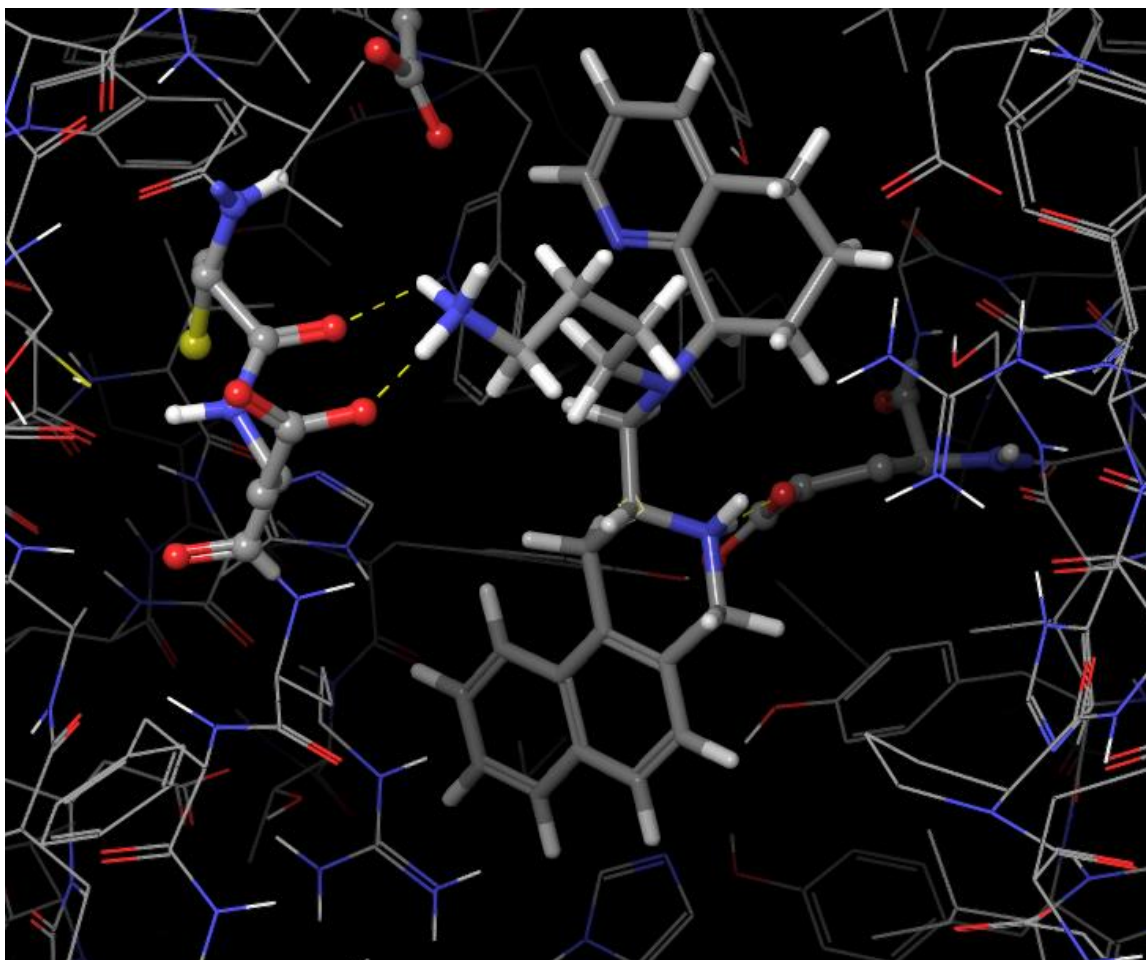


Figure 1.4: Early modeling hypothesis for 2-naphthyl **1**

We specifically expected naphthyl compound **1** to pick up higher anti-HIV potency whilst maintaining an approximately equal potency towards SDF-1 mediated signaling. This can be seen in Figure 1.4 via the naphthyls directionality towards the left side of the receptor towards helix III IV and V which are known to be responsible for HIV related activities.^{17,18} The protonated butylamine side chain also makes electrostatic interaction with aspartic acid 187 and cysteine 187 on the HIV side of the receptor. On the SDF-1 side on the other hand the TIQ nitrogen makes an electrostatic interaction with glutamic acid 288, a key residue that has been maintained in nearly all our compounds modeled.

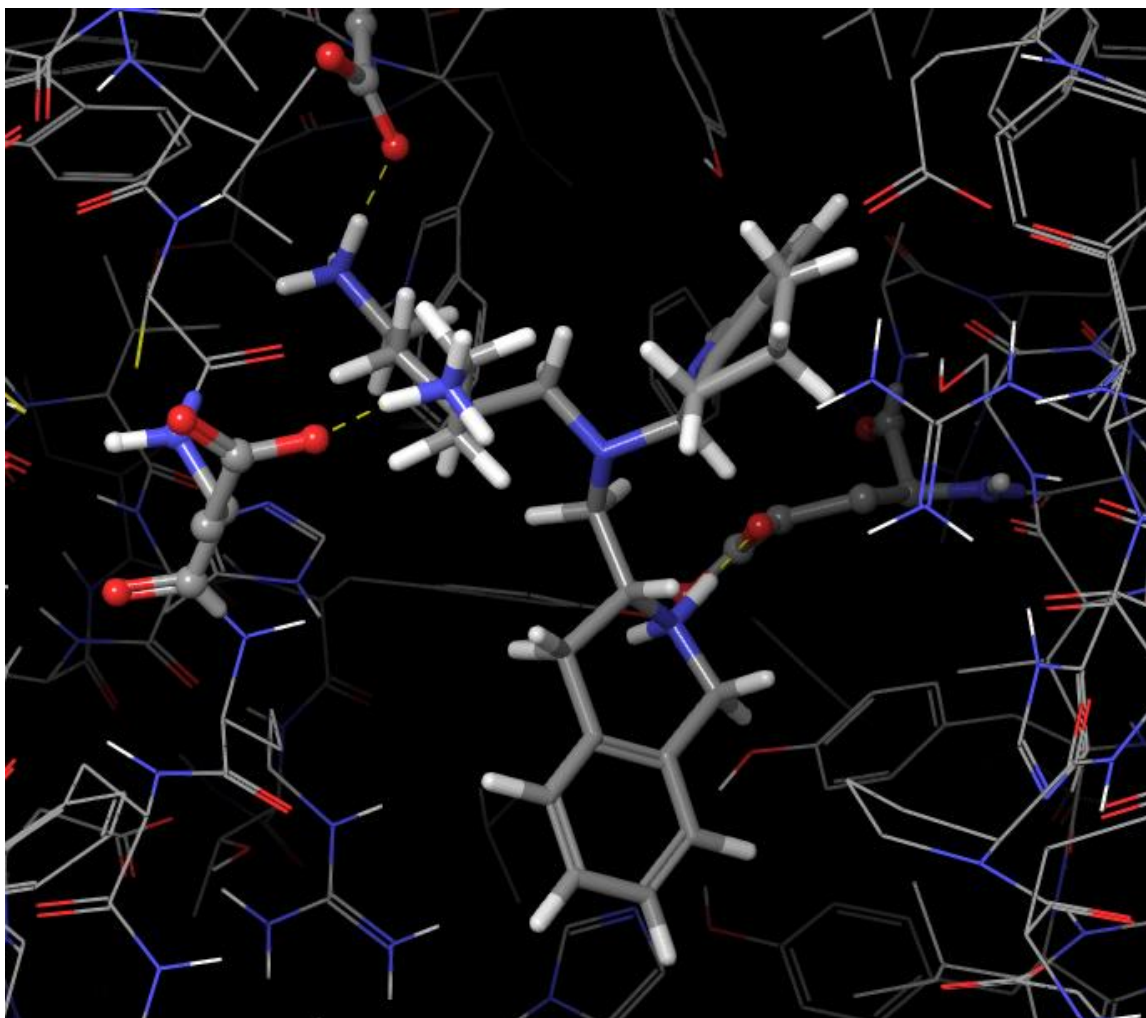
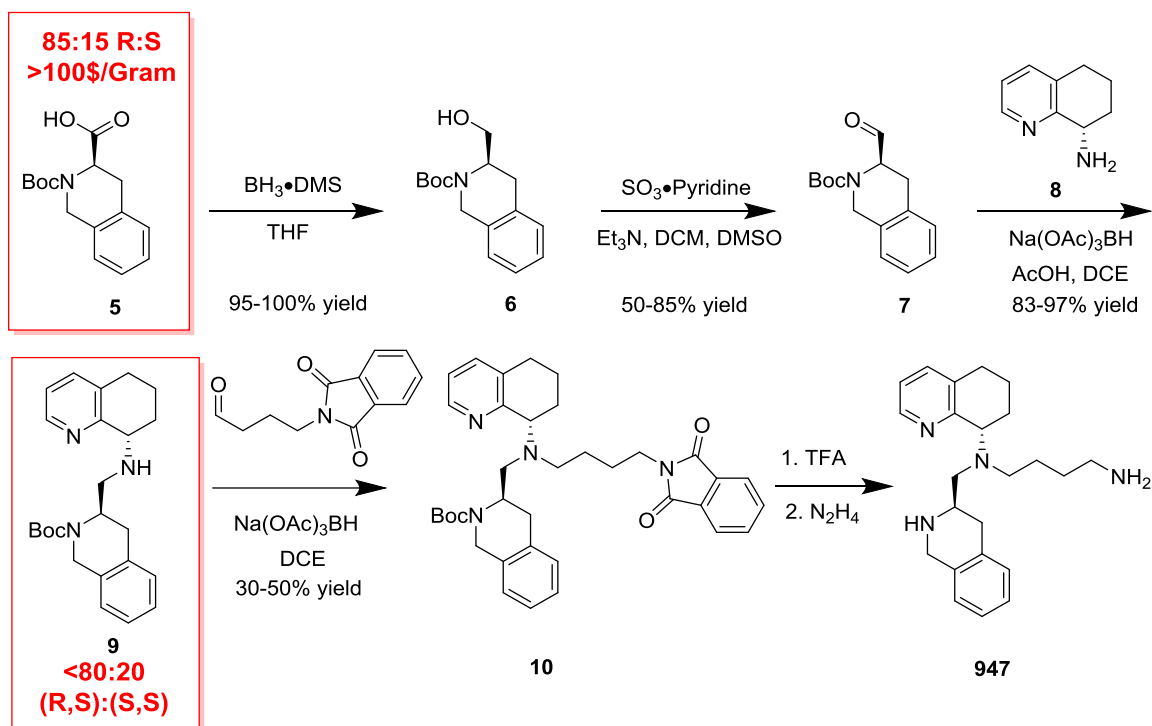


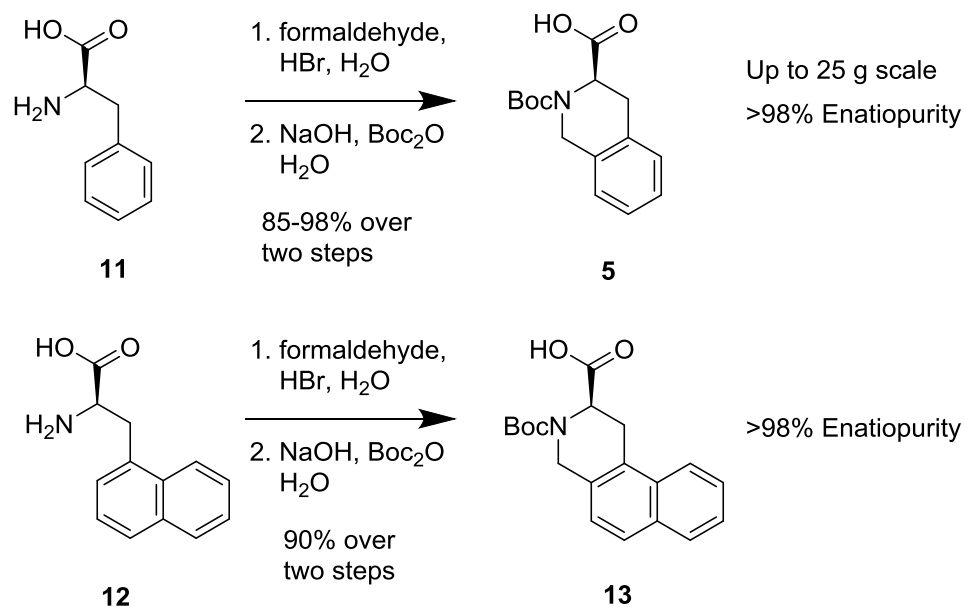
Figure 1.5: Early modeling hypothesis for di-butylamine **4**

We also expected di-butylamine **4** to pick up more potency against HIV indications while maintaining approximately the same potency for SDF-1 related indications (Figure 1.5). The two butylamines were predicted to make electrostatic interactions with aspartic acid 187 and aspartic acid 97 on the HIV side of the receptor. On the SDF-1 side of the receptor the TIQ nitrogen formed the typical electrostatic interaction with glutamic acid 288. It's worth noting that as modeled this compound carries three positive charges, which is a potential liability even in the highly acidic CXCR4 receptor.



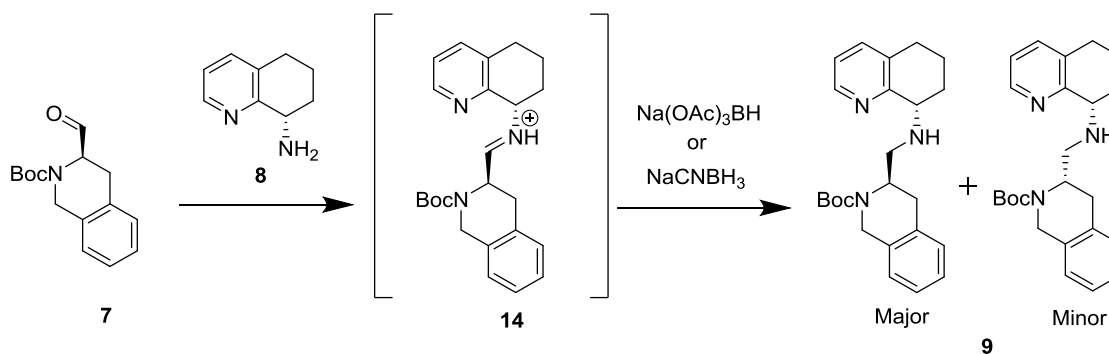
Scheme 1.1: Initial synthesis of TIQ compounds

The initial synthesis of TIQ compounds was sufficient to allow the identification and chiral assignment of **947**, but was bottlenecked by two major issues (Scheme 1.1). First, the commercially available starting material was determined to be only 85% R by chiral LCMS. Coupled with the inhibitory price tag of over 100\$ a gram and a 6+ step reaction a large scale synthesis was near impossible. Second, upon addition of the tetrahydroquinoline top piece **8** diastereomeric mixtures with a ratio of approximately 4:1 had to be separated by chromatography. This separation is very difficult and often takes several columns to achieve sufficient chiral purity.



Scheme 1.2: Synthesis of chiral building blocks **5** and **13**

Due to the high cost and insufficient chiral purity of the starting material feedstock, initial efforts in improving the synthesis were focused there. Inspection of the literature revealed a process scale synthesis of building block **5**.¹⁶ The Pictet-Spengler reaction from D-phenyl-alanine **11** followed by Boc-protection yielded tetrahydroisoquinoline **5** in high yield and enantiopurity (Scheme 1.2). Applying the same methodology to D-2-naphthyl-alanine **12** produced building block **13** without incident.

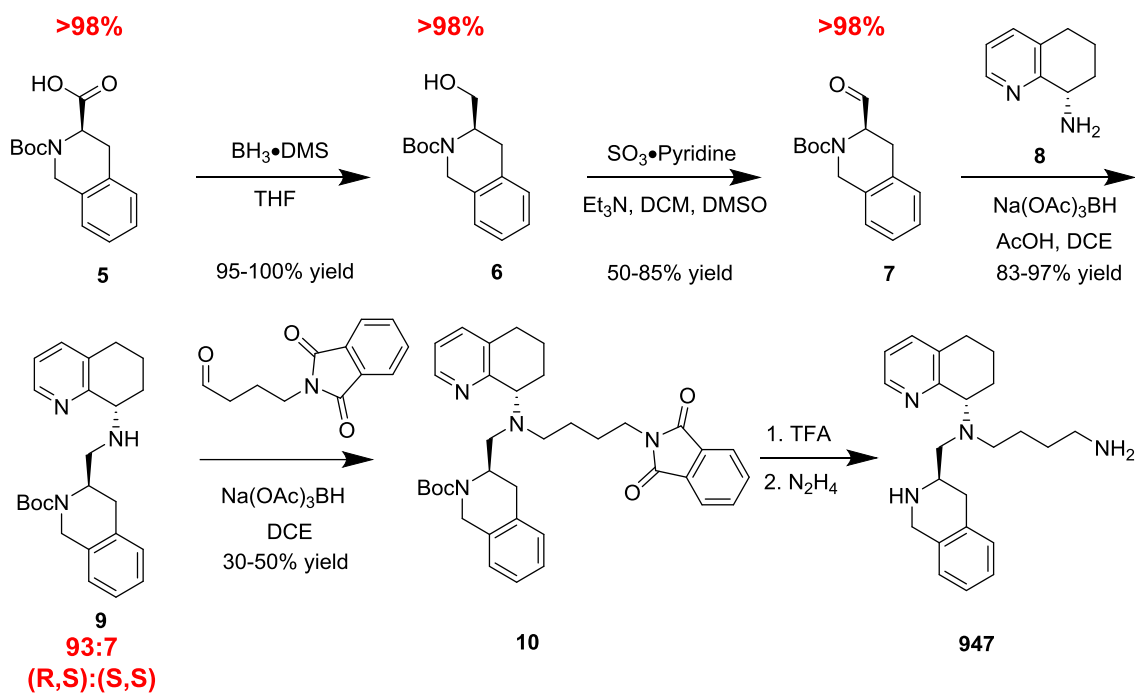
Table 1.2 Screening of Reaction Conditions^a

Entry	Solvent	Reductant	% (R,S)	Direct vs. Indirect ^b	Entry	Solvent	Reductant	% (R,S)	Direct vs. Indirect ^b
1	DCE	$\text{Na(OAc)}_3\text{BH}$	85%	Indirect	5	THF	$\text{Na(OAc)}_3\text{BH}$	90%	Direct
2	DCE/ AcOH	$\text{Na(OAc)}_3\text{BH}$	50%	Indirect	6	THF	NaCNBH_3	91%	Direct
3	DCE	$\text{Na(OAc)}_3\text{BH}$	93%	Direct	7	Toluene	$\text{Na(OAc)}_3\text{BH}$	67%	Direct
4	DCE	NaCNBH_3	92%	Direct	8	Toluene	NaCNBH_3	76%	Direct

a. Standard reductive amination reaction conditions: .1 M solution, 1:1 amine to aldehyde, 1.5 eq of reductant

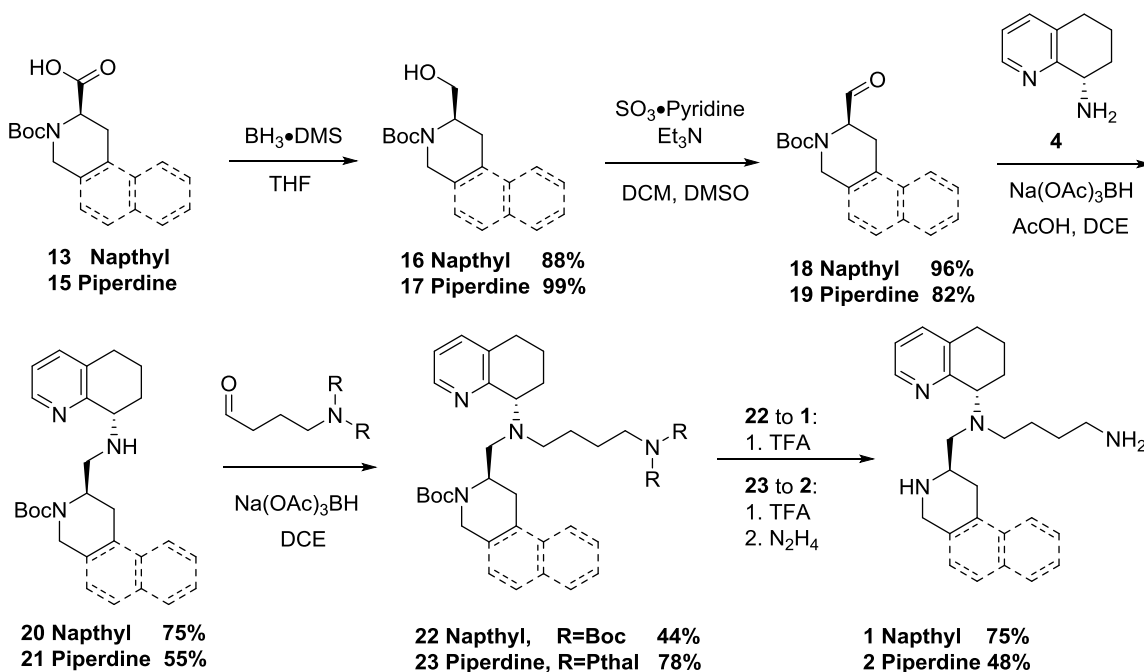
b. Direct: Addition of reductant followed by amine and aldehyde ; Indirect: Preformation of imine via 1 hour mixing of aldehyde and amine.

Even with pure chiral starting material the isolated diastereomeric ratios of intermediate **9** with our initial reductive amination methodology was unsatisfactory (table 1.2 entry 1). A screening of reaction conditions quickly identified that a direct (reductant added first) reductive amination was preferable to an indirect (reductant added after allowing imine to form) reductive amination (entries 1 vs 3). This result suggests that the imine **14** is highly racemizable and prolonged exposure of the imine to the reaction conditions causes loss of chiral purity. This hypothesis is highly supported by the addition of acetic acid (entry 2) in which case complete racemization occurs. In fact all tested indirect reaction conditions would eventually reach complete racemization is sufficient premixing was allowed (results not shown). Dichloroethane, sodium triacetoxyborohydride (STAB-H), and direct mixing conditions were used for all further chiral reductive aminations (entry 3).



Scheme 1.3: Improved synthesis of TIQ series

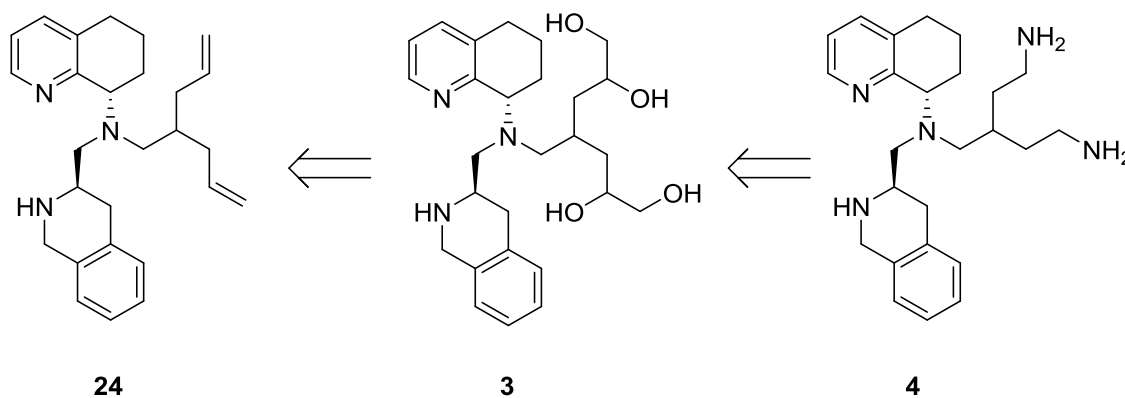
With optimized conditions for the formation of compound **9** in hand we significantly improved our chiral ratios to an average of 93:7 (R:S) to (S:S) (Scheme 1.3). Even though these ratios still required separation of the diastereomers, the separation was significantly easier and can now be accomplished in one column.



Scheme 1.4: Synthesis of compounds **20** and **21**

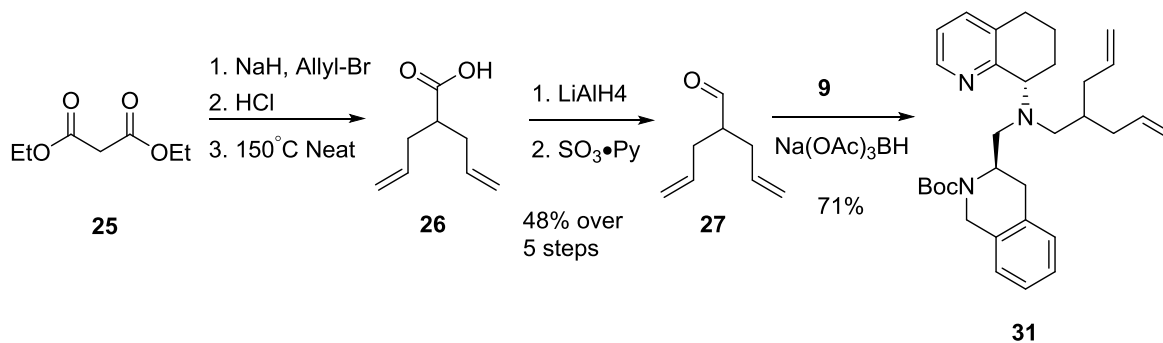
Using this synthetic methodology compounds **24** and **25** were both prepared as “one-offs” from their corresponding chiral building blocks **13** and **14** respectively (Scheme 1.4). Carboxylic acids **13** and **15** were reduced with a borane dimethyl sulfide solution to afford alcohols **16** and **17** in excellent yields. Alcohols **16** and **17** were oxidized with Parikh-Doering conditions to afford aldehydes **18** and **19** in excellent yield. Reductive amination with chiral amine **8** yielded half scaffolds **20** and **21** which were exhaustively purified and deemed diastomerically pure by HPLC. It is worth noting that though naphthyl compound **20** had a small amount of racemization that piperidine compound **21** had no detectable formation of the (S,S) adduct. This observation suggests that the aryl rings presence is a major contributor to the obliteration of the chiral center via acid. A subsequent reductive amination of **20** and **21** with protected butylamine chains yielded the protected compounds **22** and **23** in moderate to high yields. For naphthyl compound **22** a global Boc-deprotection with trifluoroacetic acid yielded final product **1** in reasonable yield. Piperidine

compound **23** on the other hand required deprotection with trifluoroacetic acid followed by deprotection with anhydrous hydrazine to remove both the Boc and phthalamide groups and yield final product **2** in moderate yield.



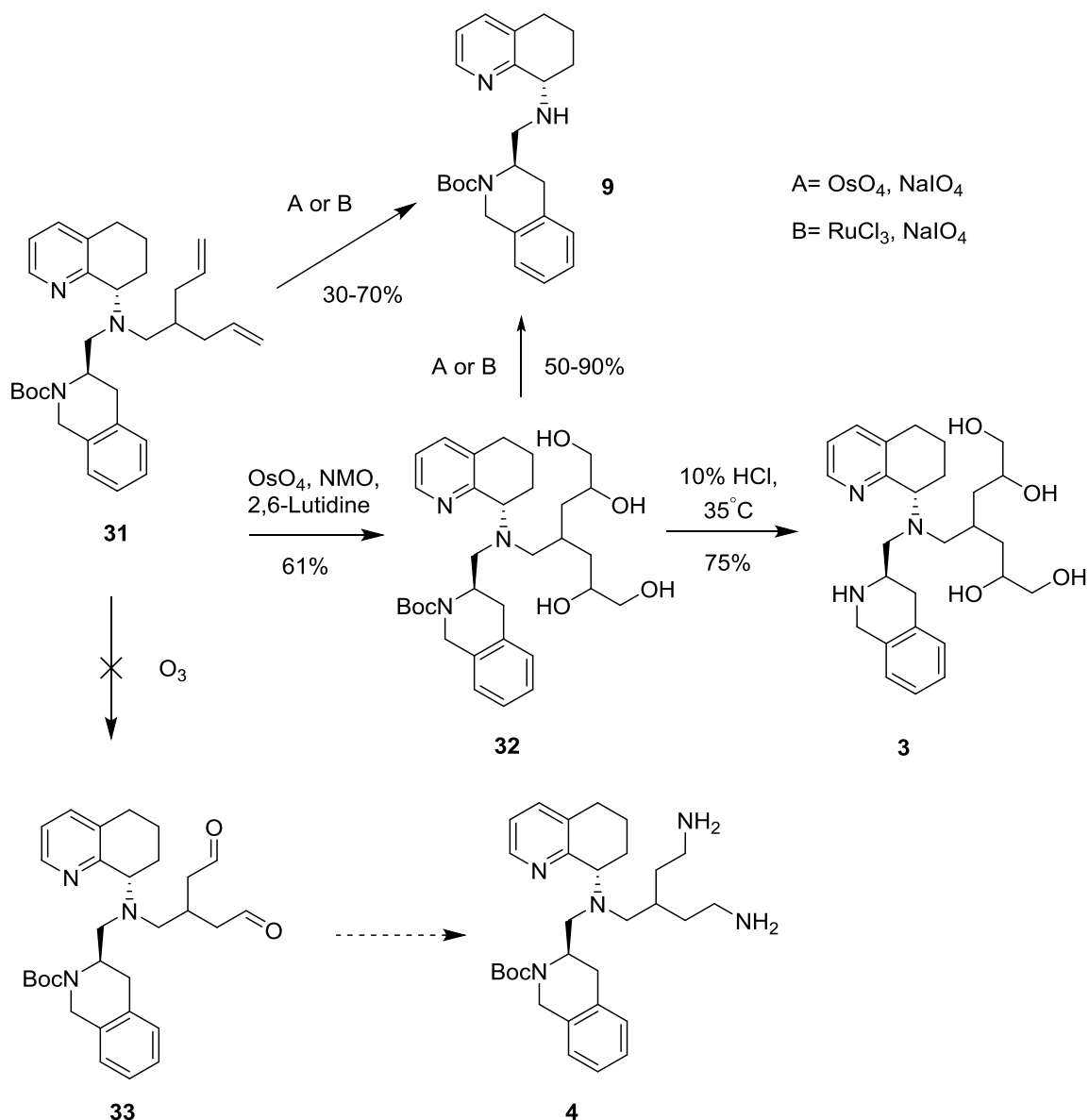
Scheme 1.5: Retrosynthetic design of target **3** and **4**

Our initial retrosynthesis of compound **3** and **4** was modular in nature and allowed both targets to be isolated in the same reaction sequence. We imagined forming compound **4** from the di-butyl aldehyde sidechain which could be procured via oxidative cleavage of di-diol **3** with appropriate protecting group chemistry. Di-diol **3** was envisioned to be formed via oxidation of di-alkene **24** in the presence of a strong oxidizing agent such as osmium or ozone.



Scheme 1.6: Synthesis of intermediate **31** in route to compounds **3** and **4**

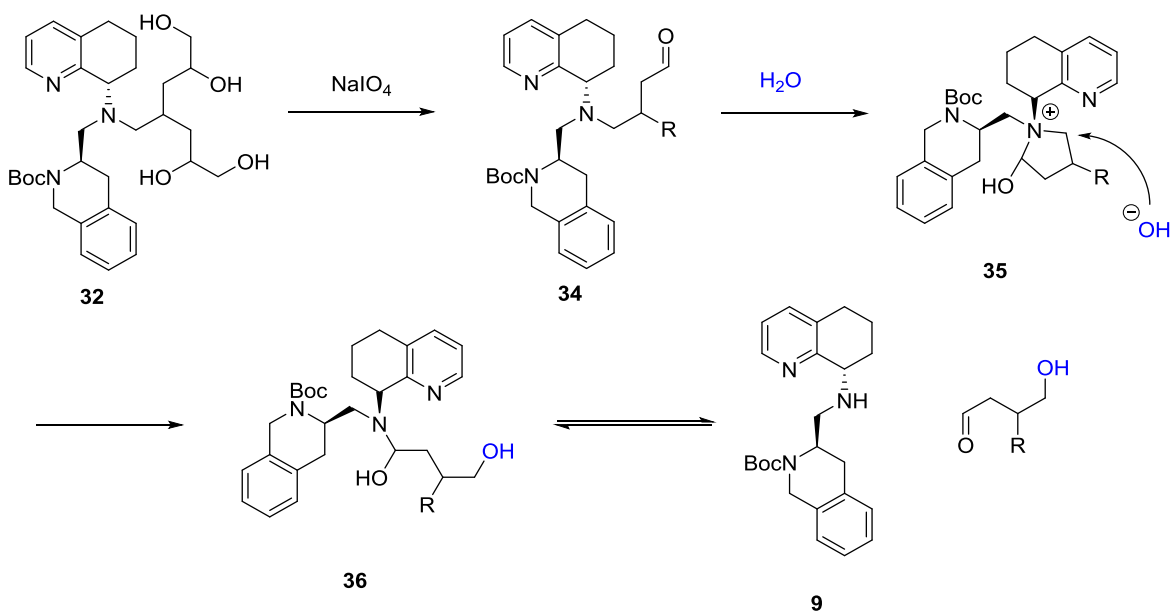
Methodology from the Alexanian lab provided an efficient synthesis of acid **26** from di-ethyl malonate **25** with no purification necessary.¹⁹ Starting from di-ethyl malonate **25** the enolate was formed by sodium hydride and two subsequent additions of allyl bromide resulted in the installation of the di-alkene moiety (Scheme 1.6). Subsequent saponification with concentrated hydrochloric acid and thermal decarboxylation neat provided acid **26** which was taken on following an acid base extraction. Reduction of carboxylic acid **26** with LiAlH and subsequent oxidation with Parikh-Doering conditions provided aldehyde **27** in nearly 50% yield over the 5 step sequence with one purification. Aldehyde **27** was coupled to half scaffold **9** via a reductive amination to form intermediate **31** in good yield.



Scheme 1.7: Synthesis of target **3** and attempted synthesis of target **4** from intermediate **31**

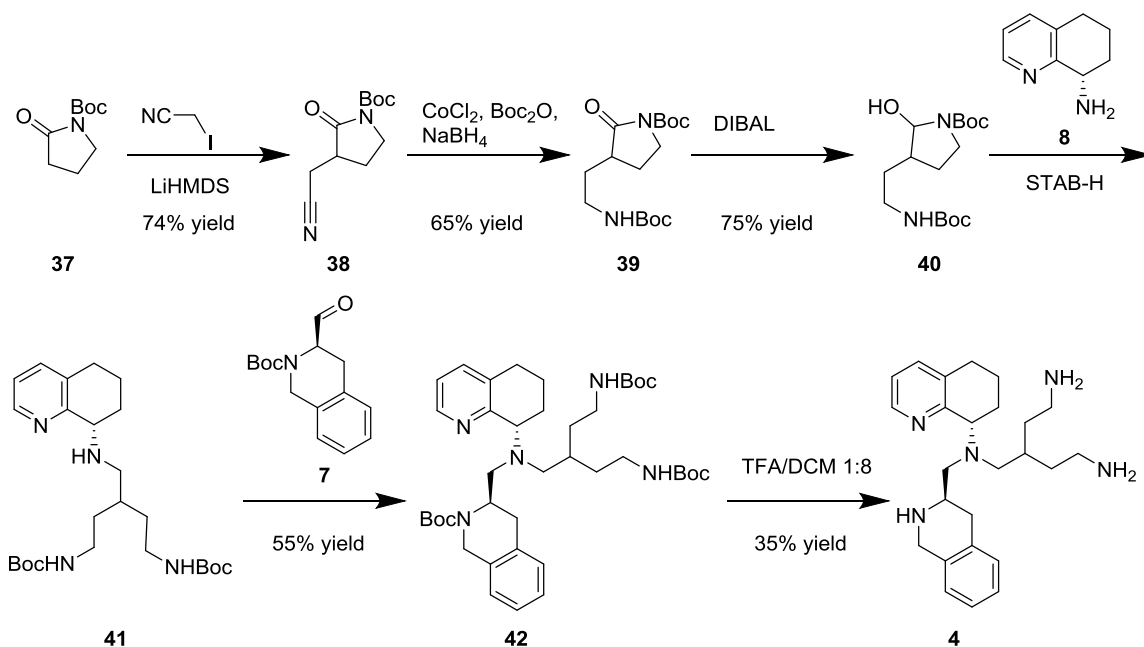
With intermediate **31** in hand we set out to find oxidation conditions that would not only yield our di-diol target **3**, but our di-butylamine target **4** as well (Scheme 1.7). Efforts towards compound **3** were fairly unremarkable. Subjecting intermediate **31** to osmium tetroxide resulted in the Boc-protected di-diol **32** in moderate yield. Subsequent Boc-deprotection with hydrochloric acid liberated target compound **3** in good yield. On the other hand subjecting intermediate **31** to osmium tetroxide and sodium periodate

(conditions known to cleave diols to aldehydes) simply resulted in isolation of the half scaffold **9**. Surprised by this result we attempted to replicate it with the comparable conditions of ruthenium chloride and sodium periodate and once again isolated the half scaffold **9**. To probe the mechanistic aspects of the reaction we started with di-diol **32** and upon addition of sodium periodate and catalyst recovered half scaffold **9**.



Scheme 1.8: Proposed mechanism for side chain cleavage of compound **32** to form **9**

We propose that intermediate **32** may be converted to half scaffold **9** via the following mechanism (Scheme 1.8). Initially sodium periodate successfully cleaves at least one of the two diols to form proposed intermediate **34** followed by subsequent intramolecular cyclization to form proposed intermediate **35**. Addition of hydroxide to release ring strain provides proposed intermediate **36** which is the rapidly exchanging hemiaminal of half scaffold **9**.



Scheme 1.9: Successful synthesis of target **4** from pyrrolidone **37**

In search for a different method to access the di-butylamine sidechain to construct target **8** we encountered a procedure to convert lactams to ethyl cyano lactams.¹⁶ We applied this method to the production of compound **38** from **37** with a good yield (Scheme 1.9). Cyanide **38** was reduced with cobalt hydride formed insitu from cobalt chloride and sodium borohydride in the presence of Boc-anhydride to form Boc protected **39** in poor yield. DIBAL reduction of pyrrolidone **39** to hemiaminal **40** followed by subsequent reductive amination with chiral amine **8** provided intermediate **41**. Chiral amine **41** was subsequently added to the TIQ aldehyde **7** with a typical reductive amination to form the boc protected **42**. The TFA mediated global deprotection of **42** successfully afforded target **4**, albeit in poor yield.

1.3 TIQ Modeling Targets -- Results

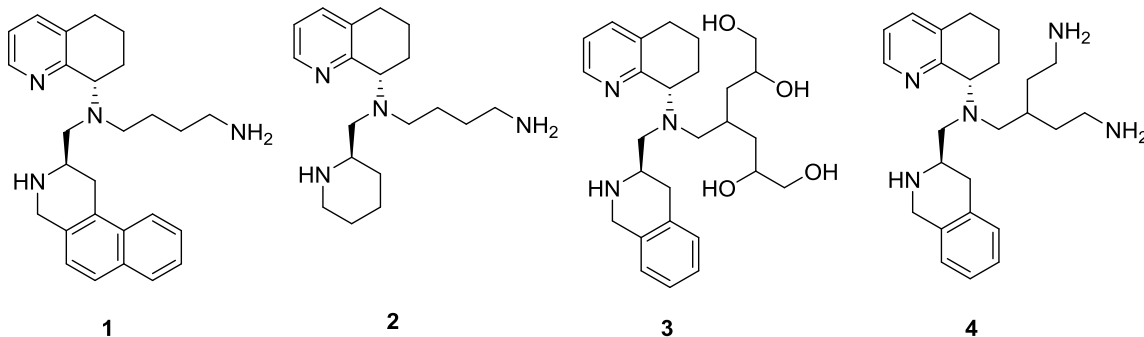
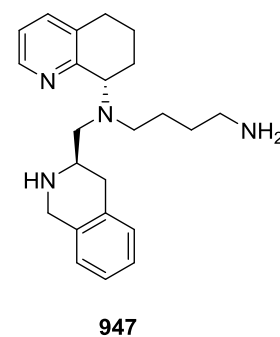


Table 1.3 Biological Testing of TIQ Modeling Targets

Compound	MAGI Assay IC ₅₀ μM	TC ₅₀ μM	Ca ²⁺ Flux	Selectivity Index
1	.01	6	.009	.9
2	1	>30	>10	>10
3	2	>10	ND	ND
4	.06	>100	.2	3.3
947	.005	>100	.003	.6

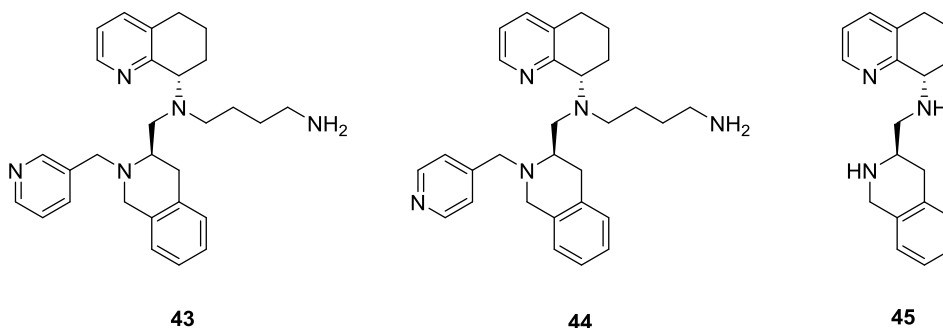


We tested our modeling targets against both the MAGI assay as a direct measure of anti-viral potency and the calcium flux assay as an indirect measure of signaling disruption (Table 1.3). 2-naphthyl compound **1** was very potent in both the MAGI and calcium flux assay, but was unfortunately one of the first toxic compounds found in the series with a TC₅₀ of only 6 μM. Ultimately, despite the high potency of **1** it did not validate our modeling hypothesis that a naphthyl ring could pick up an additional pi-stacking interaction, as the non naphthyl lead **947** was approximately equipotent. Piperidine **2** on the other hand followed our model quite closely, losing nearly over 200 fold potency when compared to parent compound **947** in the MAGI assay, and well over 1000 fold potency in the calcium

flux assay. The selectivity profile of compound **2** was the best in the group (>10), but was deemed to not be potent enough for follow up SAR towards that indication. We expected di-diol **3** to be more potent than **947** due to the addition of several hydrogen bond acceptors/donors. The data on the other hand suggested that more basic nature of an amine was quite important, as **3** had only single digit micromolar potency. We similarly and more confidently expected di-butylamine **4** to be more potent than **947**. In our models compound **4** made all the same interactions as **947** plus an extra salt bridge (see section 1.2). We were surprised to find **4** to be 12 fold less potent in the MAGI assay and 66 fold less potent in the calcium flux assay than **947**.

As a general conclusion compounds **1** and **2** which either added or deleted hydrophobic bulk from **947** modeled well, and had potencies within the expected range. On the other hand compounds **3** and **4** which added more hydrogen bond donors or acceptors than **947** modeled very poorly with potencies far off from their predicted values. Our initial hypothesis was that new interactions are hard to model via computational molecular modeling (**3** and **4**), but that attenuation of existing interactions (**1** and **2**) is predictable via molecular modeling. This hypothesis serves as the launching point for our molecular models. Though these compounds failed to produce a new lead, they did provide an important basis set for future modeling work.

1.4 TIQ Selectivity -- Chemistry



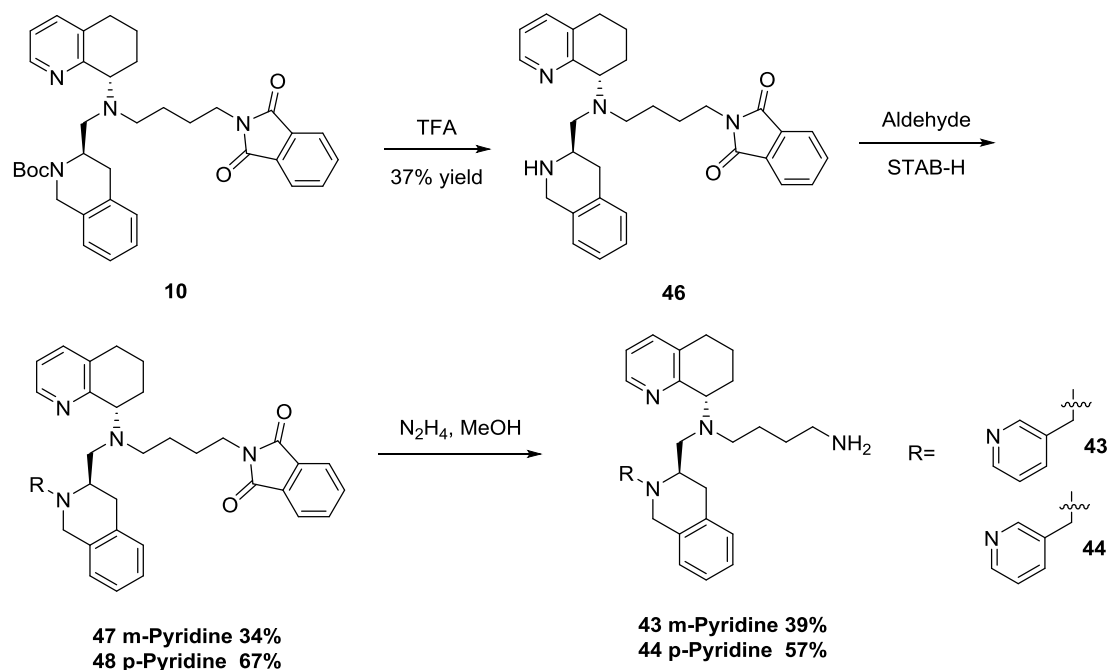
SAR Rationale:

43 and 44: Probe position of pyridine nitrogen to potentially create an HIV selective compound

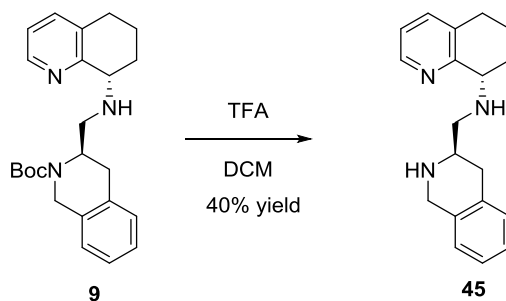
45: Delete butyl amine side chain to potentially create a mobilization selective compound

Figure 1.6: Compounds designed with medicinal chemistry rationale to probe the CXCR4 selectivity profile.

In tandem to the synthesis of our computational targets we pursued compounds based on a traditional SAR design principals in the absence of computational data (Figure 1.6). In particular we were interested in the effect of pyridine placement such as in target **43** and **44**, the corresponding ortho-analog was already synthesized and had provoking potency. Similarly, we were interested in probing the need for a butylamine sidechain, and suspected based on our models that deleting the side chain would decrease HIV potency while increasing mobilization related potency.

Scheme 1.10: Synthesis of target **43** and **44**

Starting from orthogonally protected intermediate **10** a boc deprotection with TFA yielded mono-protected **46** (Scheme 1.10). Subsequent reductive amination with nicotinaldehyde or isonicotinaldehyde yielded compounds **47** and **48** respectively. The phthalamide protecting group was cleaved using nucleophilic conditions with hydrazine to yield final compounds **43** and **44** from **47** and **48** respectively.

Scheme 1.11: Synthesis of compound **45**

Preparation of compound **45** was a simple Boc-deprotection from half scaffold **9** (Scheme 1.11) followed by a very difficult separation of the small (S,S) (approximately

7%) diastereomeric impurity. The poor yield of 40% is more a reflection of the difficult isolation than the reaction efficiency, as the Boc-deprotection proceeded cleanly and without incident. In fact it's worth noting that frequently poor yields on this project result from purification difficulties as opposed to reaction efficiencies.

1.5 Results: TIQ Selectivity

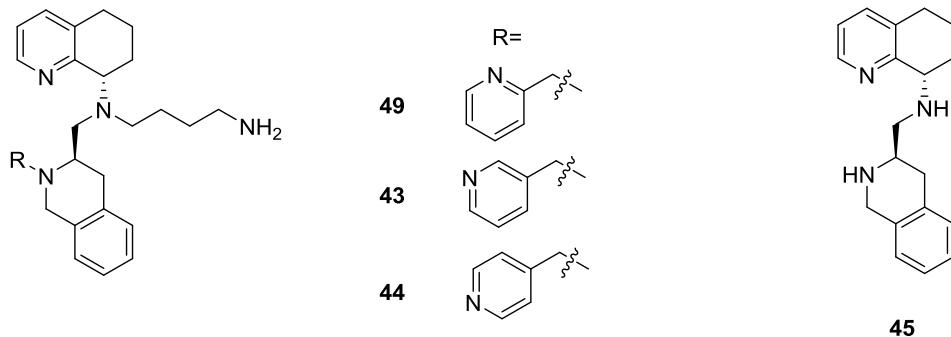
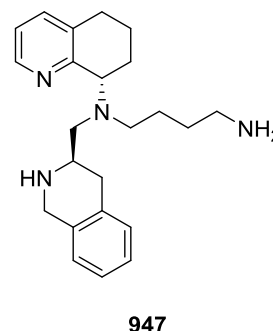


Table 1.4 Biological Testing of TIQ Selectivity Targets

Compound	MAGI Assay IC ₅₀ μM	TC ₅₀ μM	Ca ²⁺ Flux	Selectivity Index
49*	.06	>10	.06	1
43	.07	>10	.4	>5
44	.06	>10	.7	>10
45	.3	44	>10	>33
947	.005	>100	.003	.6



* Synthesized by Dr. Traux

The SAR targets were tested against both the MAGI assay as a direct measure of anti-viral potency and the calcium flux assay as an indirect measure of signaling disruption (Table 1.4). We were particularly interested in the selectivity index for these compounds, as we hoped to find compounds that were more potent against HIV and less against signaling (calcium flux). Theoretically compounds with such a profile would have fewer side-effects.

Ortho-pyridine **49** was previously synthesized by Dr. Traux and was 60 nM in both the MAGI and calcium flux assay, giving a selectivity index of 1. On the other hand, meta-pyridine **43** was approximately equally potent in the MAGI assay and 400 nM in the calcium flux assay giving a selectivity index of more than 5. This trend continued and was

particularly accented by para-pyridine **44** which had a selectivity index of greater than 10. This observation suggests that para-pyridine analogs are appropriately positioned to maintain HIV activity whilst decreasing signaling related activities. Numerous follow-up efforts are currently being conducted. Half-scaffold **45** lost 60 fold potency as compared to **947** in the MAGI assay as a result of having no butylamine side chain. Surprisingly, **45** lost over a thousand fold potency in the calcium flux assay despite our expectation that the butylamine side chain is responsible for HIV activity. Though the results were the exact opposite of what we expected, **45** provides a potentially strong entry into HIV selective compounds with a selectivity index of more than 33 fold.

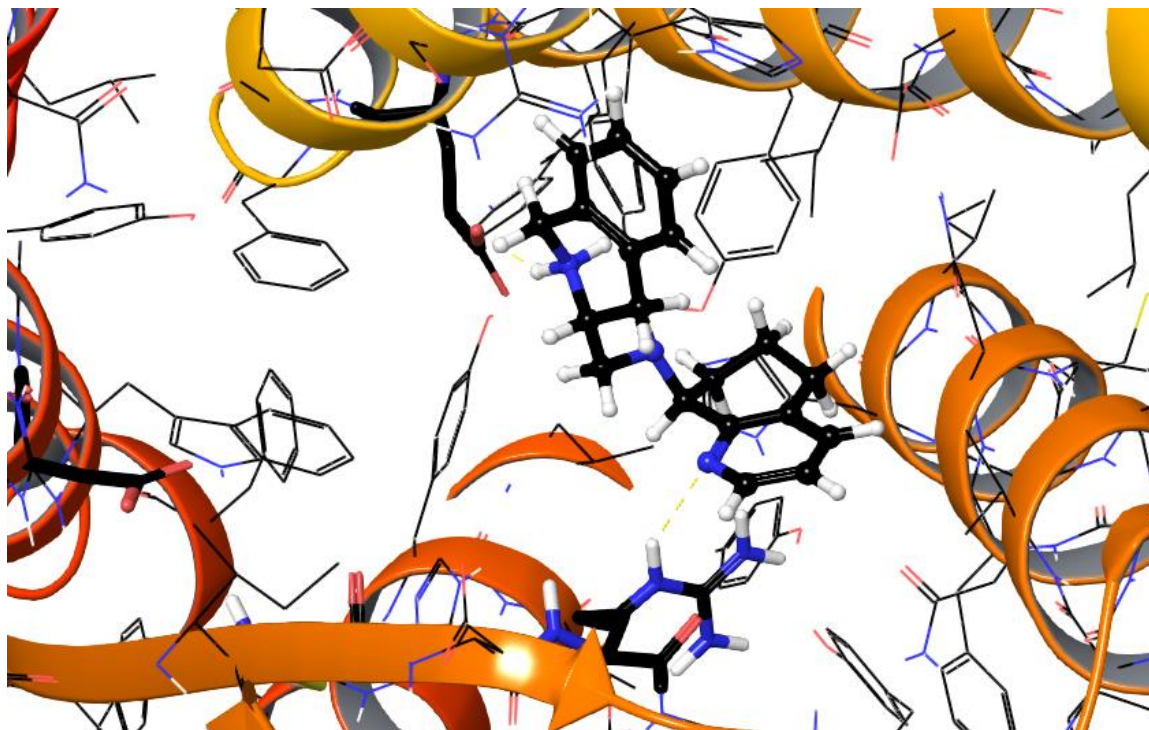


Figure 1.7: Initial modeling rationale for compound **45**

We initially expected **45** to be selective for SDF-1 related indications because the deleted butylamine side chain had been previously shown to be responsible for HIV related activity. This can be clearly seen in Figure 1.7 where compound **45** leans in the SDF-1 groove of the CXCR4 binding pocket. **45** is predicted to make a strong hydrogen bond with glutamic acid 288 and a weak interaction with arginine **188** in a similar fashion to the parent molecule **947**. It's worth noting that aspartic acid 92 often in conjunction with aspartic acid 177 is considered responsible for anti-HIV activity and is highlighted on the far left of the image.

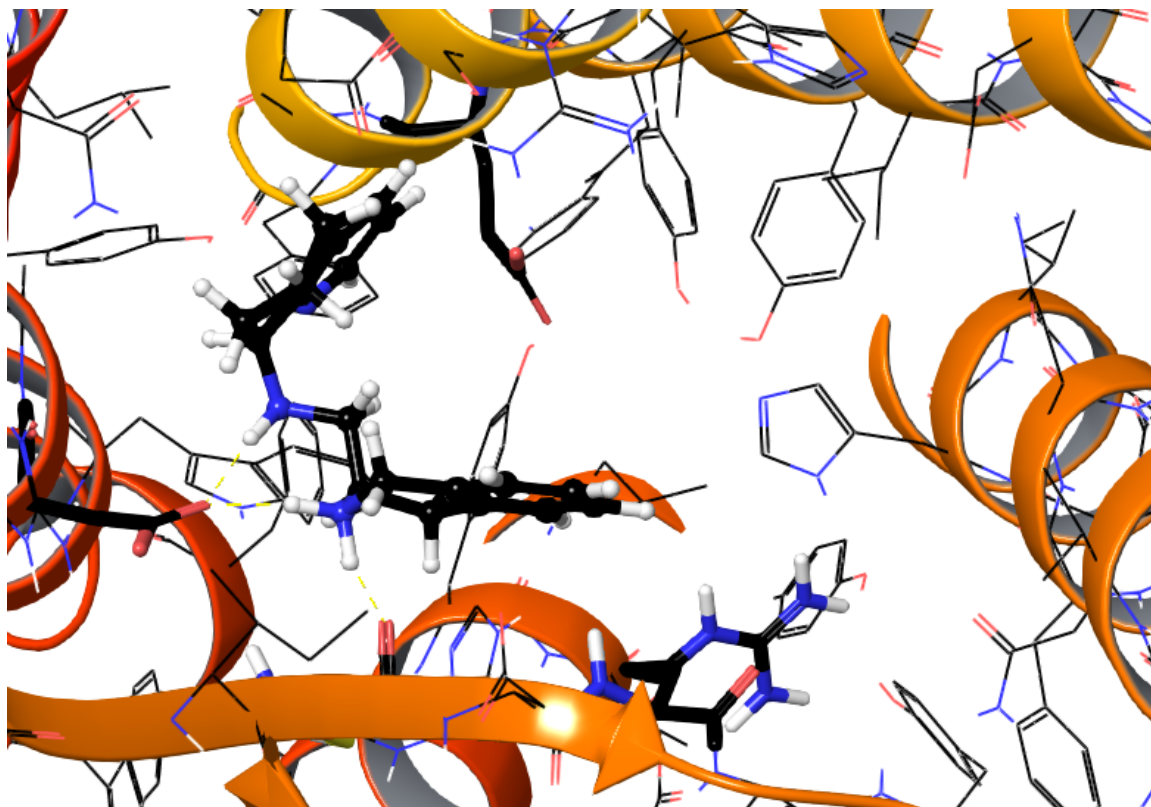
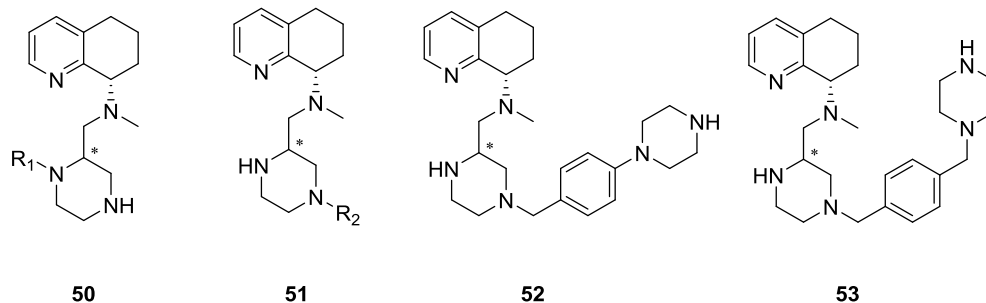


Figure 1.8: Improved modeling rationale for compound **45**'s selectivity

Our second generation models predict a far more likely binding motif for **45** considering its observed potency (Figure 1.8). In this binding motif the TIQ and central nitrogen form an electrostatic interaction with aspartic acid 97 on the HIV side of the receptor. It is worth noting that the glutamic acid and arginine residues previously interacted with are now more than 5 angstroms away. This binding pose shift potentially explains why the compound is selective for HIV related indications.

1.6 PIP SAR Targets -- Chemistry



SAR Targets:

*Synthesis and isolation of both (R,S) and (S,S) diastereomers.

50/51. Screening of various aryl groups to improve potency and probe correct nitrogen to substitute.

52/53. Replacement of butylamine side chain with iostere ate piperazine nitrogen. In a similar fashion to GSK's series.

Figure 1.9: Synthetic targets based on SAR principals on the PIP series.

Our initial computational targets centered on the **947** series because we had a reasonable modeling explanation for our observed potency difference between the diastereomers for that series, on the other hand at the time we had yet to create a model that could explain the seemingly equal potencies of both (R,S) and (S,S) **1143**. This led to targeting compounds using normal medicinal chemistry strategies. In particular we were interested in making compounds without a butyl-amine sidechain as we attributed the HERG liability as possibly stemming from that structural motif. In this pursuit we pursued compounds of four structural classes (Figure 1.9). Compounds with aryl substituents on the “top” piperazine nitrogen like **50**. Compounds with aryl substituents on the “bottom” piperazine nitrogen like **51**. Compounds with a butylamine side chain isostere like **52**. And lastly compounds with butylamine isostere with one extra methylene unite of flexibility like **53**.

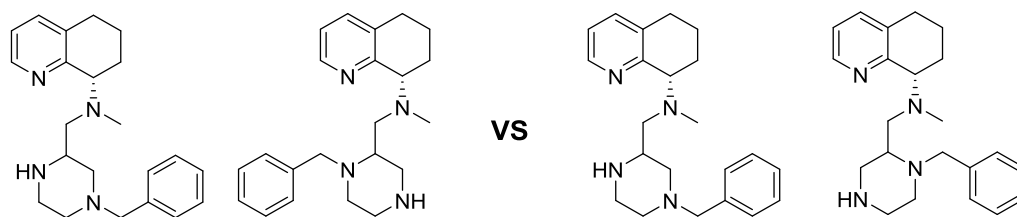


Figure 1.10 Structural similarity of substitution at either piperazine.

It was expected that compounds of type **50** and **51** would have similar potencies because of their structural similarity upon rotation of the chiral center (Figure 1.10). This hypothesis was further bolstered by the fact that the (R,S) and (S,S) diastereomers had similar potencies strongly suggesting that their placement of the benzyl group was not key. These compounds were further key initiators of modeling on the series which will be discussed in chapter 2 as it relates to the stitched series.

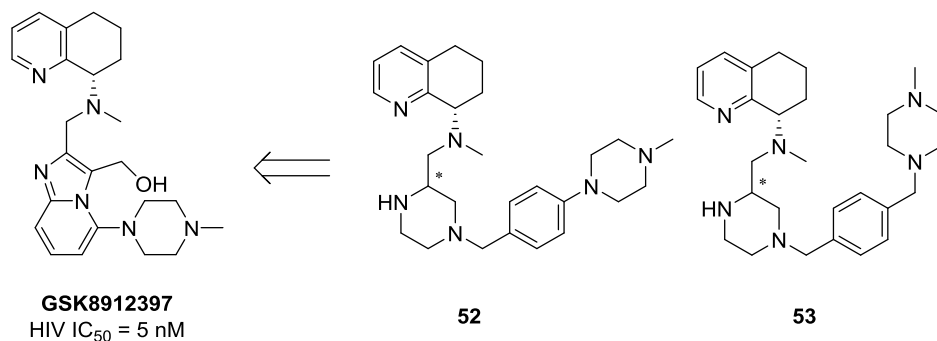
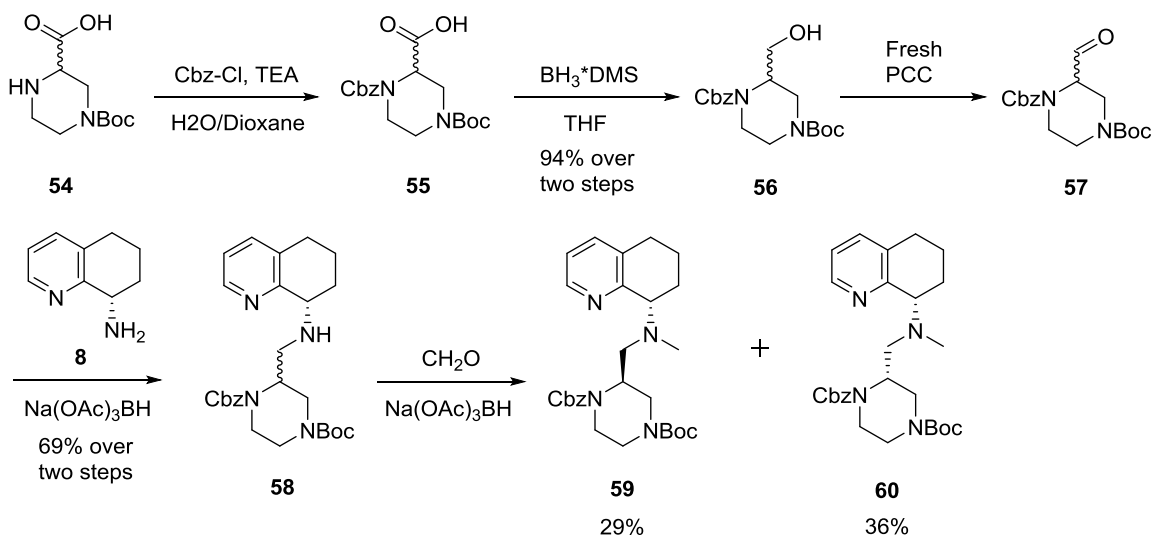


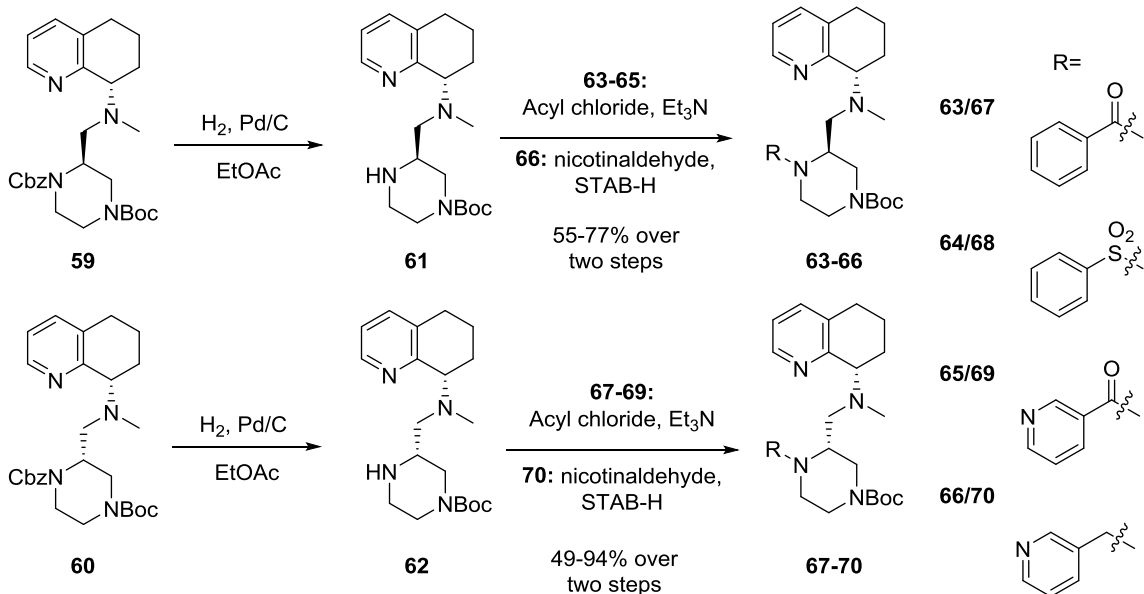
Figure 1.11: Structural comparison of GSK compound to butyl-amine isosteres **52** and **53**

Compounds **52** and **53** were designed to mimic prior-art by GSK (Figure 1.11). We suspected that our benzyl motif occupied a similar pocket as GSK's benzimidazole so appending piperazine was a logical route towards replicating GSK's ability to eliminate the butyl amine side chain. It was hypothesized that **52** and **53** would be less prone to HERG related activities whilst being similarly potent to their butyl amine counterparts.



Scheme 1.12: Synthesis and resolution of diastereomers **59** and **60**

Starting from commercially available carboxylic acid **54** bis-protected acid **55** was obtained by the Shotten-Baumann reaction with Cbz-Cl which was taken on crude. Borane reduction of acid **55** procured alcohol **56** in high yield. Oxidation of alcohol **56** with freshly synthesized PCC yielded aldehyde **57** in a pure fashion upon simple filtration. Reductive amination of aldehyde **57** with chiral amine **8** yielded half scaffold **58** in moderate yield as a mixture of two diastereomers. At this stage the diastereomers could not be adequately separated, but subsequent reductive methylation with formaldehyde formed a 50/50 mixture of scaffold **59** and **60** which were easily separated by column chromatography. This synthetic route proved amenable to scale and was conducted on a 20 gram batch.



Scheme 1.13: Synthesis of Boc-protected advanced intermediates **63-70**

Diastereomers **59** and **60** were moved through parallel synthetic routes towards products of type **50**. Fewer chemical steps would be necessary if the material was carried forward as a mixture of diastereomers and separated at the final step, but this strategy would suffer from two liabilities. First, it would run the risk that a particular substituent does not offer good enough separation to separate the diastereomers. Second, the risk of a polarity swap would delegitimize any chiral assignments. With this in mind, **59** and **60** were converted to **61** and **62** respectively via hydrogenation on a Parr hydrogenator with Degussa grade palladium on carbon. The free amines **61** and **62** were taken on crude to the next reaction. Acylations with the appropriate acyl chloride and Schotten-Bauman chemistry converted **61** and **62** to amides **63-65** and **67-69** respectively in moderate yield over two steps. Reductive aminations with nicotinaldehyde converted diastereomers **61** and **62** to amines **66** and **70**.

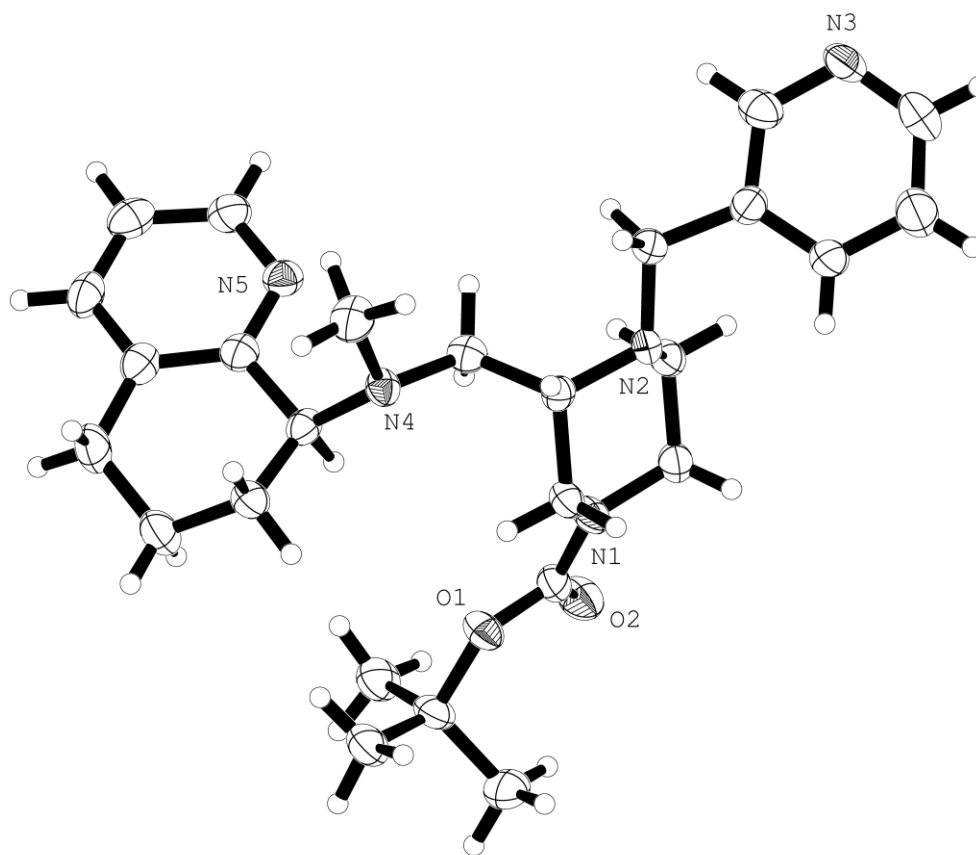
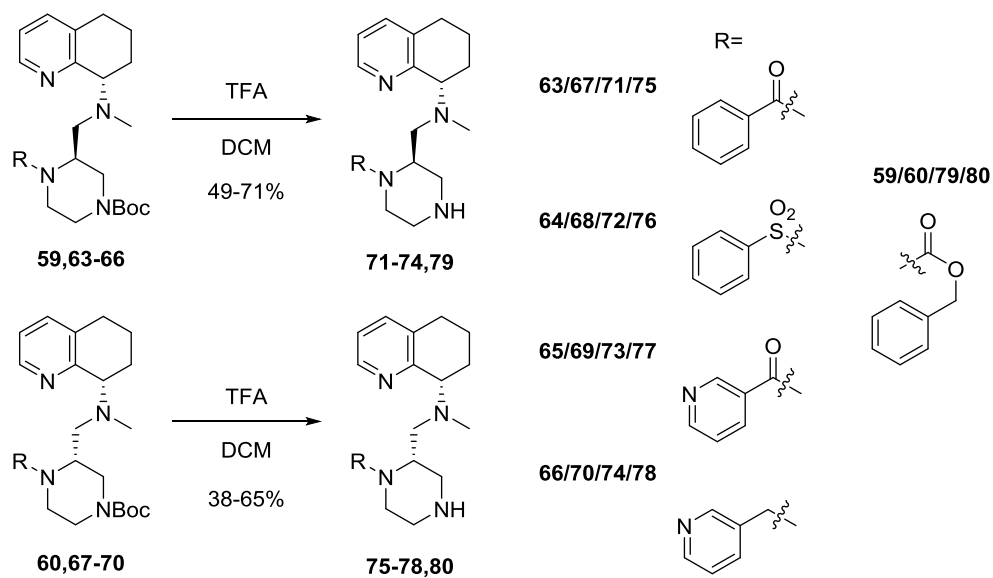


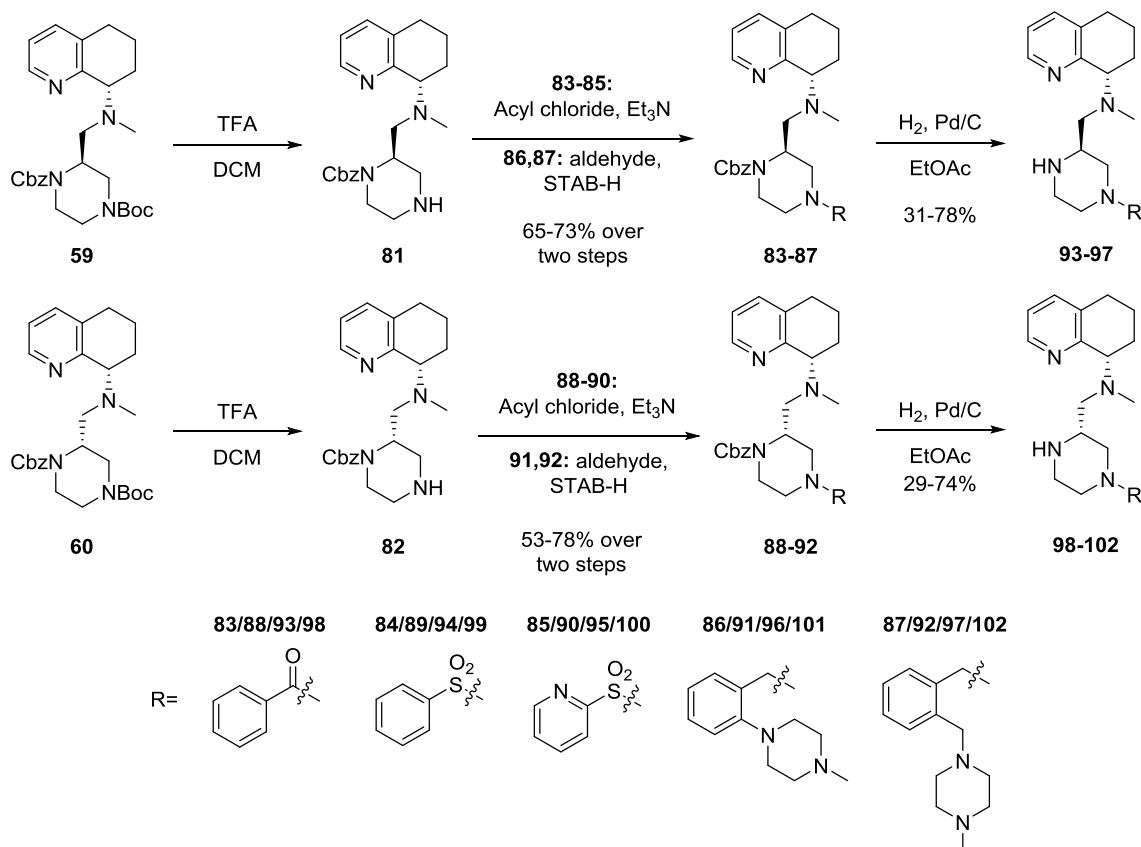
Figure 1.12: Crystal structure and chiral assignment of **66**

Amine **66** was a clear crystalline solid upon purification, subsequent recrystallization in hexanes/EtOAc yielded x-ray quality crystals (Figure 1.12). The crystal structure clearly shows (S,S) chirality which was used to assign chirality of the synthetically related materials in the series. It's worth noting that even though this material is (S,S) in the current protecting group state, that Boc-deprotection affords (R,S) material as per the chirality assignment rules. As a result chirality will be described as upper-RF (URF) for diastereomers like **66** and backwards for the lower-RF analogs as assigned by their retention times on normal phase silica. It is also worth noting that URF material on this scaffold has the same chiral assignment as the URF material on the TIQ scaffold, further bolstering our chemical assignments on a basis of polarity.



Scheme 1.14: Synthesis of final products **71-80**

Boc-deprotection of advanced intermediates **59-60**, **63-70** yielded final products **71-80** in poor to moderate yield. The compounds were all tested in parallel in the MAGI assay.



Scheme 1.15: Synthesis of final products **93-102**

From modular chiral intermediates **59** (S,S) and **60** (R,S) final products with substitution on the “bottom” piperazine nitrogen were synthesized via Scheme 1.15. Boc-deprotection of **59** and **60** yielded chiral amines **81** and **82** respectively. Acylation of **81** and **82** with the appropriate acyl chloride using Schotten-Bauman conditions yielded advanced intermediates **83-85** and **88-90** respectively. Alternatively, reductive aminations of **81** and **82** with the appropriate aldehyde yield advanced intermediates **86, 87** and **91, 92** respectively in poor to moderate yield. Cbz-protected intermediates **83** to **92** were converted to final products **93** to **102** via hydrogenation with palladium on carbon in a parr hydrogenator with highly variable yields reflecting difficulty in purification.

1.7 PIP SAR Targets – Results

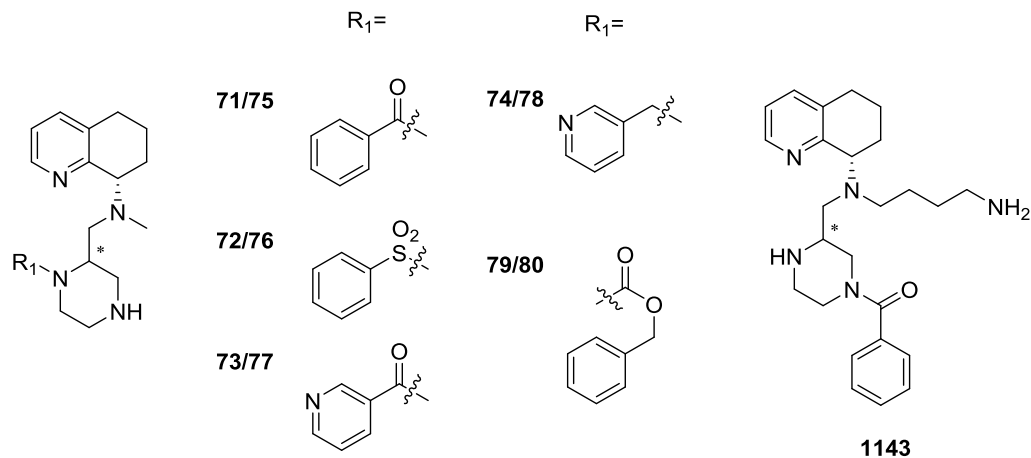
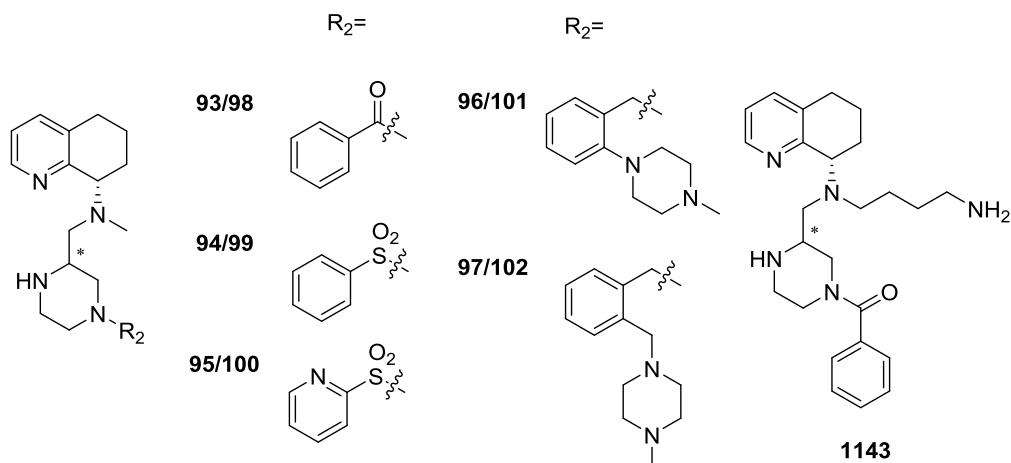


Table 1.5 Biological Testing of PIP R₁ SAR Targets

Compound	(R,S)			(S,S)		
	MAGI Assay IC ₅₀ μM	TC ₅₀ μM	Ca ²⁺ Flux	MAGI Assay IC ₅₀ μM	TC ₅₀ μM	Ca ²⁺ Flux
71/75	>100	>100	N.D.	>100	>100	N.D.
72/76	>100	>100	N.D.	>100	>100	N.D.
73/77	>100	>100	N.D.	>100	>100	N.D.
74/78	>100	>100	N.D.	>100	>100	N.D.
79/80	>100	>100	N.D.	>100	>100	N.D.
1143	.02	>100	.006	.06	>100	.002

The R₁ SAR targets were tested against both the MAGI assay as a direct measure of anti-viral potency (Table 1.5). Based on initial results in the series we suspected the compounds to have weak micromolar activity, so they were tested in parallel up to 100 μM in the MAGI assay. The advantages of testing in parallel include practical considerations such as bulk pricing, as well as scientific considerations such as increased accuracy in head to head comparisons of molecules. Unfortunately, the disadvantages include not having a good idea for potency of a series before testing.

Compounds **71** to **80** were all inactive in the MAGI assay even at 100 μ M, as such the compounds were not tested in the calcium flux assay to save resources. The apparent inactivity of this series was perplexing due to the large area of chemical space scanned and the similarity of R₁ and R₂ substitutions based on rotation through the chiral center (see Figure 1.8). Additionally compounds substituted at the R₂ position were generally less than 10 μ M in activity with sharp IC₉₀'s (see Table 1.5). Compound **71** and **75** followed lead **1143** via testing the benzamide substitution. The sulfonamides **72** and **76** were similarly inactive despite elongating the position of the aryl ring slightly. Pyridines **73** and **77** offered an accessible hydrogen bond acceptor in a similar fashion as the compounds in the TIQ series but failed to achieve measurable potency. Benzyl amines **74** and **78** allowed for protonation of the R₁ piperidine nitrogen but similarly to analogs **73** and **77** were impotent. Cbz substituted analogs **79** and **80** had several atoms of increased flexibility to potentially allow the aryl group to reach the correct hydrophobic pocket in the X₄ receptor.

Table 1.6 Biological Testing of PIP R₂ SAR Targets

(R,S)/(S,S) Compound	(R,S)			(S,S)		
	MAGI Assay IC ₅₀ μM	TC ₅₀ μM	Ca ²⁺ Flux	MAGI Assay IC ₅₀ μM	TC ₅₀ μM	Ca ²⁺ Flux
93/98	6	>30	>10	5	>100	.15
94/99	2	>30	.2	5	22	2.5
95/100	>30	>30	N.D.	>30	>30	N.D.
96/101	.7	21	2	1.5	11	.5
97/102	1.3	14	>10	5	14	>10
1143	.02	>100	.006	.06	>100	.002

The R₁ SAR targets were tested against both the MAGI assay as a direct measure of anti-viral potency and the calcium flux assay as an indirect measure of signaling disruption (Table 1.6). Based on initial results in the series we suspected the compounds to have weak micromolar activity, so they were tested in parallel up to 30 μM in the MAGI assay and 10 μM in the calcium flux assay.

Benzyl amides **93** and **98** were modestly potent with activities of approximately 5 μM in the MAGI assay. Their potency in the calcium flux assay was instructive as **93** was completely inactive and **98** was approximately 150 nM. Sulfonamides **94** and **99** were

single digit micromolar against HIV and had 10 fold differences in calcium flux activity favoring the opposite diastereomer as their benzamide analogs **93** and **98**. Remarkably, pyridine sulfonamides **95** and **100** were completely inactive in both assays. Currently no modeling rationale has been developed for why the addition of a pyridine nitrogen has such a stark impact on potency. The butylamine surrogates **96** and **101** were the most potent compounds of the series in the MAGI assay. Suspecting we were on the right track, we synthesized the elongated surrogates **97** and **102** and found them to be slightly less potent in the MAGI assay and completely inactive in the calcium flux assay. An increase in cytotoxicity was observed for all four butylamine surrogates. Ultimately, further modifications were not pursued do to the concern of enhanced cytotoxicity outweighing potential HERG liability benefits.

The (R,S) diastereomers were generally less potent in the MAGI assay than their (S,S) analogs. On the other hand, this series was typically more potent in the calcium flux assay. Ultimately the potency differences are still surprisingly small considering the chirality, but it appears that the difference is exacerbated by the lack of butylamine side chain (compare **93/98** to **1143 R/S**). This observation was important for the development of a more accurate model around the scaffold and was an important step in the development of the “stitched” series in chapter 2.

References:

1. Teicher, B. A. and S. P. Fricker (2010). "CXCL12 (SDF-1)/CXCR4 pathway in cancer." Clin Cancer Res **16**(11): 2927-2931.
2. Daar, E. S., et al. (2007). "Baseline HIV Type 1 Coreceptor Tropism Predicts Disease Progression." Clinical Infectious Diseases **45**(5): 643-649.
3. De Clercq, E. (2003). "The bicyclam AMD3100 story." Nat Rev Drug Discov **2**(7): 581-587
4. Hendrix, C. W., et al. (2000). "Pharmacokinetics and safety of AMD-3100, a novel antagonist of the CXCR-4 chemokine receptor, in human volunteers." Antimicrob Agents Chemother **44**(6): 1667-1673.
5. Han, T.-T., et al. (2014). "Role of chemokines and their receptors in chronic lymphocytic leukemia: function in microenvironment and targeted therapy." Cancer Biol. Ther. **15**(1): 3-9.
6. Song, Q.-b., et al. (2012). "Application of CXCR4 antagonist in the treatment for metastatic cancer." Zhongguo Zhongliu **21**(10): 771-774.
7. Suarez-Alvarez, B., et al. (2012). "Mobilization and homing of hematopoietic stem cells." Adv. Exp. Med. Biol. **741**(Stem Cell Transplantation): 152-170.
8. Moyle, G., et al. (2009). "Proof of activity with AMD11070, an orally bioavailable inhibitor of CXCR4-tropic HIV type 1." Clin Infect Dis **48**(6): 798-805.
9. Nyunt, M. M., et al. (2008). "Pharmacokinetic effect of AMD070, an Oral CXCR4 antagonist, on CYP3A4 and CYP2D6 substrates midazolam and dextromethorphan in healthy volunteers." J Acquir Immune Defic Syndr **47**(5): 559-565.

10. Jenkinson, S., et al. (2010). "Blockade of X4-tropic HIV-1 cellular entry by GSK812397, a potent noncompetitive CXCR4 receptor antagonist." Antimicrob Agents Chemother **54**(2): 817-824.
11. Murakami, T., et al. (2009). "The novel CXCR4 antagonist KRH-3955 is an orally bioavailable and extremely potent inhibitor of human immunodeficiency virus type 1 infection: comparative studies with AMD3100." Antimicrob Agents Chemother **53**(7): 2940-2948.
12. Truax, V. M., et al. (2013). "Discovery of Tetrahydroisoquinoline-Based CXCR4 Antagonists." ACS Med. Chem. Lett. **4**(11): 1025-1030.
13. Wong, R. S., et al. (2008). "Comparison of the potential multiple binding modes of bicyclam, monocylam, and noncyclam small-molecule CXC chemokine receptor 4 inhibitors." Mol Pharmacol **74**(6): 1485-1495.
14. Choi, W.-T., et al. (2005). "Unique Ligand Binding Sites on CXCR4 Probed by a Chemical Biology Approach: Implications for the Design of Selective Human Immunodeficiency Virus Type 1 Inhibitors." J Virol **79**(24): 15398-15404.
15. Zhao, H., et al. (2015). "Discovery of novel N-aryl piperazine CXCR4 antagonists." Bioorg. Med. Chem. Lett.: Ahead of Print.
16. Thompson, L. A., et al. (2008). Substituted Tetrahydroisoquinolines as Beta-secretase Inhibitors, Google (Kramer and Wainberg 2015) Patents.
17. Wong, R. S., et al. (2008). "Comparison of the potential multiple binding modes of bicyclam, monocylam, and noncyclam small-molecule CXC chemokine receptor 4 inhibitors." Mol Pharmacol **74**(6): 1485-1495.

18. Choi, W. T., et al. (2005). "Unique ligand binding sites on CXCR4 probed by a chemical biology approach: implications for the design of selective human immunodeficiency virus type 1 inhibitors." J Virol **79**(24): 15398-15404.
19. Schmidt, V. A. and E. J. Alexanian (2010). "Metal-Free, Aerobic Dioxygenation of Alkenes Using Hydroxamic Acids." Angewandte Chemie **122**(26): 4593-4596.
20. Murray, P. J., et al. (1998). "The enantiospecific synthesis of novel lysine analogues incorporating a pyrrolidine containing side chain." Tetrahedron Letters **39**(37): 6721-6724.

1.8 CXCR4 Experimentals

Frequently used procedures:

Hydrogenation A:

To a solution of the substrate in EtOH (.1M) and AcOH (.01 M) is added Pd/C (10-50% by mass). The reaction is hydrogenated under an atmosphere of H₂ between 45-55 psi on a parr hydrogenator overnight. Upon completion the H₂ is purged *in vacuo* and then flushed with argon. The crude reaction mixture is then filtered through two fluted pieces of filter paper and concentrated *in vacuo*. The mixture is then diluted with brine and DCM followed by basification with 10% NaOH. The layers are separated and the aqueous layer extracted with DCM (3 times). The organic layers are combined, dried over anhydrous sodium sulfate, filtered and concentrated to afford the crude product which if necessary is purified by column chromatography.

Hydrogenation B:

To a solution of the substrate in *t*-BuOH (.1M) and AcOH (.01 M) is added Pd/C (10-50% by mass). The reaction is hydrogenated under an atmosphere of H₂ between 45-55 psi on a parr hydrogenator overnight. Upon completion the H₂ is purged *in vacuo* and then flushed with argon. The crude reaction mixture is then filtered through two fluted pieces of filter paper and concentrated *in vacuo*. The mixture is then diluted with brine and DCM followed by basification with 10% NaOH. The layers are separated and the aqueous layer extracted with DCM (3 times). The organic layers are combined, dried over anhydrous sodium sulfate, filtered and concentrated to afford the crude product which if necessary is purified by column chromatography.

Hydrogenation C:

To a solution of the substrate in *t*-BuOH (.1M) and AcOH (.01 M) is added Pd/C (10-50% by mass). The reaction is then heated to 80C and ammonium formate is added portion wise (3 eq). The reaction is tracked by LCMS and usually done within 30 minutes. The reaction is then concentrated *in vacuo*. The mixture is then diluted with brine and DCM followed by basification with 10% NaOH. The layers are separated and the aqueous layer extracted with DCM (3 times). The organic layers are combined, dried over anhydrous sodium sulfate, filtered and concentrated to afford the crude product which is used without further purification.

Cbz-Deprotection:

A solution of the Cbz protected amine (1eq) and thioanisole (1eq) in DCM:methane sulfonic acid (.5 M, 1:1) was stirred under inert atmosphere. The reaction was checked by LCMS and was complete within 4 hours. The mixture was then diluted with H₂O and DCM. The layers are separated and the aqueous layer extracted with DCM (3 times). The aqueous layer was diluted with 10% NaOH until very basic. The aqueous layer was then extracted with DCM (3 times). The organic layers were combined, dried over anhydrous sodium sulfate, filtered and concentrated to afford the crude product which is purified by column chromatography.

Boc-Deprotection:

A solution of the Boc protected amine in DCM:TFA (.5 M, 4:1) was stirred under inert atmosphere. The reaction is tracked by LCMS and is usually complete within two hours. Upon completion the mixture is diluted with brine and basified with 10% NaOH. The layers are separated and the aqueous layer extracted with DCM (3 times). The organic layers were combined, dried over anhydrous sodium sulfate, filtered and concentrated to afford the crude product which is purified by column chromatography.

Reductive Amination:

To a solution of the amine in DCM (.1M) is added the aldehyde (1.1 eq) and stirred at room temperature for 30 minutes. Then sodium triacetoxyborohydride (1.5 eq) is added as one portion and the reaction is tracked by LCMS. The reaction is usually complete within 5 hours. Upon completion the mixture is diluted with brine and basified with 10% NaOH. The layers are separated and the aqueous layer extracted with DCM (3 times). The organic layers were combined, dried over anhydrous sodium sulfate, filtered and concentrated to afford the crude product which is purified by column chromatography.

Acylation A:

To a solution of the amine in DCM (.1M) is added triethylamine (2 eq). Then the acyl chloride (1.5 eq) is added dropwise with stirring. The reaction is tracked by LCMS and is usually complete within two hours. Upon completion the mixture is diluted with brine and basified with 10% NaOH. The layers are separated and the aqueous layer extracted with DCM (3 times). The organic layers were combined, dried over anhydrous sodium sulfate, filtered and concentrated to afford the crude product which is purified by column chromatography.

Acylation B:

To a solution of the amine dissolved in DCM (.2M) in a microwave vial is added triethylamine (1.5 eq). Then the acyl chloride (1.2 eq) is added dropwise. The vial is then subjected to 125°C for 20 minutes in a microwave reactor. Upon completion the mixture is diluted with brine and acidified with 10% HCl. The layers are separated and the aqueous layer extracted with DCM (3 times). The organic layers were combined, dried over anhydrous magnesium sulfate, filtered and concentrated to afford the crude product which is purified by column chromatography.

Acylation C:

To a solution of amine in DCM (.1M) is added the acyl chloride (1.5 eq) dropwise with stirring. The reaction is tracked by LCMS and is usually complete within two hours. Upon completion the mixture is diluted with brine and basified with 10% NaOH. The layers are separated and the aqueous layer extracted with DCM (3 times). The organic layers were combined, dried over anhydrous sodium sulfate, filtered and concentrated to afford the crude product which is purified by column chromatography.

Acylation D:

To a solution of the amine dissolved in DCM (.2M) in a microwave vial is added the acyl chloride (1.2 eq) dropwise. The vial is then subjected to 125°C for 20 minutes in a microwave reactor. After cooling back to room temperature triethylamine (1 eq) is added and the mixture is concentrated to afford the crude product which is purified by column chromatography.

Thioamide Formation:

To a solution of amide dissolved in toluene (.1M) in a microwave vial is added Lawesson's Reagent (1.5 eq). The reaction is then microwaved at 150°C for 20 minutes in a microwave reactor. After cooling back to room temperature the reaction is concentrated *in vacuo* to afford the crude product which is purified by column chromatography.

Suzuki Coupling:

To a solution of aryl bromide dissolved in toluene (.1M) in a microwave vial is added Potassium Carbonate (3 eq), Palladium Tetrakis (.1 eq), and the corresponding boronic acid (2 eq). The reaction is then microwaved at 150°C for 5 minutes in a microwave reactor. After cooling back to room temperature the reaction is concentrated *in vacuo* to afford the crude product which is purified by column chromatography.

Bromination of Alcohols:

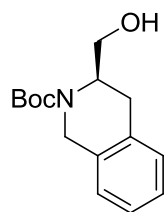
To a stirred solution of alcohol dissolved in DCM (1M) at 0°C in a round bottom flask is added CBr₄ (1.2 eq) and then triphenyl phosphine (1.2 eq) portionwise over 10 minutes. The reaction is tracked by LCMS and typically done within 1 hour. The reaction is then concentrated *in vacuo* and diethyl ether added. The resulting solids are removed by filtration and the filtrate concentrated *in vacuo* to afford the crude product which is purified by column chromatography.

Formation of Grignard Reagents:

To a flame dried flask containing finely crushed Magnesium (1.5 eq) suspended in dry THF (1 M) under argon is added the corresponding bromide. The reaction is then stirred vigorously with careful attention to temperature. The reaction is allowed to exothermically heat to the point of slight bubbling and then maintained at this sub-refluxing temperature with use of ice and water baths. If the reaction does not proceed, addition of catalytic Iodine (1 crystal) should be employed. If the reaction still does not proceed the addition of a small amount of isopropyl magnesium chloride (.01 eq) can be employed. Once the reaction stops evolving heat it's allowed to stir for one more hour at room temperature to ensure full conversion. The product is used as a solution in THF.

Weinreb Grignard one-pot Reaction:

To a stirred solution of the corresponding ester as a solution in THF (.1 M) was added to a flame dried 100 mL round bottom flask containing N,O-dimethylhydroxylamine hydrochloride (1.2 eq) and stirred at 0°C. The corresponding grignard (4.5 eq) was then added dropwise and the reaction was allowed to stir until complete conversion to ketone was observed by LCMS. The reaction mixture was quenched with a solution of saturated NH₄Cl slowly and allowed to stir for 10 minutes, then basified with 10% NaOH dropwise. The mixture was further partitioned with EtOAc and separated. The aqueous layer was extracted with EtOAc once more and then DCM twice. The organic layers were combined, dried over anhydrous sodium sulfate, filtered, and concentrated to afford the product which was generally greater than 95% pure upon extraction.

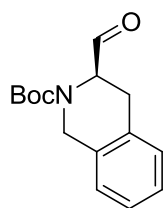
Compound 6

(R)-tert-butyl 3-(hydroperoxymethyl)-3,4-dihydroisoquinoline-2(1H)-carboxylate (5.00 g, 17.9 mmol) was dissolved in Tetrahydrofuran (45 mL, .4 M) in a 250 mL round bottom flask and stirred at 0°C. Borane Dimethyl Sulfide (18 mL, 36 mmol, 2 eq) was then added and the reaction was allowed to stir for 1.5 hours at 0°C. After 1.5 hours the reaction was allowed to warm to room temperature and continue stirring overnight. After approximately 18 hrs of stirring the reaction was cooled to 0°C and water was slowly added drop wise. The mixture was partitioned between brine and DCM. The aqueous layer was extracted with DCM (3 times). The organic layers were combined, dried over anhydrous magnesium sulfate, filtered and concentrated to afford (R)-tert-butyl 3-(hydroxymethyl)-3,4-dihydroisoquinoline-2(1H)-carboxylate (4.5 g, 96% yield).

¹H NMR (400 MHz, Chloroform-*d*) δ 7.20 – 7.15 (m, 1H), 7.15 – 7.08 (m, 1H), 4.80 – 4.58 (m, 1H), 4.57 – 4.40 (m, 1H), 4.29 (d, *J* = 16.6 Hz, 1H), 3.58 – 3.38 (m, 2H), 3.02 (dd, *J* = 16.0, 6.0 Hz, 1H), 2.77 (d, *J* = 16.4 Hz, 1H), 1.49 (s, 9H).

HRMS calc'd for C₁₅H₂₀O₃N₁ 262.14377; found 262.14377 [M+H]

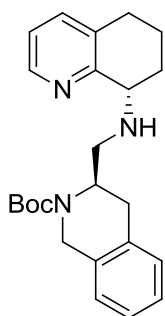
Matched known material Truax, V. M., et al. (2013). "Discovery of Tetrahydroisoquinoline-Based CXCR4 Antagonists." ACS Med. Chem. Lett. 4(11): 1025-1030.

Compound 7

(R)-tert-butyl 3-(hydroxymethyl)-3,4-dihydroisoquinoline-2(1H)-carboxylate (1.059g, 4.02 mmol) was dissolved in DMSO (20.11 ml .05 M) and DCM (20 mL .05 M). The mixture was stirred at 0°C for 20 minutes to guarantee proper equilibration. After being cooled triethylamine (2.035 g, 20.11 mmol, 5 eq) was added as well as SO₃Py (2.79 g, 20.11 mmol, 5 eq). The reaction was complete after stirring for an additional 30 minutes at 0°C. The reaction was quenched slowly with 40 mL of NH₄Cl and then the resulting suspension was broken with 10 mL of brine. After the organic and aqueous layers were separated the aqueous layer was extracted with 30 mL of DCM (2 times). The organic layers were combined, dried over anhydrous magnesium sulfate, filtered and concentrated to afford (R)-tert-butyl 3-formyl-3,4-dihydroisoquinoline-2(1H)-carboxylate (700 mg, 66% yield).

¹H NMR (400 MHz, Chloroform-*d*) δ 9.45 (d, *J* = 16.2 Hz, 1H), 7.19 – 7.09 (m, 4H), 4.84 – 4.59 (m, 1H), 4.59 – 4.38 (m, 2H), 3.10 – 2.97 (m, 2H), 1.48 (s, 4H), 1.42 (s, 5H).

Matched known material Truax, V. M., et al. (2013). "Discovery of Tetrahydroisoquinoline-Based CXCR4 Antagonists." ACS Med. Chem. Lett. 4(11): 1025-1030.

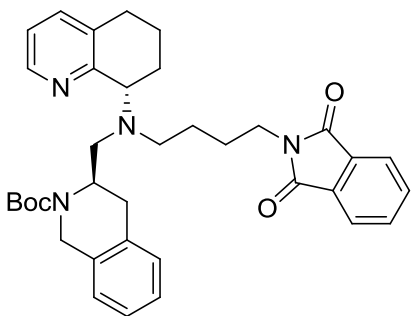
Compound 9

(R)-tert-butyl 3-formyl-3,4-dihydroisoquinoline-2(1H)-carboxylate (2.272 g, 8.70 mmol) was dissolved in DCM (87 mL, .1 M). (S)-5,6,7,8-tetrahydroquinolin-8-amine (1.482 g, 10 mmol, 1.15 eq) was added and allowed to stir for 2 hrs at room temperature, at which point sodium triacetoxyborohydride (3.69 g, 17.4 mmol, 2 eq) was added as one portion.

The reaction was allowed to stir overnight. The reaction was quenched with 10 mL NaHCO_3 carefully followed by dilution with 5 mL brine and 5 mL 1N NaOH. The aqueous layer was then extracted with 50 mL of DCM (3 times). The organic layers were combined, dried over anhydrous sodium sulfate, filtered, and concentrated to afford the crude product. The crude material was purified on a 40 gram combiflash column with a gradient from 1-5% MeOH in 1% TEA/DCM solution to afford (R)- tert-butyl 3-(((S)-5,6,7,8-tetrahydroquinolin-8-ylamino)methyl)-3,4-dihydroisoquinoline-2(1H)-carboxylate (3.31 g, 97% yield).

^1H NMR (400 MHz, Chloroform-*d*) δ 8.34 (d, $J = 4.7$ Hz, 1H), 7.33 (d, $J = 7.7$ Hz, 1H), 7.24 – 7.06 (m, 4H), 7.06 – 6.97 (m, 1H), 4.88 – 4.68 (m, 1H), 4.68 – 4.40 (m, 2H), 4.27 (d, $J = 16.9$ Hz, 1H), 3.76 – 3.58 (m, 1H), 3.05 – 2.89 (m, 2H), 2.81 – 2.63 (m, 3H), 2.63 – 2.47 (m, 1H), 1.92 (dt, $J = 10.7, 4.4$ Hz, 2H), 1.61 (dq, $J = 17.6, 9.7, 9.1$ Hz, 2H), 1.49 (s, 9H).

Matched known material Truax, V. M., et al. (2013). "Discovery of Tetrahydroisoquinoline-Based CXCR4 Antagonists." ACS Med. Chem. Lett. 4(11): 1025-1030.

Compound 10

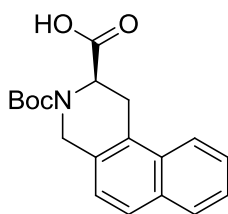
(R)-tert-butyl 3-(((S)-5,6,7,8-tetrahydroquinolin-8-ylamino)methyl)-3,4-dihydroisoquinoline-2(1H)-carboxylate (3.31 g, 8.41 mmol) was dissolved in DCM (84 mL, .1 M) and then 4-(1,3-dioxoisindolin-2-yl)butanal (2.193 g, 10.1 mmol, 1.2 eq) was added. This

mixture was stirred for 1.5 hr under inert atmosphere and then sodium triacetoxyborohydride (1.783 g, 8.41 mmol, 1 eq) was added. The reaction was then allowed to stir under inert atmosphere overnight. The reaction was quenched with aqueous 10 mL NaHCO₃ and then basified with NaOH and the organic phase was extracted (2x100 mL DCM), dried over sodium sulfate and evaporated under reduced pressure. This mixture was then subject to column chromatography with 1% MeOH in 1% TEA/DCM solution. The column was 8 inches long and allowed to drip at the rate of gravity. The column was repeated twice bringing 1.49 grams of pure major (R) diastereomer. 2.5 grams of material with an impurity of the (S) diastereomer was saved for later chromatography. (R)-tert-butyl 3-(((4-(1,3-dioxoisindolin-2-yl)butyl)((S)-5,6,7,8-tetrahydroquinolin-8-yl)amino)methyl)-3,4-dihydroisoquinoline-2(1H)-carboxylate (3.99 g, 80% combined yield).

¹H NMR (400 MHz, Chloroform-*d*) δ 8.30 (d, *J* = 8.0 Hz, 1H), 7.85 – 7.74 (m, 2H), 7.68 (td, *J* = 5.8, 2.5 Hz, 2H), 7.18 (d, *J* = 7.5 Hz, 1H), 7.11 – 7.00 (m, 3H), 7.00 – 6.93 (m, 1H), 6.93 – 6.87 (m, 1H), 4.62 (d, *J* = 17.0 Hz, 1H), 4.41 – 4.27 (m, 1H), 4.12 (d, *J* = 17.0 Hz, 1H), 3.93 – 3.76 (m, 1H), 3.58 (t, *J* = 7.3 Hz, 2H), 3.13 – 2.83 (m, 2H), 2.81 – 2.62 (m,

1H), 2.62 – 2.46 (m, 4H), 2.47 – 2.28 (m, 1H), 2.06 – 1.84 (m, 2H), 1.77 – 1.52 (m, 4H), 1.46 (s, 9H), 1.32 (p, $J = 7.7, 7.2$ Hz, 2H).

Matched known material Truax, V. M., et al. (2013). "Discovery of Tetrahydroisoquinoline-Based CXCR4 Antagonists." ACS Med. Chem. Lett. 4(11): 1025-1030.

Compound 13

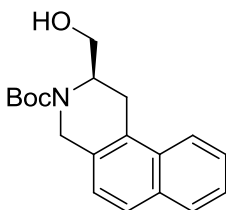
A slurry containing (R)-2-amino-3-(2-chlorophenyl)propanoic acid (2 g, 10.02 mmol) in 48% HBr (8 ml, 70.3 mmol, 7 eq) and water (10 mL) was heated to 40 °C and 37% formaldehyde (1.5 ml, 20.45 mmol, 2 eq) was added to the slurry at 3 mL/min. The reaction was then heated to 80 °C. Heating was continued at 80 °C for 20 hours, and then cooled for 46 hour after a precipitate was formed. The mixture was diluted with toluene and subsequently concentrated in vacuo until approximately half of the water was removed. The material was then filtered and dried in vacuo to afford (2R)-3-bromo-2-carboxy-1,2,3,4-tetrahydrobenzo[f]isoquinolin-3-ium as a crude solid.

To a suspension of (2R)-3-bromo-2-carboxy-1,2,3,4-tetrahydrobenzo[f]isoquinolin-3-ium (1.7 g, 5.6 mmol) in dioxane (11 mL) was added 1N aqueous sodium hydroxide (22 mL, 22 mmol, 4 eq) and BOC-Anhydride (2 ml, 8.4 mmol, 1.5 eq). The resulting reaction mixture was stirred at room temperature overnight and checked by LCMS. The mixture was then concentrated to remove solvent and dissolved in 50 mL EtOAc. To the solution was added 30% aqueous HCl to neutralize the reaction mixture to pH 2.0. The two layers were partitioned and then the water layer was extracted repeatedly with DCM until only a marginal amount of product could be pulled out (4 extractions with approximately 30 mL of DCM). The organic layers were combined, dried over anhydrous magnesium sulfate, filtered and concentrated to afford (R)-3-(tert-butoxycarbonyl)-1,2,3,4-tetrahydrobenzo[f]isoquinoline-2-carboxylic acid (1.65 g, 90% yield over two steps).

¹H NMR (400 MHz, Chloroform-*d*) δ 7.90 (t, *J* = 7.9 Hz, 1H), 7.80 – 7.74 (m, 1H), 7.63 (dd, *J* = 8.5, 5.2 Hz, 1H), 7.51 (td, *J* = 7.6, 5.3 Hz, 1H), 7.44 (td, *J* = 7.5, 2.7 Hz, 1H), 7.12 (dd, *J* = 8.5, 5.9 Hz, 1H), 5.40 – 5.34 (m, .6H), 5.09 (dd, *J* = 6.7, 2.8 Hz, .4H), 4.87 – 4.73

(m, 1H), 4.57 (dd, $J = 25.4, 17.2$ Hz, 1H), 3.90 – 3.70 (m, 1H), 3.27 (ddd, $J = 24.0, 16.3, 6.8$ Hz, 1H), 1.51 (s, 5H), 1.43 (s, 4H).

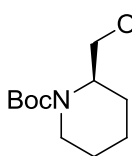
^{13}C NMR (101 MHz, cdCl_3) δ 177.26, 155.96, 132.51, 131.82, 130.36, 129.69, 128.71, 127.31, 126.73, 125.77, 124.92, 124.65, 122.90, 81.25, 53.29, 51.75, 44.90, 31.83, 28.63, 26.69.

Compound 16

(R)-3-(tert-butoxycarbonyl)-1,2,3,4-tetrahydrobenzo[f]isoquinoline-2-carboxylic acid (1.1 g, 3.36 mmol) was dissolved in Tetrahydrofuran (11 mL, .3 M) in a 250 mL round bottom flask and stirred at 0°C. Borane Dimethyl Sulfide (.85 mL, 8.5 mmol, 2.5 eq) was then added and the reaction was allowed to stir for 1.5 hrs at 0°C. At which point the ice was allowed to melt and the reaction continued stirring overnight. After approximately 18 hrs of stirring the reaction was cooled to 0°C and water was slowly added drop wise. The mixture was partitioned between brine and DCM. The aqueous layer was extracted with DCM (3 times). The organic layers were combined, dried over anhydrous magnesium sulfate, filtered and concentrated to afford (R)-tert-butyl 2-(hydroxymethyl)-1,2-dihydrobenzo[f]isoquinoline-3(4H)-carboxylate (926 mg, 88% yield).

¹H NMR (400 MHz, Chloroform-*d*) δ 7.92 (d, *J* = 8.3 Hz, 1H), 7.79 (d, *J* = 7.7 Hz, 1H), 7.66 (d, *J* = 8.4 Hz, 1H), 7.50 (dt, *J* = 6.8, 4.2 Hz, 1H), 7.45 (t, *J* = 7.5 Hz, 1H), 7.16 (d, *J* = 8.5 Hz, 1H), 5.03 – 4.69 (m, 2H), 4.44 (d, *J* = 17.9 Hz, 1H), 3.76 – 3.67 (m, 1H), 3.66 – 3.36 (m, 2H), 3.29 (d, *J* = 16.7 Hz, 1H), 3.14 (dd, *J* = 16.7, 6.4 Hz, 1H), 1.51 (s, 9H).

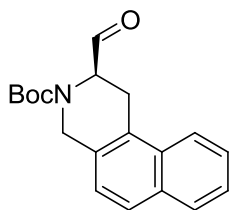
¹³C NMR (101 MHz, cdcl₃) δ 156.34, 132.63, 132.32, 129.84, 128.81, 127.56, 126.80, 126.58, 125.67, 124.73, 122.95, 80.63, 68.19, 62.72, 50.69, 43.86, 28.73, 25.62.

Compound 17

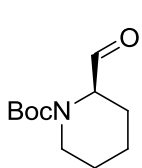
(R)-1-(tert-butoxycarbonyl)piperidine-2-carboxylic acid (3.0 g, 13 mmol) was dissolved in Tetrahydrofuran (32 mL, .4 M) in a 250 mL round bottom flask and stirred at 0°C. Borane Dimethyl Sulfide (3.2 ml, 32 mmol, 2.5 eq) was then added and the reaction was allowed to stir for 1.5 hr at 0°C. At which point the ice was allowed to melt and the reaction continued stirring overnight. After approximately 18 hrs of stirring the reaction was cooled to 0°C and water was slowly added drop wise. The mixture was partitioned between brine and DCM. The aqueous layer was extracted with DCM (3 times). The organic layers were combined, dried over anhydrous magnesium sulfate, filtered and concentrated to afford (R)-tert-butyl 2-(hydroxymethyl)piperidine-1-carboxylate (2.8 g, quantitative yield).

¹H NMR (400 MHz, Chloroform-*d*) δ 4.25 (dq, *J* = 8.8, 3.0, 2.4 Hz, 1H), 3.90 (d, *J* = 13.9 Hz, 1H), 3.77 (td, *J* = 10.1, 9.4, 4.1 Hz, 1H), 3.57 (dt, *J* = 10.7, 4.7 Hz, 1H), 2.83 (t, *J* = 12.4 Hz, 1H), 1.70 – 1.49 (m, 5H), 1.49 – 1.32 (m, 12H).

Matched known material Truax, V. M., et al. (2013). "Discovery of Tetrahydroisoquinoline-Based CXCR4 Antagonists." ACS Med. Chem. Lett. 4(11): 1025-1030.

Compound 18

SO₃Py (1.295 g, 8.14 mmol, 3 eq) and DMSO (9 mL) were combined in a 20 mL vial. 15 drops of pyridine was added and the vial was shaken for several minutes. Triethylamine (1.1 mL, 8.1 mmol, 3 eq) was then added. This mixture (biphasic as triethylamine is insoluble in DMSO) was then added to a well dried flask at 0°C containing (R)-tert-butyl 3-(hydroxymethyl)-2,3-dihydrobenzo[f]quinoline-4(1H)-carboxylate (.85 g, 2.71 mmol) and dry DCM (9 mL). This mixture was stirred at 0°C for 30 minutes checked by LCMS (approximately 80% complete) stirred at rt for 15 minutes followed by quenching with 10 mL of saturated NH₄Cl. The mixture was then diluted with EtOAc (approximately 75 mL) and enough water was added to redissolve the salts that crashed out. The layers were separated. The aqueous layer was washed several times with EtOAc. The organic layers were combined, dried over anhydrous magnesium sulfate, filtered and concentrated to afford (R)-tert-butyl 3-formyl-2,3-dihydrobenzo[f]quinoline-4(1H)-carboxylate (810 mg, 96% yield). Taken on crude.

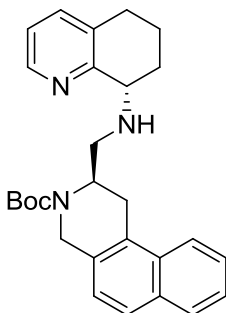
Compound 19

SO₃Py (2.162 g, 13.59 mmol, 3 eq) and DMSO (15 mL, .15 M) were combined in a 20 mL vial. 10 drops of pyridine was added and the vial was shaken for several minutes. Triethylamine (1.9 mL, 13.6 mmol, 3 eq) was then added. This mixture (biphasic as triethylamine is insoluble in DMSO) was then added to a well dried flask at 0°C containing (R)-tert-butyl 2-(hydroxymethyl)piperidine-1-carboxylate (.975 g, 4.53 mmol) and dry DCM (15 mL, .15 M). This mixture was stirred at 0°C for 30 minutes and then checked by LCMS (approximately 90% complete) and then stirred at room temperature for an additional 30 minutes before quenching with 15 mL of saturated NH₄Cl. The mixture was then diluted with EtOAc (approximately 75 mL) and enough water was added to redissolve the salts that crashed out. The layers were separated. The aqueous layer was washed several times with EtOAc. The organic layers were combined, dried over anhydrous magnesium sulfate, filtered and concentrated to afford (R)-tert-butyl 2-formylpiperidine-1-carboxylate (790 mg, 82% yield).

¹H NMR (400 MHz, Chloroform-*d*) δ 9.48 (s, 1H), 4.72 – 4.32 (m, 1H), 3.97 – 3.70 (m, 2H), 2.96 – 2.61 (m, 2H), 1.63 – 1.42 (m, 4H), 1.42 – 1.25 (m, 9H), 1.23 – 1.04 (m, 1H).

¹³C NMR (101 MHz, cdcl₃) δ 201.45, 155.52, 80.54, 80.25, 43.25, 28.53, 24.75, 23.70, 21.06.

Matched known material Truax, V. M., et al. (2013). "Discovery of Tetrahydroisoquinoline-Based CXCR4 Antagonists." ACS Med. Chem. Lett. 4(11): 1025-1030.

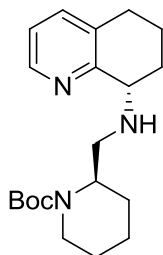
Compound 20

A 250 mL round bottom flask was charged with STAB-H (0.817 g, 3.85 mmol) and (S)-5,6,7,8-tetrahydroquinolin-8-amine (0.476 g, 3.21 mmol) dissolved in half the 1,2-Dichloroethane (25.7 ml). Then to this stirred solution (R)-tert-butyl 2-formyl-1,2-dihydrobenzo[f]isoquinoline-3(4H)-carboxylate (.8 g, 2.57 mmol) dissolved in the other half of the solvent was added. The reaction was allowed to stir for 2.5 hours before being quenched with NaHCO₃. Brine and 10% NaOH were added until the two layers had clear distinction. The DCE layer was still a little murky so ample amounts of drying agent were necessary at the end of the extraction. The water layer was extracted with DCM 3 times. The reaction mixture was purified on silica 95:5 DCM:MeOH 860 mg (75% yield).

¹H NMR (400 MHz, Chloroform-d) δ 8.33 (dd, $J = 4.8, 1.7$ Hz, 1H), 7.97 (d, $J = 8.4$ Hz, 1H), 7.80 (d, $J = 8.0$ Hz, 1H), 7.67 (d, $J = 8.5$ Hz, 1H), 7.48 (dddd, $J = 22.9, 8.0, 6.8, 1.3$ Hz, 2H), 7.31 (d, $J = 7.2$ Hz, 1H), 7.18 (d, $J = 8.6$ Hz, 1H), 7.02 (dd, $J = 7.7, 4.7$ Hz, 1H), 5.13 – 4.69 (m, 2H), 4.49-4.31 (m, 1H), 3.85 – 3.41 (m, 3H), 3.16 (dd, $J = 16.6, 6.2$ Hz, 1H), 2.85 (dd, $J = 11.7, 7.1$ Hz, 1H), 2.77 – 2.61 (m, 2H), 1.93 – 1.80 (m, 2H), 1.52 (s, 9H).

¹³C NMR (101 MHz, cdCl₃) δ 157.50, 155.40, 147.00, 137.04, 132.59, 132.55, 128.74, 126.60, 126.41, 125.53, 124.81, 124.74, 123.09, 122.96, 122.05, 80.26, 57.91, 53.71, 50.16, 48.75, 28.94, 28.74, 27.37, 26.97, 19.62.

HRMS calc'd for C₂₈H₃₄O₂N₃ 444.26455; found 444.26442 [M+H].

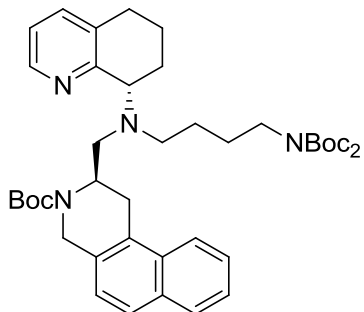
Compound 21

A 250 mL round bottom flask was charged with sodium triacetoxymethylborohydride (1.181 g, 5.57 mmol, 1.5 eq) and (S)-5,6,7,8-tetrahydroquinolin-8-amine (0.688 g, 4.64 mmol, 1.25 eq) dissolved in half the 1,2-Dichloroethane (37 mL). Then to this stirred solution (R)-tert-butyl 2-formylpiperidine-1-carboxylate (.792 g, 3.71 mmol) dissolved in the other half of the solvent was added. The reaction was allowed to stir for 2.5 hours before being quenched with NaHCO₃. Brine and 10% NaOH were added until the two layers had clear distinction. The water layer was extracted with DCM (3 times). The organic layers were combined, dried over anhydrous magnesium sulfate, filtered, and concentrated. The reaction mixture was purified on a 40gram column with a gradient going from 3-15% MeOH in DCM to afford (R)-tert-butyl 2-((((S)-5,6,7,8-tetrahydroquinolin-8-yl)amino)methyl)piperidine-1-carboxylate (704 mg, 55% yield).

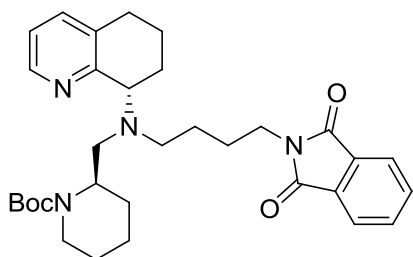
¹H NMR (400 MHz, Chloroform-d) δ 8.26 (dd, *J* = 4.6, 1.8 Hz, 1H), 7.27 – 7.23 (m, 1H), 6.94 (dd, *J* = 7.7, 4.7 Hz, 1H), 4.27 (s, 1H), 3.92 (d, *J* = 13.7 Hz, 1H), 3.69 (dd, *J* = 7.3, 5.2 Hz, 1H), 2.87 – 2.74 (m, 2H), 2.74 – 2.59 (m, 3H), 2.06 (ddd, *J* = 12.9, 8.4, 5.0 Hz, 1H), 1.97 – 1.85 (m, 1H), 1.76 (dd, *J* = 9.2, 3.5 Hz, 1H), 1.64 (tdq, *J* = 8.0, 5.5, 2.5 Hz, 1H), 1.55 – 1.42 (m, 5H), 1.37 (s, 9H).

¹³C NMR (101 MHz, cdcl₃) δ 157.62, 155.40, 146.87, 136.89, 132.34, 121.90, 79.42, 57.63, 50.66, 46.52, 39.70, 28.91, 28.63, 26.52, 25.64, 19.73, 19.40.

HRMS calc'd for C₁₉H₃₃O₂N₃ 346.24890; found 346.24889 [M+H].

Compound 22

R)-tert-butyl 2-((((S)-5,6,7,8-tetrahydroquinolin-8-yl)amino)methyl)-1,2-dihydrobenzo[f]isoquinoline-3(4H)-carboxylate (.850 g, 1.916 mmol) was dissolved in DCE (19.16 ml) in a 100 mL round bottom flask. Reactant 1 (0.716 g, 2.491 mmol) was then added and the reaction was allowed to stir for 1/2 hour. At which point STAB-H (0.609 g, 2.87 mmol) was all added as one batch. The reaction was then allowed to stir for an additional 2 hours checked by LCMS (reaction complete) and then quenched with 5 mL NaHCO₃. Brine and 10% NaOH were added until the two layers had clear distinction. The water layer was extracted with DCM 3 times. The organic layers were combined, dried over anhydrous magnesium sulfate, filtered and concentrated (600 mg, 44% yield). Taken on crude.

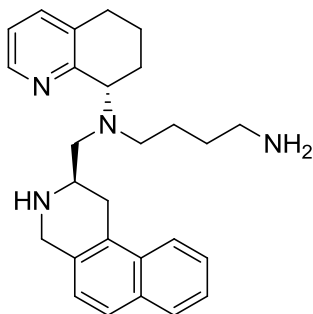
Compound 23

(R)-tert-butyl 2-(((S)-5,6,7,8-tetrahydroquinolin-8-yl)amino)methyl)piperidine-1-carboxylate (.650 g, 1.881 mmol) was dissolved in DCE (19 mL) in a 100 mL round bottom flask. 4-(1,3-dioxisoindolin-2-

yl)butanal (0.450 g, 2.07 mmol) was then added and the reaction was allowed to stir for 1 hour. At which point sodium triacetoxyborohydride (0.598 g, 2.82 mmol) was added. The reaction was then allowed to stir for an additional 3 hours checked by LCMS (reaction complete) and then quenched with 5 mL NaHCO₃. Brine and 10% NaOH were added until the two layers had clear distinction. The water layer was extracted with DCM (3 times). The crude mixture was purified on a 24g ISCO column with an eluent from 0-15% MeOH in DCM to afford (R)-tert-butyl 2-(((4-(1,3-dioxisoindolin-2-yl)butyl)((S)-5,6,7,8-tetrahydroquinolin-8-yl)amino)methyl)piperidine-1-carboxylate (800 mg, 78% yield).

¹H NMR (400 MHz, Chloroform-d) δ 8.24 (dd, *J* = 4.7, 1.6 Hz, 1H), 7.67 – 7.61 (m, 3H), 7.54 (td, *J* = 5.3, 3.0 Hz, 3H), 7.13 (dd, *J* = 7.7, 1.7 Hz, 1H), 6.83 (dd, *J* = 7.7, 4.6 Hz, 1H), 4.01 (dd, *J* = 15.4, 8.2 Hz, 1H), 3.87 (dd, *J* = 8.9, 5.9 Hz, 1H), 3.74 (d, *J* = 13.7 Hz, 1H), 3.56 (t, *J* = 6.8 Hz, 1H), 3.49 (t, *J* = 7.1 Hz, 2H), 2.80 – 2.43 (m, 4H), 2.43 – 2.26 (m, 4H), 1.94 – 1.77 (m, 2H), 1.69 – 1.40 (m, 3H), 1.29 (s, 9H), 1.15 – 1.04 (m, 6H), 0.73 – 0.64 (m, 2H).

¹³C NMR (101 MHz, cdcl₃) δ 200.81, 168.34, 155.12, 147.04, 136.35, 134.37, 133.89, 132.24, 123.13, 121.36, 78.94, 60.71, 51.73, 51.04, 41.15, 38.08, 37.16, 34.74, 31.66, 29.78, 29.40, 28.64, 26.50, 26.23, 25.49, 25.36, 25.20, 22.74, 21.51, 21.25, 19.04, 14.25.

Compound 1

N1-(((R)-1,2,3,4-tetrahydrobenzo[f]isoquinolin-2-yl)methyl)-

N1-((S)-5,6,7,8-tetrahydroquinolin-8-yl)butane-1,4-diamine

(.217 g, 0.523 mmol, 74.8 % yield) was stirred overnight in a

3:1 mixture of CH₂Cl₂ (5.25 ml) and TFA (1.748 ml). The

reaction mixture was then diluted with 10 mL of water. The

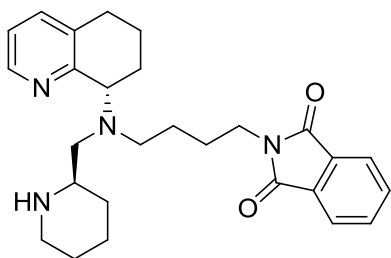
mixture was then extracted with 20mL of DCM 2 times. The water layer was bascified using NaOH pellets and then extracted with DCM 3 times. The combined organic layers from the bascified aqeous layer were then dried with sodium sulfate and concentrated in vacou. The material was a foamy solid after concentration. It was redissolved in diethyl ether and then hexane was added dropwise until the solution became cloudy. The solution was transfered to a flask scratched throughly and then let to stand and evaporate for an hour. The crystals were collected. 217 mg (75% yield).

¹H NMR (400 MHz, Chloroform-d) δ 8.46 (dd, *J* = 4.8, 1.7 Hz, 1H), 7.83 (d, *J* = 8.3 Hz, 1H), 7.74 (d, *J* = 8.3 Hz, 1H), 7.58 (d, *J* = 8.4 Hz, 1H), 7.47 – 7.35 (m, 2H), 7.30 (d, *J* = 7.7 Hz, 1H), 7.11 (d, *J* = 8.4 Hz, 1H), 7.03 (dd, *J* = 7.7, 4.8 Hz, 1H), 4.20 – 3.97 (m, 3H), 3.19 – 2.93 (m, 3H), 2.87 – 2.41 (m, 9H), 2.15 – 2.02 (m, 1H), 2.02 – 1.84 (m, 2H), 1.78 – 1.63 (m, 1H), 1.62 – 1.39 (m, 4H).

¹³C NMR (101 MHz, cdcl₃) δ 158.91, 146.97, 136.78, 134.21, 133.12, 132.54, 132.36, 129.71, 128.58, 126.07, 125.49, 125.10, 122.86, 121.67, 61.59, 58.34, 54.66, 52.39, 49.48, 42.25, 31.48, 30.83, 29.68, 29.13, 27.46, 22.23.

LCMS 75% MeOH Isocratic >95% pure rt= .887

HRMS calc'd for C₂₇H₃₅N₄ 415.28529; found 415.28562 [M+H].

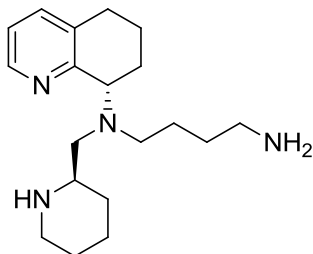
Compound 2-pre

(R)-tert-butyl 2-(((4-(1,3-dioxoisindolin-2-yl)butyl)((S)-5,6,7,8-tetrahydroquinolin-8-yl)amino)methyl)piperidine-1-carboxylate (.750 g, 1.37 mmol) was dissolved in DCM (10 mL) and then TFA (3.4

ml) was added with stirring. The reaction was stirred overnight. The reaction was then partitioned between DCM and 10% NaOH. Base was added until the aqueous layer was basic on pH paper. The crude material was then dried with sodium sulfate, concentrated in vacuo and redissolved in MeOH. In methanol solid crashed out which was filtered away, the mother liquor was concentrated. This remaining material was taken on to step 2.

¹H NMR (400 MHz, Chloroform-d) δ 8.23 (dd, $J = 4.8, 1.6$ Hz, 1H), 7.69 (dt, $J = 7.1, 3.6$ Hz, 2H), 7.58 (dd, $J = 5.4, 3.0$ Hz, 2H), 7.19 – 7.15 (m, 1H), 6.87 (dd, $J = 7.7, 4.7$ Hz, 1H), 3.90 (dd, $J = 10.3, 6.3$ Hz, 1H), 3.54 (t, $J = 7.3$ Hz, 2H), 3.04 – 2.84 (m, 2H), 2.67 – 2.15 (m, 6H), 1.94 – 1.76 (m, 2H), 1.70 (tdd, $J = 12.8, 10.1, 2.7$ Hz, 1H), 1.57 (td, $J = 15.0, 13.7, 6.0$ Hz, 2H), 1.38 (m, 3H), 1.21 – 1.03 (m, 2H), 0.92 (m, 1H).

¹³C NMR (101 MHz, cdcl₃) δ 168.49, 159.07, 146.61, 136.59, 134.10, 134.00, 132.24, 123.24, 121.42, 61.41, 58.40, 56.10, 53.09, 46.72, 38.08, 30.11, 29.50, 29.36, 27.11, 26.42, 25.99, 24.77, 22.17.

Compound 2

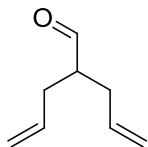
The material was then dissolved in 8 mL of MeOH and hydrazine (1 mL, 11 mmol, 8 eq) was added with stirring. The mixture was stirred overnight and then checked by LCMS in the morning (reaction complete). At this point the crude mixture was concentrated in vacuo and then diluted with 10 mL of 1N HCl. The water layer was extracted with DCM twice (both times pulling off a little bit of yellow coloration). Then the water layer was basified with 10% NaOH until blue by pH paper and extracted into DCM twice. The organic phase was dried with sodium sulfate and then concentrated to afford the product. This material was then ran through a short plug of silica to get rid of any inorganic impurities and afford N1-((R)-piperidin-2-ylmethyl)-N1-((S)-5,6,7,8-tetrahydroquinolin-8-yl)butane-1,4-diamine (190 mg, 48% yield).

¹H NMR (400 MHz, Chloroform-d) δ 8.37 (dd, $J = 4.8, 1.6$ Hz, 1H), 7.28 (dd, $J = 7.7, 1.7$ Hz, 1H), 6.99 (dd, $J = 7.7, 4.7$ Hz, 1H), 4.00 (dd, $J = 10.1, 6.3$ Hz, 1H), 3.04 (dt, $J = 12.0, 2.6$ Hz, 1H), 3.01-2.90 (m, 1H), 2.79 – 2.56 (m, 6H), 2.54 – 2.39 (m, 2H), 2.35 – 2.16 (m, 2H), 2.15-1.85 (m, 4H), 1.80 (tdd, $J = 12.5, 10.0, 2.6$ Hz, 1H), 1.73 – 1.60 (m, 2H), 1.54 – 1.33 (m, 5H), 1.21 (qt, $J = 12.7, 4.3$ Hz, 1H), 1.02 – 0.85 (m, 1H).

¹³C NMR (101 MHz, cdCl₃) δ 159.26, 146.78, 136.58, 134.18, 121.43, 61.29, 58.70, 56.01, 54.12, 47.13, 42.45, 31.80, 30.65, 29.66, 29.60, 27.47, 26.44, 25.11, 22.24.

LCMS 75% MeOH Isocratic >95% pure $rt = .996$

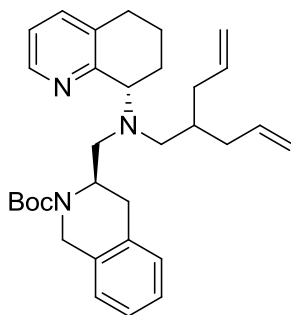
HRMS calc'd for C₁₉H₃₃N₄ 317.26997; found 317.26975 [M+H].

Compound 27

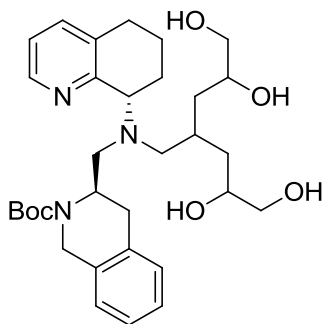
Prepared as described in reference 12. 48% yield over five steps. Spectra matched the previous description.

^1H NMR (400 MHz, Chloroform-*d*) δ 9.63 (d, $J = 1.9$ Hz, 1H), 5.73 (ddt, $J = 17.0, 10.3, 6.9$ Hz, 2H), 5.11 – 5.02 (m, 4H), 2.49 – 2.33 (m, 3H), 2.30 – 2.20 (m, 2H).

^{13}C NMR (101 MHz, cdCl_3) δ 134.90, 117.71, 50.75, 32.71.

Compound 31

The 500 mL flask containing (R)-tert-butyl 3-(((S)-5,6,7,8-tetrahydroquinolin-8-yl)amino)methyl)-3,4-dihydroisoquinoline-2(1H)-carboxylate (4.75 g, 12.08 mmol) was charged with DCE (121 ml) and then 2-allylpent-4-enal (1.5 g, 12.08 mmol, 1 eq). This mixture was stirred for 1.5 hr under inert atmosphere and then NaBH(OAc)₃ (5.12 g, 24.16 mmol, 2 eq) was added. The reaction was then allowed to stir under inert atmosphere overnight. The reaction was quenched with aqueous 10 mL NaHCO₃ and then enough 10% NaOH solution to turn pH paper blue and the organic phase was extracted (2x100ml DCM), dried over sodium sulfate and evaporated under reduced pressure. This mixture was then subject to column chromatography with 1% MeOH in 1% TEA/DCM solution. The column was 8 inches long and allowed to drip at the rate of gravity to afford (R)-tert-butyl 3-(((2-allylpent-4-en-1-yl)((S)-5,6,7,8-tetrahydroquinolin-8-yl)amino)methyl)-3,4-dihydroisoquinoline-2(1H)-carboxylate (4.3 g, 71% yield).

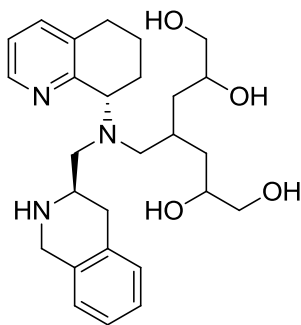
Compound 32

To a solution of (R)-tert-butyl 3-(((2-allylpent-4-en-1-yl)((S)-5,6,7,8-tetrahydroquinolin-8-yl)amino)methyl)-3,4-dihydroisoquinoline-2(1H)-carboxylate (750 mg, 1.5 mmol) in 10:1 acetone:water (0.1 M) were added 2,6-lutidine (640 mg, 6 mmol, 4 eq), 4-methylmorpholine *N*-oxide (530 mg, 4 mmol, 1.5 equiv), and osmium tetroxide (600 mg (2.5% w/w in *tert*-butanol), .06mmol, 0.04 equiv). The reaction was tracked by LCMS and complete within two hours. The mixture was extracted with ethyl acetate (3 × 10 mL). The organic layers were combined, dried over anhydrous magnesium sulfate, filtered and concentrated. The crude residue was purified on a 25 gram combiflash column with a gradient of 0-20% MeOH in DCM to afford (3R)-tert-butyl 3-(((2-(2,3-dihydroxypropyl)-4,5-dihydroxypentyl)((S)-5,6,7,8-tetrahydroquinolin-8-yl)amino)methyl)-3,4-dihydroisoquinoline-2(1H)-carboxylate (518 mg, 61% yield).

¹H NMR (400 MHz, Chloroform-*d*) δ 8.42 (t, *J* = 16.9 Hz, 1H), 7.11 (p, *J* = 9.3, 8.1 Hz, 1H), 7.05 – 6.70 (m, 4H), 5.19 – 4.77 (m, 4H), 4.44 (td, *J* = 17.7, 17.1, 6.4 Hz, 1H), 4.21 – 4.06 (m, 2H), 3.86 – 3.68 (m, 2H), 3.63 – 3.42 (m, 3H), 3.41 – 3.30 (m, 1H), 2.85 – 2.59 (m, 4H), 2.50 – 2.30 (m, 2H), 2.27 – 2.05 (m, 1H), 2.03 – 1.88 (m, 4H), 1.82 – 1.54 (m, 2H), 1.43 (s, 9H), 1.34 – 1.21 (m, 1H), 1.19 – 1.08 (m, 2H).

¹³C NMR (151 MHz, cdcl₃) δ 171.33, 155.09, 149.07, 147.62, 139.07, 132.89, 129.45, 129.26, 127.05, 126.77, 126.03, 124.08, 81.03, 73.34, 70.14, 67.24, 54.51, 53.79, 46.65, 44.70, 36.65, 29.82, 28.83, 28.64, 28.32, 27.66, 22.83, 21.23.

HRMS calc'd for C₃₂H₄₈O₆N₃ 570.35376; found 570.35359 [M+H]

Compound 3

(R)-tert-butyl 3-(((2-(2,3-dihydroxypropyl)-4,5-dihydroxypentyl)((S)-5,6,7,8-tetrahydroquinolin-8-yl)amino)methyl)-3,4-dihydroisoquinoline-2(1H)-carboxylate (300 mg, .53 mmol) was dissolved in EtOAc and a minimum amount of DCM. The organic phase was then portioned with HCl

(1 M) and stirred at 40C for 30 minutes. The layers were separated and the aqueous phase was concentrated by azeotropic distillation at 40C with toluene to afford (R)-tert-butyl 3-(((2-(2,3-dihydroxypropyl)-4,5-dihydroxypentyl)((S)-5,6,7,8-tetrahydroquinolin-8-yl)amino)methyl)heptane-1,2,6,7-tetraol (185 mg, 394 μmol, 75% yield).

¹H NMR (400 MHz, Deuterium Oxide) δ 8.40 (dt, *J* = 9.7, 5.6 Hz, 1H), 7.98 (t, *J* = 8.0 Hz, 1H), 7.54 (p, *J* = 7.7, 7.1 Hz, 1H), 7.10 – 6.97 (m, 3H), 6.95 (d, *J* = 8.0 Hz, 1H), 4.31 – 4.21 (m, 1H), 4.21 – 4.15 (m, 2H), 3.73 – 3.63 (m, 1H), 3.62 – 3.42 (m, 3H), 3.34 – 3.07 (m, 5H), 2.96 – 2.82 (m, 1H), 2.71 – 2.59 (m, 4H), 2.59 – 2.46 (m, 2H), 2.11 – 2.01 (m, 1H), 1.89 – 1.69 (m, 2H), 1.64 – 1.44 (m, 2H), 1.31 – 1.04 (m, 3H).

¹³C NMR (101 MHz, d₂O) δ 151.06, 147.04, 146.74, 139.81, 130.04, 129.22, 128.20, 127.27, 127.10, 126.53, 125.34, 70.09, 69.11, 65.85, 64.90, 63.91, 60.52, 57.72, 56.00, 53.23, 51.59, 43.92, 35.99, 30.46, 29.05, 27.50, 20.12, 19.43.

LCMS 65% MeOH:H₂O w/ .1% formic acid >95% pure rt= .509

HRMS calc'd for C₂₇H₃₉O₄N₃ 470.30133; found 470.30170 [M+H]

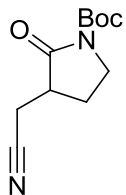
HRMS calc'd for C₂₇H₃₈D₁O₄N₃ 471.30761 found 471.30801 [M+D]

HRMS calc'd for C₂₇H₃₇D₂O₄N₃ 472.31389 found 472.31430 [M-H+2D]

HRMS calc'd for C₂₇H₃₆D₃O₄N₃ 473.32016 found 473.32053 [M-2H+3D]

HRMS calc'd for $C_{27}H_{35}D_4O_4N_3$ 474.32644 found 474.32678 [M-3H+4D]

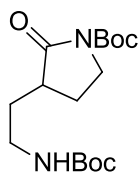
HRMS calc'd for $C_{27}H_{34}D_5O_4N_3$ 475.33272 found 475.33292 [M-4H+5D]

Compound 38

To a solution of tert-butyl 2-oxopyrrolidine-1-carboxylate (2.5 g, 13.5 mmol) in THF (90 mL, .15 M) stirred at -78 C was added a 1M solution of Lithium hexamethyldisilazide in Toluene (16.9 mL, 16.9 mmol, 1.25 eq). After stirring for 1 hr at -78 C 2-iodoacetonitrile (2.7 g, 16.2 mmol, 1.2 eq) was added and stirring continued for 2 hours. The reaction was tracked by LCMS and complete within two hours. The reaction was quenched with saturated ammonium chloride solution and then extracted with ethyl acetate (3 × 50 mL). The organic layers were combined, dried over anhydrous magnesium sulfate, filtered and concentrated to afford tert-butyl 3-(cyanomethyl)-2-oxopyrrolidine-1-carboxylate (2.23 g, 74% yield).

¹H NMR (300 MHz, Chloroform-*d*) δ 3.85 (ddd, *J* = 10.8, 8.9, 1.6 Hz, 1H), 3.60 (ddd, *J* = 11.1, 10.3, 6.8 Hz, 1H), 2.91 – 2.76 (m, 2H), 2.64 – 2.49 (m, 1H), 2.37 (dddd, *J* = 12.9, 8.5, 6.9, 1.7 Hz, 1H), 1.97 – 1.80 (m, 1H), 1.50 (s, 9H).

HRMS calc'd for C₁₁H₁₆O₃N₂Na 247.10531; found 247.10531 [M+Na]

Compound 39

Procedure adapted from reference 14

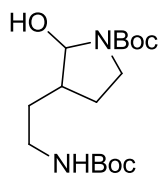
Sodium borohydride (3.7 g, 98 mmol, 10 eq) was added slowly to a stirred solution of tert-butyl 3-(cyanomethyl)-2-oxopyrrolidine-1-carboxylate (2.2 g, 9.8 mmol), $\text{CoCl}_2 \cdot 6\text{H}_2\text{O}$ (4.7 g, 19.6 mmol, 2 eq), and di-*tert*-butyl dicarbonate (2.6 g, 11.8 mmol, 1.2 eq) in methanol (100 mL, .1 M) at 0 C. The reaction was allowed to warm to room temperature and was stirred for 5 hrs. The mixture was filtered through two fluted pieces of filter paper and then water (50 mL) was added to the filtrate, and the methanol was removed in vacuo. The resulting solution was extracted with ethyl acetate (3×50 mL). The organic layers were combined, dried over anhydrous magnesium sulfate, filtered and concentrated. This mixture was then subject to column chromatography on the Isco with a gradient from 0-10% MeOH in DCM to afford tert-butyl 3-(2-((tert-butoxycarbonyl)amino)ethyl)-2-oxopyrrolidine-1-carboxylate (2.1 g, 65% yield).

^1H NMR (400 MHz, Chloroform-*d*) δ 3.74 (ddt, $J = 11.0, 8.7, 2.1$ Hz, 1H), 3.54 (dddd, $J = 11.0, 9.3, 7.1, 1.7$ Hz, 1H), 3.30 – 3.11 (m, 2H), 2.59 – 2.44 (m, 1H), 2.28 – 2.14 (m, 1H), 1.96 (dq, $J = 13.3, 6.8$ Hz, 1H), 1.69 – 1.54 (m, 2H), 1.54 – 1.36 (m, 18H).

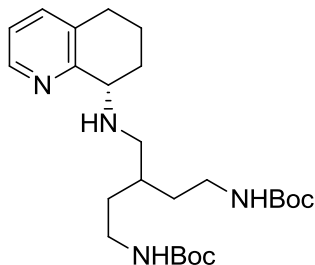
^{13}C NMR (101 MHz, cdCl_3) δ 176.20, 156.30, 150.44, 83.04, 79.35, 44.79, 41.79, 38.62, 31.18, 28.62, 28.23, 24.64.

HRMS calc'd for $\text{C}_{16}\text{H}_{29}\text{O}_5\text{N}_2$ 329.20710; found 329.20731 [M+H]

HRMS calc'd for $\text{C}_{16}\text{H}_{28}\text{O}_5\text{N}_2\text{Na}$ 351.18904; found 351.18927 [M+Na]

Compound 40

tert-butyl 3-(2-((tert-butoxycarbonyl)amino)ethyl)-2-oxopyrrolidine-1-carboxylate (2 g, 6.1 mmol) was dissolved in THF (40 mL, .15 M) under a Argon atmosphere and cooled to -78 °C. DIBAL-H (9.1 mL, 9.1 mmol, 1.5 equiv, 1.0 M in hexanes) was added slowly and reaction mixture was stirred for 1 hour. The reaction was quenched with saturated NH₄Cl (40 mL) and warmed to room temperature. The resulting solution was extracted with DCM (3 × 50 mL). The organic layers were combined, dried over anhydrous magnesium sulfate, filtered and concentrated to afford tert-butyl 3-(2-((tert-butoxycarbonyl)amino)ethyl)-2-hydroxypyrrolidine-1-carboxylate (1.5 g, 75% yield).

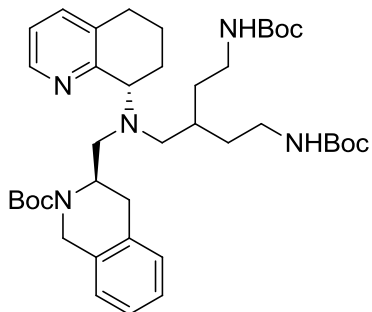
Compound 41

tert-butyl 3-(2-(((tert-butoxycarbonyl)amino)ethyl)-2-hydroxypyrrolidine-1-carboxylate (1.2 g, 3.6 mmol) was dissolved in DCM (50 ml, .075 M). (S)-5,6,7,8-tetrahydroquinolin-8-amine (.67 g, 4.5 mmol, 1.25 eq) was

added and allowed to stir for 2 hrs at room temperature, at which point sodium triacetoxo borohydride (1.55 g, 5.45 mmol, 1.5 eq) was added as one portion. The reaction was allowed to stir overnight. The reaction was quenched with 5 mL NaHCO₃ carefully followed by dilution with 5 mL NaCl and 5 mL 1N NaOH. The aqueous layer was then extracted with 50 mL of DCM (3 times). The organic layers were combined, dried over anhydrous sodium sulfate, filtered and concentrated to afford the crude product. The crude material was purified on a 25 gram combiflash column with a gradient from 1-10% MeOH in 1% TEA/DCM solution to afford (S)-di-tert-butyl (3-(((5,6,7,8-tetrahydroquinolin-8-yl)amino)methyl)pentane-1,5-diyl)dicarbamate.

¹H NMR (300 MHz, Chloroform-*d*) δ 8.33 (dd, *J* = 4.7, 1.6 Hz, 1H), 7.36 (dd, *J* = 7.7, 1.6 Hz, 1H), 7.06 (dd, *J* = 7.7, 4.7 Hz, 1H), 3.79 – 3.56 (m, 1H), 3.23 – 2.98 (m, 4H), 2.70 – 2.51 (m, 4H), 2.19 – 1.84 (m, 4H), 1.78 – 1.45 (m, 6H), 1.42 – 1.32 (m, 18H).

HRMS calc'd for C₂₅H₄₃O₄N₄ 463.32788; found 463.32786 [M+H]

Compound 42

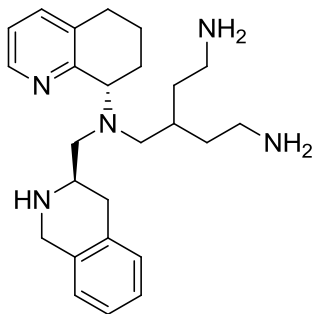
(S)-di-tert-butyl (3-(((5,6,7,8-tetrahydroquinolin-8-yl)amino)methyl)pentane-1,5-diyl)dicarbamate (110 mg, .24 mmol) was dissolved in DCM (5 ml, .05 M). (R)-tert-butyl 3-formyl-3,4-dihydroisoquinoline-2(1H)-carboxylate (68 mg, .26 mmol, 1.1 eq) was added and allowed to stir for

2 hrs at room temperature, at which point sodium triacetoxy borohydride (76 mg, .36 mmol, 1.5 eq) was added as one portion. The reaction was allowed to stir overnight. The reaction was quenched with 1 mL NaHCO₃ carefully followed by dilution with 3 mL NaCl and 3 mL 1N NaOH. The aqueous layer was then extracted with 50 mL of DCM (3 times). The organic layers were combined, dried over anhydrous sodium sulfate, filtered and concentrated to afford the crude product. The crude material was purified on a 4 gram combiflash column with a gradient from 0-10% MeOH in DCM to afford (R)-tert-butyl 3-(((4-((tert-butoxycarbonyl)amino)-2-(2-((tert-butoxycarbonyl)amino)ethyl)butyl)((S)-5,6,7,8-tetrahydroquinolin-8-yl)amino)methyl)-3,4-dihydroisoquinoline-2(1H)-carboxylate (92 mg, 55% yield).

¹H NMR (600 MHz, Chloroform-*d*) δ 8.50 (d, *J* = 67.1 Hz, 1H), 7.22 – 7.08 (m, 2H), 7.08 – 6.92 (m, 4H), 4.25 – 4.14 (m, 2H), 3.94 (dt, *J* = 55.2, 7.9 Hz, 1H), 3.40 – 2.93 (m, 4H), 2.93 – 2.72 (m, 2H), 2.59 – 2.39 (m, 6H), 2.38 – 1.97 (m, 4H), 1.93 – 1.61 (m, 2H), 1.61 – 1.29 (m, 33H).

¹³C NMR (101 MHz, cdcl₃) δ 155.24, 147.28, 132.98, 129.17, 126.08, 126.02, 121.36, 80.26, 78.47, 64.80, 61.52, 58.79, 53.66, 49.15, 38.78, 30.99, 30.43, 29.55, 28.68, 22.28.

HRMS calc'd for C₄₀H₆₂O₆N₅ 708.46946; found 708.47209 [M+H]

Compound 4

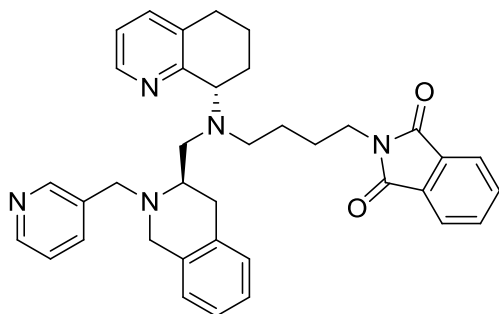
To a solution of (R)-tert-butyl 3-(((4-((tert-butoxycarbonyl)amino)-2-(2-((tert-butoxycarbonyl)amino)ethyl)butyl)((S)-5,6,7,8-tetrahydroquinolin-8-yl)amino)methyl)-3,4-dihydroisoquinoline-2(1H)-carboxylate (90 mg, .13 mmol) in DCM (.05 M) was added trifluoroacetic acid (.015 M). The reaction was tracked by LCMS and allowed to stir overnight. Upon completion the mixture was diluted 5% HCl and extracted with DCM (2 times). The aqueous layer was basified with 10% NaOH solution and then extracted with DCM (3 times) these organic layers were combined, dried over anhydrous sodium sulfate, filtered and concentrated to afford 3-(((R)-1,2,3,4-tetrahydroisoquinolin-3-yl)methyl)((S)-5,6,7,8-tetrahydroquinolin-8-yl)amino)methyl)pentane-1,5-diamine which was filtered through a silica plug (18 mg, 35% yield).

¹H NMR (400 MHz, Chloroform-*d*) δ 8.47 – 8.37 (m, 1H), 7.31 (dd, *J* = 7.8, 1.8 Hz, 1H), 7.10 – 6.94 (m, 5H), 4.09 – 3.95 (m, 2H), 3.78 (d, *J* = 15.2 Hz, 1H), 3.07 – 2.85 (m, 2H), 2.82 – 2.63 (m, 5H), 2.63 – 2.50 (m, 2H), 2.48 – 2.25 (m, 6H), 2.19 – 2.02 (m, 1H), 1.96 (dt, *J* = 11.7, 3.8 Hz, 1H), 1.85 (ddd, *J* = 13.1, 10.5, 2.9 Hz, 1H), 1.77 – 1.53 (m, 4H), 1.50 – 1.30 (m, 4H).

¹³C NMR (101 MHz, cdcl₃) δ 157.41, 147.02, 137.65, 134.08, 129.24, 126.56, 126.11, 122.39, 63.03, 61.53, 58.74, 51.93, 47.27, 38.41, 33.75, 33.28, 29.64, 29.51, 22.19.

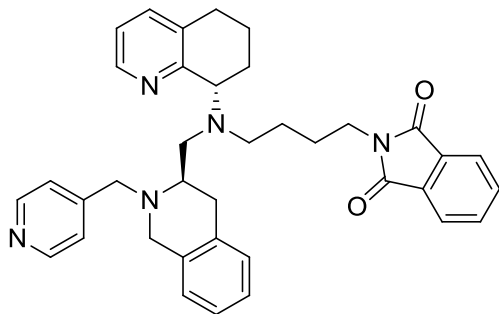
LCMS 75% MeOH Isocratic >95% pure rt= .887

HRMS calc'd for C₂₅H₃₈N₅ 408.31217; found 408.31240 [M+H]

Compound 47

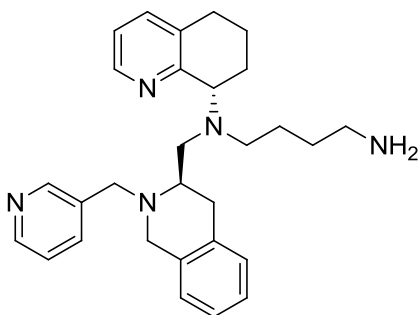
2-(4-(((R)-1,2,3,4-tetrahydroisoquinolin-3-yl)methyl)((S)-5,6,7,8-tetrahydroquinolin-8-yl)amino)butyl)isoindoline-1,3-dione (.580 g, 1.17 mmol) was dissolved in DCM (11.73 mL, .1 M) and stirred under inert atmosphere.

Nicotinaldehyde (0.151 g, 1.407 mmol, 1.2 eq) was then added and stirring was continued for 2 hrs. Sodium triacetoxyborohydride (560 mg, 2.6 mmol, 2.25 eq) was added as one portion and the reaction was allowed to stir overnight. The reaction was diluted with 10 mL NaCl and 4 mL 1N NaOH. The aqueous layer was then extracted with 20 mL of DCM (3 times). The combined organic layers were dried with MgSO₄. The material was purified on a 12g combiflash column with an eluent system of 1-5% MeOH in 1% TEA/DCM to afford 2-(4-(((R)-2-(pyridin-3-ylmethyl)-1,2,3,4-tetrahydroisoquinolin-3-yl)methyl)((S)-5,6,7,8-tetrahydroquinolin-8-yl)amino)butyl)isoindoline-1,3-dione (233 mg, 34% yield).

Compound 48

2-(4-(((R)-1,2,3,4-tetrahydroisoquinolin-3-yl)methyl)((S)-5,6,7,8-tetrahydroquinolin-8-yl)amino)butyl)isoindoline-1,3-dione (.580 g, 1.173 mmol) was dissolved in DCM (11.73 mL, .1 M) and stirred under inert atmosphere.

Isonicotinaldehyde (0.151 g, 1.41 mmol) was then added and stirring was allowed to continue for 2 hrs. The reaction was quenched with 10 mL of brine and 4 mL of 1N NaOH. The aqueous layer was then extracted with 20 mL of DCM (3 times). The combined organic layer was dried with MgSO₄. The material was purified on a 12 g combiflash column. The eluent system used was 0-3% MeOH in 1% TEA/DCM to afford 2-(4-(((R)-2-(pyridin-4-ylmethyl)-1,2,3,4-tetrahydroisoquinolin-3-yl)methyl)((S)-5,6,7,8-tetrahydroquinolin-8-yl)amino)butyl)isoindoline-1,3-dione (464 mg, 67% yield).

Compound 43

2-(4-(((R)-2-(pyridin-3-ylmethyl)-1,2,3,4-tetrahydroisoquinolin-3-yl)methyl)((S)-5,6,7,8-tetrahydroquinolin-8-yl)amino)butyl)isoindoline-1,3-dione (.205 g, 0.350 mmol) was dissolved in MeOH (3.50 mL, .1 M) in a 50 mL flask and then hydrazine

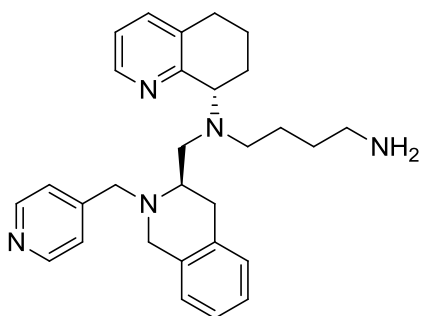
(0.374 g, 2.80 mmol, 8 eq) was added. The reaction was allowed to stir for 20 hrs and was checked by TLC prior to work up. Upon completion the reaction mixture was concentrated in vacuo. 10 mL water was added to the oily residue and extracted with DCM (3 times). The DCM layer was washed with 10 mL 1M NaOH and the aqueous layer was discarded. The organic layer was then evaporated and subjected to a 4 gram autocolumn with 5-20% MeOH gradient and 3% TEA in DCM. It eluted broadly at around 11 CV's to afford N1-(((R)-2-(pyridin-3-ylmethyl)-1,2,3,4-tetrahydroisoquinolin-3-yl)methyl)-N1-((S)-5,6,7,8-tetrahydroquinolin-8-yl)butane-1,4-diamine (62 mg, 39% yield).

¹H NMR (400 MHz, Chloroform-d) δ 8.55 – 8.39 (m, 3H), 7.66 (dt, $J = 7.9, 2.0$ Hz, 1H), 7.19 (dd, $J = 7.7, 5.0$ Hz, 2H), 7.05 – 6.91 (m, 4H), 6.84 – 6.79 (m, 1H), 3.99 (dd, $J = 8.8, 5.6$ Hz, 1H), 3.73 – 3.52 (m, 5H), 3.08 – 2.89 (m, 2H), 2.77 – 2.42 (m, 8H), 2.00 – 1.85 (m, 2H), 1.76 – 1.50 (m, 2H), 1.49 – 1.33 (m, 5H).

¹³C NMR (101 MHz, cdcl₃) δ 157.79, 150.33, 148.64, 147.33, 136.68, 136.66, 135.24, 134.40, 134.28, 134.03, 129.61, 126.56, 126.27, 125.70, 123.57, 121.70, 61.20, 56.03, 54.77, 52.79, 52.30, 50.68, 41.46, 30.63, 29.79, 29.31, 25.92, 24.77, 21.37.

LCMS 75% MeOH Isocratic >95% pure rt= .894

HRMS calc'd for C₂₉H₃₈N₅ 456.31217; found 415.31161 [M+H].

Compound 44

2-(4-(((R)-2-(pyridin-4-ylmethyl)-1,2,3,4-tetrahydroisoquinolin-3-yl)methyl)((S)-5,6,7,8-tetrahydroquinolin-8-yl)amino)butyl)isoindoline-1,3-dione (.434 g, 0.741 mmol) was dissolved in MeOH (7.41 mL, .1 M) in a 50 mL flask and then hydrazine

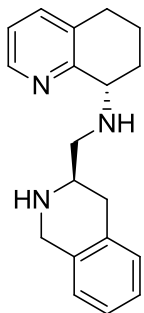
(0.791 g, 5.93 mmol) was added. The solution was allowed to stir for 20 hrs and was checked by TLC for completeness. Methanol was removed under vacuum. 10 mL of water was added to the oily residue and extracted with 20ml DCM (3 times). The DCM layer was washed with 10 mL 1M NaOH and the aqueous layer was discarded. The organic layer was then evaporated and subjected to a 4 gram autocolumn with 5-20% MeOH gradient and 3% TEA in DCM to afford N1-(((R)-2-(pyridin-4-ylmethyl)-1,2,3,4-tetrahydroisoquinolin-3-yl)methyl)-N1-((S)-5,6,7,8-tetrahydroquinolin-8-yl)butane-1,4-diamine (193 mg, 57% yield).

¹H NMR (400 MHz, Chloroform-d) δ 8.50 – 8.47 (m, 2H), 8.43 (dd, $J = 4.7, 1.7$ Hz, 1H), 7.28 – 7.25 (m, 2H), 7.23 (dd, $J = 7.4, 1.5$ Hz, 1H), 7.09 – 7.01 (m, 3H), 6.96 (dd, $J = 7.6, 4.7$ Hz, 1H), 6.86 (dd, $J = 7.5, 1.7$ Hz, 1H), 3.97 (dd, $J = 8.8, 5.2$ Hz, 1H), 3.78 – 3.56 (m, 5H), 3.02 – 2.91 (m, 2H), 2.82 (ddd, $J = 16.9, 8.7, 3.9$ Hz, 2H), 2.71 – 2.48 (m, 6H), 1.99 – 1.87 (m, 2H), 1.83 – 1.71 (m, 1H), 1.66 – 1.56 (m, 1H), 1.47 – 1.14 (m, 5H).

¹³C NMR (101 MHz, cdcl₃) δ 158.18, 149.90, 149.50, 147.18, 136.58, 134.46, 134.38, 134.16, 129.57, 126.59, 126.31, 125.71, 123.71, 121.63, 61.56, 56.40, 52.91, 52.55, 51.27, 42.18, 31.66, 29.99, 29.32, 26.31, 25.82, 21.24.

LCMS 75% MeOH Isocratic >95% pure rt= .861

HRMS calc'd for $C_{29}H_{38}N_5$ 456.31217; found 456.31174 [M+H].

Compound 45

Prepared by general Boc-deprotection procedure from material **compound 9**.

Purified on a 4 gram combiflash column with a gradient of 0-100%

DCM:MeOH:NH₄OH 9:1:5 in DCM to afford (S)-N-(((R)-1,2,3,4-

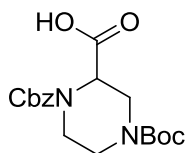
tetrahydroisoquinolin-3-yl)methyl)-5,6,7,8-tetrahydroquinolin-8-amine (60

mg, 40% yield over two steps).

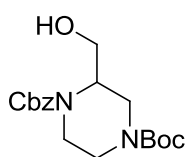
¹H NMR (400 MHz, Chloroform-*d*) δ 8.37 (dd, *J* = 4.7, 1.8 Hz, 1H), 7.40 (dd, *J* = 7.6, 1.7 Hz, 1H), 7.18 – 7.00 (m, 5H), 4.14 (d, *J* = 4.7 Hz, 2H), 3.94 – 3.80 (m, 1H), 3.73 – 3.49 (m, 3H), 3.31 – 3.14 (m, 2H), 2.93 – 2.66 (m, 3H), 2.21 (dt, *J* = 12.5, 5.9 Hz, 1H), 2.08 – 1.94 (m, 1H), 1.95 – 1.81 (m, 1H), 1.81 – 1.68 (m, 1H).

¹³C NMR (101 MHz, cdcl₃) δ 156.22, 147.01, 137.65, 133.93, 133.54, 133.02, 129.44, 126.91, 126.38, 122.65, 58.69, 55.46, 53.94, 51.57, 46.87, 32.32, 28.77, 20.05.

HRMS calc'd for C₁₉H₂₄N₃ 294.19647; found [M+H] 294.19679

Compound 55

A solution of piperazine-1,3-dicarboxylic acid 1-tert-butyl ester (14.55 g, 63.2 mmol) in 1,4-dioxane (211 mL) water (105 mL) and triethylamine (22 mL, 2.5 eq) was cooled to 0°C. Benzyl carbonochloridate (12.93 g, 76 mmol, 1.2 eq) was added dropwise over the course of 5 minutes. The reaction was allowed to warm to room temperature and was tracked by LCMS. After one hour the reaction was diluted with 1N HCl and then extracted with DCM (3 times). The organic layers were combined, dried over anhydrous magnesium sulfate, filtered and concentrated to afford 1-((benzyloxy)carbonyl)-4-(tert-butoxycarbonyl)piperazine-2-carboxylic acid (approx. 23 g). The material was used in the next step crude.

Compound 56

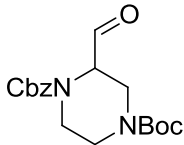
A solution of 1-((benzyloxy)carbonyl)-4-(tert-butoxycarbonyl)piperazine-2-carboxylic acid (approx 23 g, 63 mmol) in THF (316 mL, .2M) was cooled to 0°C. Borane dimethylsulfide (11.1 mL, 110 mmol, 1.75 eq) was added drop wise over the course of 5 minutes. The reaction was allowed to warm to room temperature and was tracked by LCMS. After stirring overnight the reaction was diluted with brine and then extracted with DCM (3 times). The organic layers were combined, dried over anhydrous magnesium sulfate, filtered and concentrated to afford 1-benzyl 4-tert-butyl 2-(hydroxymethyl)piperazine-1,4-dicarboxylate (21 g, 95% yield over two steps).

^1H NMR (400 MHz, Chloroform-*d*) δ 7.38 – 7.26 (m, 5H), 5.12 (d, $J = 2.3$ Hz, 2H), 4.36 – 4.07 (m, 2H), 4.04 – 3.78 (m, 2H), 3.66 – 3.50 (m, 2H), 3.16 – 2.72 (m, 4H), 1.44 (s, 9H).

^{13}C NMR (101 MHz, cdCl_3) δ 156.08, 154.98, 136.47, 128.78, 128.41, 128.19, 80.86, 67.76, 67.29, 52.77, 42.89, 39.84, 28.54.

HRMS calc'd for $\text{C}_{15}\text{H}_{27}\text{O}_5\text{N}_2$ 351.19145; found $[\text{M}+\text{H}]$ 351.19204

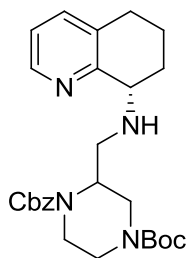
HRMS calc'd for $\text{C}_{15}\text{H}_{27}\text{O}_5\text{N}_2\text{Na}$ 373.17339; found $[\text{M}+\text{H}+\text{Na}]$ 373.17355

Compound 57

To a solution of 1-benzyl 4-tert-butyl 2-(hydroxymethyl)piperazine-1,4-dicarboxylate (21 g, 60 mmol) dissolved in DCM (300 mL, .2M) was added PCC (19.38 g, 90 mmol, 1.5 eq). The reaction was tracked by LCMS. After stirring overnight the reaction mixture was triturated with diethyl ether until no more solid (chromium waste) crashed out. The suspension was then filtered and the solution concentrated down to afford 1-benzyl 4-tert-butyl 2-formylpiperazine-1,4-dicarboxylate (approx. 20g). The material was used in the next step crude.

Alternative

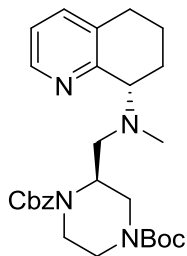
To a 0 °C solution of 1-benzyl 4-tert-butyl 2-(hydroxymethyl)piperazine-1,4-dicarboxylate (16 g, 46 mmol) in CH₂Cl₂ (100 mL) was added triethylamine (18.5 g, 183 mmol, 4 eq) followed by pyridine·SO₃ complex (21.8 g, 138 mmol, 3 eq) as a solution in DMSO (100 mL). The reaction solution was stirred at 0 °C for 1 h before quenching with sat. NaHCO₃. The solution was then extracted with Et₂O (x 3), the combined organics were washed with brine and dried (NaSO₄) to afford 1-benzyl 4-tert-butyl 2-formylpiperazine-1,4-dicarboxylate. The material was used in the next step crude

Compound 58

To a solution of 1-benzyl 4-tert-butyl 2-formylpiperazine-1,4-dicarboxylate (15.9 g, 45.6 mmol) dissolved in DCM (456 mL, .1M) was added (S)-5,6,7,8-tetrahydroquinolin-8-amine (8.45 g, 57.0 mmol, 1.25 eq). The mixture was stirred at room temperature for 30 minutes, at which point sodium triacetoxyborohydride (14.51 g, 68.5 mmol, 1.5 eq) was added. The reaction was complete after two hours as checked by LCMS. The mixture was diluted with 5 mL of 10% NaOH and 50 mL of brine. The fractions were separated and the aqueous phase extracted with DCM (3 times). The organic layers were combined dried over anhydrous sodium sulfate, filtered and concentrated. The crude mixture was then purified on a 80 gram combiflash column with a gradient from 0-20% MeOH in DCM to afford 1-benzyl 4-tert-butyl-2-(((S)-5,6,7,8-tetrahydroquinolin-8-yl)amino)methyl)piperazine-1,4-dicarboxylate (12.5 g, 57% yield over two steps).

^1H NMR (400 MHz, Chloroform-*d*) δ 8.31 – 8.22 (m, 1H), 7.38 – 7.15 (m, 6H), 6.98 (dd, $J = 7.7, 4.7$ Hz, 1H), 5.12 – 5.05 (m, 2H), 4.30 – 4.11 (m, 2H), 3.95 – 3.81 (m, 4H), 3.76 – 3.64 (m, 1H), 3.61 – 3.46 (m, 1H), 3.11 – 2.58 (m, 7H), 1.95 – 1.79 (m, 1H), 1.79 – 1.49 (m, 1H), 1.40 (s, 9H).

^{13}C NMR (101 MHz, cdcl_3) δ 157.50, 155.12, 146.97, 146.85, 136.99, 136.71, 132.53, 128.70, 128.59, 128.09, 122.00, 80.32, 67.60, 67.51, 60.55, 52.82, 51.89, 45.12, 44.14, 42.75, 39.61, 28.96, 28.49, 19.75.

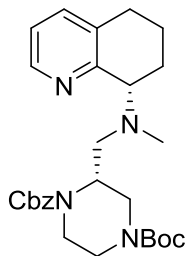
Compound 59

To a solution of 1-benzyl 4-tert-butyl-2-(((S)-5,6,7,8-tetrahydroquinolin-8-yl)amino)methyl)piperazine-1,4-dicarboxylate (5.5g, 11.4 mmol) dissolved in DCE (114 mL, .1M) was added paraformaldehyde (1.72 g, 57 mmol, 5 eq) and acetic acid (.5 mL). After stirring at room temperature for 30 minutes sodium triacetoxyborohydride (6.1 g, 29 mmol, 2.5 eq) was added as one portion. The reaction was tracked by LCMS and went to completion overnight. The mixture was filtered and then partitioned between water and DCM. The aqueous layer was basified and extracted with DCM (3 times). The organic layers were combined dried over anhydrous sodium sulfate, filtered and concentrated. The crude mixture was then purified on a 40 gram combiflash column with a step wise gradient from 0 to 5 to 10 to 15% MeOH in DCM to afford 1-benzyl 4-tert-butyl 2-((methyl((S)-5,6,7,8-tetrahydroquinolin-8-yl)amino)methyl)piperazine-1,4-dicarboxylate diastereomers (3.65 g, 7.4 mmol, 65% yield).

URF (1.6 g, 29% yield)

^1H NMR (600 MHz, Chloroform-*d*) δ 8.35 (dd, $J = 4.9, 1.7$ Hz, 1H), 7.42 – 7.14 (m, 6H), 7.04 (dd, $J = 7.7, 4.7$ Hz, 1H), 5.07 (p, $J = 11.7, 11.1$ Hz, 2H), 4.27 – 3.93 (m, 2H), 3.93 – 3.67 (m, 2H), 3.08 – 2.52 (m, 8H), 2.41 – 2.02 (m, 2H), 1.95 (s, 3H), 1.84 – 1.70 (m, 2H), 1.68 – 1.44 (m, 1H), 1.38 (s, 9H).

^{13}C NMR (101 MHz, cdcl_3) δ 155.62, 155.18, 146.35, 137.60, 136.59, 134.75, 128.61, 128.22, 122.37, 80.25, 67.59, 63.68, 55.22, 53.71, 50.16, 49.22, 43.73, 39.49, 38.54, 28.68, 28.44, 26.33, 21.71.

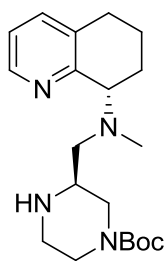
Compound 60

To a solution of 1-benzyl 4-tert-butyl-2-(((S)-5,6,7,8-tetrahydroquinolin-8-yl)amino)methyl)piperazine-1,4-dicarboxylate (5.5g, 11.4 mmol) dissolved in DCE (114 mL, .1M) was added paraformaldehyde (1.72 g, 57 mmol, 5 eq) and acetic acid (.5 mL). After stirring at room temperature for 30 minutes sodium triacetoxyborohydride (6.1 g, 29 mmol, 2.5 eq) was added as one portion. The reaction was tracked by LCMS and went to completion overnight. The mixture was filtered and then partitioned between water and DCM. The aqueous layer was basified and extracted with DCM (3 times). The organic layers were combined dried over anhydrous sodium sulfate, filtered and concentrated. The crude mixture was then purified on a 40 gram combiflash column with a step wise gradient from 0 to 5 to 10 to 15% MeOH in DCM to afford 1-benzyl 4-tert-butyl 2-((methyl((S)-5,6,7,8-tetrahydroquinolin-8-yl)amino)methyl)piperazine-1,4-dicarboxylate diastereomers (3.65 g, 7.4 mmol, 65% yield).

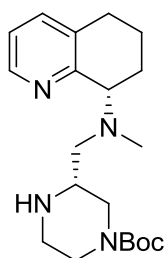
LRF (2.05 g, 36% yield)

^1H NMR (600 MHz, Chloroform-*d*) δ 8.44 – 8.23 (m, 1H), 7.37 – 7.14 (m, 6H), 7.06 – 6.98 (m, 1H), 5.18 – 4.90 (m, 2H), 4.19 – 3.94 (m, 2H), 3.94 – 3.74 (m, 2H), 2.95 – 2.51 (m, 8H), 2.42 (s, 1H), 2.24 – 2.14 (m, 1H), 1.92 (s, 3H), 2.10 – 1.83 (m, 2H), 1.83 – 1.65 (m, 1H), 1.65 – 1.46 (m, 1H), 1.29 (s, 9H).

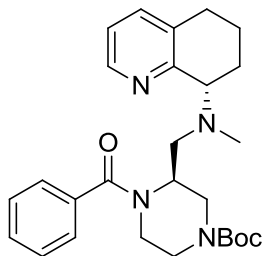
^{13}C NMR (151 MHz, cdcl_3) δ 155.80, 147.06, 146.62, 137.59, 136.42, 128.62, 128.28, 123.50, 122.16, 80.46, 67.71, 64.81, 61.77, 58.54, 55.43, 49.38, 44.16, 42.68, 39.63, 29.04, 28.39, 24.90, 21.59.

Compound 61

1-benzyl 4-tert-butyl 2-((methyl((S)-5,6,7,8-tetrahydroquinolin-8-yl)amino)methyl)piperazine-1,4-dicarboxylate (1.5 g, 3.03 mmol) was dissolved in methanol (50 mL). Degussa Pd/C (150 mg, 10% by mass) was added. The material was then hydrogenated under H₂ gas at 45 psi on a Parr hydrogenator overnight. The crude was filtered through celite and concentrated to afford (S)-tert-butyl 4-benzoyl-3-((methyl((S)-5,6,7,8-tetrahydroquinolin-8-yl)amino)methyl)piperazine-1-carboxylate material was taken onto the next step crude.

Compound 62

1-benzyl 4-tert-butyl 2-((methyl((S)-5,6,7,8-tetrahydroquinolin-8-yl)amino)methyl)piperazine-1,4-dicarboxylate (1.950 g, 3.9 mmol) was dissolved in methanol (50 mL). Degussa Pd/C (195 mg, 10% by mass) was added. The material was then hydrogenated under H₂ gas at 45 psi on a Parr hydrogenator overnight. The crude was filtered through celite and concentrated to afford (R)-tert-butyl 4-benzoyl-3-((methyl((S)-5,6,7,8-tetrahydroquinolin-8-yl)amino)methyl)piperazine-1-carboxylate material was taken onto the next step crude.

Compound 63

Prepared by general acylation procedure from crude **compound 61**.

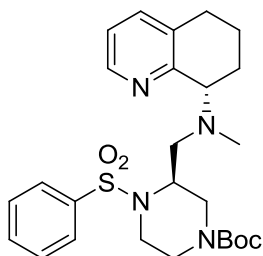
Purified on 4 gram combiflash column with a gradient of 0-20%

MeOH in DCM (190 mg, 77% yield over two steps).

¹H NMR (600 MHz, Chloroform-d) δ 8.45 (d, $J = 4.5$ Hz, 1H), 8.03 (ddd, $J = 8.2, 3.7, 1.3$ Hz, 2H), 7.55 – 7.48 (m, 1H), 7.43 – 7.35 (m, 5H), 4.23 – 3.61 (m, 2H), 3.31 – 2.65 (m, 7H), 2.58 – 2.26 (m, 2H), 2.19 – 1.93 (m, 4H), 1.92 – 1.72 (m, 2H), 1.44 (s, 9H).

¹³C NMR (151 MHz, cdcl₃) δ 169.97, 155.26, 133.11, 130.18, 128.81, 128.46, 127.61, 64.88, 56.14, 46.16, 44.59, 43.32, 38.42, 28.56, 21.07, 18.73, 8.78.

HRMS calc'd for C₂₇H₃₇O₃N₄ 465.28602; found 465.28607 [M+H]

Compound 64

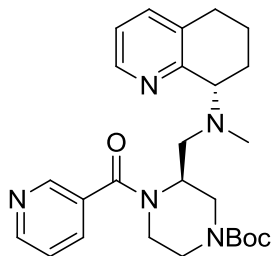
Prepared by general acylation procedure from crude **compound 61**.

Purified on 4 gram combiflash column with a gradient of 0-20%

MeOH in DCM (170 mg, 61% yield over two steps).

HRMS calc'd for C₂₆H₃₇O₄N₄S₁ 501.25300; found 501.25321

[M+H]

Compound 65

Prepared by general acylation procedure from **compound 61**.

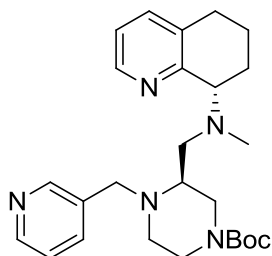
Purified on 4 gram combiflash column with a gradient of 0-15%

MeOH in DCM (253 mg, 65% yield over two steps)

¹H NMR (400 MHz, Chloroform-d) δ 8.70 (s, 1H), 8.62 (d, J = 4.4 Hz, 1H), 8.45 – 8.33 (m, 1H), 7.83 (d, J = 7.8 Hz, 1H), 7.33 (d, J = 7.4 Hz, 2H), 7.03 (t, J = 6.2 Hz, 1H), 4.37 – 3.63 (m, 3H), 3.15 – 2.59 (m, 6H), 2.37 – 2.23 (m, 1H), 2.08 – 1.79 (m, 7H), 1.73 – 1.59 (m, 2H), 1.41 (s, 10H).

¹³C NMR (101 MHz, cdcl₃) δ 150.82, 148.34, 146.80, 136.85, 135.48, 134.18, 132.26, 123.53, 121.88, 80.45, 53.66, 43.89, 37.69, 28.55, 21.25.

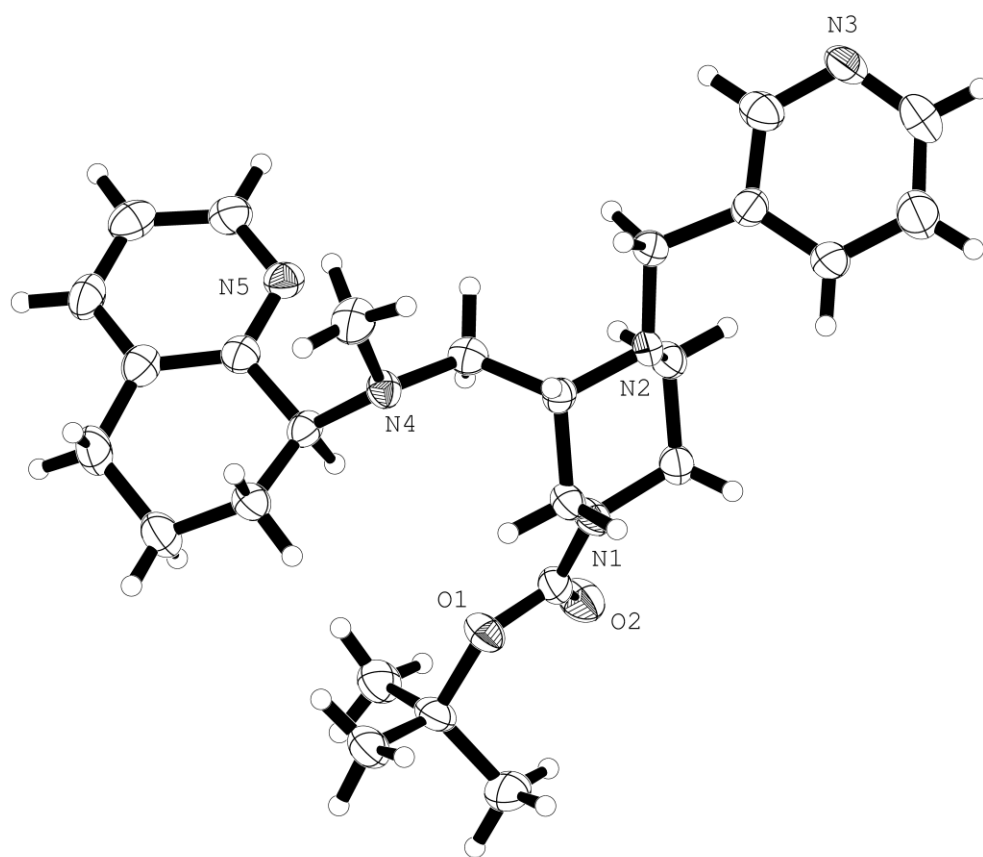
HRMS calc'd for C₂₆H₃₆O₃N₅ 466.28127; found 466.28142 [M+H]

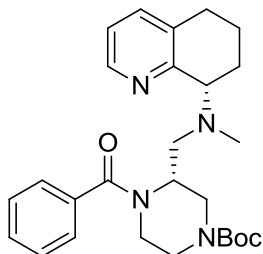
Compound 66

Prepared by general reductive amination procedure from

compound 61. Purified on 4 gram combiflash column with a gradient of 0-15% MeOH in DCM. Material further purified by

recrystallization resulting in crystal structure provided below. (205 mg, 55% yield over two steps).

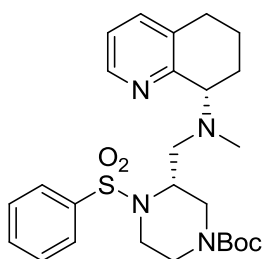


Compound 67

Prepared by general acylation procedure from crude **compound 62**.

Purified on 4 gram combiflash column with a gradient of 0-20% MeOH in DCM (248 mg, 68% yield over two steps).

HRMS calc'd for $C_{27}H_{37}O_3N_4$ 465.28602; found 465.28603 [M+H]

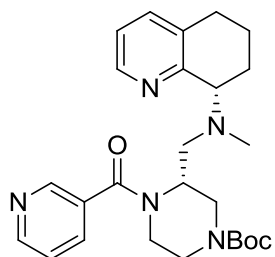
Compound 68

Prepared by general acylation procedure from crude **compound 62**.

Purified on 4 gram combiflash column with a gradient of 0-20% MeOH in DCM (201 mg, 58% yield over two steps).

HRMS calc'd for $C_{26}H_{37}O_4N_4S_1$ 501.25300; found 501.25290

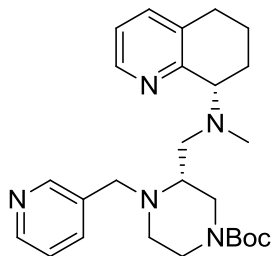
[M+H]

Compound 69

Prepared by general acylation procedure from **compound 62**.

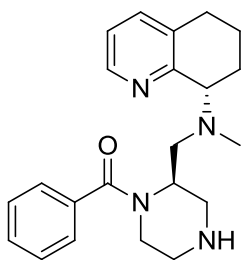
Purified on 4 gram combiflash column with a gradient of 0-15% MeOH in DCM (302 mg, 94% yield over two steps)

HRMS calc'd for $C_{26}H_{36}O_3N_5$ 466.28127; found 466.28149 [M+H]

Compound 70

Prepared by general reductive amination procedure from **compound 62**. Purified on 4 gram combiflash column with a gradient of 0-15% MeOH in DCM (152 mg, 49% yield over two steps)

HRMS calc'd for C₂₆H₃₈O₂N₅ 452.30200; found 452.30216 [M+H]

Compound 71

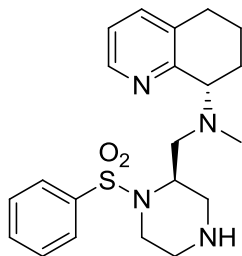
Prepared by general Boc-deprotection procedure from **compound 63**. Purified on 4 gram combiflash column with a gradient of 3-20% MeOH (3.5N NH₄) in DCM (58 mg, 49% yield)

¹H NMR (600 MHz, Chloroform-d) δ 8.56 – 8.36 (m, 1H), 7.46 – 7.29 (m, 5H), 7.07 (dd, *J* = 7.7, 4.7 Hz, 1H), 4.83 – 4.20 (m, 1H), 4.05 – 3.62 (m, 1H), 3.40 – 3.21 (m, 1H), 3.00 – 2.55 (m, 6H), 2.55 – 2.31 (m, 2H), 2.23 – 1.77 (m, 6H), 1.75 – 1.57 (m, 2H).

¹³C NMR (101 MHz, cdCl₃) δ 147.29, 137.03, 136.60, 134.48, 129.57, 128.59, 127.03, 121.92, 64.98, 53.25, 52.33, 46.07, 45.60, 39.91, 29.37, 24.13, 21.30.

LCMS 75% MeOH:H₂O w/ .1% formic acid >95% pure rt= 1.316

HRMS calc'd for C₂₂H₂₉O₁N₄ 365.23359; found 365.23372 [M+H]

Compound 72

Prepared by general Boc-deprotection procedure from **compound 64**.

Purified on 4 gram combiflash column with a gradient of 3-20%

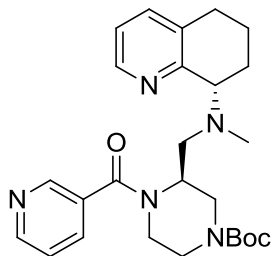
MeOH (3.5N NH₄) in DCM (67 mg, 56% yield)

¹H NMR (600 MHz, Chloroform-d) δ 8.40 (dd, *J* = 4.7, 1.6 Hz, 1H), 7.81 – 7.77 (m, 2H), 7.53 (td, *J* = 7.2, 1.3 Hz, 1H), 7.48 – 7.44 (m, 2H), 7.34 (dd, *J* = 7.9, 1.6 Hz, 1H), 7.03 (dd, *J* = 7.6, 4.7 Hz, 1H), 3.88 (ddd, *J* = 17.4, 8.2, 4.5 Hz, 2H), 3.46 – 3.40 (m, 2H), 3.32 (d, *J* = 12.7 Hz, 1H), 2.81 – 2.71 (m, 4H), 2.69 – 2.61 (m, 3H), 2.55 – 2.48 (m, 1H), 2.48 – 2.38 (m, 1H), 2.31 – 2.26 (m, 1H), 2.06 (dtd, *J* = 11.6, 5.4, 4.6, 2.6 Hz, 1H), 1.98 – 1.89 (m, 1H), 1.73 – 1.59 (m, 2H)

¹³C NMR (151 MHz, cdcl₃) δ 157.31, 147.33, 141.49, 137.09, 134.63, 132.56, 129.27, 129.20, 127.19, 121.96, 65.03, 51.26, 50.81, 50.49, 44.99, 44.71, 41.95, 39.97, 29.44, 25.56, 23.02, 21.48.

LCMS 75% MeOH:H₂O w/ .1% formic acid >95% pure rt= .981

HRMS calc'd for C₂₁H₂₉O₂N₄S₁ 401.20057; found 401.20047 [M+H]

Compound 73

Prepared by general acylation procedure from **compound 65**.

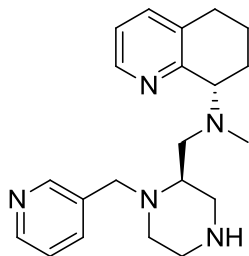
Purified on 4 gram combiflash column with a gradient of 0-15%

MeOH in DCM (253 mg, 65% yield over two steps)

¹H NMR (400 MHz, Chloroform-d) δ 8.70 (s, 1H), 8.62 (d, $J = 4.4$ Hz, 1H), 8.45 – 8.33 (m, 1H), 7.83 (d, $J = 7.8$ Hz, 1H), 7.33 (d, $J = 7.4$ Hz, 2H), 7.03 (t, $J = 6.2$ Hz, 1H), 4.37 – 3.63 (m, 3H), 3.15 – 2.59 (m, 6H), 2.37 – 2.23 (m, 1H), 2.08 – 1.79 (m, 7H), 1.73 – 1.59 (m, 2H), 1.41 (s, 10H).

¹³C NMR (101 MHz, cdcl₃) δ 150.82, 148.34, 146.80, 136.85, 135.48, 134.18, 132.26, 123.53, 121.88, 80.45, 53.66, 43.89, 37.69, 28.55, 21.25.

HRMS calc'd for C₂₆H₃₆O₃N₅ 466.28127; found 466.28142 [M+H]

Compound 74

Prepared by general Boc-deprotection procedure from **compound**

66. Purified on 4 gram combiflash column with a gradient of 3-20%

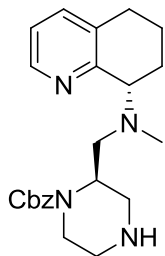
MeOH (3.5N NH₄) in DCM (96 mg, 71% yield)

¹H NMR (600 MHz, Chloroform-d) δ 8.43 (d, *J* = 2.2 Hz, 1H), 8.42 (dd, *J* = 4.6, 1.8 Hz, 2H), 7.58 (dt, *J* = 7.9, 2.0 Hz, 1H), 7.31 – 7.28 (m, 1H), 7.17 (ddd, *J* = 7.8, 4.8, 0.8 Hz, 1H), 7.02 (dd, *J* = 7.7, 4.6 Hz, 1H), 4.00 (d, *J* = 14.0 Hz, 1H), 3.82 (dd, *J* = 8.6, 4.7 Hz, 1H), 3.26 (d, *J* = 14.0 Hz, 1H), 3.17 (s, 2H), 3.09 (dd, *J* = 12.6, 3.2 Hz, 1H), 2.81 – 2.71 (m, 3H), 2.67 (ddt, *J* = 18.5, 15.9, 5.3 Hz, 3H), 2.49 (dtt, *J* = 11.6, 5.9, 3.2 Hz, 2H), 2.41 (dd, *J* = 12.8, 7.7 Hz, 1H), 2.31 (s, 3H), 2.11 (dpd, *J* = 10.8, 7.2, 4.2 Hz, 1H), 1.90 – 1.80 (m, 1H), 1.69 – 1.59 (m, 1H).

¹³C NMR (151 MHz, cdcl₃) δ 157.34, 150.28, 148.45, 147.08, 137.02, 136.57, 135.00, 134.30, 123.46, 122.02, 77.52, 77.31, 77.09, 64.97, 58.34, 56.16, 51.14, 49.64, 49.44, 45.60, 40.22, 29.09, 27.17, 23.71, 22.84, 20.76.

LCMS 75% MeOH:H₂O w/ .1% formic acid >95% pure rt= 1.101

HRMS calc'd for C₂₁H₃₀N₅ 352.24957; found 352.24963 [M+H]

Compound 79

Prepared by general Boc-deprotection procedure from **compound 59**.

Purified on 4 gram combiflash column with a gradient of 3-20% MeOH

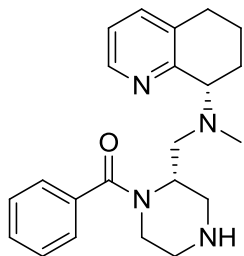
(3.5N NH₄) in DCM (97 mg, 61% yield)

¹H NMR (400 MHz, Chloroform-d) δ 8.43 (dd, *J* = 4.8, 1.7 Hz, 1H), 7.37 – 7.21 (m, 6H), 7.02 (dd, *J* = 7.7, 4.6 Hz, 1H), 5.17 – 5.00 (m, 2H), 4.17 – 3.95 (m, 1H), 3.95 – 3.81 (m, 2H), 3.78 – 3.64 (m, 2H), 3.37 – 3.23 (m, 1H), 2.81 – 2.51 (m, 7H), 2.51 – 2.24 (m, 2H), 2.14 – 2.00 (m, 1H), 1.97 – 1.85 (m, 2H), 1.81 – 1.53 (m, 1H).

¹³C NMR (101 MHz, cdcl₃) δ 157.54, 155.72, 147.29, 137.04, 136.88, 134.51, 128.63, 128.17, 121.91, 67.27, 64.91, 60.61, 53.68, 50.64, 45.28, 39.96, 29.32, 23.44, 21.24.

LCMS 75% MeOH:H₂O w/ .1% formic acid >95% pure rt= .935

HRMS calc'd for C₂₃H₃₁O₂N₄ 395.24415; found 395.24454 [M+H]

Compound 75

Prepared by general Boc-deprotection procedure from **compound 67**.

Purified on 4 gram combiflash column with a gradient of 3-20%

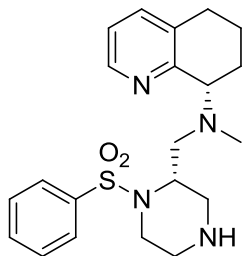
MeOH (3.5N NH₄) in DCM (94 mg, 60% yield).

¹H NMR (600 MHz, Chloroform-d) δ 8.56 – 8.31 (m, 1H), 7.49 – 7.32 (m, 6H), 7.07 (dd, *J* = 7.7, 4.7 Hz, 1H), 4.88 – 4.69 (m, 1H), 4.39 – 4.23 (m, 1H), 4.05 – 3.65 (m, 2H), 3.40 – 3.20 (m, 1H), 3.19 – 2.97 (m, 1H), 2.97 – 2.55 (m, 6H), 2.54 – 2.30 (m, 1H), 2.23 – 1.89 (m, 6H), 1.89 – 1.56 (m, 1H).

¹³C NMR (151 MHz, cdcl₃) δ 177.19, 168.48, 147.22, 146.91, 137.15, 134.56, 129.66, 128.64, 127.26, 127.04, 122.02, 72.41, 50.98, 46.07, 45.53, 39.95, 29.16, 21.28, 21.08, 7.01.

LCMS 75% MeOH:H₂O w/ .1% formic acid >95% pure rt= 1.215

HRMS calc'd for C₂₂H₂₉O₁N₄ 365.23359; found 365.23362 [M+H]

Compound 76

Prepared by general Boc-deprotection procedure from **compound 68**.

Purified on 4 gram combiflash column with a gradient of 3-20%

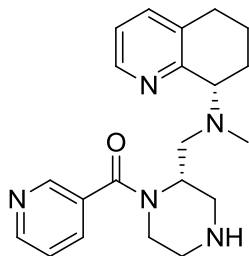
MeOH (3.5N NH₄) in DCM (71 mg, 51% yield)

¹H NMR (400 MHz, Chloroform-d) δ 8.36 (dd, *J* = 4.8, 1.6 Hz, 1H), 7.78 – 7.69 (m, 2H), 7.60 – 7.50 (m, 1H), 7.49 – 7.42 (m, 2H), 7.34 (ddt, *J* = 7.6, 1.8, 0.9 Hz, 1H), 7.06 – 7.03 (m, 1H), 4.04 – 3.89 (m, 3H), 3.73 (dd, *J* = 9.2, 5.7 Hz, 1H), 3.67 – 3.57 (m, 1H), 3.22 (dt, *J* = 12.7, 1.2 Hz, 1H), 3.17 – 3.08 (m, 1H), 2.97 (dt, *J* = 12.6, 2.5 Hz, 1H), 2.80 – 2.54 (m, 5H), 2.20 (s, 3H), 2.00 – 1.72 (m, 3H), 1.59 (dddd, *J* = 18.0, 7.4, 5.5, 2.9 Hz, 1H).

¹³C NMR (101 MHz, cdcl₃) δ 156.87, 147.00, 140.66, 137.52, 134.39, 132.99, 129.50, 127.13, 122.40, 77.64, 77.52, 77.32, 77.00, 64.76, 54.91, 51.07, 50.63, 45.11, 44.10, 41.15, 39.11, 28.98, 23.62, 22.74, 20.98.

LCMS 75% MeOH:H₂O w/ .1% formic acid >95% pure rt= .957

HRMS calc'd for C₂₁H₂₉O₂N₄S₁ 401.20057; found 401.20047 [M+H]

Compound 77

Prepared by general Boc-deprotection procedure from **compound**

69. Purified on 4 gram combiflash column with a gradient of 3-20%

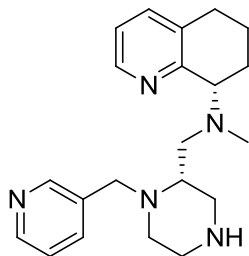
MeOH (3.5N NH₄) in DCM (77 mg, 38% yield)

¹H NMR (400 MHz, Chloroform-d) δ 8.69 – 8.45 (m, 2H), 8.36 – 8.27 (m, 1H), 7.77 (dt, *J* = 7.8, 1.9 Hz, 1H), 7.33 – 7.16 (m, 2H), 7.04 – 6.90 (m, 1H), 4.83 – 4.08 (m, 1H), 3.96 – 3.48 (m, 2H), 3.12 – 2.45 (m, 9H), 2.33 (dt, *J* = 38.9, 8.7 Hz, 1H), 2.01 – 1.79 (m, 3H), 1.76 – 1.48 (m, 2H).

¹³C NMR (101 MHz, cdcl₃) δ 173.24, 169.72, 157.69, 150.56, 150.26, 148.30, 147.96, 146.88, 137.14, 135.60, 134.35, 132.63, 123.39, 121.81, 65.69, 64.65, 56.20, 53.88, 47.46, 46.40, 45.94, 38.99, 38.78, 38.14, 29.20, 27.09, 22.72, 21.33, 21.15.

LCMS 75% MeOH:H₂O w/ .1% formic acid >95% pure rt= 1.262

HRMS calc'd for C₂₁H₂₈O₁N₅ 366.22884; found 366.22895 [M+H]

Compound 78

Prepared by general Boc-deprotection procedure from **compound**

70. Purified on 4 gram combiflash column with a gradient of 3-20%

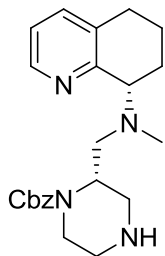
MeOH (3.5N NH₄) in DCM (74 mg, 58% yield)

¹H NMR (400 MHz, Chloroform-d) δ 8.46 – 8.36 (m, 2H), 8.22 (dd, *J* = 4.7, 1.6 Hz, 1H), 7.52 (dt, *J* = 7.8, 2.0 Hz, 1H), 7.30 (dd, *J* = 7.7, 1.7 Hz, 1H), 7.15 (dd, *J* = 7.8, 4.7 Hz, 1H), 6.93 (dd, *J* = 7.7, 4.7 Hz, 1H), 4.27 (d, *J* = 14.2 Hz, 1H), 3.88 (t, *J* = 6.6 Hz, 1H), 3.15 (d, *J* = 14.2 Hz, 1H), 3.03 – 2.95 (m, 1H), 2.81 – 2.67 (m, 3H), 2.67 – 2.58 (m, 1H), 2.53 (ddd, *J* = 11.9, 4.7, 3.3 Hz, 2H), 2.50 – 2.41 (m, 2H), 2.36 (s, 3H), 2.16 – 2.01 (m, 1H), 1.98 (s, 2H), 1.96 – 1.87 (m, 2H), 1.70 – 1.56 (m, 1H).

¹³C NMR (101 MHz, cdcl₃) δ 157.43, 150.41, 148.18, 147.13, 136.84, 136.67, 135.41, 134.37, 123.34, 121.82, 77.58, 77.47, 77.26, 76.94, 64.93, 59.54, 56.29, 55.54, 52.55, 50.93, 45.99, 40.53, 29.26, 24.46, 22.85, 21.08.

LCMS 75% MeOH:H₂O w/ .1% formic acid >95% pure rt= 1.022

HRMS calc'd for C₂₁H₃₀N₅ 352.24957; found 352.24965 [M+H]

Compound 80

Prepared by general Boc-deprotection procedure from **compound 60**.

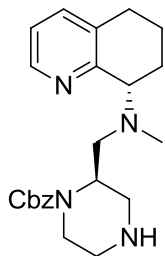
Purified on 4 gram combiflash column with a gradient of 3-20% MeOH (3.5N NH₄) in DCM (104 mg, 65% yield)

¹H NMR (600 MHz, Chloroform-d) δ 8.43 (dd, *J* = 4.8, 1.7 Hz, 1H), 7.39 – 7.26 (m, 6H), 7.05 (dd, *J* = 7.7, 4.7 Hz, 1H), 5.18 – 5.04 (m, 2H), 4.28 – 4.01 (m, 1H), 3.98 – 3.78 (m, 2H), 3.59 – 3.33 (m, 2H), 3.17 (d, *J* = 12.6 Hz, 1H), 3.04 (dd, *J* = 13.3, 7.8 Hz, 1H), 3.00 – 2.88 (m, 2H), 2.87 – 2.60 (m, 5H), 2.38 – 2.15 (m, 3H), 2.04 – 1.79 (m, 3H), 1.72 – 1.57 (m, 1H).

¹³C NMR (151 MHz, cdCl₃) δ 157.67, 147.00, 137.12, 136.82, 134.23, 128.65, 128.21, 123.96, 122.06, 67.45, 64.93, 54.76, 49.86, 45.77, 45.29, 40.43, 39.25, 29.11, 20.97.

LCMS 75% MeOH:H₂O w/ .1% formic acid >95% pure rt= .823

HRMS calc'd for C₂₃H₃₁O₂N₄ 395.24415; found 395.24461 [M+H]

Compound 81

Prepared by general Boc-deprotection procedure from **compound 59**.

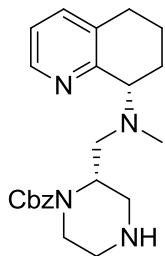
Purified on 4 gram combiflash column with a gradient of 3-20% MeOH (3.5N NH₄) in DCM (97 mg, 61% yield)

¹H NMR (400 MHz, Chloroform-d) δ 8.43 (dd, *J* = 4.8, 1.7 Hz, 1H), 7.37 – 7.21 (m, 6H), 7.02 (dd, *J* = 7.7, 4.6 Hz, 1H), 5.17 – 5.00 (m, 2H), 4.17 – 3.95 (m, 1H), 3.95 – 3.81 (m, 2H), 3.78 – 3.64 (m, 2H), 3.37 – 3.23 (m, 1H), 2.81 – 2.51 (m, 7H), 2.51 – 2.24 (m, 2H), 2.14 – 2.00 (m, 1H), 1.97 – 1.85 (m, 2H), 1.81 – 1.53 (m, 1H).

¹³C NMR (101 MHz, cdcl₃) δ 157.54, 155.72, 147.29, 137.04, 136.88, 134.51, 128.63, 128.17, 121.91, 67.27, 64.91, 60.61, 53.68, 50.64, 45.28, 39.96, 29.32, 23.44, 21.24.

LCMS 75% MeOH:H₂O w/ .1% formic acid >95% pure rt= .935

HRMS calc'd for C₂₃H₃₁O₂N₄ 395.24415; found 395.24454 [M+H]

Compound 82

Prepared by general Boc-deprotection procedure from **compound 60**.

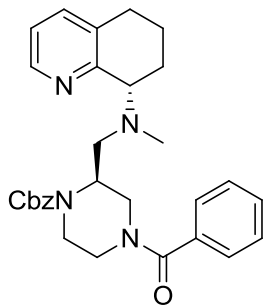
Purified on 4 gram combiflash column with a gradient of 3-20% MeOH (3.5N NH₄) in DCM (104 mg, 65% yield)

¹H NMR (600 MHz, Chloroform-d) δ 8.43 (dd, *J* = 4.8, 1.7 Hz, 1H), 7.39 – 7.26 (m, 6H), 7.05 (dd, *J* = 7.7, 4.7 Hz, 1H), 5.18 – 5.04 (m, 2H), 4.28 – 4.01 (m, 1H), 3.98 – 3.78 (m, 2H), 3.59 – 3.33 (m, 2H), 3.17 (d, *J* = 12.6 Hz, 1H), 3.04 (dd, *J* = 13.3, 7.8 Hz, 1H), 3.00 – 2.88 (m, 2H), 2.87 – 2.60 (m, 5H), 2.38 – 2.15 (m, 3H), 2.04 – 1.79 (m, 3H), 1.72 – 1.57 (m, 1H).

¹³C NMR (151 MHz, cdCl₃) δ 157.67, 147.00, 137.12, 136.82, 134.23, 128.65, 128.21, 123.96, 122.06, 67.45, 64.93, 54.76, 49.86, 45.77, 45.29, 40.43, 39.25, 29.11, 20.97.

LCMS 75% MeOH:H₂O w/ .1% formic acid >95% pure rt= .823

HRMS calc'd for C₂₃H₃₁O₂N₄ 395.24415; found 395.24461 [M+H]

Compound 83

Prepared by general acylation procedure from **compound 81**.

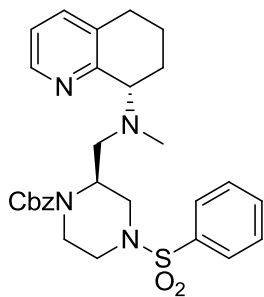
Purified on 4 gram combiflash column with a gradient of 0-20%

MeOH in DCM (173 mg, 78% yield over two steps)

¹H NMR (400 MHz, Chloroform-d) δ 8.36 (s, 1H), 7.46 – 7.20 (m, 11H), 7.00 (dd, $J = 7.7, 4.7$ Hz, 1H), 5.16 – 5.08 (m, 2H), 4.93 – 4.43 (m, 1H), 4.15 – 3.78 (m, 2H), 3.60 – 3.25 (m, 2H), 3.09 – 2.47 (m, 6H), 2.34 – 1.68 (m, 4H), 1.67 – 1.34 (m, 2H).

¹³C NMR (101 MHz, cdcl₃) δ 171.10, 158.52, 155.71, 146.66, 136.79, 134.31, 130.07, 128.69, 128.31, 127.68, 121.76, 113.72, 67.59, 65.44, 50.06, 41.91, 39.47, 30.88, 28.87, 21.29, 19.53.

HRMS calc'd for C₃₀H₃₅O₃N₄ 499.27037; found 499.27026 [M+H]

Compound 84

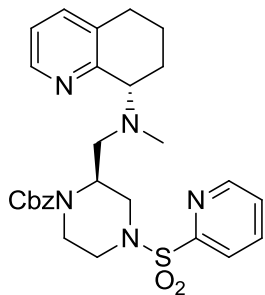
Prepared by general acylation procedure from **compound 81**.

Purified on 4 gram combiflash column with a gradient of 0-15%

MeOH in DCM (93 mg, 69% yield over two steps)

HRMS calc'd for C₂₉H₃₅O₄N₄S₁ 535.23735; found 535.23759

[M+H]

Compound 85

Prepared by general acylation procedure from **compound 81**.

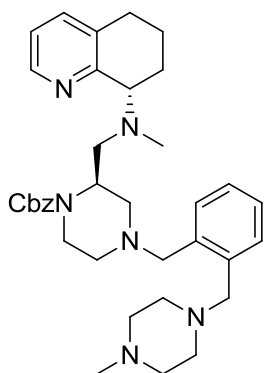
Purified on 4 gram combiflash column with a gradient of 0-20%

MeOH in DCM (290 mg, 71% yield over two steps)

^1H NMR (600 MHz, Chloroform-*d*) δ 8.66 (ddd, $J = 4.8, 1.7, 0.9$ Hz, 1H), 8.41 (d, $J = 4.4$ Hz, 1H), 7.92 – 7.86 (m, 2H), 7.46 (ddd, $J = 7.1, 4.7, 1.6$ Hz, 1H), 7.33 – 7.25 (m, 6H), 7.01 (dd, $J = 7.6, 4.7$ Hz, 1H), 5.09 (q, $J = 12.4$ Hz, 2H), 4.30 – 4.07 (m, 1H), 4.06 – 3.89 (m, 2H), 3.83 – 3.75 (m, 1H), 3.35 – 3.25 (m, 1H), 3.15 – 2.97 (m, 1H), 2.98 – 2.87 (m, 1H), 2.75 – 2.67 (m, 4H), 2.63 (dt, $J = 16.4, 4.8$ Hz, 1H), 2.28 – 2.00 (m, 4H), 1.99 – 1.88 (m, 1H), 1.84 – 1.73 (m, 1H), 1.73 – 1.62 (m, 1H).

^{13}C NMR (151 MHz, cdcl_3) δ 158.38, 156.24, 150.24, 146.89, 138.16, 136.64, 134.28, 128.68, 128.30, 128.24, 126.91, 123.28, 121.58, 67.60, 65.41, 56.36, 53.72, 46.87, 46.65, 39.90, 37.63, 29.34, 28.71, 21.58.

HRMS calc'd for $\text{C}_{28}\text{H}_{34}\text{O}_4\text{N}_5\text{S}$ 536.23260; found 536.23248 [M+H]

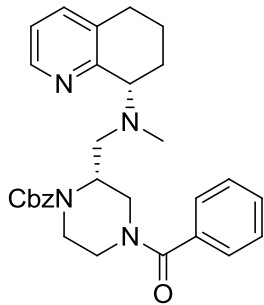
Compound 87

Prepared by general reductive amination procedure from

compound 81. Purified on 4 gram combiflash column with a

gradient of 0-15% MeOH in DCM (127 mg, 53% yield over two steps)

HRMS calc'd for $\text{C}_{36}\text{H}_{49}\text{O}_2\text{N}_6$ 597.39115; found 597.39174 [M+H]

Compound 88

Prepared by general acylation procedure from **compound 82**.

Purified on 4 gram combiflash column with a gradient of 0-20%

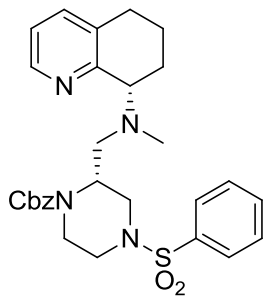
MeOH in DCM (185 mg, 73% yield over two steps)

¹H NMR (400 MHz, Chloroform-d) δ 8.39 (s, 1H), 7.49 – 7.16 (m, 11H), 7.01 (d, *J* = 5.8 Hz, 1H), 5.18 – 5.02 (m, 2H), 4.78 – 4.38 (m,

1H), 4.31 – 3.77 (m, 2H), 3.20 – 2.52 (m, 9H), 2.48 – 1.68 (m, 5H), 1.74 – 1.47 (m, 2H).

¹³C NMR (101 MHz, cdcl₃) δ 171.38, 147.00, 136.71, 132.09, 130.04, 128.74, 128.65, 128.65, 128.32, 128.27, 127.62, 121.72, 77.63, 77.46, 77.31, 76.99, 67.63, 64.85, 53.70, 39.68, 29.27, 28.52, 20.99.

HRMS calc'd for C₃₀H₃₅O₃N₄ 499.27037; found 499.27019 [M+H]

Compound 89

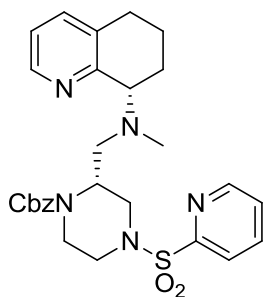
Prepared by general acylation procedure from **compound 82**.

Purified on 4 gram combiflash column with a gradient of 0-15%

MeOH in DCM (87 mg, 65% yield over two steps)

HRMS calc'd for C₂₉H₃₅O₄N₄S₁ 535.23735; found 535.23749

[M+H]

Compound 90

Prepared by general acylation procedure from **compound 82**.

Purified on 4 gram combiflash column with a gradient of 0-20%

MeOH in DCM (311 mg, 68% yield over two steps)

^1H NMR (400 MHz, Chloroform-*d*) δ 8.62 (dt, $J = 4.8, 1.3$ Hz, 1H),

8.38 – 8.34 (m, 1H), 7.84 (d, $J = 1.3$ Hz, 1H), 7.84 – 7.82 (m, 1H),

7.42 (ddd, $J = 6.0, 4.7, 3.0$ Hz, 1H), 7.29 (d, $J = 7.4$ Hz, 1H), 7.23 (d, $J = 11.8$ Hz, 5H),

6.98 (dd, $J = 7.7, 4.6$ Hz, 1H), 5.06 – 4.95 (m, 2H), 4.39 – 4.08 (m, 1H), 4.03 – 3.93 (m,

1H), 3.92 – 3.71 (m, 1H), 3.11 – 2.92 (m, 2H), 2.92 – 2.82 (m, 1H), 2.74 (dd, $J = 13.0, 5.7$

Hz, 2H), 2.66 (dd, $J = 11.9, 3.9$ Hz, 2H), 2.63 – 2.53 (m, 1H), 2.47 – 2.24 (m, 3H), 1.99 –

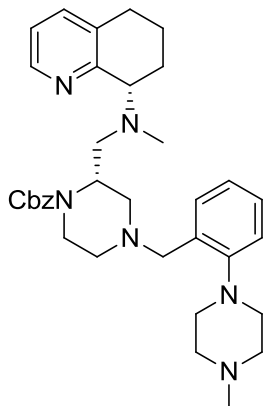
1.86 (m, 2H), 1.86 – 1.72 (m, 1H), 1.68 – 1.47 (m, 1H).

^{13}C NMR (101 MHz, cdcl_3) δ 157.80, 155.83, 150.23, 146.78, 138.22, 136.91, 134.27,

128.61, 128.25, 127.01, 123.39, 121.71, 67.58, 64.79, 53.74, 46.68, 39.82, 29.32, 27.32,

21.48.

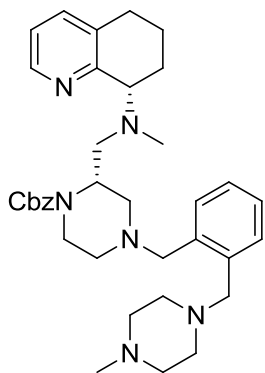
HRMS calc'd for $\text{C}_{28}\text{H}_{34}\text{O}_4\text{N}_5\text{S}$ 536.23260; found 536.23279 [M+H]

Compound 91

Prepared by general reductive amination procedure from **compound 82**. Purified on 4 gram combiflash column with a gradient of 0-15% MeOH in DCM (400 mg, 71% yield over two steps)

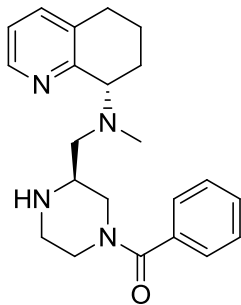
^1H NMR (600 MHz, Chloroform-*d*) δ 8.45 – 8.27 (m, 1H), 7.39 – 7.17 (m, 7H), 7.17 – 7.07 (m, 1H), 7.02 – 7.00 (m, 1H), 6.96 – 6.91 (m, 2H), 5.10 – 5.02 (m, 2H), 4.32 – 4.03 (m, 1H), 3.91 – 3.60 (m, 3H), 3.57 – 3.42 (m, 1H), 3.35 (d, $J = 12.8$ Hz, 1H), 3.11 – 2.94 (m, 4H), 2.94 – 2.83 (m, 3H), 2.83 – 2.58 (m, 3H), 2.58 – 2.35 (m, 4H), 2.29 (s, 3H), 2.17 – 2.06 (m, 1H), 1.96 (dtd, $J = 45.9, 11.4, 5.9$ Hz, 1H), 1.85 – 1.69 (m, 2H), 1.68 – 1.43 (m, 3H).

^{13}C NMR (151 MHz, cdcl_3) δ 158.41, 152.51, 146.86, 136.51, 133.92, 132.91, 131.24, 128.55, 128.19, 128.01, 123.29, 121.48, 119.86, 67.19, 65.07, 57.84, 55.98, 55.30, 54.15, 53.72, 53.09, 52.87, 46.41, 40.48, 40.17, 29.31, 21.49.

Compound 92

Prepared by general reductive amination procedure from material 3-25 LRF. Purified on 4 gram combiflash column with a gradient of 0-15% MeOH in DCM (200 mg, 73% yield over two steps)

HRMS calc'd for $\text{C}_{36}\text{H}_{49}\text{O}_2\text{N}_6$ 597.39115; found 597.39205 [M+H]

Compound 93

Prepared by general hydrogenation procedure from **compound 83**.

Purified on 4 gram combiflash column with a gradient of 3-20% MeOH (3.5N NH₄) in DCM (73 mg, 67% yield)

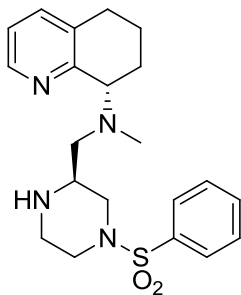
¹H NMR (400 MHz, Chloroform-d) δ 8.35 (d, *J* = 25.4 Hz, 1H), 7.38 – 7.25 (m, 6H), 7.01 (d, *J* = 6.3 Hz, 1H), 4.47 (dd, *J* = 22.8,

13.1 Hz, 1H), 3.93 – 3.74 (m, 1H), 3.61 – 3.43 (m, 1H), 3.16 – 2.97 (m, 1H), 2.95 – 2.47 (m, 7H), 2.46 – 2.37 (m, 1H), 2.37 – 2.24 (m, 4H), 1.99 – 1.84 (m, 2H), 1.70 – 1.55 (m, 1H).

¹³C NMR (101 MHz, cdcl₃) δ 173.30, 157.68, 147.03, 136.99, 134.18, 129.79, 128.66, 127.10, 121.84, 57.63, 54.09, 48.75, 46.39, 45.48, 39.98, 29.42, 25.03, 22.84, 21.46.

LCMS 75% MeOH:H₂O w/ .1% formic acid >95% pure rt= .721

HRMS calc'd for C₂₂H₂₉O₁N₄ 365.23359; found 365.23373 [M+H]

Compound 94

Prepared by general hydrogenation procedure from **compound 84**.

Purified on 4 gram combiflash column with a gradient of 3-20%

MeOH (3.5N NH₄) in DCM (47 mg, 78% yield)

¹H NMR (600 MHz, Chloroform-d) δ 8.41 (dd, *J* = 4.7, 1.7 Hz, 1H),

7.73 – 7.70 (m, 2H), 7.59 – 7.54 (m, 1H), 7.52 – 7.48 (m, 2H), 7.33

(dd, *J* = 7.7, 1.6 Hz, 1H), 7.05 (dd, *J* = 7.7, 4.7 Hz, 1H), 3.87 (dd, *J* = 9.4, 5.6 Hz, 1H),

3.59 (dq, *J* = 11.0, 2.6 Hz, 1H), 3.55 – 3.50 (m, 1H), 2.98 (dt, *J* = 11.6, 2.9 Hz, 1H), 2.80

– 2.62 (m, 4H), 2.56 (dd, *J* = 12.8, 3.8 Hz, 2H), 2.40 (s, 3H), 2.40 – 2.27 (m, 2H), 1.99 –

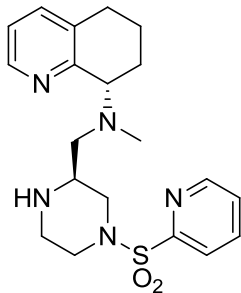
1.92 (m, 2H), 1.92 – 1.77 (m, 3H), 1.72 – 1.61 (m, 1H).

¹³C NMR (151 MHz, cdcl₃) δ 157.74, 147.11, 136.98, 135.63, 134.10, 132.96, 129.19,

127.97, 121.86, 64.71, 57.17, 52.98, 50.16, 46.74, 45.00, 41.00, 29.45, 25.39, 21.59.

LCMS 75% MeOH:H₂O w/ .1% formic acid >95% pure rt= .885

HRMS calc'd for C₂₁H₂₉O₂N₄S₁ 401.20057; found 401.20049 [M+H]

Compound 95

Prepared by general hydrogenation procedure from **compound 85**.

Purified on 4 gram combiflash column with a gradient of 3-20%

MeOH (3.5N NH₄) in DCM.

¹H NMR (600 MHz, Chloroform-*d*) δ 8.66 (dt, *J* = 4.7, 1.2 Hz, 1H),

8.40 – 8.37 (m, 1H), 7.91 – 7.84 (m, 2H), 7.45 (ddd, *J* = 6.9, 4.7, 2.3

Hz, 1H), 7.35 – 7.32 (m, 1H), 7.04 (dd, *J* = 7.7, 4.7 Hz, 1H), 3.89 (dd, *J* = 9.5, 5.7 Hz,

1H), 3.72 (dq, *J* = 12.0, 2.6 Hz, 1H), 3.69 – 3.65 (m, 1H), 3.05 (dt, *J* = 11.7, 3.0 Hz, 1H),

2.88 (td, *J* = 11.4, 3.0 Hz, 1H), 2.80 – 2.71 (m, 3H), 2.65 (dt, *J* = 12.8, 5.1 Hz, 1H), 2.59

(dd, *J* = 13.0, 3.5 Hz, 1H), 2.49 – 2.42 (m, 3H), 2.32 (s, 2H), 2.02 – 1.90 (m, 3H), 1.85 –

1.77 (m, 1H), 1.65 (ttq, *J* = 13.4, 8.0, 2.6 Hz, 1H).

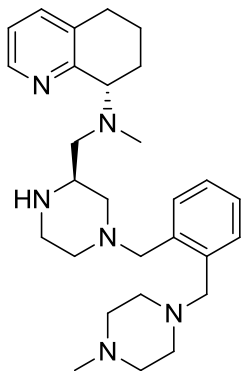
¹³C NMR (151 MHz, cdcl₃) δ 157.46, 156.12, 150.27, 146.94, 138.07, 137.25, 134.24,

126.82, 123.24, 121.97, 64.75, 56.86, 53.14, 50.05, 46.80, 44.76, 39.88, 29.41, 24.88,

21.54.

LCMS 25-95% MeOH:H₂O w/ .1% formic acid >95% pure rt= .605

HRMS calc'd for C₂₀H₂₈O₂N₅S 402.19582; found 402.19586 [M+H]

Compound 97

Prepared by general acidic CBZ removal procedure from **compound**

87. Purified by acid extraction followed by being ran through a plug of silica in a pipette with MeOH:DCM 1:3 (30 mg, 31% yield)

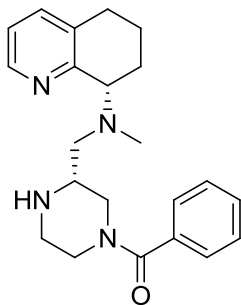
^1H NMR (400 MHz, Chloroform-*d*) δ 8.53 – 8.23 (m, 1H), 7.46 – 7.16 (m, 3H), 7.11 (ddd, $J = 7.1, 3.2, 1.4$ Hz, 2H), 6.98 (dd, $J = 7.6, 4.7$ Hz, 1H), 3.94 – 3.72 (m, 1H), 3.73 – 3.64 (m, 2H), 3.62 – 3.51

(m, 2H), 3.51 – 3.32 (m, 2H), 3.07 – 2.77 (m, 2H), 2.77 – 2.49 (m, 7H), 2.49 – 2.25 (m, 10H), 2.23 – 2.12 (m, 2H), 2.12 – 2.03 (m, 2H), 2.03 – 1.71 (m, 3H), 1.71 – 1.41 (m, 2H).

^{13}C NMR (101 MHz, cdCl_3) δ 146.91, 141.94, 136.52, 131.40, 130.30, 128.80, 127.92, 65.08, 62.07, 54.99, 46.06, 31.80, 22.87, 14.36.

LCMS 75-95% MeOH:H₂O w/ .1% formic acid >95% pure $t_r = .475$

HRMS calc'd for C₂₀H₂₈O₂N₅S 462.34712; found 462.34706 [M+H]

Compound 98

Prepared by general hydrogenation procedure from **compound 88**.

Purified on 4 gram combiflash column with a gradient of 3-20%

MeOH (3.5N NH₄) in DCM (79 mg, 66% yield)

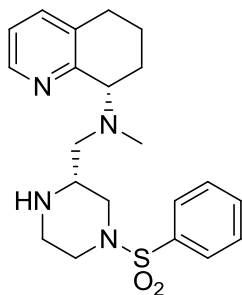
¹H NMR (400 MHz, Chloroform-d) δ 8.49 – 8.34 (m, 1H), 7.44 – 7.28 (m, 6H), 7.04 (dd, *J* = 7.7, 4.8 Hz, 1H), 4.57 – 4.37 (m, 1H),

3.98 – 3.74 (m, 1H), 3.62 – 3.45 (m, 1H), 3.20 – 2.92 (m, 1H), 2.90 – 2.57 (m, 5H), 2.51 – 2.33 (m, 4H), 2.29 – 2.20 (m, 3H), 2.18 – 2.02 (m, 1H), 1.87 – 1.57 (m, 2H).

¹³C NMR (101 MHz, cdcl₃) δ 172.79, 157.44, 147.52, 137.00, 136.22, 134.43, 129.76, 128.67, 127.17, 122.02, 64.42, 57.88, 53.65, 46.10, 39.98, 29.91, 28.63, 23.70, 22.86, 21.57.

LCMS 75% MeOH:H₂O w/ .1% formic acid >95% pure rt= .718

HRMS calc'd for C₂₂H₂₉O₁N₄ 365.23359; found 365.23383 [M+H]

Compound 99

Prepared by general hydrogenation procedure from **compound 89**.

Purified on 4 gram combiflash column with a gradient of 3-20%

MeOH (3.5N NH₄) in DCM (26 mg, 46% yield)

¹H NMR (600 MHz, Chloroform-d) δ 8.39 (dd, *J* = 4.6, 1.8 Hz, 1H),

7.70 – 7.67 (m, 2H), 7.56 – 7.52 (m, 1H), 7.47 (dd, *J* = 8.4, 7.0 Hz,

2H), 7.30 (dd, *J* = 7.6, 1.6 Hz, 1H), 7.00 (dd, *J* = 7.7, 4.7 Hz, 1H), 3.84 (dd, *J* = 9.6, 5.9

Hz, 1H), 3.55 – 3.50 (m, 1H), 3.46 – 3.42 (m, 1H), 3.38 (q, *J* = 7.2 Hz, 1H), 3.30 (q, *J* =

7.2 Hz, 1H), 2.94 – 2.79 (m, 4H), 2.77 – 2.60 (m, 2H), 2.52 – 2.47 (m, 1H), 2.34 (s, 3H),

2.12 – 2.04 (m, 2H), 1.97 – 1.90 (m, 2H), 1.73 (tdd, *J* = 12.5, 9.4, 2.8 Hz, 1H), 1.64 (qdd,

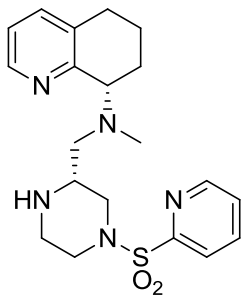
J = 10.8, 5.1, 2.4 Hz, 1H).

¹³C NMR (101 MHz, cdcl₃) δ 157.23, 147.36, 137.04, 135.51, 134.44, 132.97, 129.19,

127.94, 122.07, 64.64, 57.33, 53.67, 49.91, 46.60, 44.87, 39.92, 29.48, 24.02, 21.57.

LCMS 75% MeOH:H₂O w/ .1% formic acid >95% pure rt= .722

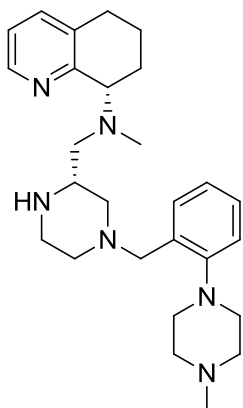
HRMS calc'd for C₂₁H₂₉O₂N₄S₁ 401.20057; found 401.20046 [M+H]

Compound 100

Prepared by general acidic Cbz deprotection procedure from **compound 90**. Purified on 4 gram combiflash column with a gradient of 3-20% MeOH (3.5N NH₄) in DCM (83 mg, 74% yield)

¹H NMR (400 MHz, Chloroform-*d*) δ 8.66 (dt, $J = 4.8, 1.3$ Hz, 1H), 8.41 (dd, $J = 4.7, 1.7$ Hz, 1H), 7.93 – 7.81 (m, 2H), 7.44 (ddd, $J = 6.8, 4.7, 2.2$ Hz, 1H), 7.31 (dd, $J = 7.7, 1.7$ Hz, 1H), 7.02 (dd, $J = 7.7, 4.6$ Hz, 1H), 3.89 – 3.81 (m, 1H), 3.73 – 3.59 (m, 2H), 2.98 – 2.60 (m, 7H), 2.54 – 2.46 (m, 1H), 2.43 – 2.37 (m, 1H), 2.35 (s, 3H), 2.14 – 2.04 (m, 1H), 2.02 – 1.90 (m, 1H), 1.82 – 1.60 (m, 2H).

LCMS 50-95% MeOH:H₂O w/ .1% formic acid >95% pure rt= .503

Compound 101

Prepared by general hydrogenation procedure from **compound 91**.

Purified on 4 gram combiflash column with a gradient of 3-20%

MeOH (3.5N NH₄) in DCM (174 mg, 60% yield)

¹H NMR (400 MHz, Chloroform-*d*) δ 8.39 (dd, *J* = 5.0, 1.5 Hz, 1H),

7.33 – 7.28 (m, 2H), 7.20 – 7.15 (m, 1H), 7.06 – 6.96 (m, 3H), 3.86

– 3.81 (m, 1H), 3.55 – 3.40 (m, 2H), 3.05 – 2.82 (m, 8H), 2.82 –

2.57 (m, 4H), 2.57 – 2.46 (m, 4H), 2.46 – 2.41 (m, 2H), 2.30 (s, 3H), 2.26 (s, 3H), 2.22 –

2.12 (m, 1H), 2.01 (dddd, *J* = 13.2, 8.3, 6.1, 2.5 Hz, 1H), 1.97 – 1.86 (m, 1H), 1.85 – 1.70

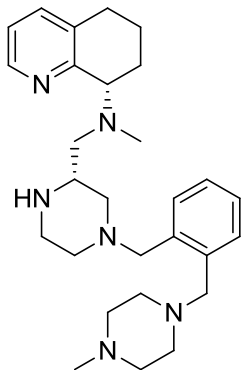
(m, 2H), 1.62 (dtdd, *J* = 13.2, 10.6, 5.2, 2.6 Hz, 1H).

¹³C NMR (101 MHz, cdcl₃) δ 157.58, 152.53, 147.29, 136.93, 134.42, 133.07, 131.20,

127.93, 123.43, 121.88, 120.00, 77.51, 64.37, 58.11, 57.33, 55.88, 53.66, 53.29, 52.78,

50.47, 46.31, 39.65, 29.48, 24.21, 21.46.

LCMS 50-95% MeOH:H₂O w/ .1% formic acid >95% pure rt= .460

Compound 102

Prepared by general acidic CBZ removal procedure from **compound**

92. Purified by acid extraction followed by being ran through a plug of silica in a pipette with MeOH:DCM 1:3 (45 mg, 29% yield)

^1H NMR (600 MHz, Chloroform-*d*) δ 8.41 (dd, $J = 4.7, 1.7$ Hz, 1H), 7.31 (dd, $J = 7.7, 1.7$ Hz, 1H), 7.28 – 7.23 (m, 2H), 7.19 – 7.14 (m, 2H), 7.01 (dd, $J = 7.7, 4.6$ Hz, 1H), 3.84 (dd, $J = 9.3, 6.0$ Hz, 1H),

3.65 – 3.56 (m, 2H), 3.52 (dd, $J = 13.1, 10.9$ Hz, 2H), 2.92 – 2.70 (m, 6H), 2.64 (dt, $J = 16.8, 4.7$ Hz, 2H), 2.60 – 2.30 (m, 8H), 2.31 – 2.20 (m, 7H), 2.09 – 1.99 (m, 2H), 1.95 (dtd, $J = 15.5, 9.4, 7.7, 4.6$ Hz, 2H), 1.86 – 1.74 (m, 2H), 1.65 (tddd, $J = 13.2, 10.4, 6.5, 4.0$ Hz, 1H).

^{13}C NMR (151 MHz, cdcl_3) δ 157.82, 147.30, 137.74, 136.84, 134.31, 130.43, 130.37, 126.86, 121.87, 60.55, 60.31, 55.51, 46.29, 39.36, 29.48, 21.56.

LCMS 75-95% MeOH:H₂O w/ .1% formic acid >95% pure $r_t = .456$

HRMS calc'd for $\text{C}_{20}\text{H}_{28}\text{O}_2\text{N}_5\text{S}$ 462.34712; found 462.34723 [M+H]

Chapter 2: Dual X4/R5 Modulators

2.1 CXCR4/CCR5 as a Therapeutic Target

Current HIV regimens require multiple antiviral drugs to arrest ongoing viral replication and restore immune function.^{1,2} These so-called “drug cocktails” work by utilizing several mechanisms of action to disrupt HIV replication. The drugs typically employed in this strategy include entry/fusion inhibitors, non-nucleoside and nucleoside reverse transcriptase inhibitors (NNRTIs/NRTIs), integrase inhibitors, and protease inhibitors. Unfortunately, these so-called “drug cocktails” come with significant financial burden, a continually emerging set of long term side effects, and the potential for resistance if not taken as prescribed.^{3,4} We propose that a multi-target single agent treatment for HIV may decrease cost of treatment and help alleviate side effects due to drug-drug interactions.⁵⁻⁷

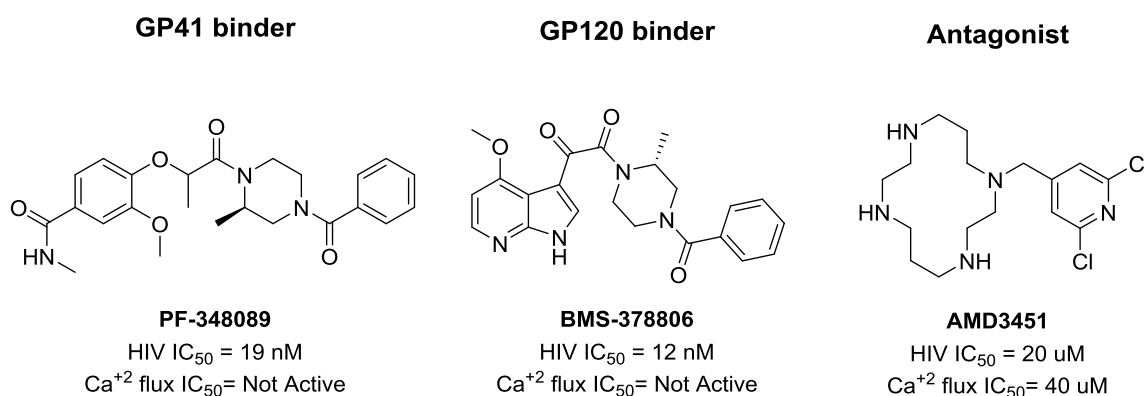


Figure 2.1: Tropism independent small molecule entry inhibitors

We are particularly interested in the development of chemokine HIV entry inhibitors because they offer a host of potential resistance advantages.⁸⁻¹¹ Central to the development of entry inhibitors is tropism dependence. Due to the evolution of different

HIV glycoproteins it exists as three tropic forms; M-tropic targeting CCR5, T-tropic targeting CXCR4, and mixed tropic strains that target both CCR5 and CXCR4.¹² Small molecules (Figure 2.1) that bind to the viral entry proteins are inherently tropism independent. Glycoprotein binders can be split into two major therapeutic targets gp41 and gp120, both of which are necessary for viral entry. Gp41 binders such as PF-348089 have been the subject of intense research as gp41 is tightly conserved between HIV strains. The FDA approved poly-peptide Enfuvirtide binds to gp41 and interferes with all three tropisms of HIV, unfortunately because gp41 is a viral target the risk of mutations are elevated.^{13,14} BMS's highly potent BMS-378806 binds to gp120 very tightly, and is effective against both CXCR4 and CCR5 using virus. The only previously reported dual-tropic antagonist of CXCR4 and CCR5 is AMD3451 which was weakly potent (approximately 20 μ M against both tropic strains). It hasn't been conclusively proven that AMD3451 is a chemokine based entry inhibitor (active in both signaling assays, but very little mechanistic data), but it was still considered a proof of concept molecule for our studies.

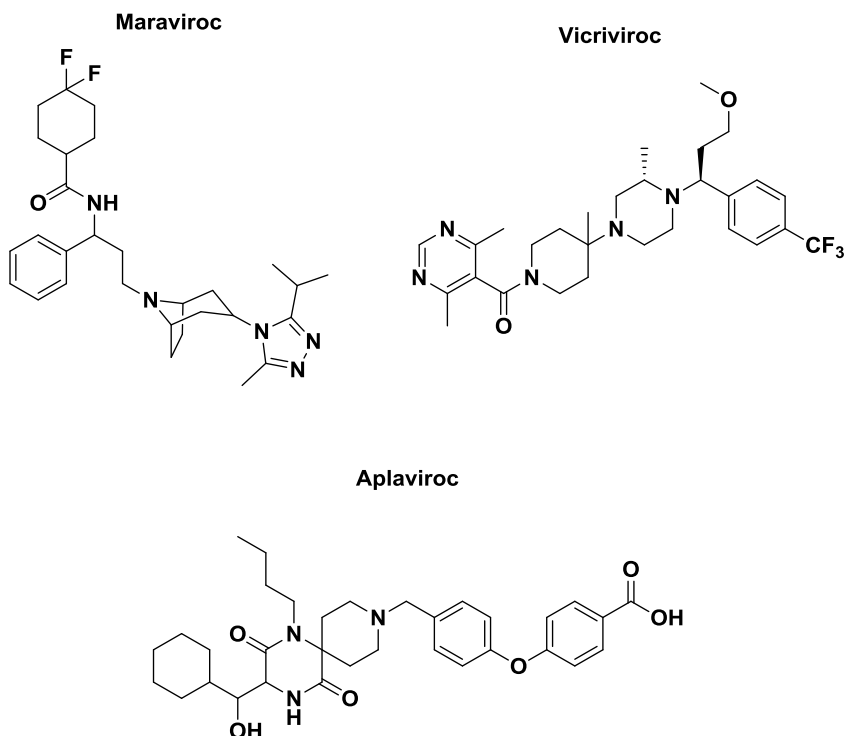


Figure 2.2: Potent CCR5 antagonists

Maraviroc, Vicriviroc, and Aplaviroc bind specifically to CCR5 making them only effective against the M-tropic virus, but offering a robust resistance profile (Figure 2.2).^{15,16} Maraviroc is FDA approved and is frequently used in the clinical setting due to its chemokine specific properties. Currently there are no FDA approved CXCR4 antagonists for HIV treatment. AMD3100 was initially pursued for T-tropic HIV but proved too toxic for chronic treatment, though it is approved for stem cell mobilization.¹⁷ Tropism dependent treatments such as Maraviroc require expensive tropism tests limiting their use in the developing world. In recent years our pursuit of entry inhibition has been to develop a tropism independent entry inhibitor that targets the GPCR's CXCR4 and CCR5. Additionally, simultaneous inhibition of both the CXCR4 and CCR5 chemokine may have

a plethora of possible therapeutic effects including: anti-inflammatory, anti-cancer, and as lesion detection agents.

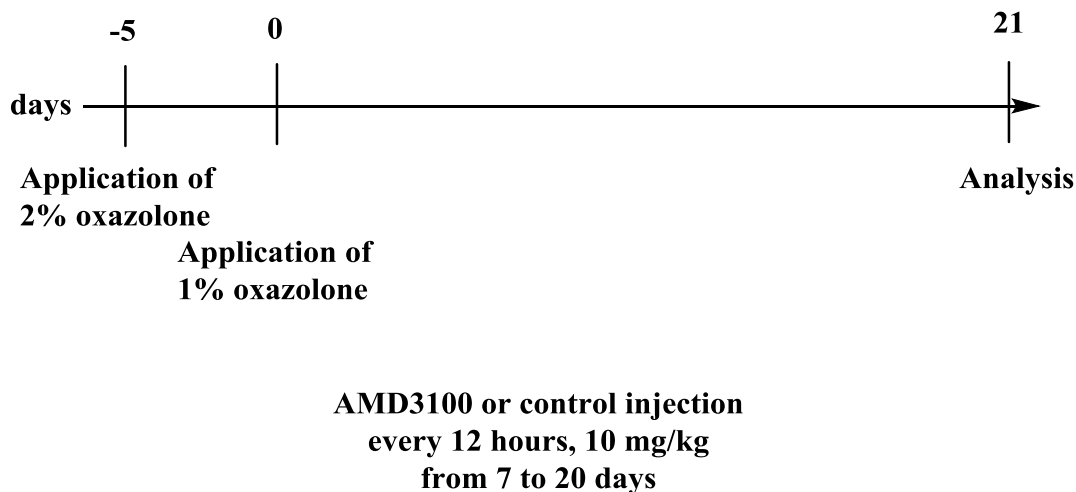


Figure 2.3: Anti-inflammatory effects of AMD3100 in mouse model¹⁸

AMD3100 dosed twice daily to mice at 10 mg/kg has been shown to profoundly decrease chronic skin inflammation as compared to the control PBS vehicle in mice challenged with an injection of oxazolone (Figure 2.3).¹⁸ It is worth noting that due to the large sample size the difference in ear thickness between control and experimental groups is significant to three standard deviations via the student T test. Visible improvement was also obtained in less than a week of dosing.

Though results are still mixed, preliminary data also suggests that CCR5 antagonists may play an anti-inflammatory role in the human body.¹⁹ If proven to be the case, a CCR5/CXCR4 dual-active antagonist may provide a very robust treatment for inflammatory diseases such as arthritis. Regardless of CCR5's involvement in inflammation, the widely accepted anti-inflammatory nature of CXCR4 antagonists offers an advantage for the treatment of HIV when compared to the current standard of care.

Normal cells	Corresponding tumor
Prostate gland epithelial stem cells	Prostate cancer
Hematopoietic stem cells	Leukemia
Neural stem cells	Brain tumors
Mammary gland epithelial stem cells	Breast cancer
Skeletal muscle satellite cells	Rhabdomyosarcoma
Neuroectodermal stem cells	Neuroblastoma
Renal tubular epithelium stem cells	Wilms' tumor
Retina pigment epithelium stem cells	Retinoblastoma
Liver oval stem cells	Hepatoblastoma
Ovarian epithelium stem cells	Ovarian cancer
Cervical epithelium stem cells	Cervical cancer

Table 2.1: Normal CXCR4 Expressing Cells and Analogous CXCR4 Expressing Tumor²⁰

Kulcia and more recently Furusato have produced a large body of literature tracking CXCR4's involvement in various types of cancer (Table 2.1).²⁰ Research indicates that the CXCR4 SDF-1 activity axis has a large influence on the metastasis of tumor cells. More specifically the upregulation of vascular endothelial growth factor and nuclear factor kappa B by the tumor increases CXCR4 expression, which in turn increases metastasis through the chemotactic paths described in Chapter 1. This biological action not only increases the robustness of cancer to normal physiological responses, but also provides a potential target for CXCR4 antagonists.²¹

CXCR4 antagonists have been known to be effective in chemotherapy for some time. AMD3100 (Plerixafor) is currently used in leukemia patients for stem cell mobilization followed by targeting by conventional anti-cancer agents. More recently, AMD3100 has been shown in several animal models as an effective anti-cancer agent in its own right. Unpublished results from the Bond lab demonstrate that our own CXCR4 antagonists are quite active against breast cancer cell lines. In fact **947** is very potent with a subnanomolar IC₅₀. The controls are also quite robust; none of the tested compounds were toxic to healthy jurkat cells, and Maraviroc had no activity, suggesting a CXCR4

specific mechanism for this specific cancer line (engineered to have only CXCR4 expression).

The Pestell group amongst others have shown CCR5 antagonists such as Maraviroc and Vicriviroc to be potent inhibitors of cancer metastasis.²² Recently, Maraviroc was demonstrated to not only reduce metastasis but also have a profound effect on tumor size in a mouse lung cancer model. In **A** MDA-MB-231 cells were injected into the mice and *in vivo* bioluminescent signals showed mice dosed with 8 mg/kg every 12 hours of Maraviroc to be far more resistant to tumor progression. The graph **B** shows the difference at 5 weeks to be quite profound passing statistical tests with confidence levels of $P = .048$. The excised lungs in **C** show a representative visible comparison of the treated vs control lungs.

Considering the mountain of evidence for GPCR antagonists being used against various strains of cancer, it stands to reason that an X4-R5 dual active antagonist may have a synergistic effect. We are particularly interested in breast cancer, which has been shown to be sensitive to both CXCR4 and CCR5 antagonists. Even if no synergistic effect is found for common cancer cell lines, dual-active antagonists may represent a more robust treatment of cancer than mono-active via being effective against a greater number of cell lines.

2.2 Design of “Stitched” Dual X4/R5 Antagonists

Due to Maraviroc’s clinical success several extremely potent CCR5 antagonists have been developed (Figure 2.2). We hypothesized that appending one of these very potent CCR5 antagonists to one of our potent CXCR4 antagonists may produce a

compound that could bind to both receptors. This strategy relies on the assumption that the X4 potency deriving moiety can be accommodated by the CCR5 binding pocket and vice-versa. This could be envisioned in two ways: first the X4 active motif binds to X4 and the R5 motif hangs out extracellularly and second the X4 active motif binds to X4 and the R5 motif also rests in the receptor potentially making positive interactions as well. Both possibilities are reasonable considering the very large size of the two surface receptors.

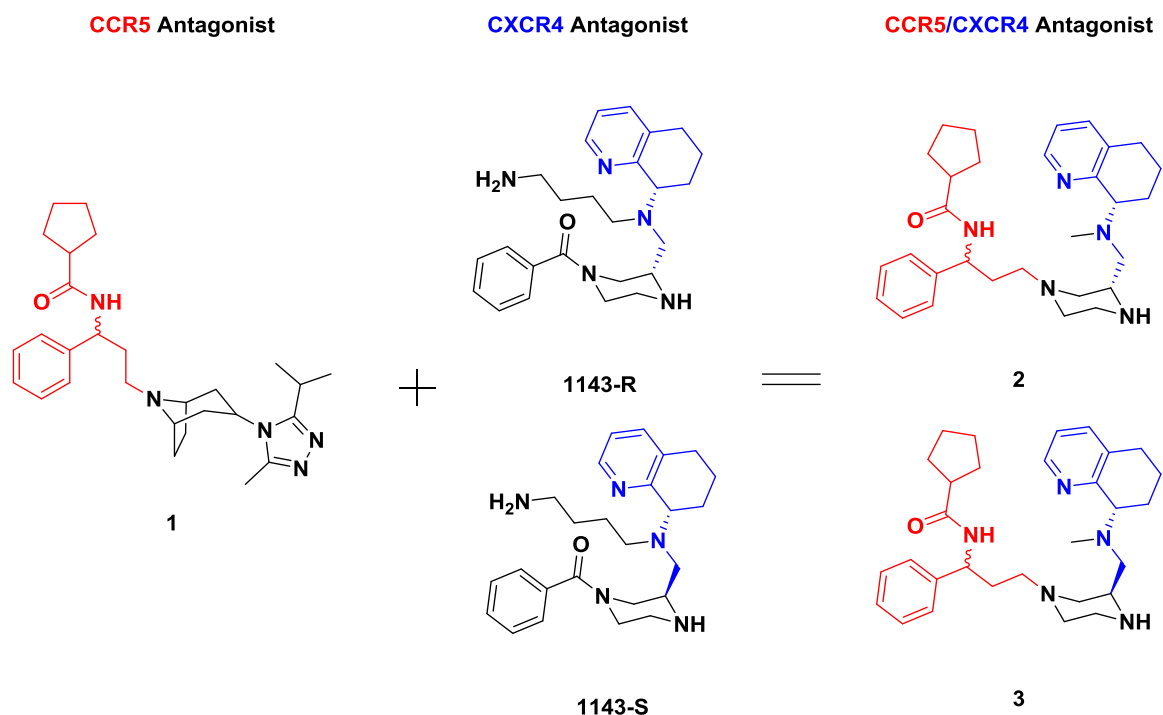


Figure 2.4: Compound stitching strategy in the pursuit of dual-active CCR5/CXCR4 antagonists

To minimize the risk of the two structural motifs not being compatible with each other, we choose CCR5 antagonists with either a piperidine or a piperazine that could be directly overlaid with the piperazine of our own series. One such resulting molecule is stitched from an extremely potent Maraviroc precursor **1** and our own **1143** (Figure 2.4). We choose to not include the butylamine side-chain in the resulting compounds (**2** and **3**)

because CCR5 is not nearly as acidic as CXCR4 and we suspected the butylamine side-chain may be incompatible.

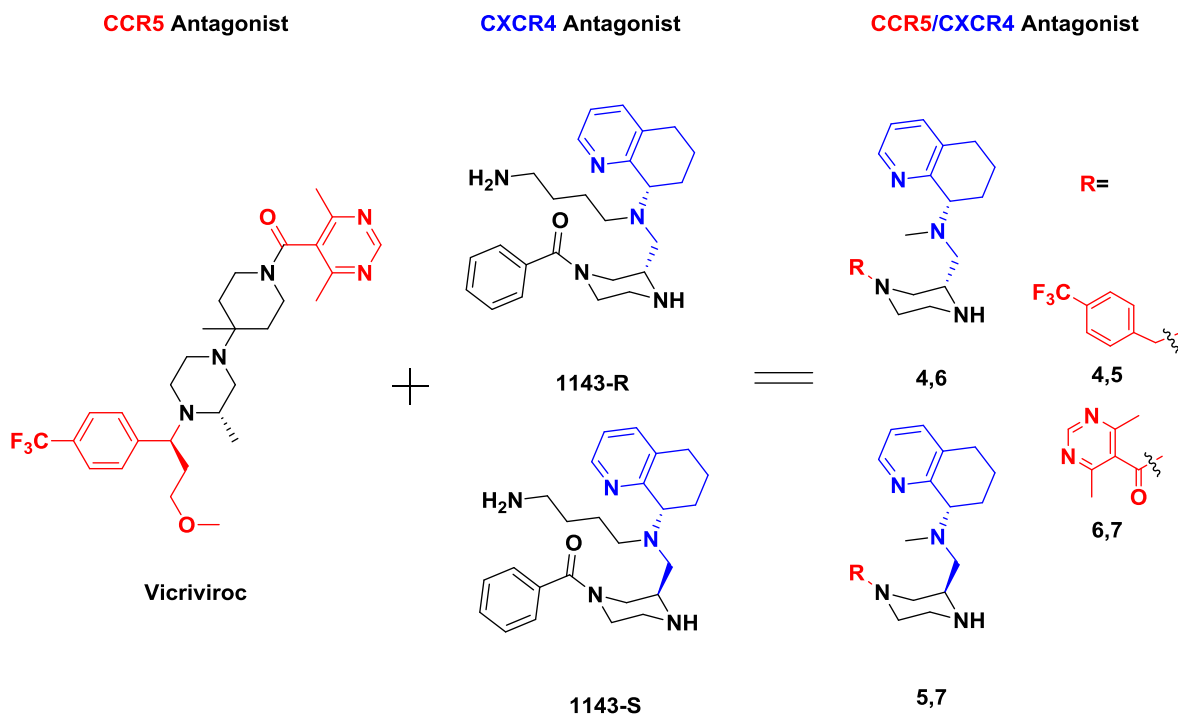
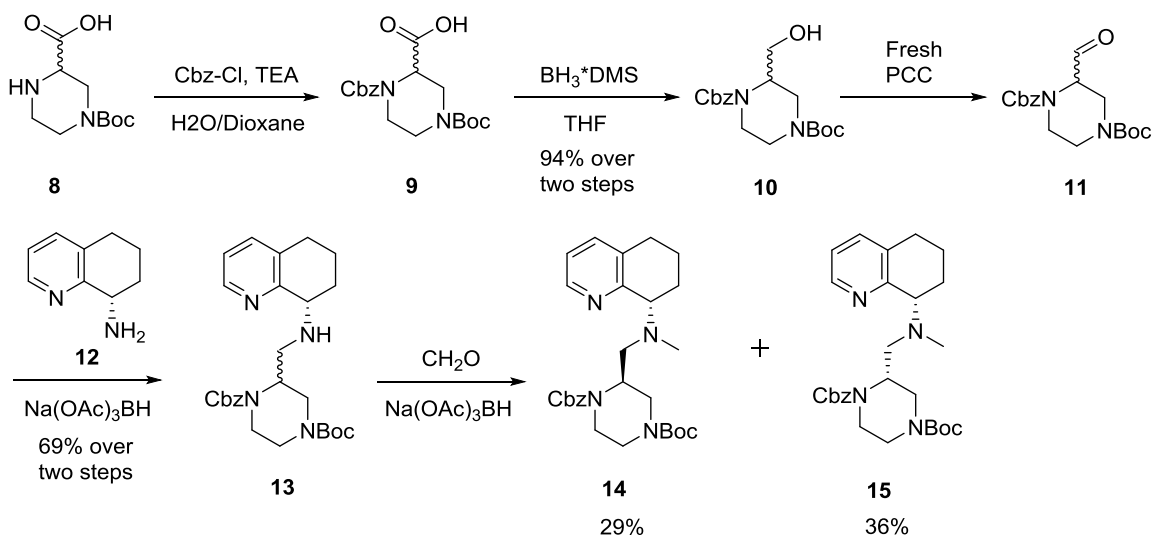


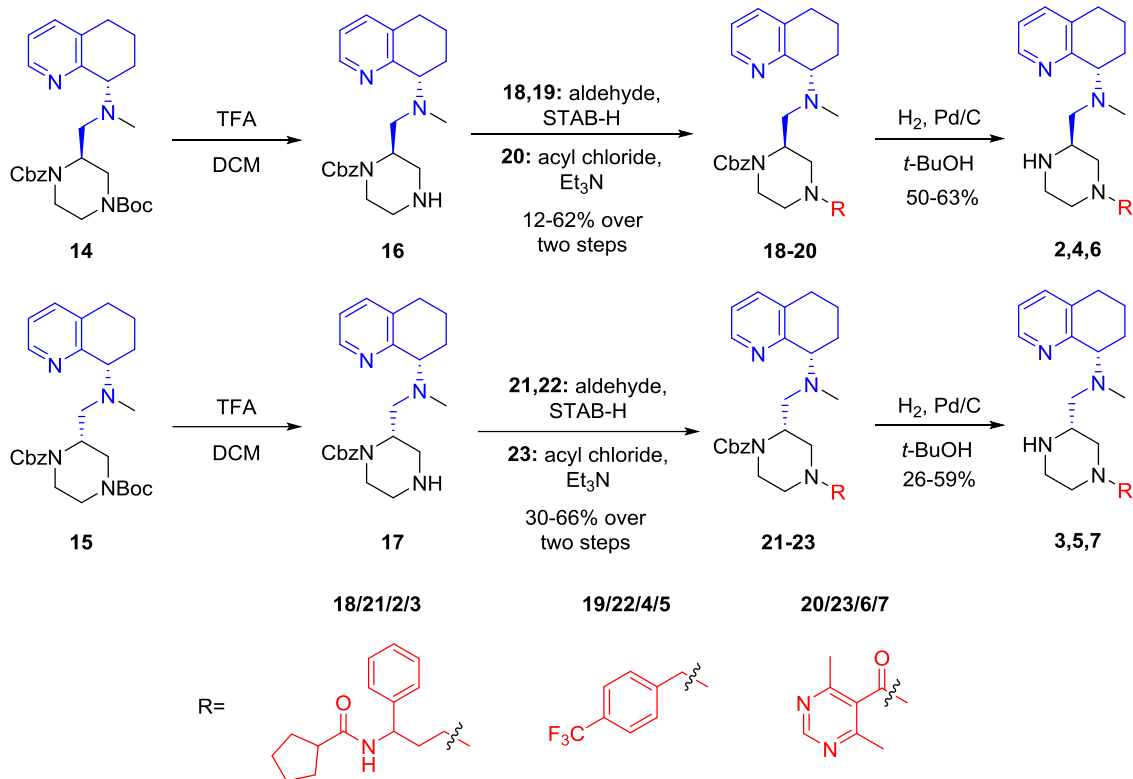
Figure 2.5: Design of “stitched”-compounds **4-7**

We similarly designed compounds **4-7** from Vicriviroc instead of Maraviroc precursor **1**. In this case the chiral center (**4,5**) which required nearly 6 synthetic steps was ablated both for synthetic simplicity and to increase the chances of compatibility. Based on previous SAR of the piperazine series the bottom nitrogen was substituted, and a baseline X4 activity in the single digit micromolar range was expected. In the absence of crystallographic data on Vicriviroc, we suspected that choosing a stitching fragment from both sides of the molecule (**4-7**) would increase the chances of successfully developing a dual-active program.



Scheme 2.1: Synthesis and resolution of diastereomers **14** and **15**

Starting from commercially available carboxylic acid **8** bis-protected acid **9** was obtained by the Shotten-Baumann reaction with Cbz-Cl which was taken on crude (Scheme 2.1). Borane reduction of acid **9** procured alcohol **10** in high yield. Oxidation of alcohol **10** with freshly synthesized PCC yielded aldehyde **11** in a pure fashion upon simple filtration. Reductive amination of aldehyde **11** with chiral amine **12** yielded half scaffold **13** in moderate yield as a mixture of two diastereomers. At this stage the diastereomers could not be adequately separated, but subsequent reductive methylation with formaldehyde formed a 50/50 mixture of scaffold **14** and **15** which were easily separated by column chromatography. This synthetic route proved amenable to scale and was conducted on a 20 gram batch.

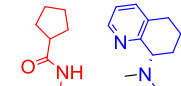
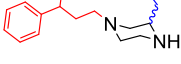
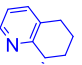
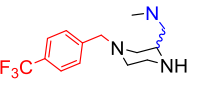
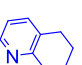
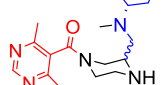


Scheme 2.2: Synthesis of final products **2-7**

From modular chiral intermediates **14** (S,S) and **15** (R,S) final products with substitution on the “bottom” piperazine nitrogen were synthesized via Scheme 2.2. Boc-deprotection of **14** and **15** yielded chiral amines **16** and **17** respectively. Reductive aminations of **16** and **17** with the appropriate aldehyde yield advanced intermediates **18**, **19**, **21**, and **22** respectively in poor to moderate yield. Alternatively, acylation of **16** and **17** with the appropriate acyl chloride using Schotten-Bauman conditions yielded advanced intermediates **20** and **23** respectively. Cbz-protected intermediates **18** to **23** were converted to final products **2** to **7** via hydrogenation with palladium on carbon in a Parr hydrogenator with highly variable yields reflecting difficulty in purification.

2.3 “Stitched” Dual X4/R5 Antagonists – Results

Table 2.2: Anti-HIV and Antagonist Activity of “Stitched” Series

#	Structure	Chirality	MAGI Assay IC ₅₀ uM		TC ₅₀ uM	SDF-1 % inhibition @ 100uM	MIP1-B% inhibition @ 100uM	RT % inhibition @ 100uM
			CCR5	CXCR4				
2		S,S	22	33	136	11%	97%	<5%
3		R,S	22	28	108	30%	71%	<5%
4		R,S	11	8	17	47%	75%	<5%
5		S,S	7	8	>300	66%	59%	<5%
6		R,S	>100	>100	>100			
7		S,S	>100	>100	>100			

The SAR targets were tested against both the MAGI assay as a direct measure of anti-viral potency and ligand displacement as an indirect measure of signaling disruption (Table 2.3). Gratifyingly, two of the three “stitched” fragments tested were μM potent inhibitors of both R5 and X4 tropic HIV. The Maraviroc fragment (compounds **2** and **3**) was similarly potent against both R5 and X4 tropic HIV, which suggested the potential of a tropism independent mechanism. Follow-up testing against SDF-1 (CXCR4) and MIP-1 β (CCR5) showed at least moderate activity against both chemokines, but the activity was significantly higher against CCR5. Both diastereomers were moderately toxic with TC50's just over 100 μM . The CF₃ Vicriviroc fragment was also two to three fold more potent than the Maraviroc fragment in the MAGI assay. The potency difference between CXCR4 and CCR5 ligand displacement was noticeably more similar and strongly suggests a pure and classic antagonist profile. Remarkably, **4** was quite toxic against MAGI cells, whereas **5** caused no measurable cytotoxicity even up to 300 μM . This suggests that the

diastereomers clearly can have different and unpredictable differences in activity profile. All four active compounds were further profiled against reverse transcriptase and were essentially inactive. The acyl Vicriviroc fragment was startlingly not active against either strain. We suspected compounds **6** and **7** would at-least have potency against the X4 tropic virus. In fact, pyridyl benzamides tested in Chapter 1 were active against the X4 tropic virus. This suggests that the bulky ortho substitutions have a strongly detrimental effect on binding potency in the CXCR4 receptor.

2.4 Second Generation “Stitched” Dual X4/R5 Antagonists

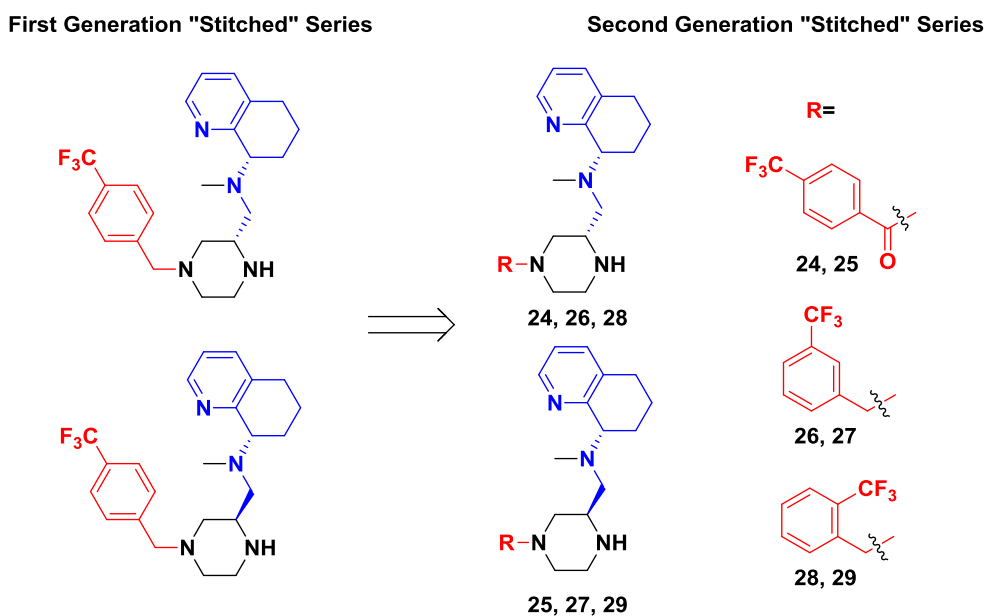
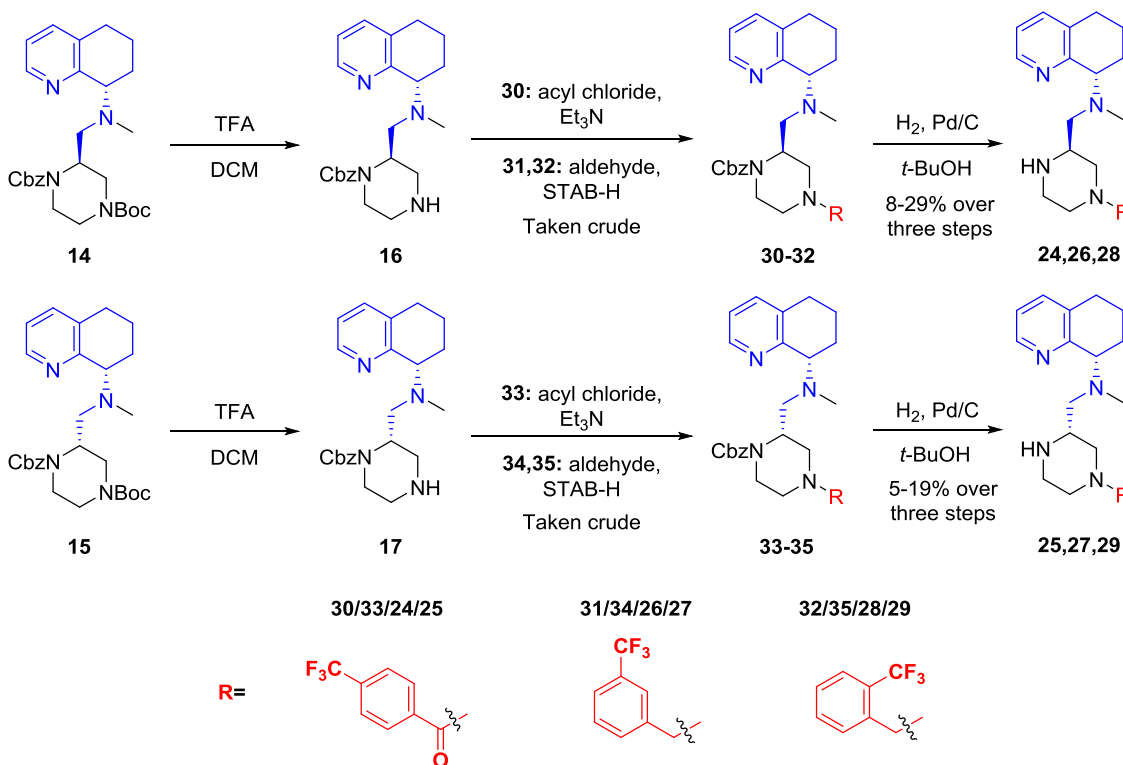


Figure 2.6: Design of “stitched”-compounds **24-29**

Of the two hit fragment series the Vicriviroc trifluoromethyl group was chosen for follow-up SAR studies due to the simplicity of its synthesis as well as the lack of observed toxicity (at least in the case of **5**). Additionally, characterizing why the simple addition of a trifluoromethyl group could have such a profound effect on tropism of the molecule was an academic question with considerable weight. To probe whether this dual-tropic

scaffold followed our X4 piperazine SAR or Vicriviroc R5 piperidine SAR, compounds **24** and **25** were synthesized. In the Vicriviroc series amides were significantly less active than amines at the fragments bonding location, on the other hand in our own CXCR4 series amides are often more potent than their amine counterparts (see Chapter 1). We were also interested in a more conventional SAR manner whether the position of the trifluoromethyl group would affect potency. If the trifluoromethyl group was making a specific interaction we suspected to see a decrease in potency, on the other hand in the case of an electronic effect we suspected to see no major change in potency at any of the three positions.



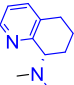
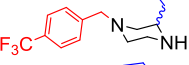
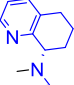
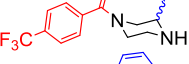
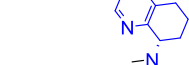
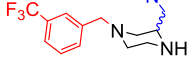
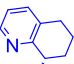
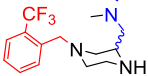
Scheme 2.3: Synthesis of final products **24** to **29**

From modular chiral intermediates **14** (S,S) and **15** (R,S) final products with substitution on the “bottom” piperazine nitrogen were synthesized via Scheme 2.3. Boc-deprotection of **14** and **15** yielded chiral amines **16** and **17** respectively. Acylation of **16**

and **17** with the appropriate acyl chloride using Schotten-Bauman conditions yielded advanced intermediates **30** and **33** respectively. Alternatively, reductive aminations of **16** and **17** with the appropriate aldehyde yield advanced intermediates **31**, **32** and **34**, **35** respectively which were taken on crude. Cbz-protected intermediates **30** to **35** were converted to final products **24** to **29** via hydrogenation with palladium on carbon in a Parr hydrogenator with highly variable yields reflecting difficulty in purification and three synthetic steps.

2.5 Second Generation “Stitched” Dual X4/R5 Antagonists – Results

Table 2.3: Anti-HIV Activity of Second Generation “Stitched” Series

#	Structure	Chirality	MAGI Assay % inhibition at 10 μ M		% Cell Viability at 10 μ M	SDF-1 % inhibition @ 100uM	MIP1-B% inhibition @ 100uM	RT % inhibition @ 100uM
			CCR5	CXCR4				
4		R,S	41%	57%	76%	47%	75%	<5%
5		S,S	61%	57%	95%	66%	59%	<5%
24		S,S	41%	13%	100%			
25		R,S	24%	54%	89%			
26		R,S	55%	70%	96%			
27		S,S	58%	36%	62%			
28		R,S	94%	93%	9%			
29		S,S	96%	82%	25%			

The SAR targets were tested in the MAGI assay as a direct measure of anti-viral potency at a single data point to conserve resources (Table 2.3). Compounds **4** and **5** are provided here with their percent inhibitions at 10 μ M for ease of comparison, it's worth noting that this percent inhibition is extracted from their IC₅₀'s in Table 2.2. The chiral designations of amides **24** and **25** is flipped as compared to the analogous amines in Table

2.3. This is because even though the group priorities are changed by the addition of a carbonyl, the (S,S) amide has the same stereo-fingerprint as the (R,S) amine (IE: in both cases the chiral bond is pointed “up”). The (S,S) amide **24** was similarly potent against R5 tropic HIV as the analogous (R,S) amine **4**, but was less active against the X4 tropic HIV virus. In contrast, the (R,S) amide **25** was similarly potent against the X4 tropic virus as the analogous (S,S) amine **5**, but was less active against the R5 tropic HIV virus. In both cases cell viability was within experimental error of control cells. The meta-substituted amines **26** and **27** were similarly potent to their para-substituted analogues **4** and **5** against both strains of the virus. In this case the (R,S) diastereomer had a slight edge both in terms of potency and more significantly in terms of cell viability as compared to the (S,S) diastereomer. This observation is in sharp contrast to the initial hits wherein the (R,S) diastereomer was significantly more toxic than the (S,S). Further, taken in combination these results suggest a specific mechanism of toxicity as opposed to a general mechanism of toxicity which would be attenuated by hydrophobicity but not chirality. The ortho-substituted amines **28** and **29** were far too toxic to reliably interpret their potencies, and once again the more toxic diastereomer “flipped”.

In conclusion, the compound “stitching” strategy was highly successful with the discovery of the first set of dual-tropic antagonists of CXCR4 and CCR5 resulting from the effort (compounds **2** to **5**). Unfortunately, study of the series is resource intensive as each compound has to be tested against X4 and R5 tropic strains independently as compared to traditional series which are only tested against one. This resource drain is further exacerbated by the chirality of the series, as neither diastereomer was revealed to be superior in the initial study. In fact, the superior diastereomer in terms of potency was

statistically completely random, and the amides **24** and **25** were mono-tropic in R5 and X4 respectively. All these observations taken in conjunction with the apparent flatness of the SAR led us to table this exciting series temporarily to explore an alternative strategy in the dual-tropic chemical space with no chiral centers.

2.6 Virtual Screen and Discovery of Pyrazole Dual X4/R5 Series

Anecdotal data in the form of cell culture experiments as well as a handful of clinical studies have shown that treatment of the HIV virus with a single chemokine antagonist will cause shifts in tropic loads. Clinical data of **AMD11070** showed a pronounced shift in viral tropism when **AMD11070** was taken as a single drug anti-viral agent.²³ Of the nine patients, only three maintained their original tropism of the virus for the entirety of the dosing regimen. Four of the nine patients had no detectable level of X4 virus in at least one tropism test, whilst maintaining a detectable amount of the R5 virus.

Due to the ability of the HIV virus to quickly mutate to CXCR4 using virus from CCR5 and vice versa, we suspected that there must be some structurally similar binding site in the CXCR4 and CCR5 receptors that allowed tropism shift with small modifications in protein structure. This hypothesis was further supported by our positive results with the “stitched” series which could be interpreted in one of two ways. First the ability of the compounds to bind to both CXCR4 and CCR5 could be from disparate binding sites where the X4 fragment binds in CXCR4 with the CCR5 fragment making no essential interactions and vice versa. Or, second the ability of the compounds to bind to both CXCR4 and CCR5 may be a result of similar interactions being made in a homologous binding site. Believing this second possibility to be at least plausible, we designed a virtual screening protocol to discover a commercially available compound with the desired dual tropic activity.

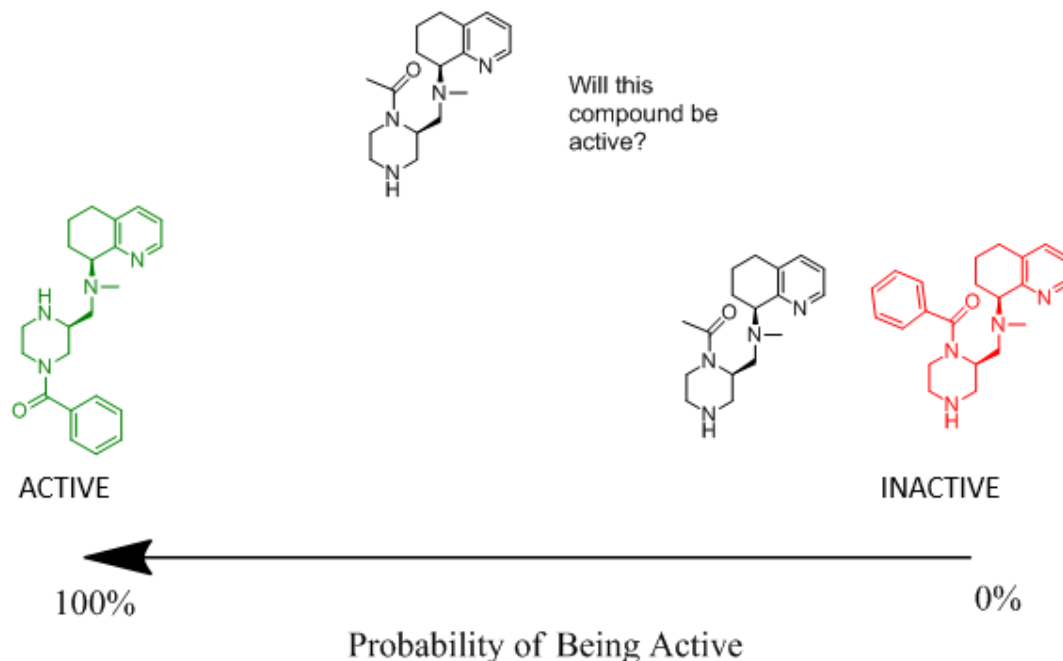


Figure 2.7: Example of Bayesian statistics

The virtual screening protocol was designed around Bayesian statistical analysis of 2D fingerprints to both save computational power and eliminate concerns of chirality which was one of the objectives of the study. Bayesian statistics is defined as “a subset of the field of statistics in which the evidence about the true state of the world is expressed in terms of degrees of belief or, more specifically, Bayesian probabilities.” An example of Bayesian statistics is provided in Figure 2.7 wherein a known active (green) and a known inactive (red) are used as a basis set for prediction of an untested compound (black). The known active has a 100% probability of being active because it has been tested and as such we know it is true, similarly the known inactive has a 0% chance of being active. Because the 2D fingerprint of the untested compound is more similar to the known inactive than active its probability of being active is less than 50%. This is a simplified example wherein one’s own intuition would probably come to the same conclusion, but with pipeline pilot

we were able to run this analysis on over 5 million compounds against a basis set of thousands of actives and inactive compounds.

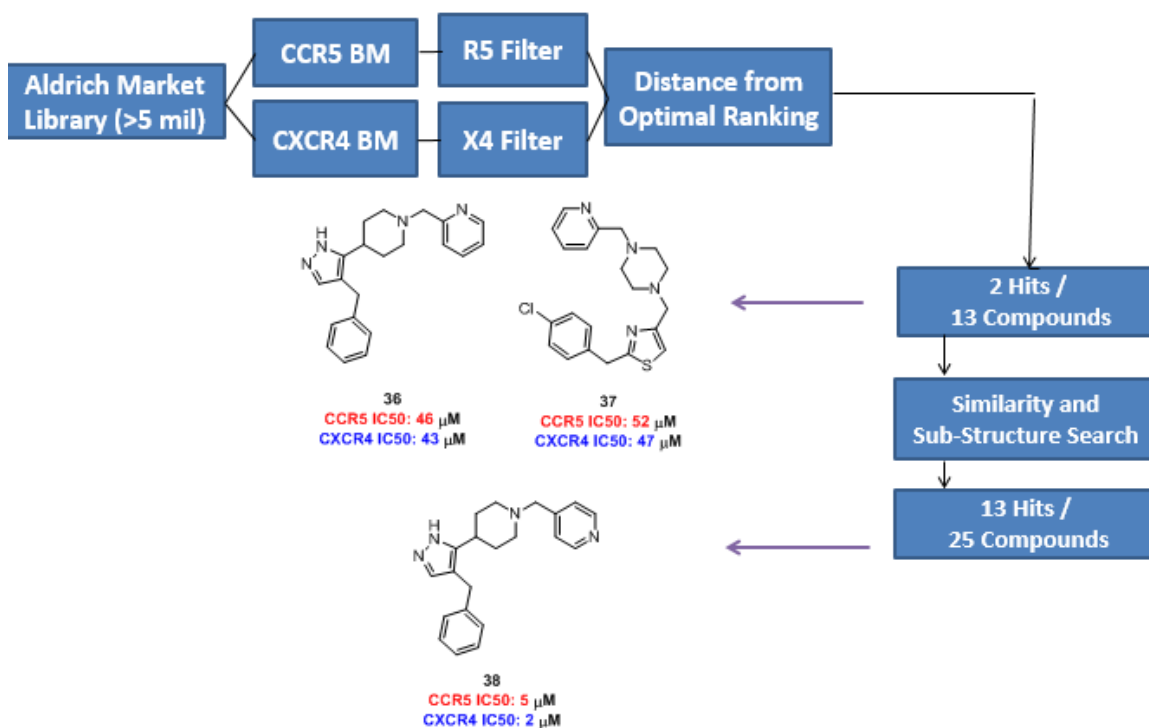
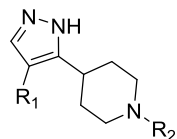


Figure 2.8: Virtual screening work flow and active hits

The virtual screening protocol was designed and ran by Dr. Cox (Figure 2.8). The workflow converted the entire Aldrich marketplace select library of over five million compounds into two dimensional fingerprints. Then, the protocol compared these five million fingerprints versus Bayesian statistics constructed from the known CCR5 and CXCR4 active and known inactive compounds in the Zinc database. The R5 and X4 filter ranked the fingerprints by their probability of being CCR5 or CXCR4 binders respectively, and then the 13 top most compounds that showed up in both lists was selected for purchase and screening with the MAGI assay. Of the 13 compounds purchased two (**36** and **37**) had potency against both X4 and R5 tropic HIV with IC₅₀'s less than 100 μM. We next rescreened the Aldrich marketplace select library for compounds that were structurally

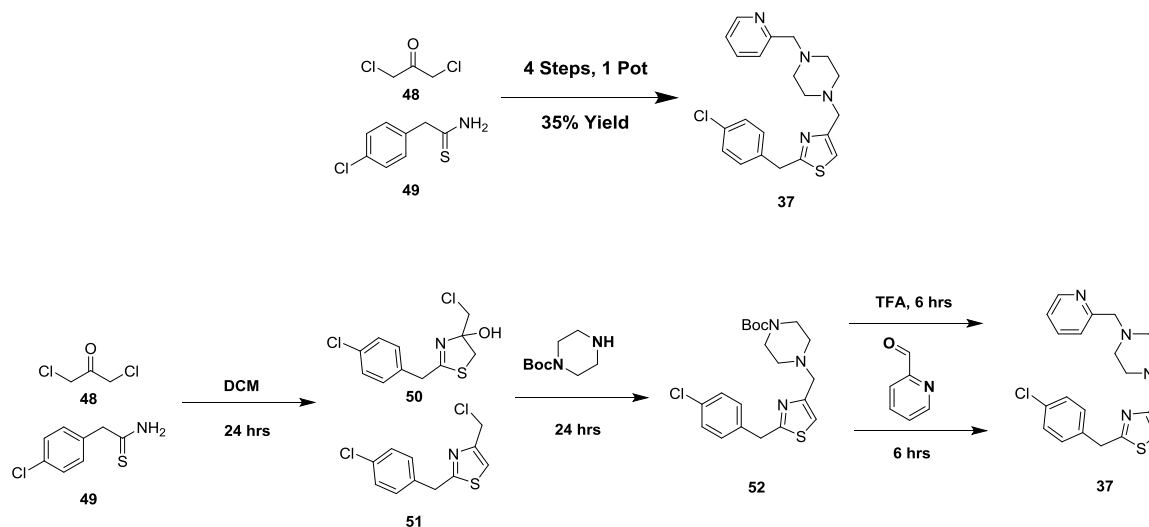
similar or substructures of the pyrazole hit compound **36**. This rescreen resulted in 13 more compounds with IC₅₀'s under 100 μ M against either R5 or X4 tropic HIV out of 25 compounds purchased. The most potent compound from the rescreen (**38**) had IC₅₀'s under 10 μ M against both strains of HIV, making this screening hit essentially equally potent to the "stitched" series.



#	R1=	R2=	MAGI Assay IC ₅₀ μM		TC ₅₀ μM
			CCR5	CXCR4	
36	Benzyl-		46	43	>100
39	Benzyl-		16	6	>300
38	Benzyl-		5	2	>100
40	Phenyl-		64	44	>300
41	Benzyl-		60	68	>300
42	Benzyl-		83	81	>300
43	Benzyl-		17	13	>100
44	Benzyl-		66	57	172
45	Benzyl-		13	6	>100
46	Benzyl-		95	105	>300
47	Benzyl-		72	264	>300

The activities of the pyrazole screening hits that were >95% pure by LCMS analysis are provided in Table 2.5. Generally all the compounds were non-toxic with potencies ranging from 2 to 264 μM. A few clear SAR trends become apparent when inspecting the data. First, a pyridine nitrogen in the para position **38** is superior to the meta **39** and ortho

37 positions, strongly suggesting the existence of a hydrogen bond interaction. Second, a benzyl ring coming off the R1 position **39** appears superior to the phenyl analog **40**. Third, though no direct comparison was available, anilino analogs like compounds **46** and **47** appear to be less potent than benzyl analogs like **36**, **38-47** in the R2 position. Additionally, several other weak SAR trends were apparent necessitating follow up synthesis and testing.



Scheme 2.4: Synthesis of screening hit **37**

With the Aldrich marketplace tapped out of compounds with high similarity to our pyrazole hit and having few compounds of high similarity to our thiazole hit we endeavored to synthesize the thiazole hit and consider synthetic SAR around the scaffold. In an attempt to expeditiously create a synthetic sample of **37** to test we attempted the entire synthetic sequence in one pot with DCM as a solvent. DCM was an important choice as a solvent, because we envisioned using TFA to afford a Boc-deprotection, and few solvents other than DCM are compatible with high ratios of TFA. Starting from dichloroacetone **48** and an appropriately substituted thioamide **49** a mixture of cyclization products was afforded upon simple mixing for 24 hours (Figure 2.9). The reaction was tracked by LCMS and after the initial formation of the nonaromatic ring **50** and the thiazole **51** in an approximately 2

to 1 mixture no more conversion was detected. It was hypothesized that the acid formed from alkylation of **51** and **50** with mono-Boc-piperazine may afford the conversion to a thiazole. Additionally, the consumption of the HCl byproduct by affording dehydration most likely increased the stability of the Boc-protecting group. As expected, the mixture of **50** and **51** were successfully converted to **52** within 24 hours. Subsequent deprotection of the Boc group with TFA afforded an amine which was then subjected to an aldehyde and sodium triacetoxy borohydride to afford final product **37** in a high 35% yield over 4 steps and one purification. Upon retesting the analytically pure sample of **37** we were surprised to see no activity separable from the steep toxicity curve. We suspect that the initial sample may have actually been of a different compound, or that the testing contractor may have mixed up samples from our initial screening. Regardless, we moved our synthetic efforts back towards pyrazole compounds.

2.7 Design of One-pot Methodology for the Conversion of Esters to Ketones

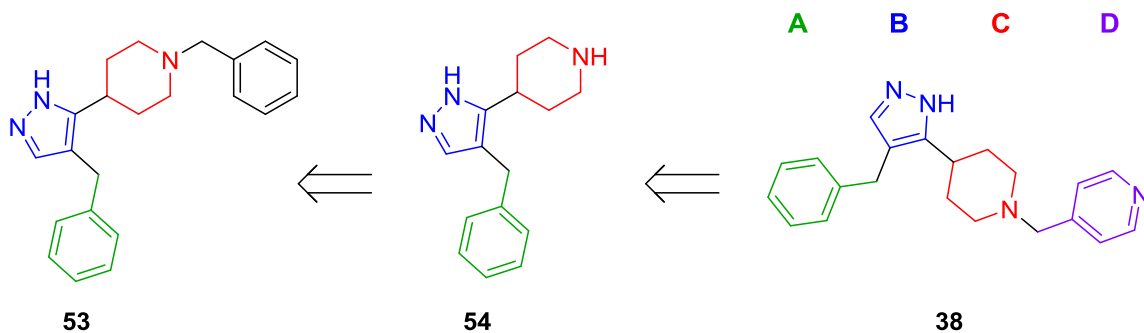
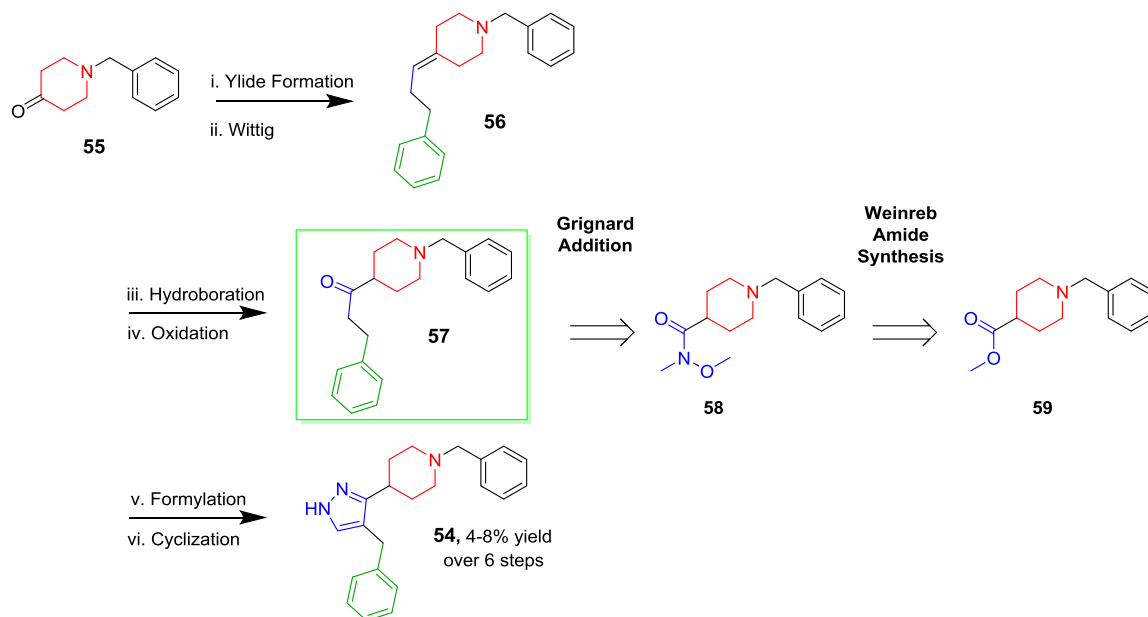


Figure 2.9: Retrosynthetic analysis and ring designation for screening hit **38**

In an effort to scale up compound **38** for further testing as well as to produce modular building blocks that would allow further SAR we split the molecule into 4 regions aptly named the A, B, C, and D rings (Figure 2.9). We desired a synthesis that would allow quick and easy SAR around the D ring through coupling of various acyl chlorides and aldehydes with piperidine **54**. We further envisioned that piperidine **54** could come from nearly any protected **54** precursor in the literature and found the benzyl protected compound **53** in a series of papers published by Merck.²⁴⁻²⁶



Scheme 2.5: Merck's synthesis of common intermediate **54** and an alternative retrosynthetic analysis of precursor **57**

Our lab initially attempted to scale up compound **54** using the conditions alluded to in the original set of publications (Scheme 2.5). We found that, in the absence of an explicit procedure, we were only able to prepare small amounts of the desired material over the course of six steps. To address this problem, it appeared that developing a one-pot route to intermediate **57** might be the quickest way of improving the efficiency of the synthesis. To achieve this, we focused our attention on the Weinreb amide synthesis and subsequent Grignard reaction used for the conversion of ester **A** to ketone **57** (Table 2.5).²⁷⁻²⁸ Specifically, when we used "standard" conditions for forming the Weinreb amides (i.e., multiple equivalents of alkyl-aluminum chlorides), followed by addition/elimination with a Grignard reagent,²⁷ we observed significant quantities of impurities that necessitated a separate purification step. As an alternative, we considered the use of Grignard/N,O-dimethylhydroxylamine combinations to form Weinreb amides, a strategy used in several publications.²⁹⁻³⁰ In this regard there are numerous reports that generate Weinreb amides

from esters using non-nucleophilic Grignard reagents, followed by subsequent addition of nucleophilic Grignard reagents to afford the corresponding ketone in a two-step fashion with isolation and purification in between.³¹ Surprisingly, however, we were unable to find any literature that discussed single pot ketone forming reactions that utilize Weinreb amide/Grignard reagent combinations.²⁹⁻³⁰ As a consequence, we decided to explore the scope and limitation of this approach.

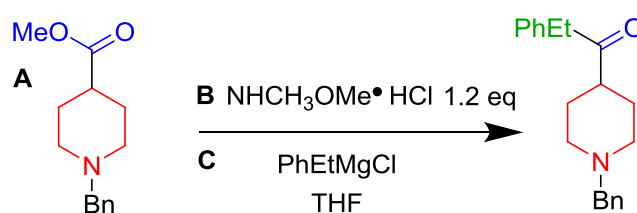


Table 2.5: Screen of Reaction Conditions

#	Temp.	Eq. of C	Order of add.	Yield
1	-5°C	4.5	A,B,C	>95%
2	0°C ^a	4.5	A,B,C	>95%
3	RT	4.5	A,B,C	>95%
4	0°C	3.5	A,B,C	>95%
5	0°C	4.5 ^a	A,B,C	>95%
6	0°C	10	A,B,C	>95%
7	0°C	4.5	A,B,C ^a	>95%
8	0°C	4.5	B,A,C ^a	>95%
9	0°C	4.5	B,C,A	>95%

^a Selected conditions

Initial attempts at the one pot process provided surprisingly straightforward and robust results (Table 2.5). We initially chose to use 4.5 eq of the relevant Grignard, 1.2 eq

of N,O-dimethylhydroxylamine hydrochloride, and an A-B-C addition paradigm. Varying the temperatures (entry 1-3) using these conditions on a half mmol scale produced excellent results, with no double addition by-products and yields over 95% of pure material after a simple work up. Since chemical intuition might suggest that room temperature additions might have selectivity issues, all nine permutations were tested in duplicate. Although cooling was not required on this scale, the exotherm that was produced led us to select 0°C for all further attempts. Variation in the number of equivalents of Grignard reagent had virtually no effect on the observed product ratios (entry 4-6). When we used 3.5 equivalents with careful drying and handling of reagents, the yields were consistently over 95% yield and the products that were isolated by simple extractions exhibited excellent purity. Reactions performed with 4.5 equivalents were much less sensitive to small amounts of water (i.e., non-distilled THF could be used). Indeed, even when 10 equivalents of Grignard reagents were used, we only observed trace amounts of double addition. As a consequence 4.5 equivalents of Grignard reagent were used in all subsequent experiments. Next, we probed the order of addition (entries 7-9). As expected, adding either the ester or N,O-dimethylhydroxylamine hydrochloride first did not affect the outcome of the reactions. Similarly, addition of the Grignard reagent in excess prior to the addition of the ester did not result in any over addition and pure material was still obtained after a simple extraction. From a mechanistic perspective these results suggest that both tetrahedral intermediates (i.e., the orthoamide intermediate formed from addition of the hydroxylamine and the ketal intermediate formed by addition of the Grignard reagent) must be exceedingly stable at 0°C in THF. From a practical perspective it suggests that, if a given reaction failed to go to completion (due to wetness, bulkiness of substrate, or old Grignard reagent), one can

simply add more Grignard to finish the reaction with no fear of byproducts. For simplicity, we decided to move forward with the more logical order of addition where the Grignard is added last.

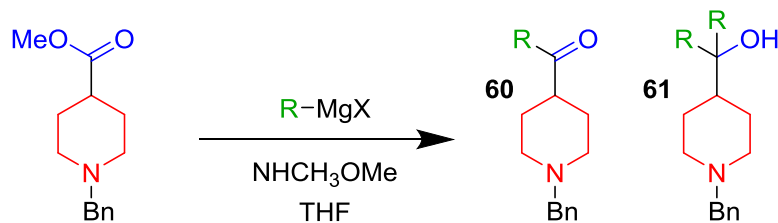


Table 2.6 Reaction Scope Versus Piperidine Moiety

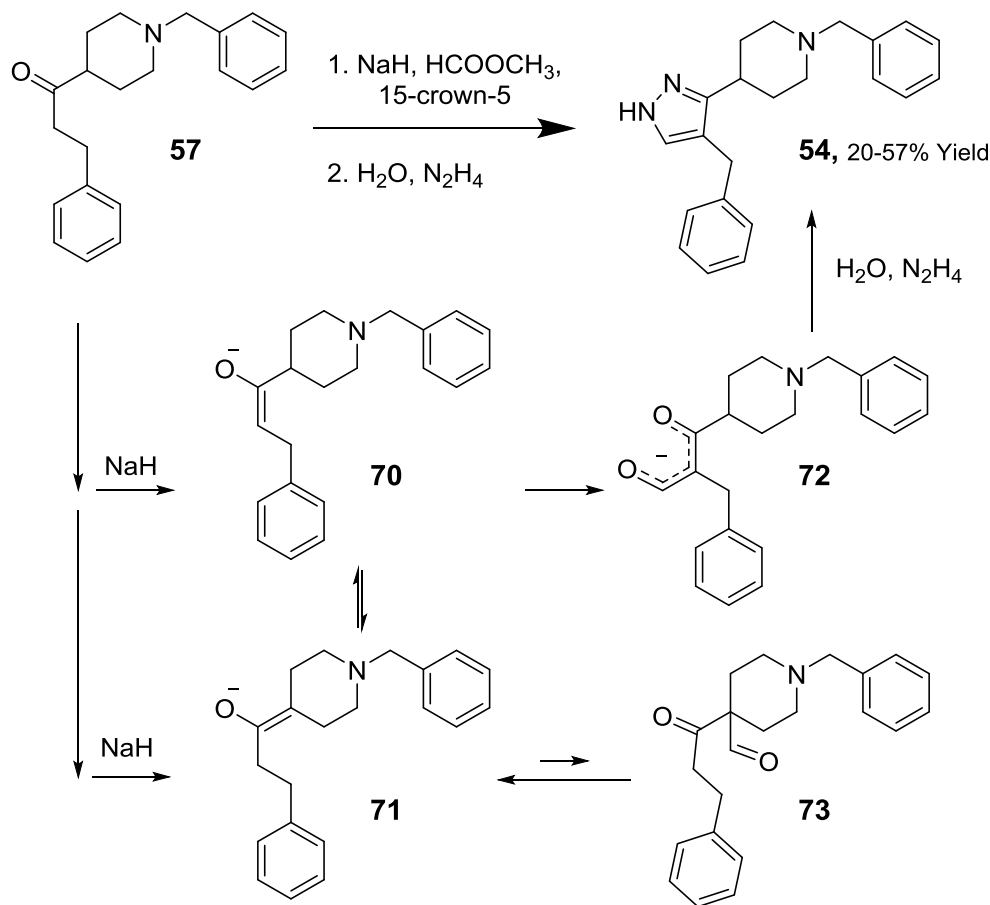
#	R	Nucleophile/Base	Yield	60:61 ^a
62	Me	MeMgBr	98%	>25:1
63	Me	MeLi	96%	6:1
64	Bu	BuMgBr	98%	>25:1
65	iPr	iPrMgCl	quant ^b	NA ^b
66	Cy	CyMgBr	quant ^b	NA ^b
67	HCC	HCCMgBr ^c	97%	>25:1
68	PhCH ₂ CH ₂	PhCH ₂ CH ₂ MgCl	98%	>25:1
69	PhCH ₂ CH ₂	PhCH ₂ CH ₂ MgBr	99%	>25:1

^a Mono to di-adduct ratio was determined by ¹H NMR ^b Produced pure Weinreb amide with no conversion to ketone ^c Used iPrMgCl as base followed by Nu

To illustrate the reaction scope, we first varied the identity of the Grignard (Table 2.6). Being significantly more nucleophilic than phenethyl, we wondered if methylmagnesium bromide might result in over addition (entry 62). This was not the case, since the reaction product was once again produced in high yield and high purity after a simple extraction. By contrast, addition of methyl lithium under the same conditions

produced a significantly poorer mono to di-addition ratio (entry 63), suggesting that magnesium-stabilized tetrahedral intermediates are more stable than their lithium counterparts. Continuing our exploration of aliphatic Grignard reagents, we next demonstrated that additions of primary alkyl Grignard reagents (entries 64) proceeded smoothly. By contrast, attempts to add secondary Grignard reagents, such as isopropylmagnesium chloride and cyclohexylmagnesium bromide, resulted only in the formation of the Weinreb amide with no detectable ketone being observed (entries 65 and 66).

We realized that the low reactivity of bulky Grignard reagents could, in selective cases, be used to our advantage. Having to use several equivalents of highly reactive Grignards could easily be avoided. For example, by first forming the Weinreb amide *in situ* using isopropylmagnesium chloride, we only needed to add ethynyl magnesium bromide in slight excess to produce the corresponding ethynyl ketone in high yield and purity (entry 15). This example is particularly noteworthy as the resulting ethynyl ketone is not stable to column chromatography and polymerizes upon concentration. Being able to use entry 15 as a pure solution in THF in subsequent reactions was highly advantageous compared to previous procedures.



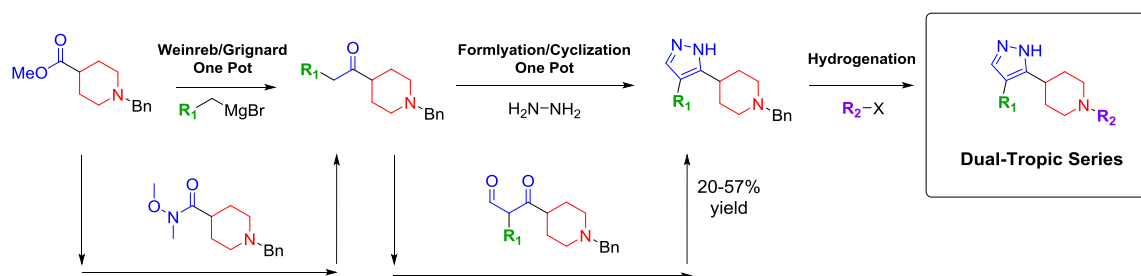
Scheme 2.6: Conversion of intermediate **57** to target **54**

With our reaction scope and limitations established, we returned to our original task of making compound **54** on a multi-gram scale (Scheme 2.6). Upon subjecting up to 25 grams of ester **A** to our optimized conditions, quantitative yields of ketone **57** were obtained. This material was then subjected to the formylation/cyclization reaction. We initially attempted to combine the formylation and cyclization reagents shown in Scheme 2.5 and were disappointed to largely recover our starting material. Since quenching the reaction mixture generated ample amounts of hydrogen gas, we concluded that the first deprotonation event was failing (Scheme 2.6). Fortunately, addition of catalytic 15-crown-5 caused rapid evolution of hydrogen gas and allowed us to produce pyrazole **54** in good yield.

LC-MS monitoring suggests the initial formation of enolate **8** and **9**. Enolate **9** is nonproductive and would not form the intended product, but disappeared rapidly. We believe this suggests a thermodynamic equilibrium is in play. Enolate **70** formylates with methyl formate and becomes trapped as the conjugated system **72**. On the other hand, enolate **71** produces the non-conjugated compound **73**, which is unstable and quickly decomposes back to enolate **71**, which through proton transfer is in equilibrium with enolate **70**. When all of ketone **57** is converted to desired intermediate **72** hydrazine is added and the cyclization occurs.

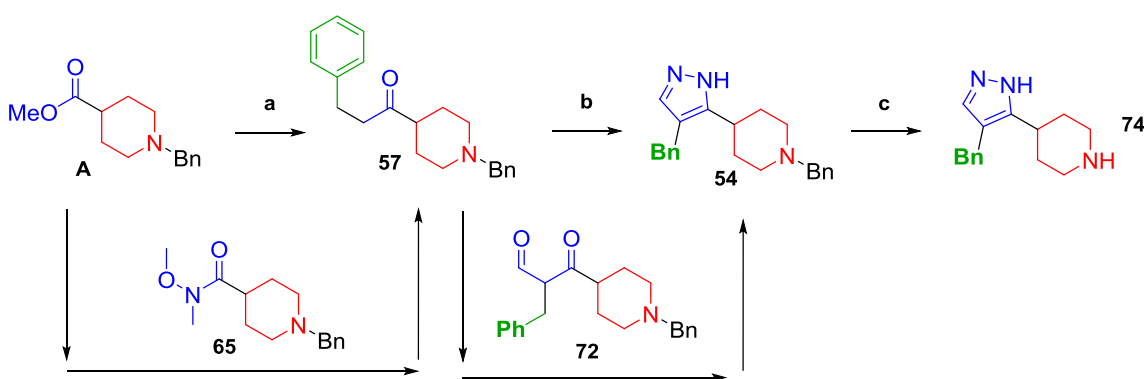
In conclusion, we have developed a new method for the formation of ketones from esters using two classic reactions in a one-pot fashion. The reaction is quite robust and tolerates a large excess of exogenous nucleophile/base, a wide range of temperatures, and any order of addition. To demonstrate its utility, we showed that incorporating the one-pot reaction in a telescopic process towards biologically relevant pyrazole **54** resulted in a nearly tenfold increase in yield and decreased the number of synthetic operations from six to two.

2.8 Initial Synthetic Studies on Dual-tropic Pyrazoles (D ring SAR)



Scheme 2.7: General route to A and D ring SAR

With synthetic methodology in hand to easily access large amounts of our pyrazole scaffold we began SAR studies on the D ring (R_2 , Scheme 2.7). As a strategy we intended to choose our C ring substituent by choice of ester, our A ring substituent by choice of Grignard reagent and our D ring substituent by choice of aldehyde or acyl chloride. Though this strategy immediately opened up a plethora of potential SAR targets we choose to focus on the initial A, B, and C ring substituents and vary the D ring in an attempt to increase potency.



Reagents: (a) *N,O*-dimethylhydroxylamine hydrochloride, Grignard reagent, sat NH_4Cl , THF; (b) NaH, 15-crown-5, Methyl Formate, MeOH, N_2H_4 , THF; (c) 10% Pd/C, *t*-BuOH

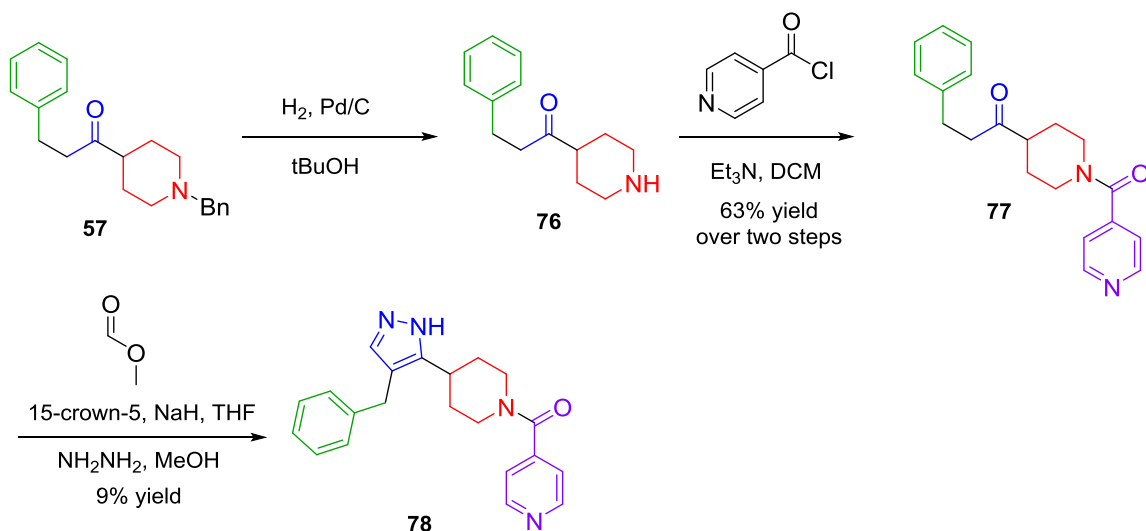
Scheme 2.8: Synthesis of modular intermediate **74**

Starting from commercially available ester **A** the Weinreb amide **65** is formed by nucleophilic attack of the Weinreb amine after deprotonation via the appropriate Grignard reagent at 0°C (Scheme 2.8). Upon warming the reaction to room temperature the Grignard acts as a nucleophile and affords analytically pure ketone **57** upon simple work-up. The ketone **57** is then subjected to sodium hydride, 15-crown-5, and reagent grade methyl formate to form intermediate **72**. Upon quenching with methanol and subsequent addition of hydrazine the pyrazole **54** is formed. The benzyl group is hydrogenated off on a Parr shaker to afford **74** which is taken on crude.



Scheme 2.9: Synthesis of compounds with various D rings

From modular intermediate **74** various D ring substituents could easily be assessed from aldehydes in a single step fashion. Of particular note is the highly variable yields which reflects the occasional difficulty of purification as well as potential variation in the hydrogenations effectiveness.



Scheme 2.10: Synthesis of compound **78**

Unfortunately synthesis of amides proved far more difficult because of the inherent nucleophilicity of pyrazoles. As a result we installed a test amido group prior to formation of the pyrazole ring (Scheme 2.10). Starting from the ketone we previously optimized (**57**) hydrogenation with Degussa grade palladium on carbon in *tert*-butanol afforded piperidine **76** which was taken on crude. Acylation of **76** with standard conditions yielded the acylated

piperidine **77**. Subjection of ketone **77** to our single-pot formylation cyclization reaction produced final compound **78** in mediocre yield.

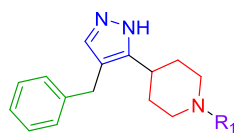


Table 2.6: Anti-HIV Data for D Ring Analogs

#	R=	MAGI Assay IC ₅₀ μM		TC ₅₀ μM	#	R=	MAGI Assay IC ₅₀ μM		TC ₅₀ μM
		CCR5	CXCR4				CCR5	CXCR4	
38		4	.8	>100	86		2	1	>100
36		17	25	>300	87		5	NA	49
79		18	13	>100	88		4	3	>100
80		>100	>100	>100	89		4	4	17
81		>100	>100	>100	90		8	7	18
82		50	59	142	91		.3	.2	34
78		>100	>100	>100	92		.2	.1	67
83		9	5	60					
84		6	5	19					
85		10	13	18					

We previously reported that the pyridine in the para position **38** was significantly more potent than in the ortho position **36**, suggesting the existence of a hydrogen bond at that position. We further corroborated this result by preparing the benzyl compound **79** which lost a similar amount of potency (Table 2.7). The replacement of the entire aryl group with a hydrogen atom **80** completely ablates activity suggesting a hydrophobic pocket or pi- stacking interaction. The phenethyl and cyclohexyl substitutions **81** and **82** also significantly decreased activity suggesting the pivotal feature is more likely pi-stacking

than hydrophobic bulk. Curious if the piperidine needed to be basic, we synthesized amide **78** and found a complete loss in potency. Looking at the electronic factors of the ring (**83-88**) we found that electronic withdrawing groups increase potency, with compound **86** being essentially equipotent to the hydrogen bond accepting pyridine **38**. Interestingly, the electron rich aniline **87** appeared to only be active against the R5 tropic virus, but being sure of this conclusion is difficult due to the low therapeutic index present. The meta analog **88** of compound **86** suggests that there is room in that portion of the binding pocket, and though we choose para substitutions for simplicity meta and ortho substitutions are likely just as active. The two naphthyl isomers **89** and **90** were also similarly potent to pyridine **1**, but were far more toxic. As electron withdrawing groups could produce potency similar to our pyridines, we decided to substitute the pyridine with chlorines **91** and **92** both of which were significantly more potent than the previous lead **38**. **91** and **92** also demonstrated slight toxicity.

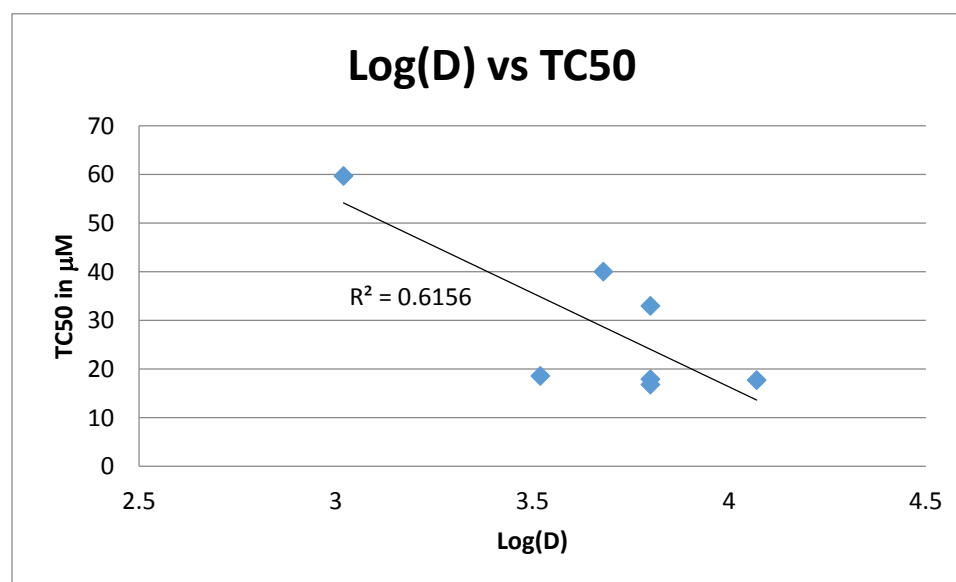


Figure 2.10: Correlation between hydrophobicity and toxicity

Plotting hydrophobicity (log D) vs toxicity reveals a modest correlation suggesting that the series' toxicity is related to hydrophobic bulk (Figure 2.10). In the above graph the Log(D) of **83**, **84**, **85**, **89**, **90**, **91**, and **92** as calculated by chemsketch is plotted against TC50's from the MAGI assay yielding a modest correlation of $R^2 = .62$. Considering the high standard deviation of MAGI results, we suspected that this correlation was highly meaningful and to some extent have avoided making hydrophobic compounds since.

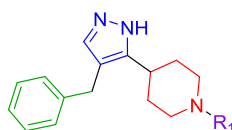


Table 2.8: Anti-HIV (% Inhibition) Data for D Ring Analogs

#	R=	MAGI Assay % inhibition @ 10 μ M		% viability @ 10 μ M	#	R=	MAGI Assay % inhibition @ 10 μ M		% viability @ 10 μ M
		CCR5	CXCR4				CCR5	CXCR4	
38		67%	73%	95%	94		33%	32%	97%
93		38%	0%	97%	95		54%	47%	94%

A resource saving strategy initiated during the screening of R1 derivatives was to initially screen compounds for percent inhibition at 10 μ M before following up with IC50 determinations. Three such compounds are presented in Table 2.8. Compound **93** was significantly less potent against the R5 tropic virus and completely inactive against the X4 tropic virus at 10 μ M, which is in sharp contrast to the 3,5 pyrimidine **45** with the analogous meta substituted isopropyl. Phenol **94** was tested to probe the ability of a hydroxyl group to potentially pick up a hydrogen bond in an analogous fashion to the lead pyridine **38**, we suspect this isn't the case as the percent inhibition was halved. The fluoro compound **95** probed the electronics of the pocket and we suspected based on a Hansch analysis of **83-86** that the fluoro substituent would not be very potent as it is only weakly electron

withdrawing. Surprisingly **95** actually had an IC₅₀ under 10 μ M based on the percent inhibitions at 10 μ M suggesting that a halogen hydrogen bond may occur.

Compound	MAGI Assay IC ₅₀ μ M		TC ₅₀ μ M	HIV 8X ActOne X4 Fusion μ M	Time of Addition Fold Loss	Inhibition of RT K103N/Y181C Fold loss
	CCR5	CXCR4				
38	4	.8	>100	24	2	21
86	2	1	>100	45	1.5	19
91	.3	.2	34	14	3	66
92	.2	.1	67	9	1.5	1.5

Based on our initial D ring SAR we choose a handful of compounds for further characterization as part of a collaboration with Bristol-Myers Squibb (BMS). BMS initially tested **38** (pyridyl), **86** (SO₂Me), **91**, and **92** (chloropyridines) in the CXCR4 fusion assay with ActOne cells (Table 2.9). All four compounds were significantly less potent in the fusion assay than MAGI which is surprising due to our presumed mechanism of action being stopping HIV entry. Follow up testing with a time of addition loss calculation found that even if we allowed HIV enter cells before addition of our compound that there was still a reduction of viral replication (albeit 2-3 fold lower than preincubation with compound). This data strongly suggested the existence of a second mechanism of action that was operable after HIV entry occurred, but also further confirmed our entry mechanism when compared to the fusion results. When ran against a NRTI resistant HIV strain all four compounds lost appreciable activity as compared to wildtype controls. Taken together this data strongly suggests that our compounds act as HIV entry inhibitors with concurrent inhibition of HIV reverse transcriptase. Interestingly, the NNRTI mutant was still very

sensitive to compound **92**, thought this result is dampened by the fact that nearly every modern NNRTI on the market shares this activity.

With this initial set of structurally similar analogs we set out to make CCR5, CXCR4, and Reverse Transcriptase binding models in silico.³³ We started with the GPCR's CCR5 and CXCR4 because their crystal structures were recently published.³⁴⁻³⁵ GPCRs are composed of seven transmembrane helices numbered consecutively from I to VII starting from the N-terminus. Chemokine receptors possess a spacious extracellular ligand binding pocket containing two sub-pockets. The minor sub-pocket is shallow composed of helices I-III, and the major sub-pocket penetrates deep into the receptor composed of helices VI through VII. To better understand the SAR for this series, studies were initiated to determine binding models for this series interacting with the CCR5 and CXCR4 receptors.

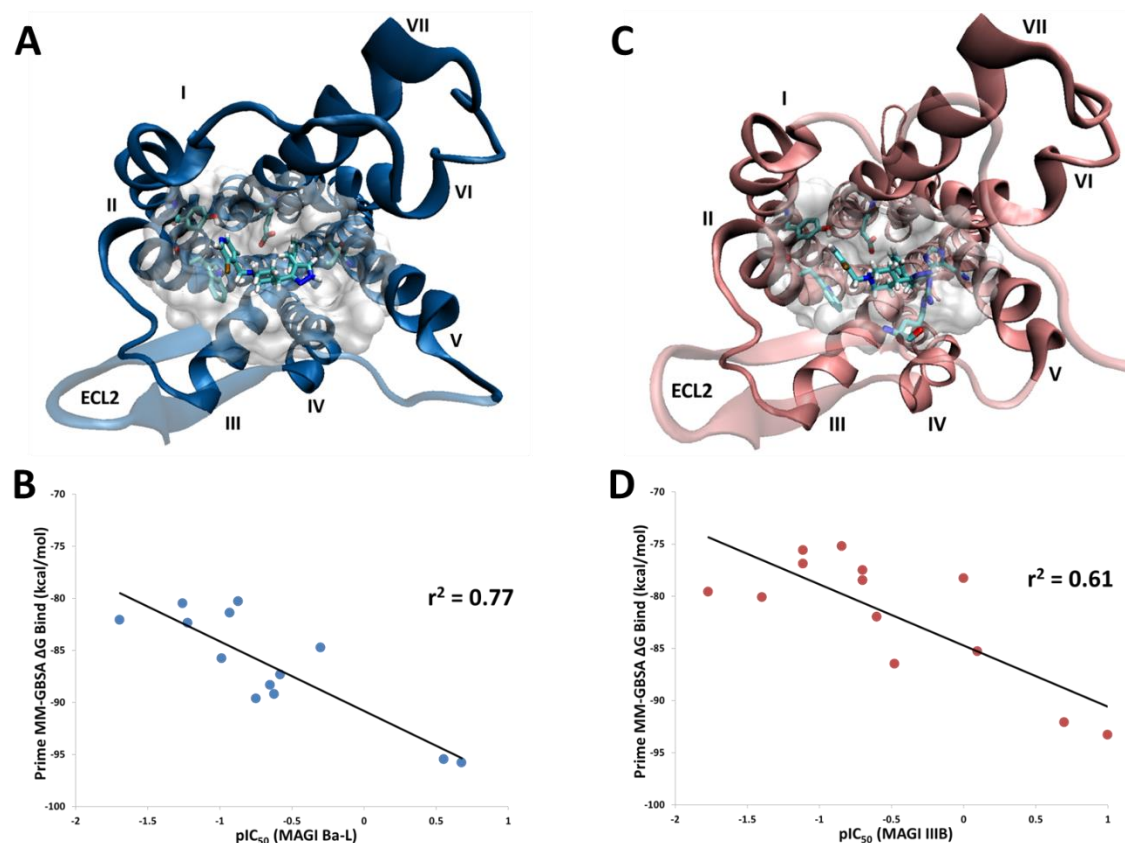


Figure 2.11: Binding of pyrazolo-piperidines to CCR5 (A/B) and CXCR4 (C/D) predicted by molecular modeling.

Our initial modeling of compounds provided in Table 2.6 is provided herein. A) Docked pose of compound **92** as determined from the CCR5:Maraviroc crystal structure (PDBID – 4MBS, Chain A). B) Correlation of Prime MM-GBSA scores from this model with experimental anti-HIV activity from the MAGI Ba-L assay. C) Docked pose of compound **92** as determined from the CXCR4 model based on the CCR5 crystal structure. D) Correlation of Prime MM-GBSA scores from this model with experimental anti-HIV activity from the MAGI IIIB assay.

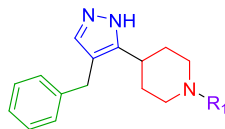


Table 2.10: R5 vs X4 vs RT activity for D Ring Analogs

#	R=	MAGI Assay IC ₅₀ μM		RT IC ₅₀ μM	#	R=	MAGI Assay IC ₅₀ μM		RT IC ₅₀ μM
		CCR5	CXCR4				CCR5	CXCR4	
38		4	.8	9	97		1	2	1.5
91		.3	.2	10	98		.6	.4	4
92		.2	.1	10	99		.4	1	7
82		49	59	>200	100		.8	1.5	4
89		4	4	20	101		1	4	35
90		8	7	23	102		20	>100	146
96		.8	1	3	103		43	>100	211
					104		>100	>100	>100

Due to the serendipity of having RT activity in our series we decided to return to SAR of the D ring to get a better modeling handle for the reverse transcriptase (RT) activity. Starting with screening pyridine **38** and chloropyridines **91** and **92** we discovered that their RT activity was essentially the same despite an approximately 10 fold difference in anti-viral potency (Table 2.9). The cyclohexyl compound **82** on the other hand was completely inactive against reverse transcriptase. These observations suggest that the identity of the D ring is a more important structural element for RT activity than chemokine activity and provides an interesting starting point for development of a dual-tropic/chemokine anti-HIV compound without RT activity. On the other hand the naphthyl isomers **89** and **90** had

potencies that leaned slightly more towards the RT side of activity. Postulating that a hydrogen bond acceptor could improve our selectivity we synthesized the quinolone **96** and found it to be far more potent against RT than its non-hydrogen bond accepting predecessor **90**. Based on our initial models we suspected that a properly placed methoxide could accept a hydrogen bond whilst simultaneously providing steric bulk. Gratifyingly, compound **97** demonstrated this hypothesis with similar potency in the RT and MAGI assay. We theorized that compounds with negligible potency differences between the RT and MAGI assay were essentially just inhibitors of reverse transcriptase. Follow up fusion testing for both **96** and **97** found no activity in the fusion assay (Table 4) further validating our analysis of MAGI vs RT data. Next we turned our attention to electron withdrawing groups with varying levels of bulk. The sulfoxide **98** leaned slightly towards RT activity compared to the meta-chloro analog **92**. The ortho-bromo analog **99** was synthesized instead of the meta isomer due to stability concerns, it also leaned slightly towards RT activity. The 2,3 dichloropyridine **100** had a similar profile further corroborating our bulk to NNRTI hypothesis. The very electron deficient compound **101** had potency leaning towards the chemokines, and we suspect this is due to the relative lack of steric bulk in conjunction with a strong pi-stacking interaction. Interestingly, the 2,4 pyrimidine **102** and cyano-substituted pyridine **103** appeared to only have CCR5 and RT activity, albeit with very little potency in both. The N-oxide **104** was completely inactive.

With a basis set in hand (Table 2.10) we tested several models of the series binding to HIV-RT using available co-crystal structures with Etravirine (pdb 3M8P), Delavirdine (pdb 1KLM), and Nevirapine. The only model that reasonably correlated Prime MM-GBSA ΔG binding with the experimental HIV-RT IC_{50} potencies was obtained from

induced fit docking into the HIV-RT:Nevirapine co-crystal structure in the presence of the RNA/DNA:template/primer (pdb 4PUO). In this model, compound **92** occupies a solvent-exposed cavity flanked by V108 and F227 (Figure 3A). The piperidine ring establishes hydrophobic interactions with P236 and Y318. The pyrazole acts as a hydrogen bond donor to K101, and the benzyl ring buries in a hydrophobic pocket surrounded by W229, Y188, and Y181. The 13 active compounds with HIV-RT IC₅₀ values were docked into this model and re-scored using Prime MM-GBSA (Figure 3B). This model correctly assigns the most potent compound as **97** and the least potent compounds as **102** and **103**. Fitting the scores to a linear model, a modest correlation is observed ($r^2 \sim 0.5$) (Figure 2.12).

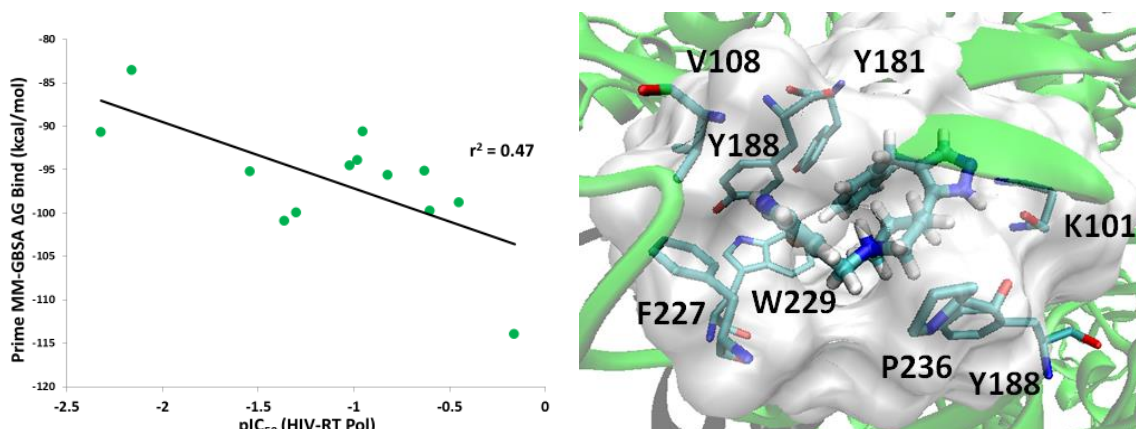
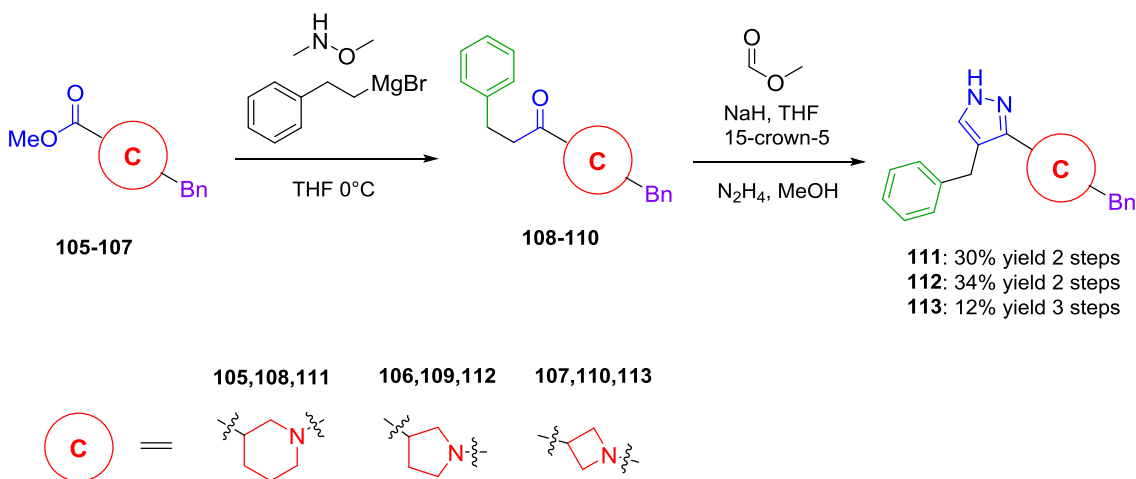


Figure 2.12: Binding of pyrazolo-piperidines to HIV-RT predicted by molecular modeling.

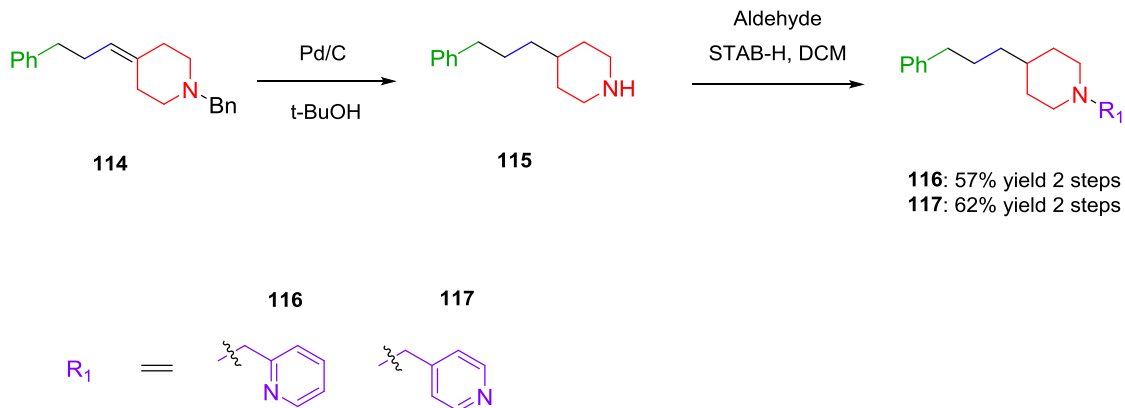
2.9 Additional Synthetic Studies on Dual-tropic Pyrazoles (A, B, C-ring SAR)

With a thorough screening of D-ring substituents being completed and an initial gain of 100 fold potency from this effort, we next turned our attention to the synthesis of A, B, and C ring analogs by tuning of our initial synthetic strategy. We envisioned varying our A ring through choice of Grignard reagent, B ring through different synthetic pathways and C ring through choice of initial ester.



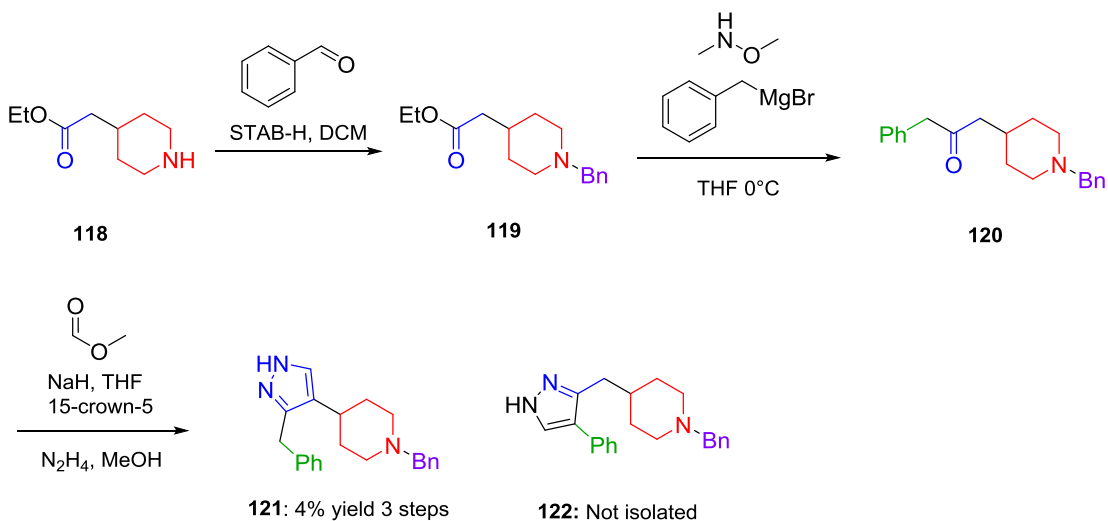
Scheme 2.11: Synthesis of C ring analogs

The isopiperidine ester **105** and pyrrolidine ester **106** were both commercially available with benzyl protecting groups. Ester **107** was prepared by reductive amination and taken on crude through the 3 step sequence. Ketone formation with our optimized conditions of esters **105-107** afforded ketones **108-110** which were taken on crude. The enolates of **108-110** were formed with sodium hydride and 15-crown-5 and subsequently quenched with methyl formate, the thermodynamically favored enolate is then trapped with hydrazine to afford **111-113** in moderate yield over 2 or 3 steps.



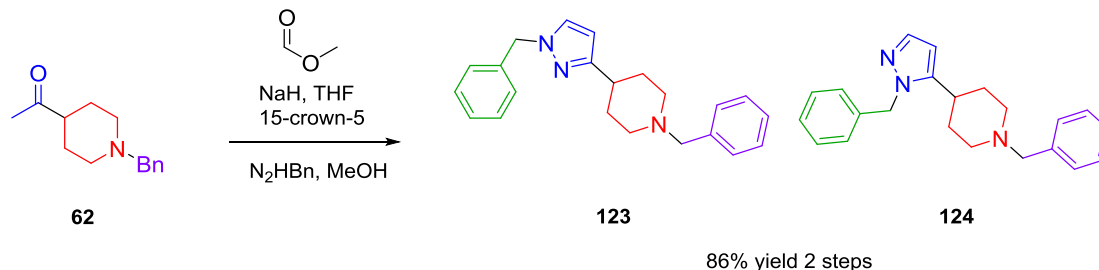
Scheme 2.12: Synthesis of compounds **116** and **117**

B ring modifications had to be pursued on a fairly un-modular basis. The first two B ring analogs **116** and **117** were chosen to probe the need for a pyrazole ring as well as if in this binding motif if the hydrogen bond accepting interaction was still in place (Scheme 2.12). We suspected both compounds to be active in CCR5 based on previous work by Merck, and we had no preconceived notions as to whether the ortho **116** or para **117** pyridine would be more potent. Starting from the piperidino-alkene **114** hydrogenation with Degussa grade palladium on carbon in *tert*-butanol afforded piperidine **115** which was both deprotected and reduced in one step. Subsequent reductive amination on crude **115** with the ortho and para pyridine aldehyde yielded **116** and **117** respectively.



Scheme 2.13: Synthesis of compound **121**

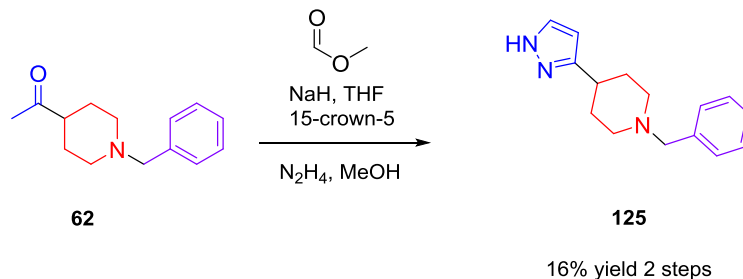
Commercially available ester **118** was benzylated with standard reductive amination conditions to afford the protected piperidine **119** (Scheme 2.13). Subjecting ester **119** to our standard one pot ketone synthesis with freshly prepared benzyl Grignard afforded ketone **120** which was taken on crude. Subjecting internal ketone **120** to our enolate forming and trapping conditions afforded a mixture of **121** and **122** as detected by LCMS, but upon purification only the intended product **121** was isolated. The very poor 4% yield comes as a result of the difficulty in separating **121** from **122**, and though only 4% of **121** was recovered completely pure well more than twice as much of the material was isolated as a mixture with **122**. **121** was identified as the correct isomer as compared to **122** via coupling constant comparisons for the signals in ^1H NMR versus that of the parent compound. In particular **121** has a singlet benzyl peak that integrates for 2 protons whereas **122** is split into a triplet.



Scheme 2.14: Synthesis of compounds **123** and **124**

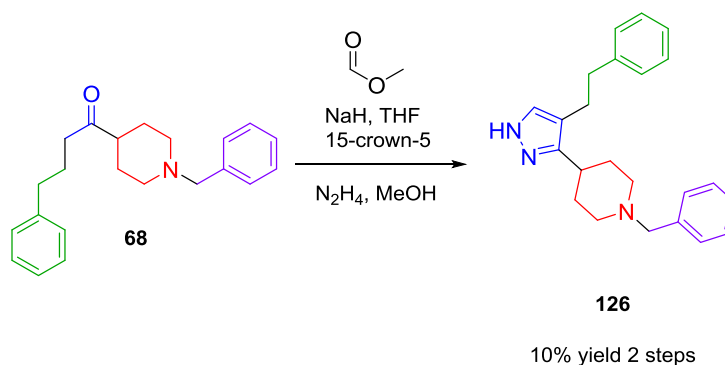
We were particularly interested in probing the bond configuration around the pyrazole ring, as it wasn't clear if a hydrogen bond donor was even necessary. We envisioned that compound **124** which is isosteric to our parent series would probe the need of an N-H bond in the B core (Scheme 2.14). With the synthetic strategy pursued **123** was also formed as an unavoidable byproduct and was thus also tested. Starting with methyl ketone **62** that was prepared in route to our synthetic methodology application of our enolate formation and subsequent cyclization conditions with benzyl hydrazine afforded **123** and **124** as a difficult to separate mixture. Multiple columns with tight gradients eventually afforded **123** and **124** as pure compounds in good yield.

Next we turned our attention to A ring analogs, which were easily obtained by variation of Grignard reagents. It is worth noting that there were several functional groups that ultimately were not compatible with Grignard formation such as pyridines, halogenated aromatic rings, and electron deficient aryl rings. As a result, the tested A rings were ultimately chosen to probe specific SAR questions while being quite limited to only simplistic motifs.



Scheme 2.15: Synthesis of compound **125**

The first analog to probe the SAR around the A ring we tested was the compound with no A ring at all. Starting from previously synthesized compound **62** from our methodology study the pyrazole formation reaction we optimized afforded compound **125** in poor yield over two steps (Scheme 2.15).

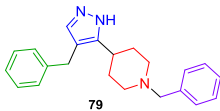
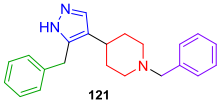
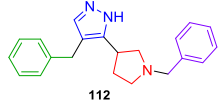
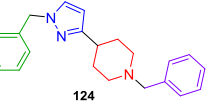
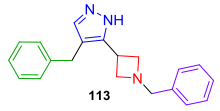
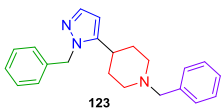
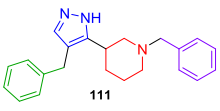
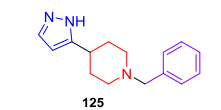
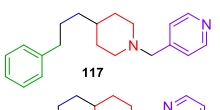
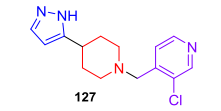
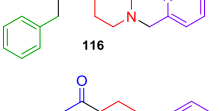
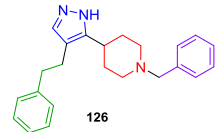
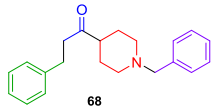


Scheme 2.16: Synthesis of compound **126**

We also endeavored to probe the symmetry of the binding pockets in regards to length of the compounds. Having observed that the addition of a single methylene unit to the D ring (compound **81**) completely killed activity, we were curious if such an addition to the A ring would similarly kill activity against one, two, or all three targets. This hypothesis was particularly interesting because one could imagine the compound binding with a flipped pose between any two of the three targets, based on the current level of SAR collected. Starting from previously synthesized compound **68** from our methodology study

the pyrazole formation reaction we optimized afforded compound **126** in poor yield over two steps (Scheme 2.16).

Table 2.11: SAR of the A, B, C Rings

Structure	MAGI Assay IC ₅₀ μM		TC ₅₀ μM	Structure	MAGI Assay IC ₅₀ μM		TC ₅₀ μM
	CCR5	CXCR4			CCR5	CXCR4	
	18	13	>100		NA	16	53
	NA	NA	70		>100	>100	>100
	NA	NA	70		>100	>100	>100
	70	>100	>100		>100	>100	>100
	24	NA	125		>100	>100	>100
	74	NA	153		>50	>50	>50
	>100	>100	>100				

*NA denotes activities that are within 5% of toxicity.

With D ring modifications **91** and **92** increasing our potency into the nanomolar range, we sought to modify the A, B, and C rings to further increase potency. Starting with modifications of the C ring (Table 2.11, **111-113**) we discovered that the piperidine moiety was essential for good anti-viral activity. Ring contracting the C ring to the pyrrolidine **112** or the azetidine **113** completely ablates activity. Similarly the shifted piperidine **114** also significantly decreased activity as compared to parent compound **79**. Moving to the B ring we were unsurprised that deletion of the pyrazole ring **117** led to an approximately 5 fold loss of CCR5 activity but complete loss of CXCR4 activity and loss of reverse transcriptase

activity. The loss in reverse transcriptase activity is most likely responsible for the associated loss in total activity against the R5 tropic HIV virus, as opposed to a loss in binding to CCR5. This SAR is similar to that previously observed by Merck.³⁶⁻³⁸ Additionally, moving the hydrogen bond accepting pyridine nitrogen from the para to ortho position **116** resulted in a threefold loss in potency, suggesting that the previous SAR still follows in this binding motif. Comparing compounds **36** and **38** to the congeners **116** and **117** suggests that the CCR5 binding motif is conserved between the four compounds, while the pyrazole moiety is linked more to the other two target activities, namely CXCR4 and reverse transcriptase. Surprisingly, replacing the pyrazole with a ketone **68** resulted in complete loss of activity against all three targets. The ortho pyrazole **121** was only active against the X4 tropic HIV virus, but due a low TC50 of only 53 μM it is possible that there is CCR5 activity that is not separable from the cytotoxicity. Moving the position of the A ring to either of the pyrazole nitrogens **123** and **124** ablates anti-viral activity. It is worth noting that compound **124** is isosteric to the other tautomer of **79**. For CCR5 activity the presence of a pyrazole seems unnecessary, but when present only one isomer appears to be active. Moving to SAR of the A ring both removing the benzyl group **125** and increasing its length by one methylene unit **126** caused complete loss of activity. Due to the low activity window of the benzyl D rings an undergraduate in our lab synthesized the chloropyridine **127** version of **125** which is similarly inactive. Taken together the SAR of the A and B ring suggests that reverse transcriptase activity requires a benzyl/pyrazole pharmacophore, R5 activity requires a benzyl group but tolerates deletion of the pyrazole functionality, and that X4 activity requires a benzyl group and either arrangement of the pyrazole functionality.

2.10 Dual-tropic Pyrazole Series Conclusions

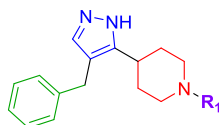


Table 2.12 Profiling of Two Sub-Series

#	R=	MAGI Assay IC ₅₀ μM		RT IC ₅₀ μM	Fusion Assay IC ₅₀ μM		M.O.A.
		CCR5	CXCR4		CCR5	CXCR4	
38		4	.8	9	35	52 ^b	CXCR4 CCR5 NNRTI
91		.3	.2	10	19 ^a	14 ^b	
92		.2	.1	10	20 ^a	9 ^b	
96		.8	1	3	>40	>40	NNRTI
97		1	2	1.5	>40	>40	

^a Single cycle fusion with clinical envelope 1-16C17

^b Single cycle fusion with CD4 independent 8XActOneX4 cells

In conclusion SAR and models developed around our pyrazolo-piperidine series is allowing the concurrent tuning of three separate mechanisms of action, namely against CCR5 and CXCR4 chemokine receptors as well as HIV reverse transcriptase. As a result our most potent compound (**92**) has sub-μM potency and is nearly 10 fold more potent than the initial hit **38** in the MAGI assay. Moreover, compounds **91** and **92** appear to have a balanced activity between the three targets. Whilst, modifications that completely ablate the CXCR4 and CCR5 mechanism of action were also identified producing μM potent NNRTI compounds **96** and **97**. The increase in RT activity and concurrent decrease in chemokine activity in going from balanced compounds **91** and **92** to the screening hit **38** to the RT only compounds **96** and **97** indicates that multi-target compounds can be tuned

to single targets with small chemical modifications. While the NNRTI compounds are interesting spin-offs from this study, the tunability towards dual chemokine entry inhibition observed with the discovery of compounds **91** and **92** offer a more desirable direction for future work.

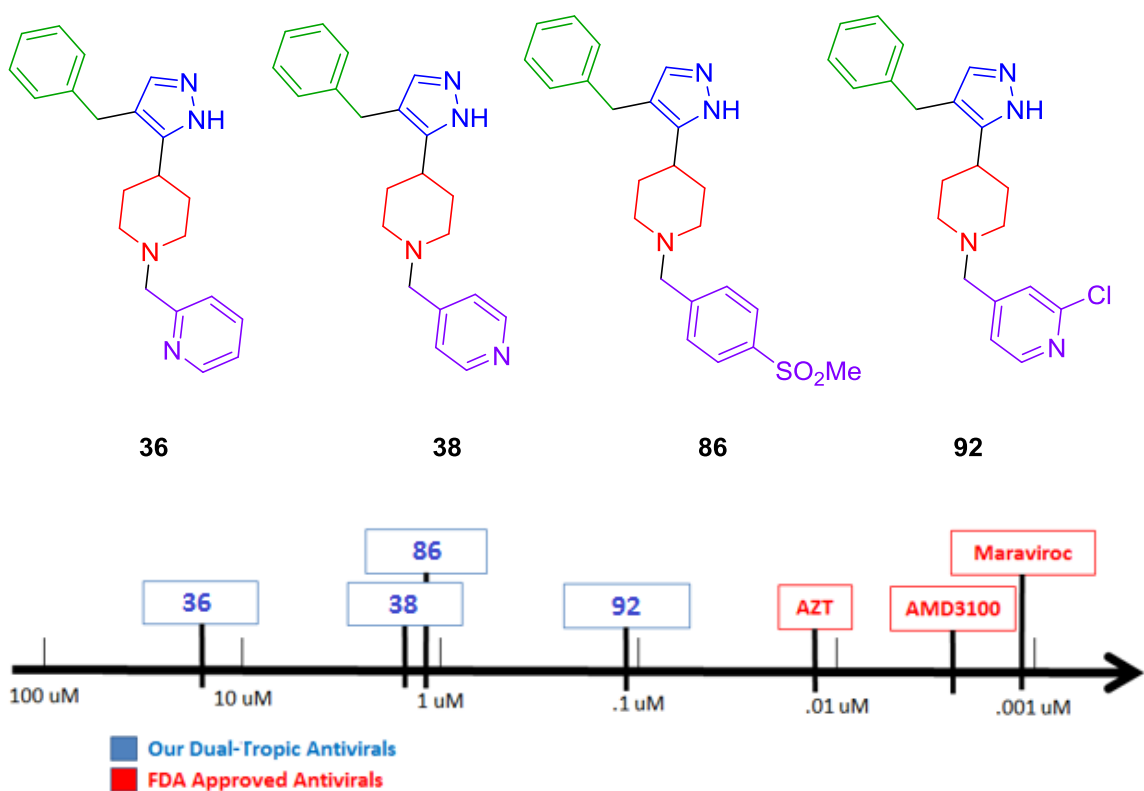


Figure 2.13: Potency gains from virtual screening hit to compound **92**

In addition to finding compounds that bind just X4 and R5, compounds that bind X4, R5, and RT, and compounds that bind just RT, we significantly improved our potency from the initial virtual screening effort in terms of total antiviral potency (Figure 2.13). From ortho pyridine **36** moving the pyridine to the para position **38** brought a potency increase of approximately 10 fold by picking up a hydrogen bond. A similar potency jump was also achieved by replacing the pyridine nitrogen with a sulfonyl methyl substituent **86**

by withdrawing electron density from the ring. Combining both the electron withdrawing activity and the hydrogen bond accepting nitrogen in compound **92** resulted in another approximately 10 fold increase in potency. In total, even with such a large increase in potency **92** is still 10 fold from being comparable to AZT and 100 fold from being similarly potent to AMD3100 and Maraviroc. On the other hand, if the series were to achieve such potency it would have the same mechanisms of action of the three previously mentioned compounds in one single agent. This proof of concept reveals a new direction of antiviral research, but based on our initial results we suspect achieving subnanomolar potencies against three targets with one compound may require a herculean effort.

References:

1. Fauci, A. S., et al. (2013). "HIV-AIDS: much accomplished, much to do." Nat Immunol **14**(11): 1104-1107.
2. Moss, J. A. (2013). "HIV/AIDS Review." Radiol Technol **84**(3): 247-267; quiz p.268-270.
3. Solomon, D. A. and P. E. Sax (2015). "Current state and limitations of daily oral therapy for treatment." Curr. Opin. HIV AIDS **10**(4): 219-225.
4. Phillips, A., et al. (2014). "Cost-effectiveness of HIV drug resistance testing to inform switching to second line antiretroviral therapy in low income settings." PLoS One **9**(10): e109148/109141-e109148/109110, 109110 pp.
5. Herschhorn, A., et al. (2014). "A broad HIV-1 inhibitor blocks envelope glycoprotein transitions critical for entry." Nat Chem Biol **10**(10): 845-852.
6. Jenwitheesuk, E., et al. (2008). "Novel paradigms for drug discovery: computational multitarget screening." Trends Pharmacol Sci **29**(2): 62-71.
7. Watson Buckheit, K., et al. (2011). "Development of Dual-Acting Pyrimidinediones as Novel and Highly Potent Topical Anti-HIV Microbicides." Antimicrobial Agents and Chemotherapy **55**(11): 5243-5254.
8. Tilton, J. C. and R. W. Doms (2010). "Entry inhibitors in the treatment of HIV-1 infection." Antiviral Research **85**(1): 91-100.
9. Kramer, V. G. and M. A. Wainberg (2015). "Resistance against inhibitors of HIV-1 entry into target cells." Future Virol. **10**(2): 97-112.
10. Truax, V. M., et al. (2013). "Discovery of Tetrahydroisoquinoline-Based CXCR4 Antagonists." ACS Med. Chem. Lett. **4**(11): 1025-1030.

11. Zhao, H., et al. (2015). "Discovery of novel N-aryl piperazine CXCR4 antagonists." Bioorg. Med. Chem. Lett.: Ahead of Print.
12. Poveda, E., et al. (2006). "HIV tropism: diagnostic tools and implications for disease progression and treatment with entry inhibitors." AIDS **20**(10): 1359-1367.
13. Ashkenazi, A., et al. (2011). "Multifaceted action of Fuzeon as virus-cell membrane fusion inhibitor." Biochim. Biophys. Acta, Biomembr. **1808**(10): 2352-2358.
14. Morozov, V. A., et al. (2007). "Transmembrane protein polymorphisms and resistance to T-20 (Enfuvirtide, Fuzeon) in HIV-1 infected therapy-naive seroconverters and AIDS patients under HAART-T-20 therapy." Virus Genes **35**(2): 167-174.
15. Veljkovic, N., et al. (2015). "Preclinical discovery and development of maraviroc for the treatment of HIV." Expert Opin. Drug Discovery **10**(6): 671-684.
16. Llibre, J. M., et al. (2015). "Safety, efficacy and indications of prescription of maraviroc in clinical practice: Factors associated with clinical outcomes." Antiviral Res. **120**: 79-84.
17. Wilson, L. J. and D. C. Liotta (2011). "Emergence of small-molecule CXCR4 antagonists as novel immune and hematopoietic system regulatory agents." Drug Dev. Res. **72**(7): 598-602.
18. Zraggen, S., et al. (2014). "An Important Role of the SDF-1/CXCR4 Axis in Chronic Skin Inflammation." PLoS One **9**(4): e93665.
19. Ness, T. L., et al. (2006). "CCR5 antagonists: the answer to inflammatory disease?" Expert Opin Ther Pat **16**(8): 1051-1065.
20. Furusato, B., et al. (2010). "CXCR4 and cancer." Pathol Int **60**(7): 497-505.

21. Burger, J. A., et al. (2011). "Potential of CXCR4 antagonists for the treatment of metastatic lung cancer." Expert Rev Anticancer Ther **11**(4): 621-630.
22. Velasco-Velazquez, M., et al. (2012). "CCR5 antagonist blocks metastasis of basal breast cancer cells." Cancer Res **72**(15): 3839-3850.
23. Moyle, G., et al. (2009). "Proof of Activity with AMD11070, an Orally Bioavailable Inhibitor of CXCR4-Tropic HIV Type 1." Clinical Infectious Diseases **48**(6): 798-805.
24. Shen, D. M., et al. (2004). "Antagonists of human CCR5 receptor containing 4-(pyrazolyl)piperidine side chains. Part 1: Discovery and SAR study of 4-pyrazolylpiperidine side chains." Bioorg Med Chem Lett **14**(4): 935-939.
25. Shen, D. M., et al. (2004). "Antagonists of human CCR5 receptor containing 4-(pyrazolyl)piperidine side chains. Part 2: Discovery of potent, selective, and orally bioavailable compounds." Bioorg Med Chem Lett **14**(4): 941-945.
26. Merk Chapman, K.; Hale, J.; Kim, D.; Lynch, C.; Shah, S.; Shankaran, K.; Shen, D.-m.; Willoughby, C.; Maccoss, M.; Mills, S. G.; Loebach, J. L.; Guthikonda, R. N. WO2000059502A1, 2000.
27. Nahm, S. and S. M. Weinreb (1981). "N-Methoxy-N-methylamides as effective acylating agents." Tetrahedron Lett. **22**(39): 3815-3818.
28. Grignard, V. (1900). "About some new organo-metallic compounds of the magnesium and their application to the synthesis of alcohols and hydrocarbons. [machine translation]." C. r. d. l'Acad. des Sciences **130**: 1322-1324.
29. Pedrosa, R., et al. (2005). "Sequential diastereoselective addition of allylic and homoallylic Grignard reagents to 2-acyl-perhydro-1,3-benzoxazines and ring-closing

- metathesis: An asymmetric route to azepin-3-ol and azocin-3-ol derivatives." Eur. J. Org. Chem.(12): 2449-2458. Calvo, L.; Gonzalez-Ortega, A.; Navarro, R.; Perez, M.; Sanudo, M. C., *Synthesis* **2005**, (18), 3152-3158.
30. Balasubramaniam, S. and I. S. Aidhen (2008). "The Growing Synthetic Utility of the Weinreb Amide." Synthesis **2008**(23): 3707-3738.
31. Seyferth, D. (2009). "The Grignard Reagents." Organometallics **28**(6): 1598-1605.
32. Beight, D. W.; Burkholder, T. P.; Clayton, J. R.; Eggen, M.; Henry, K. J. J.; Johns, D. M.; Parthasarathy, S.; Pei, H.; Rempala, M. E.; Sawyer, J. S. WO2011050016A1, 2011.
33. Cox, B. D., et al. (2014). "Anti-HIV Small-Molecule Binding in the Peptide Subpocket of the CXCR4:CVX15 Crystal Structure." ChemBioChem **15**(11): 1614-1620.
34. Tan, Q., et al. (2013). "Structure of the CCR5 Chemokine Receptor–HIV Entry Inhibitor Maraviroc Complex." Science **341**(6152): 1387-1390.
35. Wu, B., et al. (2010). "Structures of the CXCR4 Chemokine GPCR with Small-Molecule and Cyclic Peptide Antagonists." Science **330**(6007): 1066-1071.
36. Shen, D.-M., et al. (2004). "Antagonists of human CCR5 receptor containing 4-(pyrazolyl)piperidine side chains. Part 1: Discovery and SAR study of 4-pyrazolylpiperidine side chains." Bioorganic & Medicinal Chemistry Letters **14**(4): 935-939.
37. Shen, D.-M., et al. (2004). "Antagonists of human CCR5 receptor containing 4-(pyrazolyl)piperidine side chains. Part 2: Discovery of potent, selective, and orally

- bioavailable compounds." Bioorganic & Medicinal Chemistry Letters **14**(4): 941-945.
38. Shu, M., et al. (2004). "Antagonists of human CCR5 receptor containing 4-(pyrazolyl)piperidine side chains. Part 3: SAR studies on the benzylpyrazole segment." Bioorganic & Medicinal Chemistry Letters **14**(4): 947-952.

2.11 Dual-Tropic Experimental

Frequently used procedures:

Hydrogenation A:

To a solution of the substrate in EtOH (.1M) and AcOH (.01 M) is added Pd/C (10-50% by mass). The reaction is hydrogenated under an atmosphere of H₂ between 45-55 psi on a parr hydrogenator overnight. Upon completion the H₂ is purged *in vacuo* and then flushed with argon. The crude reaction mixture is then filtered through two fluted pieces of filter paper and concentrated *in vacuo*. The mixture is then diluted with brine and DCM followed by basification with 10% NaOH. The layers are separated and the aqueous layer extracted with DCM (3 times). The organic layers are combined, dried over anhydrous sodium sulfate, filtered and concentrated to afford the crude product which if necessary is purified by column chromatography.

Hydrogenation B:

To a solution of the substrate in *t*-BuOH (.1M) and AcOH (.01 M) is added Pd/C (10-50% by mass). The reaction is hydrogenated under an atmosphere of H₂ between 45-55 psi on a parr hydrogenator overnight. Upon completion the H₂ is purged *in vacuo* and then flushed with argon. The crude reaction mixture is then filtered through two fluted pieces of filter paper and concentrated *in vacuo*. The mixture is then diluted with brine and DCM followed by basification with 10% NaOH. The layers are separated and the aqueous layer extracted with DCM (3 times). The organic layers are combined, dried over anhydrous sodium sulfate, filtered and concentrated to afford the crude product which if necessary is purified by column chromatography.

Hydrogenation C:

To a solution of the substrate in *t*-BuOH (.1M) and AcOH (.01 M) is added Pd/C (10-50% by mass). The reaction is then heated to 80C and ammonium formate is added portion wise (3 eq). The reaction is tracked by LCMS and usually done within 30 minutes. The reaction is then concentrated *in vacuo*. The mixture is then diluted with brine and DCM followed by basification with 10% NaOH. The layers are separated and the aqueous layer extracted with DCM (3 times). The organic layers are combined, dried over anhydrous sodium sulfate, filtered and concentrated to afford the crude product which is used without further purification.

Cbz-Deprotection:

A solution of the Cbz protected amine (1eq) and thioanisole (1eq) in DCM:methane sulfonic acid (.5 M, 1:1) was stirred under inert atmosphere. The reaction was checked by LCMS and was complete within 4 hours. The mixture was then diluted with H₂O and DCM. The layers are separated and the aqueous layer extracted with DCM (3 times). The aqueous layer was diluted with 10% NaOH until very basic. The aqueous layer was then extracted with DCM (3 times). The organic layers were combined, dried over anhydrous sodium sulfate, filtered and concentrated to afford the crude product which is purified by column chromatography.

Boc-Deprotection:

A solution of the Boc protected amine in DCM:TFA (.5 M, 4:1) was stirred under inert atmosphere. The reaction is tracked by LCMS and is usually complete within two hours. Upon completion the mixture is diluted with brine and basified with 10% NaOH. The layers are separated and the aqueous layer extracted with DCM (3 times). The organic layers were combined, dried over anhydrous sodium sulfate, filtered and concentrated to afford the crude product which is purified by column chromatography.

Reductive Amination:

To a solution of the amine in DCM (.1M) is added the aldehyde (1.1 eq) and stirred at room temperature for 30 minutes. Then sodium triacetoxyborohydride (1.5 eq) is added as one portion and the reaction is tracked by LCMS. The reaction is usually complete within 5 hours. Upon completion the mixture is diluted with brine and basified with 10% NaOH. The layers are separated and the aqueous layer extracted with DCM (3 times). The organic layers were combined, dried over anhydrous sodium sulfate, filtered and concentrated to afford the crude product which is purified by column chromatography.

Acylation A:

To a solution of the amine in DCM (.1M) is added triethylamine (2 eq). Then the acyl chloride (1.5 eq) is added dropwise with stirring. The reaction is tracked by LCMS and is usually complete within two hours. Upon completion the mixture is diluted with brine and basified with 10% NaOH. The layers are separated and the aqueous layer extracted with DCM (3 times). The organic layers were combined, dried over anhydrous sodium sulfate, filtered and concentrated to afford the crude product which is purified by column chromatography.

Acylation B:

To a solution of the amine dissolved in DCM (.2M) in a microwave vial is added triethylamine (1.5 eq). Then the acyl chloride (1.2 eq) is added dropwise. The vial is then subjected to 125°C for 20 minutes in a microwave reactor. Upon completion the mixture is diluted with brine and acidified with 10% HCl. The layers are separated and the aqueous layer extracted with DCM (3 times). The organic layers were combined, dried over anhydrous magnesium sulfate, filtered and concentrated to afford the crude product which is purified by column chromatography.

Acylation C:

To a solution of amine in DCM (.1M) is added the acyl chloride (1.5 eq) dropwise with stirring. The reaction is tracked by LCMS and is usually complete within two hours. Upon completion the mixture is diluted with brine and basified with 10% NaOH. The layers are separated and the aqueous layer extracted with DCM (3 times). The organic layers were combined, dried over anhydrous sodium sulfate, filtered and concentrated to afford the crude product which is purified by column chromatography.

Acylation D:

To a solution of the amine dissolved in DCM (.2M) in a microwave vial is added the acyl chloride (1.2 eq) dropwise. The vial is then subjected to 125°C for 20 minutes in a microwave reactor. After cooling back to room temperature triethylamine (1 eq) is added and the mixture is concentrated to afford the crude product which is purified by column chromatography.

Thioamide Formation:

To a solution of amide dissolved in toluene (.1M) in a microwave vial is added Lawesson's Reagent (1.5 eq). The reaction is then microwaved at 150°C for 20 minutes in a microwave reactor. After cooling back to room temperature the reaction is concentrated *in vacuo* to afford the crude product which is purified by column chromatography.

Suzuki Coupling:

To a solution of aryl bromide dissolved in toluene (.1M) in a microwave vial is added Potassium Carbonate (3 eq), Palladium Tetrakis (.1 eq), and the corresponding boronic acid (2 eq). The reaction is then microwaved at 150°C for 5 minutes in a microwave reactor. After cooling back to room temperature the reaction is concentrated *in vacuo* to afford the crude product which is purified by column chromatography.

Bromination of Alcohols:

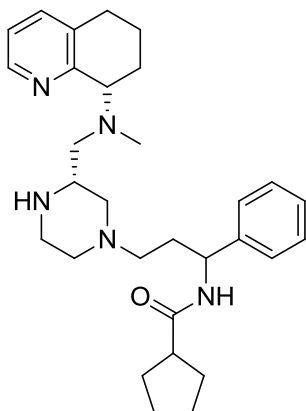
To a stirred solution of alcohol dissolved in DCM (1M) at 0°C in a round bottom flask is added CBr₄ (1.2 eq) and then triphenyl phosphine (1.2 eq) portionwise over 10 minutes. The reaction is tracked by LCMS and typically done within 1 hour. The reaction is then concentrated *in vacuo* and diethyl ether added. The resulting solids are removed by filtration and the filtrate concentrated *in vacuo* to afford the crude product which is purified by column chromatography.

Formation of Grignard Reagents:

To a flame dried flask containing finely crushed Magnesium (1.5 eq) suspended in dry THF (1 M) under argon is added the corresponding bromide. The reaction is then stirred vigorously with careful attention to temperature. The reaction is allowed to exothermically heat to the point of slight bubbling and then maintained at this sub-refluxing temperature with use of ice and water baths. If the reaction does not proceed, addition of catalytic Iodine (1 crystal) should be employed. If the reaction still does not proceed the addition of a small amount of isopropyl magnesium chloride (.01 eq) can be employed. Once the reaction stops evolving heat it's allowed to stir for one more hour at room temperature to ensure full conversion. The product is used as a solution in THF.

Weinreb Grignard one-pot Reaction:

To a stirred solution of the corresponding ester as a solution in THF (.1 M) was added to a flame dried 100 mL round bottom flask containing N,O-dimethylhydroxylamine hydrochloride (1.2 eq) and stirred at 0°C. The corresponding grignard (4.5 eq) was then added dropwise and the reaction was allowed to stir until complete conversion to ketone was observed by LCMS. The reaction mixture was quenched with a solution of saturated NH₄Cl slowly and allowed to stir for 10 minutes, then basified with 10% NaOH dropwise. The mixture was further partitioned with EtOAc and separated. The aqueous layer was extracted with EtOAc once more and then DCM twice. The organic layers were combined, dried over anhydrous sodium sulfate, filtered, and concentrated to afford the product which was generally greater than 95% pure upon extraction.

Compound 2

Prepared by general hydrogenation B procedure from **compound 21**. Purified on a 4 gram combiflash column with a gradient of 0-70% DCM:MeOH:NH₄OH 90:10:.5 in DCM to afford N-(3-((S)-3-((methyl((S)-5,6,7,8-tetrahydroquinolin-8-yl)amino)methyl)piperazin-1-yl)-1-phenylpropyl)cyclopentanecarboxamide (40 mg, 26% yield).

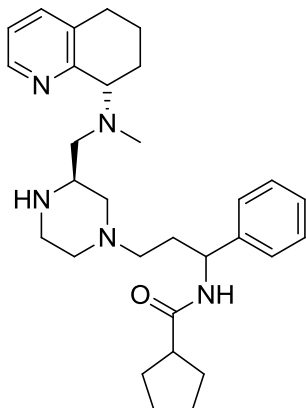
¹H NMR (400 MHz, Chloroform-d) δ 8.31 (t, *J* = 4.1 Hz, 1H), 7.36 (t, *J* = 9.3 Hz, 1H), 7.26 (td, *J* = 8.0, 3.1 Hz, 2H), 7.23 – 7.15 (m, 2H), 7.06 (dd, *J* = 7.7, 4.7 Hz, 1H), 6.90 (s, 1H), 5.10 – 4.95 (m, 2H), 3.78 (dd, *J* = 15.3, 8.6 Hz, 1H), 3.29 – 3.07 (m, 2H), 3.07 – 2.72 (m, 5H), 2.72 – 2.42 (m, 4H), 2.42 – 2.23 (m, 5H), 2.13 – 1.94 (m, 3H), 1.94 – 1.85 (m, 2H), 1.85 – 1.73 (m, 3H), 1.73 – 1.57 (m, 5H), 1.57 – 1.38 (m, 3H).

LCMS 25-95% 8 minutes MeOH:H₂O gradient >95% pure rt= 4.450

LCMS 75-95% 3 minutes MeOH:H₂O gradient >95% pure rt= .538

HRMS calc'd for C₃₀H₄₄ON₅ 490.35404; found [M+H] 490.35328

¹³C NMR (101 MHz, Chloroform-d) δ 175.94, 157.82, 146.83, 141.92, 137.61, 134.47, 128.13, 127.71, 127.02, 122.34, 55.40, 51.89, 46.18, 38.67, 32.42, 30.63, 29.14, 25.58, 23.53, 21.76.

Compound 3

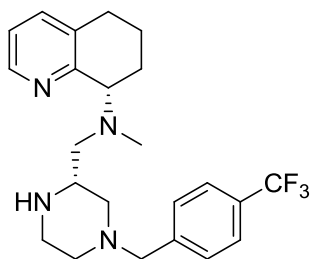
Prepared by general hydrogenation B procedure from **compound 18**. Purified on a 4 gram combiflash column with a gradient of 0-70% DCM:MeOH:NH₄OH 90:10:.5 in DCM to afford N-(3-((S)-3-((methyl((S)-5,6,7,8-tetrahydroquinolin-8-yl)amino)methyl)piperazin-1-yl)-1-phenylpropyl)cyclopentanecarboxamide (35 mg, 50% yield).

¹H NMR (400 MHz, Chloroform-d) δ 8.40 (t, *J* = 4.7 Hz, 1H), 7.45 – 7.10 (m, 6H), 7.12 – 6.93 (m, 1H), 5.06 (s, 1H), 3.93 (s, 1H), 3.60 (dd, *J* = 10.7, 3.9 Hz, 1H), 3.49 (dd, *J* = 10.6, 6.9 Hz, 1H), 2.91 (ddd, *J* = 23.1, 17.2, 10.2 Hz, 5H), 2.81 – 2.57 (m, 4H), 2.50 (dd, *J* = 9.2, 4.4 Hz, 2H), 2.44 – 2.15 (m, 9H), 2.04 (dd, *J* = 24.9, 13.6 Hz, 4H), 1.72 (ddd, *J* = 71.7, 43.2, 22.4 Hz, 11H).

LCMS 25-95% 8 minutes MeOH:H₂O gradient >95% pure rt= 4.802

LCMS 75-95% 3 minutes MeOH:H₂O gradient >95% pure rt= .541

HRMS calc'd for C₃₀H₄₄ON₅ 490.35404; found [M+H] 490.35314

Compound 4

Prepared by general acid CBZ deprotection procedure from material **compound 22**. Purified on a 4 gram combiflash column with a gradient from 0-70% DCM:MeOH:NH₄OH (90:10:.5) in DCM to afford (R)-N-methyl-N-(((R)-4-(4-(trifluoromethyl)benzyl)piperazin-2-yl)methyl)-5,6,7,8-tetrahydroquinolin-8-amine (125 mg, 59% yield).

¹H NMR (400 MHz, Chloroform-*d*) δ 8.42 – 8.39 (m, 1H), 7.52 (d, *J* = 7.9 Hz, 2H), 7.38 (d, *J* = 8.1 Hz, 2H), 7.30 (dd, *J* = 7.6, 1.7 Hz, 1H), 7.00 (dd, *J* = 7.7, 4.7 Hz, 1H), 3.84 (dd, *J* = 9.4, 5.7 Hz, 1H), 3.49 (s, 2H), 2.93 – 2.53 (m, 8H), 2.53 – 2.43 (m, 2H), 2.28 (s, 3H), 2.12 (td, *J* = 10.7, 3.5 Hz, 1H), 2.03 (ddd, *J* = 12.6, 6.9, 4.3 Hz, 1H), 1.98 – 1.90 (m, 1H), 1.76 (m, 2H), 1.69 – 1.56 (m, 2H).

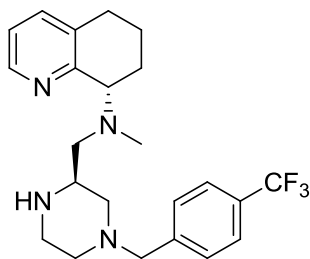
¹³C NMR (101 MHz, Chloroform-*d*) δ 157.71, 147.31, 142.71, 136.83, 134.33, 129.48, 125.27, 121.86, 64.72, 62.98, 58.77, 57.61, 53.79, 53.65, 53.49, 45.50, 39.52, 29.49, 24.77, 21.55.

¹⁹F NMR (376 MHz, Chloroform-*d*) δ -63.03.

HRMS calc'd for C₂₃H₃₀N₄F₃ 419.24171; found [M+H] 419.24099

LCMS 50-95% 5 minutes MeOH:H₂O gradient >95% pure rt= 1.878

LCMS 75-95% 3 minutes MeOH:H₂O gradient >95% pure rt= .767

Compound 5

Prepared by general acid CBZ deprotection procedure from material **compound 19**. Purified on a 4 gram combiflash column with a gradient from 0-70% DCM:MeOH:NH₄OH (90:10:.5) in DCM to afford (S)-N-methyl-N-(((R)-4-(4-

(trifluoromethyl)benzyl)piperazin-2-yl)methyl)-5,6,7,8-tetrahydroquinolin-8-amine (110 mg, 52% yield).

¹H NMR (400 MHz, Chloroform-*d*) δ 8.34 (dd, *J* = 4.7, 1.7 Hz, 1H), 7.53 – 7.47 (m, 2H), 7.39 – 7.34 (m, 2H), 7.32 – 7.27 (m, 1H), 7.00 (ddd, *J* = 7.7, 4.6, 0.7 Hz, 1H), 3.92 (dd, *J* = 9.4, 5.7 Hz, 1H), 3.57 – 3.43 (m, 2H), 3.01 (dt, *J* = 11.7, 3.0 Hz, 1H), 2.90 (tt, *J* = 9.6, 3.7 Hz, 1H), 2.82 (td, *J* = 11.3, 2.9 Hz, 1H), 2.77 – 2.55 (m, 6H), 2.46 (dd, *J* = 12.9, 4.2 Hz, 1H), 2.27 (s, 3H), 2.02 – 1.72 (m, 5H), 1.61 (qdd, *J* = 10.7, 5.4, 3.2 Hz, 1H).

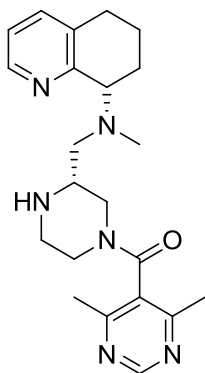
¹³C NMR (101 MHz, Chloroform-*d*) δ 157.59, 146.90, 142.44, 137.15, 134.34, 129.44, 125.35, 125.32, 121.86, 64.68, 62.68, 57.36, 56.69, 53.64, 52.73, 44.71, 39.08, 29.40, 24.62, 21.50.

¹⁹F NMR (376 MHz, Chloroform-*d*) δ -63.06.

HRMS calc'd for C₂₃H₃₀N₄F₃ 419.24171; found [M+H] 419.24105

LCMS 50-95% 5 minutes MeOH:H₂O gradient >95% pure rt= 2.208

LCMS 75-95% 3 minutes MeOH:H₂O gradient >95% pure rt= .762

Compound 6

Prepared by general hydrogenation B procedure from **compound 23**.

Purified on a 4 gram combiflash column with a gradient of 0-70%

DCM:MeOH:NH₄OH 90:10:.5 in DCM to afford (4,6-

dimethylpyrimidin-5-yl)((R)-3-((methyl((S)-5,6,7,8-

tetrahydroquinolin-8-yl)amino)methyl)piperazin-1-yl)methanone (60

mg, 40% yield).

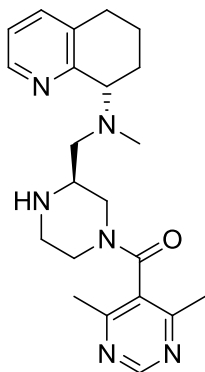
¹H NMR (600 MHz, Chloroform-*d*) δ 8.96 – 8.87 (m, 1H), 8.42 – 8.31 (m, 1H), 7.41 – 7.28 (m, 1H), 7.04 (dddd, *J* = 8.7, 7.7, 4.6, 0.9 Hz, 1H), 4.66 – 4.43 (m, 1H), 3.83-3.70 (m, 1H), 3.36 – 3.09 (m, 1H), 2.96 – 2.54 (m, 5H), 2.53 – 2.18 (m, 14H), 2.13 – 1.93 (m, 3H), 1.93 – 1.53 (m, 2H).

¹³C NMR (151 MHz, Chloroform-*d*) δ 166.36, 162.65, 157.91, 157.28, 147.24, 137.44, 134.62, 129.02, 122.30, 63.42, 56.86, 53.72, 50.95, 47.21, 45.61, 42.52, 39.59, 39.11, 29.40, 25.39, 22.27.

LCMS 25-95% 5 minutes MeOH:H₂O gradient >95% pure rt= .539

LCMS 75-95% 3 minutes MeOH:H₂O gradient >95% pure rt= .525

HRMS calc'd for C₂₂H₃₁ON₆ 395.25539; found [M+H] 395.25581

Compound 7

Prepared by general hydrogenation B procedure from **compound 20**.

Purified on a 4 gram combiflash column with a gradient of 0-70% DCM:MeOH:NH₄OH 90:10:.5 in DCM to afford (4,6-dimethylpyrimidin-5-yl)((S)-3-((methyl((S)-5,6,7,8-tetrahydroquinolin-8-yl)amino)methyl)piperazin-1-yl)methanone (70 mg, 63% yield).

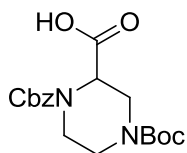
¹H NMR (400 MHz, Chloroform-*d*) δ 8.90 (d, *J* = 12.8 Hz, 1H), 8.44 – 8.31 (m, 1H), 7.39 – 7.27 (m, 1H), 7.08 – 6.99 (m, 1H), 4.70 – 4.50 (m, 1H), 3.97 – 3.72 (m, 1H), 3.17 – 3.09 (m, 1H), 2.98 – 2.85 (m, 1H), 2.80 – 2.58 (m, 4H), 2.56 – 2.26 (m, 15H), 2.10 – 1.82 (m, 3H), 1.82 – 1.56 (m, 2H).

¹³C NMR (101 MHz, Chloroform-*d*) δ 166.27, 162.93, 162.77, 157.81, 147.14, 137.00, 134.15, 129.33, 121.88, 64.90, 57.45, 53.65, 50.96, 47.31, 45.61, 42.52, 40.68, 29.47, 25.35, 22.35, 21.49.

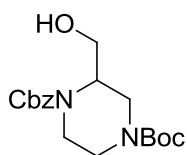
LCMS 25-95% 5 minutes MeOH:H₂O gradient >95% pure rt= .546

LCMS 75-95% 3 minutes MeOH:H₂O gradient >95% pure rt= .526

HRMS calc'd for C₂₂H₃₁ON₆ 395.25539; found [M+H] 395.25440

Compound 9

A solution of piperazine-1,3-dicarboxylic acid 1-tert-butyl ester (14.55 g, 63.2 mmol) in 1,4-dioxane (211 mL) water (105 mL) and triethylamine (22 mL, 2.5 eq) was cooled to 0°C. Benzyl carbonochloridate (12.93 g, 76 mmol, 1.2 eq) was added dropwise over the course of 5 minutes. The reaction was allowed to warm to room temperature and was tracked by LCMS. After one hour the reaction was diluted with 1N HCl and then extracted with DCM (3 times). The organic layers were combined, dried over anhydrous magnesium sulfate, filtered and concentrated to afford 1-((benzyloxy)carbonyl)-4-(tert-butoxycarbonyl)piperazine-2-carboxylic acid (approx. 23 g). The material was used in the next step crude.

Compound 10

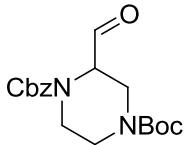
A solution of 1-((benzyloxy)carbonyl)-4-(tert-butoxycarbonyl)piperazine-2-carboxylic acid (approx 23 g, 63 mmol) in THF (316 mL, .2M) was cooled to 0°C. Borane dimethylsulfide (11.1 mL, 110 mmol, 1.75 eq) was added drop wise over the course of 5 minutes. The reaction was allowed to warm to room temperature and was tracked by LCMS. After stirring overnight the reaction was diluted with brine and then extracted with DCM (3 times). The organic layers were combined, dried over anhydrous magnesium sulfate, filtered and concentrated to afford 1-benzyl 4-tert-butyl 2-(hydroxymethyl)piperazine-1,4-dicarboxylate (21 g, 95% yield over two steps).

^1H NMR (400 MHz, Chloroform-*d*) δ 7.38 – 7.26 (m, 5H), 5.12 (d, $J = 2.3$ Hz, 2H), 4.36 – 4.07 (m, 2H), 4.04 – 3.78 (m, 2H), 3.66 – 3.50 (m, 2H), 3.16 – 2.72 (m, 4H), 1.44 (s, 9H).

^{13}C NMR (101 MHz, Chloroform-*d*) δ 156.08, 154.98, 136.47, 128.78, 128.41, 128.19, 80.86, 67.76, 67.29, 52.77, 42.89, 39.84, 28.54.

HRMS calc'd for $\text{C}_{15}\text{H}_{27}\text{O}_5\text{N}_2$ 351.19145; found $[\text{M}+\text{H}]$ 351.19204

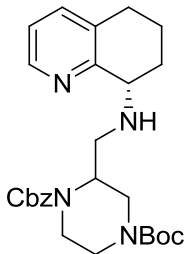
HRMS calc'd for $\text{C}_{15}\text{H}_{27}\text{O}_5\text{N}_2\text{Na}$ 373.17339; found $[\text{M}+\text{H}+\text{Na}]$ 373.17355

Compound 11

To a solution of 1-benzyl 4-tert-butyl 2-(hydroxymethyl)piperazine-1,4-dicarboxylate (21 g, 60 mmol) dissolved in DCM (300 mL, .2M) was added PCC (19.38 g, 90 mmol, 1.5 eq). The reaction was tracked by LCMS. After stirring overnight the reaction mixture was triturated with diethyl ether until no more solid (chromium waste) crashed out. The suspension was then filtered and the solution concentrated down to afford 1-benzyl 4-tert-butyl 2-formylpiperazine-1,4-dicarboxylate (approx. 20g). The material was used in the next step crude.

Alternative

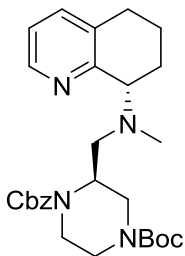
To a 0 °C solution of 1-benzyl 4-tert-butyl 2-(hydroxymethyl)piperazine-1,4-dicarboxylate (16 g, 46 mmol) in CH₂Cl₂ (100 mL) was added triethylamine (18.5 g, 183 mmol, 4 eq) followed by pyridine·SO₃ complex (21.8 g, 138 mmol, 3 eq) as a solution in DMSO (100 mL). The reaction solution was stirred at 0 °C for 1 h before quenching with sat. NaHCO₃. The solution was then extracted with Et₂O (x 3), the combined organics were washed with brine and dried (NaSO₄) to afford 1-benzyl 4-tert-butyl 2-formylpiperazine-1,4-dicarboxylate. The material was used in the next step crude

Compound 13

To a solution of 1-benzyl 4-tert-butyl 2-formylpiperazine-1,4-dicarboxylate (15.9 g, 45.6 mmol) dissolved in DCM (456 mL, .1M) was added (S)-5,6,7,8-tetrahydroquinolin-8-amine (8.45 g, 57.0 mmol, 1.25 eq). The mixture was stirred at room temperature for 30 minutes, at which point sodium triacetoxyborohydride (14.51 g, 68.5 mmol, 1.5 eq) was added. The reaction was complete after two hours as checked by LCMS. The mixture was diluted with 5 mL of 10% NaOH and 50 mL of brine. The fractions were separated and the aqueous phase extracted with DCM (3 times). The organic layers were combined dried over anhydrous sodium sulfate, filtered and concentrated. The crude mixture was then purified on a 80 gram combiflash column with a gradient from 0-20% MeOH in DCM to afford 1-benzyl 4-tert-butyl-2-(((S)-5,6,7,8-tetrahydroquinolin-8-yl)amino)methyl)piperazine-1,4-dicarboxylate (12.5 g, 57% yield over two steps).

^1H NMR (400 MHz, Chloroform-*d*) δ 8.31 – 8.22 (m, 1H), 7.38 – 7.15 (m, 6H), 6.98 (dd, $J = 7.7, 4.7$ Hz, 1H), 5.12 – 5.05 (m, 2H), 4.30 – 4.11 (m, 2H), 3.95 – 3.81 (m, 4H), 3.76 – 3.64 (m, 1H), 3.61 – 3.46 (m, 1H), 3.11 – 2.58 (m, 7H), 1.95 – 1.79 (m, 1H), 1.79 – 1.49 (m, 1H), 1.40 (s, 9H).

^{13}C NMR (101 MHz, Chloroform-*d*) δ 157.50, 155.12, 146.97, 146.85, 136.99, 136.71, 132.53, 128.70, 128.59, 128.09, 122.00, 80.32, 67.60, 67.51, 60.55, 52.82, 51.89, 45.12, 44.14, 42.75, 39.61, 28.96, 28.49, 19.75.

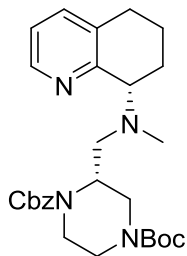
Compound 14

To a solution of 1-benzyl 4-tert-butyl-2-(((S)-5,6,7,8-tetrahydroquinolin-8-yl)amino)methyl)piperazine-1,4-dicarboxylate (5.5g, 11.4 mmol) dissolved in DCE (114 mL, .1M) was added paraformaldehyde (1.72 g, 57 mmol, 5 eq) and acetic acid (.5 mL). After stirring at room temperature for 30 minutes sodium triacetoxyborohydride (6.1 g, 29 mmol, 2.5 eq) was added as one portion. The reaction was tracked by LCMS and went to completion overnight. The mixture was filtered and then partitioned between water and DCM. The aqueous layer was basified and extracted with DCM (3 times). The organic layers were combined dried over anhydrous sodium sulfate, filtered and concentrated. The crude mixture was then purified on a 40 gram combiflash column with a step wise gradient from 0 to 5 to 10 to 15% MeOH in DCM to afford 1-benzyl 4-tert-butyl 2-((methyl((S)-5,6,7,8-tetrahydroquinolin-8-yl)amino)methyl)piperazine-1,4-dicarboxylate diastereomers (3.65 g, 7.4 mmol, 65% yield).

URF (1.6 g, 29% yield)

^1H NMR (600 MHz, Chloroform-*d*) δ 8.35 (dd, $J = 4.9, 1.7$ Hz, 1H), 7.42 – 7.14 (m, 6H), 7.04 (dd, $J = 7.7, 4.7$ Hz, 1H), 5.07 (p, $J = 11.7, 11.1$ Hz, 2H), 4.27 – 3.93 (m, 2H), 3.93 – 3.67 (m, 2H), 3.08 – 2.52 (m, 8H), 2.41 – 2.02 (m, 2H), 1.95 (s, 3H), 1.84 – 1.70 (m, 2H), 1.68 – 1.44 (m, 1H), 1.38 (s, 9H).

^{13}C NMR (101 MHz, Chloroform-*d*) δ 155.62, 155.18, 146.35, 137.60, 136.59, 134.75, 128.61, 128.22, 122.37, 80.25, 67.59, 63.68, 55.22, 53.71, 50.16, 49.22, 43.73, 39.49, 38.54, 28.68, 28.44, 26.33, 21.71.

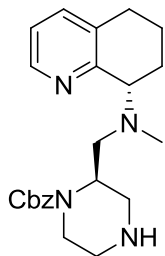
Compound 15

To a solution of 1-benzyl 4-tert-butyl-2-(((S)-5,6,7,8-tetrahydroquinolin-8-yl)amino)methyl)piperazine-1,4-dicarboxylate (5.5g, 11.4 mmol) dissolved in DCE (114 mL, .1M) was added paraformaldehyde (1.72 g, 57 mmol, 5 eq) and acetic acid (.5 mL). After stirring at room temperature for 30 minutes sodium triacetoxyborohydride (6.1 g, 29 mmol, 2.5 eq) was added as one portion. The reaction was tracked by LCMS and went to completion overnight. The mixture was filtered and then partitioned between water and DCM. The aqueous layer was basified and extracted with DCM (3 times). The organic layers were combined dried over anhydrous sodium sulfate, filtered and concentrated. The crude mixture was then purified on a 40 gram combiflash column with a step wise gradient from 0 to 5 to 10 to 15% MeOH in DCM to afford 1-benzyl 4-tert-butyl 2-((methyl((S)-5,6,7,8-tetrahydroquinolin-8-yl)amino)methyl)piperazine-1,4-dicarboxylate diastereomers (3.65 g, 7.4 mmol, 65% yield).

LRF (2.05 g, 36% yield)

^1H NMR (600 MHz, Chloroform-*d*) δ 8.44 – 8.23 (m, 1H), 7.37 – 7.14 (m, 6H), 7.06 – 6.98 (m, 1H), 5.18 – 4.90 (m, 2H), 4.19 – 3.94 (m, 2H), 3.94 – 3.74 (m, 2H), 2.95 – 2.51 (m, 8H), 2.42 (s, 1H), 2.24 – 2.14 (m, 1H), 1.92 (s, 3H), 2.10 – 1.83 (m, 2H), 1.83 – 1.65 (m, 1H), 1.65 – 1.46 (m, 1H), 1.29 (s, 9H).

^{13}C NMR (151 MHz, Chloroform-*d*) δ 155.80, 147.06, 146.62, 137.59, 136.42, 128.62, 128.28, 123.50, 122.16, 80.46, 67.71, 64.81, 61.77, 58.54, 55.43, 49.38, 44.16, 42.68, 39.63, 29.04, 28.39, 24.90, 21.59.

Compound 16

Prepared by general Boc-deprotection procedure from **compound 14**.

Purified on 4 gram combiflash column with a gradient of 3-20% MeOH

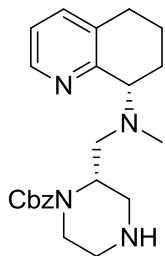
(3.5N NH₄) in DCM (97 mg, 61% yield)

¹H NMR (400 MHz, Chloroform-d) δ 8.43 (dd, *J* = 4.8, 1.7 Hz, 1H), 7.37 – 7.21 (m, 6H), 7.02 (dd, *J* = 7.7, 4.6 Hz, 1H), 5.17 – 5.00 (m, 2H), 4.17 – 3.95 (m, 1H), 3.95 – 3.81 (m, 2H), 3.78 – 3.64 (m, 2H), 3.37 – 3.23 (m, 1H), 2.81 – 2.51 (m, 7H), 2.51 – 2.24 (m, 2H), 2.14 – 2.00 (m, 1H), 1.97 – 1.85 (m, 2H), 1.81 – 1.53 (m, 1H).

¹³C NMR (101 MHz, Chloroform-d) δ 157.54, 155.72, 147.29, 137.04, 136.88, 134.51, 128.63, 128.17, 121.91, 67.27, 64.91, 60.61, 53.68, 50.64, 45.28, 39.96, 29.32, 23.44, 21.24.

LCMS 75% MeOH:H₂O w/ .1% formic acid >95% pure rt= .935

HRMS calc'd for C₂₃H₃₁O₂N₄ 395.24415; found 395.24454 [M+H]

Compound 17

Prepared by general Boc-deprotection procedure from **compound 15**.

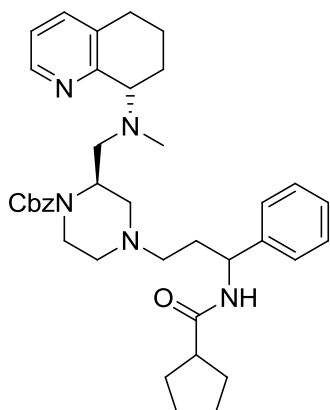
Purified on 4 gram combiflash column with a gradient of 3-20% MeOH (3.5N NH₄) in DCM (104 mg, 65% yield)

¹H NMR (600 MHz, Chloroform-d) δ 8.43 (dd, *J* = 4.8, 1.7 Hz, 1H), 7.39 – 7.26 (m, 6H), 7.05 (dd, *J* = 7.7, 4.7 Hz, 1H), 5.18 – 5.04 (m, 2H), 4.28 – 4.01 (m, 1H), 3.98 – 3.78 (m, 2H), 3.59 – 3.33 (m, 2H), 3.17 (d, *J* = 12.6 Hz, 1H), 3.04 (dd, *J* = 13.3, 7.8 Hz, 1H), 3.00 – 2.88 (m, 2H), 2.87 – 2.60 (m, 5H), 2.38 – 2.15 (m, 3H), 2.04 – 1.79 (m, 3H), 1.72 – 1.57 (m, 1H).

¹³C NMR (151 MHz, Chloroform-d) δ 157.67, 147.00, 137.12, 136.82, 134.23, 128.65, 128.21, 123.96, 122.06, 67.45, 64.93, 54.76, 49.86, 45.77, 45.29, 40.43, 39.25, 29.11, 20.97.

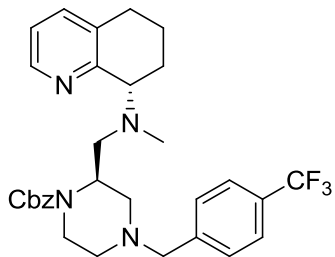
LCMS 75% MeOH:H₂O w/ .1% formic acid >95% pure rt= .823

HRMS calc'd for C₂₃H₃₁O₂N₄ 395.24415; found 395.24461 [M+H]

Compound 18

To a solution of N-(3-hydroxy-1-phenylpropyl)cyclopentanecarboxamide (.35 g, 1.4 mmol, 1 eq) in MeCN (14 mL, .1 M) in a 100 mL round bottom flask was added tetrakisacetonitrile copper(1) triflate (53 mg, .14 mmol, .1 eq), 2,2'-bipyridine (22 mg, .14 mmol, .1 eq), TEMPO (22 mg, .14 mmol, .1 eq) sequentially. NMI (23 mg, .28 mmol, .2 eq) was then added drop wise. The reaction was allowed to stir exposed to the ambient atmosphere. Upon turning bright green the reaction was checked by LCMS and deemed complete. **Compound 14** (469 mg, 1.12 mmol, .8 eq) was then added followed rapidly by STAB-H (.38 g, 1.8 mmol, 2.1 eq). The reaction was tracked by LCMS for 30 minutes and then quenched with sat. NaHCO₃. The aqueous layer was extracted with DCM (3 times). The organic layers were combined, dried over anhydrous sodium sulfate, filtered and concentrated. The crude mixture was then purified on a 12 gram combiflash column with a gradient from 0-50% DCM:MeOH:NH₄OH (90:10:.5) in DCM to afford (2R)-benzyl 4-(3-(cyclopentanecarboxamido)-3-phenylpropyl)-2-((methyl((S)-5,6,7,8-tetrahydroquinolin-8-yl)amino)methyl)piperazine-1-carboxylate (.09 g, 12% yield over 2 steps).

HRMS calc'd for C₃₈H₅₀O₃N₅ 624.39082; found [M+H] 624.38987

Compound 19

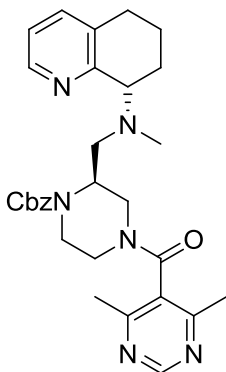
Prepared by general reductive amination procedure from material **compound 14**. Purified on 4 gram combiflash column with a gradient of 0-50% DCM:MeOH:NH₄OH 90:10:.5 in DCM to afford (R)-benzyl 2-((methyl((S)-5,6,7,8-tetrahydroquinolin-8-yl)amino)methyl)-4-(4-(trifluoromethyl)benzyl)piperazine-1-carboxylate (305 mg, 62% yield over two steps).

¹H NMR (400 MHz, Chloroform-*d*) δ 8.43 – 8.34 (m, 1H), 7.57 (d, *J* = 8.0 Hz, 1H), 7.48 (d, *J* = 8.0 Hz, 2H), 7.41 (dd, *J* = 14.4, 8.1 Hz, 1H), 7.36 – 7.27 (m, 4H), 7.17 (d, *J* = 7.9 Hz, 2H), 6.90 (dd, *J* = 7.7, 4.6 Hz, 1H), 5.19 – 5.03 (m, 2H), 4.25-3.92 (m, 1H), 3.89 – 3.70 (m, 2H), 3.66 – 3.38 (m, 2H), 3.27 (d, *J* = 13.6 Hz, 1H), 3.17 – 3.01 (m, 2H), 2.88 – 2.59 (m, 3H), 2.46 (s, 3H), 2.35-2.20 (m, 1H), 2.19-2.02 (m, 1H), 2.00 – 1.50 (m, 6H).

¹³C NMR (101 MHz, Chloroform-*d*) δ 147.12, 142.93, 136.90, 136.74, 134.51, 129.30, 128.75, 128.63, 128.32, 128.18, 125.64, 125.16, 121.84, 77.44, 65.28, 62.16, 53.76, 53.38, 52.79, 52.08, 41.27, 39.56, 29.39, 24.99, 21.16.

¹⁹F NMR (376 MHz, Chloroform-*d*) δ -62.80.

HRMS calc'd for C₃₁H₃₆O₂N₄F₃ 553.77849; found [M+H] 553.27775

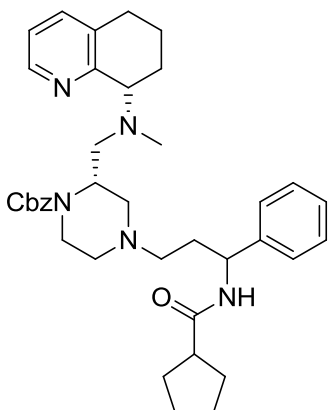
Compound 20

4,6-dimethylpyrimidine-5-carboxylic acid (174 mg, 1.14 mmol, 1.5 eq) as a solution in dry DMF (8 mL, .1 M) was added to a flame dried 50 mL round bottom flask containing HATU (578 mg, 1.52 mmol, 2 eq) and stirred at RT. Hunig's base (295 mg, 2.28 mmol, 3 eq) was added to the solution dropwise. After stirring for 15 minutes **compound 14** (300 mg, 7.6 mmol, 1 eq) was added and allowed to stir overnight. The reaction was then quenched with deionized water (4 mL) and basified with 10% NaOH. The mixture was further partitioned with EtOAc and separated. The organic layer was extracted with D.I. water (2 times). The organic layer was dried over anhydrous magnesium sulfate, filtered and concentrated. The crude mixture was then purified on a 4 gram combiflash column with a gradient from 0-100% DCM:MeOH:NH₄OH (90:10:.5) in DCM to afford (S)-benzyl 4-(4,6-dimethylpyrimidine-5-carbonyl)-2-((methyl((S)-5,6,7,8-tetrahydroquinolin-8-yl)amino)methyl)piperazine-1-carboxylate (150 mg, 37% yield over two steps).

¹H NMR (400 MHz, Chloroform-*d*) δ 8.91 (d, *J* = 8.1 Hz, 1H), 8.34 (dd, *J* = 39.0, 4.7 Hz, 1H), 7.39 – 7.25 (m, 7H), 7.02 (dd, *J* = 7.7, 4.7 Hz, 1H), 5.11 (s, 2H), 4.91 – 3.94 (m, 3H), 3.93 – 3.79 (m, 1H), 3.79 – 3.59 (m, 1H), 3.48 – 3.22 (m, 1H), 3.22 – 2.85 (m, 4H), 2.83 – 2.56 (m, 3H), 2.55 – 2.42 (m, 1H), 2.41 – 2.29 (m, 6H), 2.28 – 1.99 (m, 2H), 1.99 – 1.71 (m, 2H), 1.71 – 1.47 (m, 2H).

¹³C NMR (101 MHz, Chloroform-*d*) δ 167.07, 163.94, 162.67, 157.92, 146.91, 146.65, 136.90, 136.37, 134.32, 128.72, 128.39, 121.88, 77.52, 67.77, 65.41, 64.39, 56.35, 46.43, 45.85, 41.35, 38.35, 29.07, 28.09, 28.02, 22.43, 22.08.

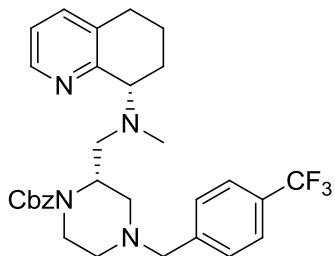
HRMS calc'd for $C_{30}H_{37}O_3N_6$ 529.29217; found [M+H] 529.29115

Compound 21

Prepared using the exact same procedure and scale as above with the exception of using **compound 15** to yield (2*S*)-benzyl 4-(3-(cyclopentanecarboxamido)-3-phenylpropyl)-2-((methyl((*S*)-5,6,7,8-tetrahydroquinolin-8-yl)amino)methyl)piperazine-1-carboxylate (.225 g, 30% yield over 2 steps).

^1H NMR (400 MHz, Chloroform-*d*) δ 8.29 (t, $J = 4.6$ Hz, 1H), 7.39 – 7.17 (m, 11H), 6.96 (ddd, $J = 12.2, 7.7, 4.7$ Hz, 1H), 5.19 – 5.01 (m, 2H), 5.01 – 4.86 (m, 1H), 4.13 (s, 1H), 4.06 – 3.78 (m, 2H), 3.15 – 2.41 (m, 7H), 2.22 (s, 3H), 2.03 – 1.86 (m, 4H), 1.85 – 1.70 (m, 4H), 1.70-1.55 (m, 4H), 1.55 – 1.38 (m, 2H), 1.34 – 1.16 (m, 2H).

HRMS calc'd for $\text{C}_{38}\text{H}_{50}\text{O}_3\text{N}_5$ 624.39082; found $[\text{M}+\text{H}]$ 624.39033

Compound 22

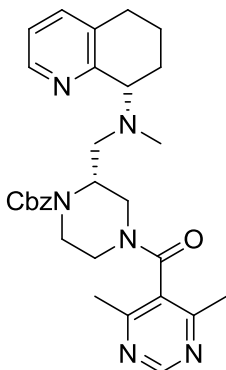
Prepared by general reductive amination procedure from material **compound 15**. Purified on 4 gram combiflash column with a gradient of 0-50% DCM:MeOH:NH₄OH 90:10:.5 in DCM to afford (S)-benzyl 2-((methyl((S)-5,6,7,8-tetrahydroquinolin-8-yl)amino)methyl)-4-(4-(trifluoromethyl)benzyl)piperazine-1-carboxylate (325 mg, 66% yield over two steps).

¹H NMR (400 MHz, Chloroform-*d*) δ 8.43 – 8.35 (m, 1H), 7.57 (d, *J* = 8.0 Hz, 1H), 7.48 (d, *J* = 8.0 Hz, 2H), 7.42 – 7.22 (m, 7H), 7.00 (dd, *J* = 7.5, 4.7 Hz, 1H), 5.19 – 5.02 (m, 2H), 4.29 – 4.01 (m, 1H), 4.00 – 3.67 (m, 2H), 3.55 – 3.35 (m, 2H), 3.06 (d, *J* = 11.4 Hz, 2H), 3.01 – 2.85 (m, 2H), 2.81 – 2.49 (m, 3), 2.50 – 2.17 (m, 3H), 2.11 (td, *J* = 11.7, 3.9 Hz, 1H), 2.03 – 1.48 (m, 6H).

¹³C NMR (101 MHz, Chloroform-*d*) δ 146.99, 142.68, 136.66, 134.00, 129.34, 129.27, 128.74, 128.59, 128.31, 128.10, 125.73, 125.27, 121.62, 77.45, 67.31, 65.06, 62.53, 53.66, 52.80, 40.45, 39.96, 29.33, 26.94, 21.32.

¹⁹F NMR (376 MHz, Chloroform-*d*) δ -62.78.

HRMS calc'd for C₃₁H₃₆O₂N₄F₃ 553.77849; found [M+H] 553.27811

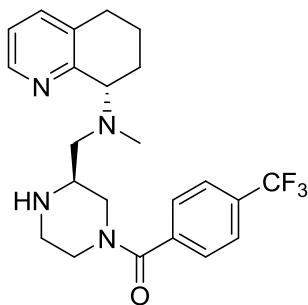
Compound 23

4,6-dimethylpyrimidine-5-carboxylic acid (174 mg, 1.14 mmol, 1.5 eq) as a solution in dry DMF (8 mL, .1 M) was added to a flame dried 50 mL round bottom flask containing HATU (578 mg, 1.52 mmol, 2 eq) and stirred at RT. Hunig's base (295 mg, 2.28 mmol, 3 eq) was added to the solution dropwise. After stirring for 15 minutes **compound 15** (300 mg, 7.6 mmol, 1 eq) was added and allowed to stir overnight. The reaction was then quenched with deionized water (4 mL) and basified with 10% NaOH. The mixture was further partitioned with EtOAc and separated. The organic layer was extracted with D.I. water (2 times). The organic layer was dried over anhydrous magnesium sulfate, filtered and concentrated. The crude mixture was then purified on a 4 gram combiflash column with a gradient from 0-100% DCM:MeOH:NH₄OH (90:10:.5) in DCM to afford (R)-benzyl 4-(4,6-dimethylpyrimidine-5-carbonyl)-2-((methyl((S)-5,6,7,8-tetrahydroquinolin-8-yl)amino)methyl)piperazine-1-carboxylate (200 mg, 50% yield over two steps).

¹H NMR (400 MHz, Chloroform-*d*) δ 9.05 – 8.76 (m, 1H), 8.44 – 8.27 (m, 1H), 7.40 – 7.18 (m, 6H), 7.01 (ddd, *J* = 10.1, 7.6, 4.6 Hz, 1H), 5.10 (s, 2H), 4.81 – 4.02 (m, 3H), 4.02 – 3.79 (m, 1H), 3.79 – 3.37 (m, 1H), 3.37 – 2.76 (m, 5H), 2.75 – 2.41 (m, 4H), 2.42 – 2.26 (m, 4H), 2.26 – 1.72 (m, 5H), 1.76 – 1.50 (m, 2H), 1.33 – 1.14 (m, 1H).

¹³C NMR (101 MHz, Chloroform-*d*) δ 167.54, 166.98, 162.67, 162.42, 157.91, 157.82, 147.20, 136.89, 136.72, 134.01, 128.82, 128.67, 128.35, 121.79, 77.48, 67.76, 65.36, 53.67, 46.99, 46.03, 41.41, 39.61, 38.88, 31.79, 29.47, 22.07, 21.60.

HRMS calc'd for C₃₀H₃₇O₃N₆ 529.29217; found [M+H] 529.29211

Compound 24

Prepared by general acid CBZ deprotection procedure from material **Compound 30**. Purified on a 4 gram combiflash column with a gradient from 0-70% DCM:MeOH:NH₄OH (90:10:.5) in DCM to afford ((S)-3-((methyl((S)-5,6,7,8-tetrahydroquinolin-8-yl)amino)methyl)piperazin-1-yl)(4-

(trifluoromethyl)phenyl)methanone (80 mg, 29% yield three two steps).

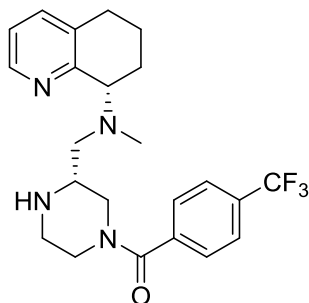
¹H NMR (400 MHz, Chloroform-*d*) δ 8.35 (d, *J* = 22.0 Hz, 1H), 7.69 – 7.60 (m, 2H), 7.47 (d, *J* = 7.7 Hz, 2H), 7.35 (t, *J* = 9.3 Hz, 1H), 7.05 (s, 1H), 4.51 (dd, *J* = 22.2, 12.6 Hz, 1H), 3.93 (d, *J* = 49.0 Hz, 1H), 3.58 – 3.45 (m, 1H), 3.19 – 2.96 (m, 2H), 2.73 (d, *J* = 44.1 Hz, 6H), 2.54 – 2.43 (m, 1H), 2.40 (s, 3H), 1.91 (d, *J* = 36.4 Hz, 2H), 1.74 (d, *J* = 40.8 Hz, 2H).

¹⁹F NMR (376 MHz, cd₃od) δ -63.22.

HRMS calc'd for C₂₃H₂₈O N₄F₃ 433.22097; found [M+H] 433.22201

LCMS 75-95% 3 minutes MeOH:H₂O gradient >95% pure rt= 1.120

LCMS 50-95% 8 minutes MeOH:H₂O gradient >95% pure rt= 2.401

Compound 25

Prepared by general acid CBZ deprotection procedure from **compound 33**. Purified on a 4 gram combiflash column with a gradient from 0-70% DCM:MeOH:NH₄OH (90:10:.5) in DCM to afford ((R)-3-((methyl((S)-5,6,7,8-tetrahydroquinolin-8-yl)amino)methyl)piperazin-1-yl)(4-

(trifluoromethyl)phenyl)methanone (53 mg, 19% yield over three steps).

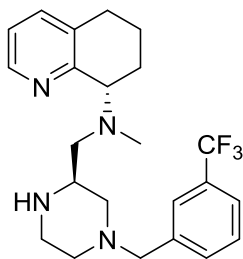
¹H NMR (400 MHz, Chloroform-*d*) δ 8.44 – 8.32 (m, 1H), 7.61 (t, *J* = 6.9 Hz, 2H), 7.42 (d, *J* = 7.9 Hz, 2H), 7.33 – 7.26 (m, 1H), 7.04 – 6.96 (m, 1H), 4.52 – 4.36 (m, 1H), 3.81 (ddd, *J* = 41.7, 9.1, 5.8 Hz, 1H), 3.45 – 3.30 (m, 1H), 3.19 – 2.88 (m, 2H), 2.87 – 2.68 (m, 2H), 2.62 (ddt, *J* = 19.0, 13.5, 4.8 Hz, 3H), 2.54 – 2.38 (m, 2H), 2.35 (s, 3H), 2.17 – 2.01 (m, 1H), 1.93 (tdd, *J* = 21.1, 7.9, 4.2 Hz, 2H), 1.83 – 1.52 (m, 2H).

¹⁹F NMR (376 MHz, cd₃od) δ -63.19.

HRMS calc'd for C₂₃H₂₈O N₄F₃ 433.22097; found [M+H] 433.22207

LCMS 75-95% 3 minutes MeOH:H₂O gradient >95% pure rt= 1.056

LCMS 50-95% 8 minutes MeOH:H₂O gradient >95% pure rt= 1.690

Compound 26

Prepared by general acid CBZ deprotection procedure from **compound 31**. Purified on a 4 gram combiflash column with a gradient from 0-70% DCM:MeOH:NH₄OH (90:10:.5) in DCM to afford (S)-N-methyl-N-(((R)-4-(3-

(trifluoromethyl)benzyl)piperazin-2-yl)methyl)-5,6,7,8-tetrahydroquinolin-8-amine (18 mg, 7% yield over three steps).

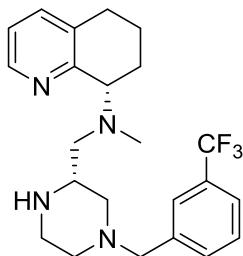
¹H NMR (400 MHz, Chloroform-*d*) δ 8.39 (dd, *J* = 4.8, 1.7 Hz, 1H), 7.53 (t, *J* = 1.5 Hz, 1H), 7.47 (tt, *J* = 6.8, 1.1 Hz, 2H), 7.42 – 7.38 (m, 1H), 7.33 (ddt, *J* = 7.7, 1.6, 0.9 Hz, 1H), 7.03 (ddd, *J* = 7.6, 4.7, 0.7 Hz, 1H), 3.99 – 3.91 (m, 1H), 3.53 (q, *J* = 37.8, 12.6 Hz, 2H), 3.03 (d, *J* = 11.7 Hz, 1H), 2.97 – 2.81 (m, 2H), 2.77 – 2.70 (m, 3H), 2.70 – 2.64 (m, 1H), 2.64 – 2.48 (m, 1H), 2.37 (s, 3H), 2.24 (d, *J* = 11.4 Hz, 1H), 2.06 – 1.90 (m, 3H), 1.89 – 1.78 (m, 2H), 1.73 – 1.60 (m, 1H), 1.22 (d, *J* = 5.2 Hz, 1H).

¹⁹F NMR (376 MHz, cd₃od) δ -62.79.

HRMS calc'd for C₂₃H₃₀N₄F₃ 419.24171; found [M+H] 419.24283

LCMS 75-95% 3 minutes MeOH:H₂O gradient >95% pure rt= 1.724

LCMS 50-95% 8 minutes MeOH:H₂O gradient >95% pure rt= 3.645

Compound 27

Prepared by general acid CBZ deprotection procedure from **compound 32**. Purified on a 4 gram combiflash column with a gradient from 0-70% DCM:MeOH:NH₄OH (90:10:.5) in DCM to afford (S)-N-methyl-N-(((S)-4-(3-(trifluoromethyl)benzyl)piperazin-

2-yl)methyl)-5,6,7,8-tetrahydroquinolin-8-amine (25 mg, 9% yield over three steps).

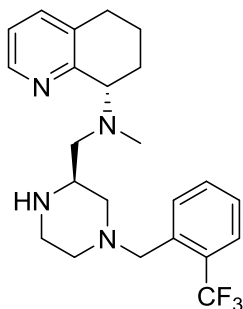
¹H NMR (400 MHz, Chloroform-*d*) δ 8.39 (dd, *J* = 4.8, 1.7 Hz, 1H), 7.53 (s, 1H), 7.47 (tt, *J* = 6.8, 1.1 Hz, 2H), 7.42 – 7.36 (m, 1H), 7.33 (ddt, *J* = 7.7, 1.6, 0.9 Hz, 1H), 7.03 (ddd, *J* = 7.6, 4.7, 0.7 Hz, 1H), 3.98 – 3.90 (m, 1H), 3.59 – 3.46 (m, 2H), 3.03 (d, *J* = 11.7 Hz, 1H), 2.97 – 2.82 (m, 2H), 2.78 – 2.70 (m, 3H), 2.70 – 2.65 (m, 1H), 2.64 – 2.48 (m, 1H), 2.37 (s, 3H), 2.24 (d, *J* = 11.3 Hz, 1H), 2.06 – 1.90 (m, 2H), 1.90 – 1.78 (m, 2H), 1.74 – 1.61 (m, 1H), 1.22 (s, 1H).

¹⁹F NMR (376 MHz, cd₃od) δ -62.85.

HRMS calc'd for C₂₃H₃₀N₄F₃ 419.24171; found [M+H] 419.24277

LCMS 75-95% 3 minutes MeOH:H₂O gradient >95% pure rt= 1.587

LCMS 50-95% 8 minutes MeOH:H₂O gradient >95% pure rt= 3.483

Compound 28

Prepared by general acid CBZ deprotection procedure from **compound 32**. Purified on a 4 gram combiflash column with a gradient from 0-70% DCM:MeOH:NH₄OH (90:10:.5) in DCM to afford (S)-N-methyl-N-(((R)-4-(2-(trifluoromethyl)benzyl)piperazin-2-yl)methyl)-5,6,7,8-

tetrahydroquinolin-8-amine (22 mg, 8% yield over three steps).

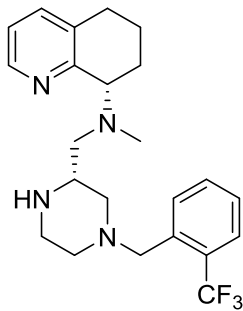
¹H NMR (400 MHz, Chloroform-*d*) δ 8.36 (dd, *J* = 4.9, 1.6 Hz, 1H), 7.65 (d, *J* = 7.8 Hz, 1H), 7.59 (dt, *J* = 7.8, 1.6 Hz, 1H), 7.47 (t, *J* = 7.6 Hz, 1H), 7.34 (t, *J* = 9.0 Hz, 2H), 7.06 – 7.01 (m, 1H), 3.98 (dd, *J* = 9.2, 5.5 Hz, 1H), 3.64 (s, 3H), 3.08 (td, *J* = 14.7, 13.6, 7.5 Hz, 2H), 2.97 – 2.87 (m, 1H), 2.79 (dd, *J* = 10.3, 3.6 Hz, 1H), 2.77 – 2.69 (m, 2H), 2.67 (d, *J* = 4.2 Hz, 1H), 2.63 – 2.54 (m, 1H), 2.49 – 2.36 (m, 1H), 2.31 (s, 3H), 2.11 (d, *J* = 19.4 Hz, 1H), 2.04 – 1.90 (m, 2H), 1.83 (tdt, *J* = 11.7, 9.3, 1.9 Hz, 1H), 1.67 (dtq, *J* = 15.9, 7.8, 2.5 Hz, 1H).

¹⁹F NMR (376 MHz, cd₃od) δ -59.60.

HRMS calc'd for C₂₃H₃₀N₄F₃ 419.24171; found [M+H] 419.24283

LCMS 75-95% 3 minutes MeOH:H₂O gradient >95% pure rt= 1.292

LCMS 50-95% 8 minutes MeOH:H₂O gradient >95% pure rt= 3.459

Compound 29

Prepared by general acid CBZ deprotection procedure from **compound 35**. Purified on a 4 gram combiflash column with a gradient from 0-70% DCM:MeOH:NH₄OH (90:10:.5) in DCM to afford (S)-N-methyl-N-(((S)-4-(2-(trifluoromethyl)benzyl)piperazin-

2-yl)methyl)-5,6,7,8-tetrahydroquinolin-8-amine (14 mg, 5% yield over two steps).

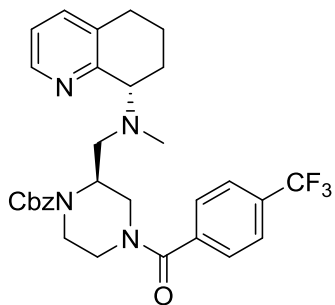
¹H NMR (400 MHz, Chloroform-*d*) δ 8.34 (d, *J* = 4.5 Hz, 1H), 7.60 (d, *J* = 7.6 Hz, 2H), 7.47 (t, *J* = 7.6 Hz, 1H), 7.34 (t, *J* = 9.6, 8.6 Hz, 2H), 7.05 (ddd, *J* = 7.7, 4.7, 0.8 Hz, 1H), 3.82 – 3.74 (m, 1H), 3.67 (d, *J* = 7.4 Hz, 2H), 3.09 (q, *J* = 6.6 Hz, 2H), 3.01 – 2.90 (m, 1H), 2.89 – 2.80 (m, 1H), 2.79 – 2.70 (m, 4H), 2.69 – 2.61 (m, 1H), 2.35 (s, 3H), 2.09 – 1.92 (m, 4H), 1.85 (tdd, *J* = 12.2, 9.5, 2.5 Hz, 1H), 1.67 (dtdd, *J* = 18.7, 11.4, 5.0, 2.3 Hz, 1H).

¹⁹F NMR (376 MHz, cd₃od) δ -59.65.

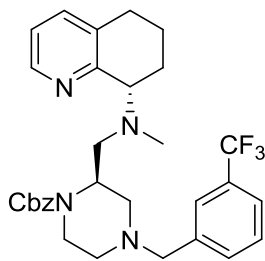
HRMS calc'd for C₂₃H₃₀N₄F₃ 419.24171; found [M+H] 419.24275

LCMS 75-95% 3 minutes MeOH:H₂O gradient >95% pure rt= 1.356

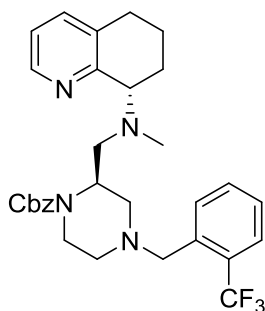
LCMS 50-95% 8 minutes MeOH:H₂O gradient >95% pure rt= 3.513

Compound 30

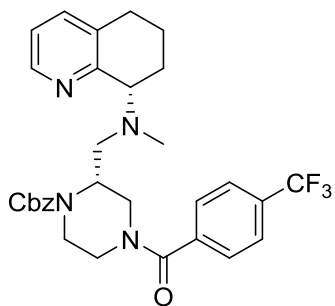
Prepared by general acylation procedure A from **compound 14** to afford (S)-benzyl 2-((methyl((S)-5,6,7,8-tetrahydroquinolin-8-yl)amino)methyl)-4-(4-(trifluoromethyl)benzoyl)piperazine-1-carboxylate, taken on crude to the next step.

Compound 31

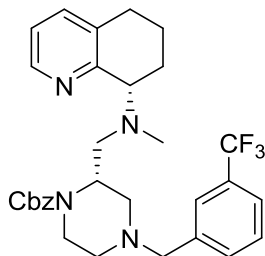
Prepared by general reductive amination from **compound 14** to afford (R)-benzyl 2-((methyl((S)-5,6,7,8-tetrahydroquinolin-8-yl)amino)methyl)-4-(3-(trifluoromethyl)benzyl)piperazine-1-carboxylate, taken on crude to the next step.

Compound 32

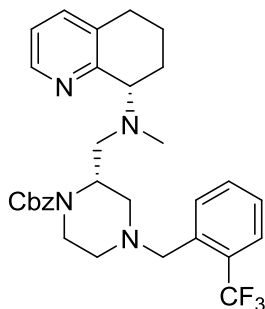
Prepared by general reductive amination from **compound 14** to afford (R)-benzyl 2-((methyl((S)-5,6,7,8-tetrahydroquinolin-8-yl)amino)methyl)-4-(2-(trifluoromethyl)benzyl)piperazine-1-carboxylate, taken on crude to the next step.

Compound 33

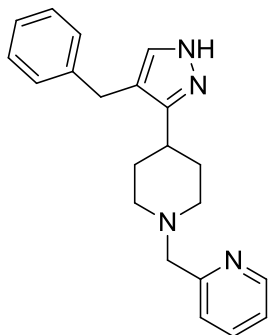
Prepared by general acylation procedure A from material **compound 15** to afford (R)-benzyl 2-((methyl((S)-5,6,7,8-tetrahydroquinolin-8-yl)amino)methyl)-4-(4-(trifluoromethyl)benzoyl)piperazine-1-carboxylate, taken on crude to the next step.

Compound 34

Prepared by general reductive amination from **compound 15** to afford (S)-benzyl 2-((methyl((S)-5,6,7,8-tetrahydroquinolin-8-yl)amino)methyl)-4-(3-(trifluoromethyl)benzyl)piperazine-1-carboxylate, taken on crude to the next step.

Compound 35

Prepared by general reductive amination from material **compound 15** to afford (S)-benzyl 2-((methyl((S)-5,6,7,8-tetrahydroquinolin-8-yl)amino)methyl)-4-(2-(trifluoromethyl)benzyl)piperazine-1-carboxylate, taken on crude to the next step.

Compound 36

Prepared by general reductive amination procedure from **compound 74**. Purified on a 12 gram combiflash column with a gradient from 0-70% DCM:MeOH:NH₄OH (90:10:.5) in DCM to afford 2-((4-(4-benzyl-1H-pyrazol-3-yl)piperidin-1-yl)methyl)pyridine (275 mg, 62% yield over two steps).

¹H NMR (400 MHz, Chloroform-*d*) δ 8.53 (ddd, *J* = 5.0, 1.9, 0.9 Hz, 1H), 7.63 (td, *J* = 7.6, 1.8 Hz, 1H), 7.40 (d, *J* = 7.8 Hz, 1H), 7.30 – 7.21 (m, 3H), 7.19 – 7.11 (m, 3H), 3.79 (s, 2H), 3.65 (s, 2H), 2.95 (d, *J* = 11.4 Hz, 2H), 2.62 (tt, *J* = 12.1, 4.0 Hz, 1H), 2.10 (td, *J* = 11.8, 2.7 Hz, 2H), 1.84 (qd, *J* = 12.3, 3.8 Hz, 2H), 1.72 (d, *J* = 12.3 Hz, 2H).

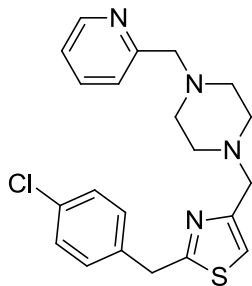
¹³C NMR (101 MHz, Chloroform-*d*) δ 158.23, 149.12, 141.20, 136.54, 128.38, 125.95, 123.53, 122.33, 115.71, 64.79, 54.19, 33.18, 31.51, 29.80.

HRMS calc'd for C₂₁H₂₅N₄ 333.20737; found [M+H] 333.20695

LCMS 75-95% 3 minutes MeOH:H₂O gradient >95% pure rt= .555

HIV-1_{BaL} inhibition in MAGI Cells- IC₅₀=16.7 μM IC₉₀ 300 μM

HIV-1_{IIIIB} inhibition in MAGI Cells- IC₅₀=24.8 μM IC₉₀> 300 μM

Compound 37

To a solution 2-(4-chlorophenyl)ethanethioamide (1.00 g, 5.39 mmol) in DCM (18 mL, .3 M) in a 50 mL round bottom flask was added 1,3-dichloroacetone (.821 g, 6.46 mmol, 1.2 eq) and stirred at RT for 24 hours. After 24 hours of stirring the solution was determined to be a mixture of the unaromatized and aromatized thioazole by LCMS. Addition of tert-butyl piperazine-1-carboxylate (1.204 g, 6.46 mmol, 1.2 eq) allowed for nucleophilic addition and the additional HCl produced caused complete aromatization of the thioazole after an additional 24 hours at RT. Next TFA (2.456 g, 21.5 mmol, 4 eq) was added drop wise. After six hours complete deprotection of the boc group was realized. To this solution was added picolinaldehyde (.692 g, 6.46 mmol, 1.2 eq) followed by STAB-H (2.283 g, 10.8 mmol, 2 eq). After six hours of stirring the reaction was quenched with 2 mL H₂O. The crude mixture was partitioned between water and DCM and basified with 10% NaOH solution. The layers were separated and the aqueous layer was extracted with DCM (3 times). The organic layers were combined, dried over anhydrous magnesium sulfate, filtered and concentrated. The crude mixture was then purified on a 40 gram combiflash column with a gradient from 0-50% DCM:MeOH:NH₄OH (90:10:.5) in DCM to afford 2-(4-chlorobenzyl)-4-((4-(pyridin-2-ylmethyl)piperazin-1-yl)methyl)thiazole (.745 g, 35% yield over 5 steps in one pot).

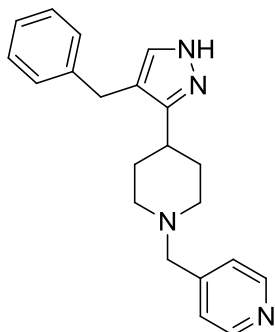
¹H NMR (400 MHz, Chloroform-*d*) δ 8.52 – 8.44 (m, 1H), 7.56 (td, *J* = 7.7, 1.8 Hz, 1H), 7.36 – 7.27 (m, 2H), 7.23 – 7.18 (m, 2H), 7.18 – 7.13 (m, 2H), 7.07 (ddd, *J* = 7.5, 4.9, 1.3 Hz, 1H), 4.20 (s, 2H), 3.66 – 3.55 (m, 4H), 2.65 – 2.38 (m, 8H).

^{13}C NMR (101 MHz, Chloroform- d) δ 169.40, 158.35, 153.32, 149.15, 136.31, 132.89, 130.30, 128.80, 123.22, 121.95, 116.39, 64.45, 58.17, 53.00, 38.91.

HRMS calc'd for $\text{C}_{21}\text{H}_{24}\text{N}_4\text{ClS}$ 399.14047; found $[\text{M}+\text{H}]$ 399.14029

LCMS 25-95% 8 minutes MeOH:H₂O gradient >95% pure rt= 5.308

LCMS 75-95% 3 minutes MeOH:H₂O gradient >95% pure rt= .706

Compound 38

Prepared by general reductive amination procedure from **compound 74**. Purified on a 12 gram combiflash column with a gradient of 0-70% DCM:MeOH:NH₄OH 90:10:.5 in DCM to afford 4-((4-(4-benzyl-1H-pyrazol-3-yl)piperidin-1-yl)methyl)pyridine (225 mg, 51% yield over two steps).

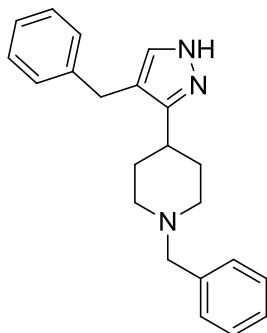
¹H NMR (400 MHz, Chloroform-*d*) δ 8.71 – 8.36 (m, 2H), 7.35 (s, 1H), 7.27 – 7.21 (m, 4H), 7.19 – 7.12 (m, 3H), 3.82 (s, 2H), 3.48 (s, 2H), 2.88 (dt, *J* = 11.5, 3.1 Hz, 2H), 2.62 (tt, *J* = 12.0, 3.9 Hz, 1H), 2.03 (td, *J* = 11.5, 2.3 Hz, 2H), 1.89 (qd, *J* = 12.4, 3.6 Hz, 2H), 1.79 – 1.65 (m, 2H).

¹³C NMR (101 MHz, Chloroform-*d*) δ 149.62, 148.08, 141.13, 128.34, 125.98, 123.80, 115.74, 61.98, 54.13, 33.32, 31.69, 29.82.

LCMS 25-95% 8 minutes MeOH:H₂O gradient >95% pure rt= 3.410

LCMS 75-95% 3 minutes MeOH:H₂O gradient >95% pure rt= .589

HRMS calc'd for C₂₁H₂₅N₄ 333.20737; found [M+H] 333.20729

Compound 53

To a solution of 1-(1-benzylpiperidin-4-yl)-3-phenylpropan-1-one (.45 g, 1.5 mmol) in THF (15 mL, .1 M) in a flame dried 100 mL round bottom flask was added NaH (.21 g, 8.8 mmol, 6 eq) and stirred at RT. Methyl formate (1.76 g, 29 mmol, 20 eq) was then added followed by 15-crown-5 (.16 g, .73 mmol, .5 eq). The reaction was tracked by LCMS and after 1 hour was quenched with 1 mL of H₂O dropwise. The reaction was then diluted with MeOH (15 mL, .1 M) followed by the dropwise addition of hydrazine (.7 g, 22 mmol, 15 eq) and tracked by LCMS. After an additional hour of stirring the reaction was concentrated in vacuo to remove MeOH. The oily residue was partitioned between water and DCM and basified with 10% NaOH solution. The layers were separated and the aqueous layer was extracted with DCM (3 times). The organic layers were combined, dried over anhydrous magnesium sulfate, filtered and concentrated. The crude mixture was then purified on a 12 gram combiflash column with a gradient from 0-70% DCM:MeOH:NH₄OH (90:10:.5) in DCM to afford 1-benzyl-4-(4-benzyl-1H-pyrazol-3-yl)piperidine (.235 g, 48% yield).

Scaleup: Conducted as described above with minor variations to equivalents: NaH(4.5 eq), 15-crown-5 (.25 eq), MeOH (.33 M), Hydrazine (10 eq). (2.51 g, 35% yield).

¹H NMR (600 MHz, Chloroform-*d*) δ 7.32 – 7.21 (m, 8H), 7.18 – 7.13 (m, 2H), 3.79 (s, 2H), 3.67 (s, 1H), 3.50 (s, 2H), 2.94 (dt, *J* = 11.3, 2.9 Hz, 2H), 2.66 – 2.56 (m, 1H), 1.99 (tt, *J* = 11.7, 1.5 Hz, 2H), 1.89 – 1.80 (m, 2H), 1.75 – 1.67 (m, 2H).

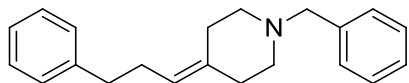
¹³C NMR (151 MHz, Chloroform-*d*) δ 161.70, 141.37, 138.29, 129.49, 128.58, 128.41, 127.27, 126.18, 116.00, 70.74, 63.60, 54.14, 31.84, 30.03.

LCMS 75-95% 3 minutes MeOH:H₂O gradient >95% pure rt= .620

HRMS calc'd for C₂₂H₂₆N₃ 332.21212; found [M+H] 332.21145

HIV-1_{BaL} inhibition in MAGI Cells- IC₅₀=18.1 μ M IC₉₀= 68.4 μ M

HIV-1_{IIIb} inhibition in MAGI Cells- IC₅₀=13.0 μ M IC₉₀= 57.7 μ M

Compound 56

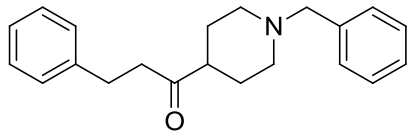
Synthesized using the exact procedure from. Shen, D.-M., et al. (2004). "Antagonists of human CCR5 receptor

containing 4-(pyrazolyl)piperidine side chains. Part 1: Discovery and SAR study of 4-pyrazolylpiperidine side chains." Bioorganic & Medicinal Chemistry Letters **14**(4): 935-939.

^1H NMR (400 MHz, Chloroform-*d*) δ 7.56 – 7.01 (m, 10H), 5.22 – 5.12 (m, 1H), 2.74 (q, $J = 7.9, 6.9$ Hz, 1H), 2.64 (dd, $J = 8.5, 6.8$ Hz, 2H), 2.48 (dt, $J = 12.4, 6.6$ Hz, 2H), 2.40 (dd, $J = 6.4, 4.9$ Hz, 2H), 2.35 – 2.24 (m, 4H), 2.24 – 2.12 (m, 4H).

HRMS calc'd for $\text{C}_{15}\text{H}_{20}\text{O}_3\text{N}_1$ 262.14377; found [M+H]

Matched known material

Compound 57

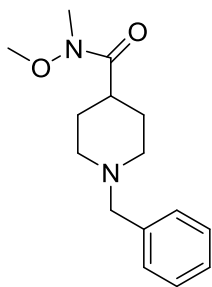
Methyl 1-benzylpiperidine-4-carboxylate (.50 g, 2.1 mmol) as a solution in THF (43 mL, .05 M) was added

to a flame dried 250 mL round bottom flask containing the Weinreb amine salt (.26 g, 2.7 mmol, 1.25 eq) and stirred at -5°C . Phenethylmagnesium chloride (8.6 mL, 8.6 mmol, 4 eq) was then added dropwise and the reaction was allowed to stir until complete consumption of starting material at -5°C . After formation of the Weinreb amide the reaction was slowly warmed to room temperature and tracked by LCMS. After an additional 2 hours of stirring at room temperature the reaction was quenched with NH_4Cl (20 mL) and basified with 10% NaOH . The mixture was further partitioned with EtOAc and separated. The aqueous layer was extracted with DCM (3 times). The organic layers were combined, dried over anhydrous magnesium sulfate, filtered and concentrated to afford 1-(1-benzylpiperidin-4-yl)-3-phenylpropan-1-one (.630 g, 96% yield).
Scaleup: Conducted as described above but scaled to 5 g of starting material. Taken on crude to hydrazine reaction.

^1H NMR (400 MHz, Chloroform-*d*) δ 7.34 – 7.29 (m, 4H), 7.29 – 7.21 (m, 3H), 7.21 – 7.15 (m, 3H), 3.48 (s, 2H), 2.94 – 2.82 (m, 4H), 2.80 – 2.71 (m, 2H), 2.26 (tt, $J = 11.5, 4.0$ Hz, 1H), 1.98 (tt, $J = 11.6, 6.6$ Hz, 2H), 1.80 – 1.73 (m, 2H), 1.65 (dtd, $J = 13.1, 11.5, 3.7$ Hz, 2H).

^{13}C NMR (101 MHz, Chloroform-*d*) δ 212.28, 141.50, 138.54, 129.30, 128.70, 128.56, 128.43, 127.22, 126.30, 63.43, 53.29, 49.19, 42.29, 29.88, 27.97.

HRMS calc'd for $\text{C}_{21}\text{H}_{26}\text{ON}$ 308.20089; found $[\text{M}+\text{H}]$ 308.20037

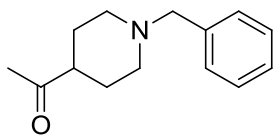
Compound 58

Methyl 1-benzylpiperidine-4-carboxylate (2 g, 8.1 mmol) as a solution in THF (40 mL, .2 M) was added to a flame dried 100 mL round bottom flask containing N,O-dimethylhydroxylamine hydrochloride (.95 g, 9.7 mmol, 1.2 eq) and stirred at 0°C. Isopropyl magnesium chloride (24 mL, 24 mmol, 3 eq) was then added dropwise and the reaction was allowed to stir until complete conversion to ketone was observed by LCMS. The reaction mixture was quenched with a solution of saturated NH₄Cl (10 mL) slowly and allowed to stir for 10 minutes, then basified with 10% NaOH dropwise. The mixture was further partitioned with EtOAc and separated. The aqueous layer was extracted with EtOAc once more and then DCM twice. The organic layers were combined, dried over anhydrous sodium sulfate, filtered, and concentrated to afford 1-benzyl-N-methoxy-N-methylpiperidine-4-carboxamide (2.05 g, 97% yield).

¹H NMR (400 MHz, Chloroform-d) δ 7.31 – 7.24 (m, 4H), 7.23 – 7.18 (m, 1H), 3.63 (s, 3H), 3.48 (s, 2H), 3.13 (s, 3H), 2.95 – 2.86 (m, 2H), 2.60 (d, *J* = 17.7 Hz, 1H), 2.01 (td, *J* = 11.6, 2.5 Hz, 2H), 1.79 (tt, *J* = 20.1, 6.0 Hz, 2H), 1.72 – 1.64 (m, 2H).

¹³C NMR (101 MHz, Chloroform-d) δ 138.05, 129.12, 128.15, 126.97, 63.14, 61.49, 52.95, 38.07, 28.18.

HRMS calc'd for C₁₅H₂₂O₂N₂ 262.12513; found [M+H] 262.12500

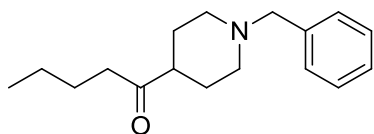
Compound 62

Yellow oil, 213 mg, 98% yield

^1H NMR (400 MHz, Chloroform-*d*) δ 7.34 – 7.28 (m, 4H), 7.28 – 7.21 (m, 1H), 3.49 (s, 2H), 2.94 – 2.86 (m, 2H), 2.28 (tt, $J = 11.5, 3.9$ Hz, 1H), 2.13 (s, 3H), 2.00 (td, $J = 11.6, 2.6$ Hz, 2H), 1.86 – 1.78 (m, 2H), 1.66 (dtd, $J = 13.2, 11.6, 3.8$ Hz, 2H). ^{13}C NMR (101 MHz, Chloroform-*d*) δ 211.15, 138.22, 129.07, 128.19, 127.00, 63.17, 53.01, 49.37, 27.75, 27.69

IR: 2941, 2801, 2759, 1705, 1447, 1143 cm^{-1}

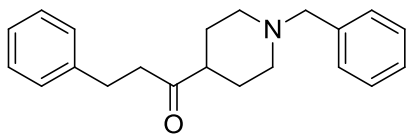
HRMS calc'd for $\text{C}_{14}\text{H}_{20}\text{ON}$ 218.15394; found $[\text{M}+\text{H}]$ 218.15372

Compound 64

Yellow oil, 253 mg, 98%

$^1\text{H NMR}$ (400 MHz, Chloroform-*d*) δ 7.32 – 7.28 (m, 4H), 7.27 – 7.21 (m, 1H), 3.49 (s, 2H), 2.96 – 2.83 (m, 2H), 2.42 (t, $J = 7.4$ Hz, 2H), 2.29 (tt, $J = 11.5, 4.0$ Hz, 1H), 1.99 (td, $J = 11.6, 2.7$ Hz, 2H), 1.81 – 1.74 (m, 2H), 1.73 – 1.63 (m, 2H), 1.53 (p, $J = 7.5$ Hz, 2H), 1.28 (h, $J = 7.5$ Hz, 2H), 0.89 (t, $J = 7.4$ Hz, 3H). $^{13}\text{C NMR}$ (101 MHz, Chloroform-*d*) δ 213.28, 138.34, 129.05, 128.16, 126.95, 63.20, 53.11, 48.80, 40.11, 27.85, 25.74, 22.40, 13.91.

IR: 2934, 2800, 2758, 1706, 1449, 1130 cm^{-1} HRMS calc'd for $\text{C}_{17}\text{H}_{26}\text{ON}$ 260.20089; found $[\text{M}+\text{H}]$ 260.20079

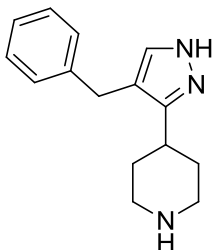
Compound 68

Clear oil, 302 mg, 98% yield

^1H NMR (400 MHz, Chloroform-*d*) δ 7.34 – 7.29 (m, 4H), 7.29 – 7.21 (m, 3H), 7.21 – 7.15 (m, 3H), 3.48 (s, 2H), 2.94 – 2.82 (m, 4H), 2.80 – 2.71 (m, 2H), 2.26 (tt, $J = 11.5, 4.0$ Hz, 1H), 1.98 (tt, $J = 11.6, 6.6$ Hz, 2H), 1.80 – 1.73 (m, 2H), 1.65 (dtd, $J = 13.1, 11.5, 3.7$ Hz, 2H). ^{13}C NMR (101 MHz, Chloroform-*d*) δ 212.28, 141.50, 138.54, 129.30, 128.70, 128.56, 128.43, 127.22, 126.30, 63.43, 53.29, 49.19, 42.29, 29.88, 27.97.

IR: 2940, 2800, 2758, 1705, 1450, 1121 cm^{-1}

HRMS calc'd for $\text{C}_{21}\text{H}_{26}\text{ON}$ 308.20089; found $[\text{M}+\text{H}]$ 308.20037

Compound 74

Prepared by general hydrogenation procedure B from **compound 53**.

Material filtered through celite to remove the Pd/C, concentrated, and then taken on to the next step crude. Analytical sample purified for magi assay on a 12 gram combiflash column with a gradient from 0-70%

DCM:MeOH:NH₄OH (90:10:.5) in DCM to afford 4-(4-benzyl-1H-pyrazol-3-yl)piperidine.

¹H NMR (400 MHz, Chloroform-*d*) δ 7.30 (s, 1H), 7.27 – 7.20 (m, 2H), 7.18 – 7.08 (m, 3H), 3.77 (s, 2H), 3.41 (dt, *J* = 12.8, 3.0 Hz, 2H), 2.91 (td, *J* = 13.1, 3.2 Hz, 2H), 2.81 (tt, *J* = 11.7, 3.8 Hz, 1H), 2.02 – 1.91 (m, 2H), 1.85 – 1.74 (m, 2H).

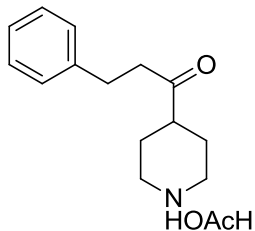
¹³C NMR (101 MHz, Chloroform-*d*) δ 177.14, 149.03, 140.68, 131.58, 128.74, 128.52, 126.51, 116.92, 43.99, 31.80, 31.23, 29.91, 28.64.

LCMS 75-95% 3 minutes MeOH:H₂O gradient >95% pure rt= .581

HRMS calc'd for C₁₅H₂₀N₃ 242.16517; found [M+H] 242.16551

HIV-1_{BaL} inhibition in MAGI Cells- less than 10% inhibition at 100 □M

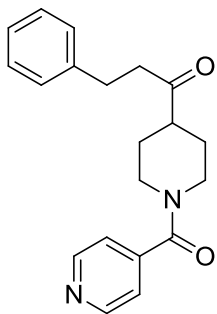
HIV-1_{IIIIB} inhibition in MAGI Cells- less than 10% inhibition at 100 □M

Compound 76

Prepared by general hydrogenation procedure B. Material filtered through celite to remove the Pd/C and concentrated to afford 3-phenyl-1-(piperidin-4-yl)propan-1-one which was taken on to the next step crude.

Amorphous solid

HRMS calc'd for $C_{14}H_{20}ON$ 218.15394; found $[M+H]$ 218.15385

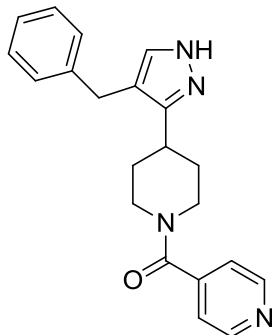
Compound 77

Prepared by general acylation procedure from **compound 76**. Purified on a 12 gram combiflash column with a gradient of 0-70% DCM:MeOH:NH₄OH 90:10:.5 in DCM to afford 1-(1-isonicotinoylpiperidin-4-yl)-3-phenylpropan-1-one (515 mg, 63% yield over two steps).

¹H NMR (400 MHz, Chloroform-*d*) δ 8.78 – 8.59 (m, 2H), 7.27 – 7.21 (m, 4H), 7.21 – 7.12 (m, 3H), 4.66 – 4.43 (m, 1H), 3.68 – 3.52 (m, 1H), 3.06 – 2.95 (m, 1H), 2.89 (t, *J* = 11.1 Hz, 3H), 2.81 – 2.69 (m, 2H), 2.55 (tt, *J* = 11.0, 3.9 Hz, 1H), 1.93 (d, *J* = 13.7 Hz, 1H), 1.70 (d, *J* = 13.9 Hz, 1H), 1.58 (tt, *J* = 21.4, 8.0 Hz, 2H).

¹³C NMR (101 MHz, Chloroform-*d*) δ 210.42, 167.65, 150.31, 143.48, 140.81, 128.52, 128.27, 126.23, 120.96, 48.17, 46.72, 42.39, 41.44, 29.60, 27.65, 27.24.

HRMS calc'd for C₂₀H₂₃O₂N₂ 323.17540; found [M+H] 323.17534

Compound 78

To a solution of 1-(1-isonicotinoylpiperidin-4-yl)-3-phenylpropan-1-one ARP5-70 (.500 g, 1.55 mmol) in THF (16 mL, .1 M) in a flame dried 100 mL round bottom flask was added NaH (.172 g, 4.65 mmol, 3 eq) and stirred at RT. Methyl formate (1.86 g, 31.0 mmol, 20 eq) was then added followed by 15-crown-5 (.034 g, .155 mmol, .1 eq). The reaction was tracked by LCMS and after 30 minutes was quenched with 1 mL of H₂O dropwise. The reaction was then diluted with MeOH (16 mL, .1 M) followed by the dropwise addition of hydrazine (.174 g, 5.43 mmol, 3.5 eq) and tracked by LCMS. After an additional hour of stirring the reaction was concentrated in vacuo to remove MeOH. The oily residue was partitioned between water and DCM and basified with 10% NaOH solution. The layers were separated and the aqueous layer was extracted with DCM (3 times). The organic layers were combined, dried over anhydrous magnesium sulfate, filtered and concentrated. The crude mixture was then purified on a 4 gram combiflash column with a gradient from 0-70% DCM:MeOH:NH₄OH (90:10:.5) in DCM to afford 4-(4-benzyl-1H-pyrazol-3-yl)piperidin-1-yl)piperidin-1-yl(pyridine-4-yl)methanone (.050 g, 9% yield.)

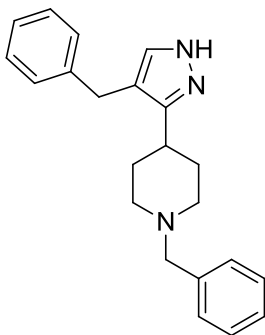
¹H NMR (400 MHz, Chloroform-*d*) δ 8.73 – 8.59 (m, 1H), 7.37 – 7.20 (m, 5H), 7.21 – 7.10 (m, 2H), 4.71 (d, *J* = 13.4 Hz, 1H), 3.81 (s, 2H), 3.75 – 3.53 (m, 1H), 3.02 (dd, *J* = 16.5, 8.4 Hz, 1H), 2.83 (q, *J* = 13.2, 12.1 Hz, 2H), 2.06 – 1.90 (m, 1H), 1.90 – 1.75 (m, 2H), 1.69 (d, *J* = 11.9 Hz, 1H).

¹³C NMR (101 MHz, Chloroform-*d*) δ 167.63, 150.18, 143.86, 140.72, 128.46, 128.32, 126.19, 121.06, 116.34, 47.87, 42.48, 33.88, 31.89, 31.14, 29.82.

HRMS calc'd for $C_{21}H_{23}ON_4$ 347.18664; found [M+H] 347.18658

LCMS 25-95% 8 minutes MeOH:H₂O gradient >95% pure rt= 6.362

LCMS 75-95% 3 minutes MeOH:H₂O gradient >95% pure rt= .897

Compound 79

To a solution of 1-(1-benzylpiperidin-4-yl)-3-phenylpropan-1-one (.45 g, 1.5 mmol) in THF (15 mL, .1 M) in a flame dried 100 mL round bottom flask was added NaH (.21 g, 8.8 mmol, 6 eq) and stirred at RT. Methyl formate (1.76 g, 29 mmol, 20 eq) was then added followed by 15-crown-5 (.16 g, .73 mmol, .5 eq). The reaction was tracked by LCMS and after 1 hour was quenched with 1 mL of H₂O dropwise. The reaction was then diluted with MeOH (15 mL, .1 M) followed by the dropwise addition of hydrazine (.7 g, 22 mmol, 15 eq) and tracked by LCMS. After an additional hour of stirring the reaction was concentrated in vacuo to remove MeOH. The oily residue was partitioned between water and DCM and basified with 10% NaOH solution. The layers were separated and the aqueous layer was extracted with DCM (3 times). The organic layers were combined, dried over anhydrous magnesium sulfate, filtered and concentrated. The crude mixture was then purified on a 12 gram combiflash column with a gradient from 0-70% DCM:MeOH:NH₄OH (90:10:.5) in DCM to afford 1-benzyl-4-(4-benzyl-1H-pyrazol-3-yl)piperidine (.235 g, 48% yield).

Scaleup: Conducted as described above with minor variations to equivalents: NaH(4.5 eq), 15-crown-5 (.25 eq), MeOH (.33 M), Hydrazine (10 eq). (2.51 g, 35% yield).

¹H NMR (600 MHz, Chloroform-*d*) δ 7.32 – 7.21 (m, 8H), 7.18 – 7.13 (m, 2H), 3.79 (s, 2H), 3.67 (s, 1H), 3.50 (s, 2H), 2.94 (dt, *J* = 11.3, 2.9 Hz, 2H), 2.66 – 2.56 (m, 1H), 1.99 (tt, *J* = 11.7, 1.5 Hz, 2H), 1.89 – 1.80 (m, 2H), 1.75 – 1.67 (m, 2H).

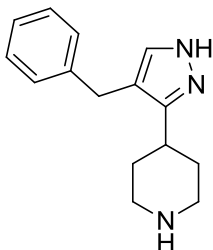
¹³C NMR (151 MHz, Chloroform-*d*) δ 161.70, 141.37, 138.29, 129.49, 128.58, 128.41, 127.27, 126.18, 116.00, 70.74, 63.60, 54.14, 31.84, 30.03.

LCMS 75-95% 3 minutes MeOH:H₂O gradient >95% pure rt= .620

HRMS calc'd for C₂₂H₂₆N₃ 332.21212; found [M+H] 332.21145

HIV-1_{BaL} inhibition in MAGI Cells- IC₅₀=18.1 μ M IC₉₀= 68.4 μ M

HIV-1_{IIIb} inhibition in MAGI Cells- IC₅₀=13.0 μ M IC₉₀= 57.7 μ M

Compound 80

Prepared by general hydrogenation procedure B from material 5-12.

Material filtered through celite to remove the Pd/C, concentrated, and then taken on to the next step crude. Analytical sample purified for magi assay on a 12 gram combiflash column with a gradient from 0-70%

DCM:MeOH:NH₄OH (90:10:.5) in DCM to afford 4-(4-benzyl-1H-pyrazol-3-yl)piperidine.

¹H NMR (400 MHz, Chloroform-*d*) δ 7.30 (s, 1H), 7.27 – 7.20 (m, 2H), 7.18 – 7.08 (m, 3H), 3.77 (s, 2H), 3.41 (dt, *J* = 12.8, 3.0 Hz, 2H), 2.91 (td, *J* = 13.1, 3.2 Hz, 2H), 2.81 (tt, *J* = 11.7, 3.8 Hz, 1H), 2.02 – 1.91 (m, 2H), 1.85 – 1.74 (m, 2H).

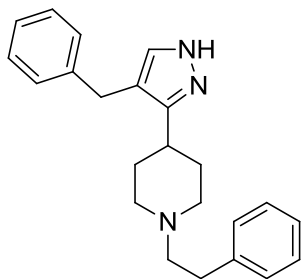
¹³C NMR (101 MHz, Chloroform-*d*) δ 177.14, 149.03, 140.68, 131.58, 128.74, 128.52, 126.51, 116.92, 43.99, 31.80, 31.23, 29.91, 28.64.

LCMS 75-95% 3 minutes MeOH:H₂O gradient >95% pure rt= .581

HRMS calc'd for C₁₅H₂₀N₃ 242.16517; found [M+H] 242.16551

HIV-1_{BaL} inhibition in MAGI Cells- less than 10% inhibition at 100 □M

HIV-1_{III_B} inhibition in MAGI Cells- less than 10% inhibition at 100 □M

Compound 81

Prepared by general reductive amination procedure from **compound 74**. Purified on a 12 gram combiflash column with a gradient of 0-70% DCM:MeOH:NH₄OH 90:10:.5 in DCM to afford 4-(4-benzyl-1H-pyrazol-3-yl)-1-phenethylpiperidine.

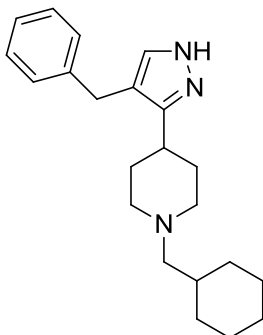
¹H NMR (400 MHz, Chloroform-*d*) δ 7.33 – 7.23 (m, 6H), 7.23 – 7.14 (m, 5H), 3.82 (s, 2H), 3.09 (dt, *J* = 11.3, 3.3 Hz, 2H), 2.86 – 2.78 (m, 2H), 2.66 – 2.58 (m, 4H), 2.08 (td, *J* = 11.7, 2.6 Hz, 2H), 1.92 (tdd, *J* = 12.3, 7.4, 2.8 Hz, 2H), 1.83 – 1.74 (m, 2H).

¹³C NMR (101 MHz, Chloroform-*d*) δ 148.02, 141.15, 140.26, 128.69, 128.38, 126.05, 125.97, 115.79, 60.78, 53.99, 33.54, 33.45, 31.53, 29.85.

LCMS 25-95% 8 minutes MeOH:H₂O gradient >95% pure rt= 5.547

LCMS 75-95% 3 minutes MeOH:H₂O gradient >95% pure rt= .614

HRMS calc'd for C₂₃H₂₈N₃ 346.22777; found [M+H] 346.22797

Compound 82

Prepared by general reductive amination procedure from **compound 74**. Purified on a 12 gram combiflash column with a gradient of 0-70% DCM:MeOH:NH₄OH 90:10:.5 in DCM to afford 4-(4-benzyl-1H-pyrazol-3-yl)-1-(cyclohexylmethyl)piperidine (305 mg, 68% yield over two steps).

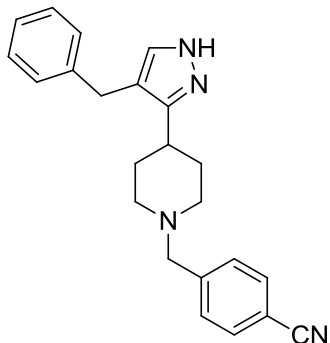
¹H NMR (600 MHz, Chloroform-*d*) δ 7.33 (s, 1H), 7.26 – 7.23 (m, 2H), 7.18 – 7.13 (m, 3H), 3.80 (s, 2H), 2.97 – 2.88 (m, 2H), 2.59 (ddq, *J* = 12.1, 8.2, 4.0 Hz, 1H), 2.11 (d, *J* = 7.1 Hz, 2H), 1.93 – 1.82 (m, 4H), 1.78 – 1.61 (m, 8H), 1.47 (ttt, *J* = 10.8, 7.2, 3.5 Hz, 1H), 1.26 – 1.09 (m, 3H), 0.85 (qd, *J* = 12.2, 3.3 Hz, 2H).

¹³C NMR (151 MHz, Chloroform-*d*) δ 141.50, 128.58, 128.54, 126.12, 115.81, 66.25, 54.83, 35.39, 33.69, 32.21, 31.89, 30.03, 27.00, 26.38.

HRMS calc'd for C₂₂H₃₂N₃ 338.25907; found [M+H] 338.25881

LCMS 50-95% 5 minutes MeOH:H₂O gradient >95% pure rt= 2.918

LCMS 75-95% 3 minutes MeOH:H₂O gradient >95% pure rt= .746

Compound 83

Prepared by general reductive amination procedure from **compound 74**. Purified on a 12 gram combiflash column with a gradient of 0-70% DCM:MeOH:NH₄OH 90:10:.5 in DCM to afford 4-((4-(4-benzyl-1H-pyrazol-3-yl)piperidin-1-yl)methyl)benzonitrile (190 mg, 41% yield over two steps).

¹H NMR (400 MHz, Chloroform-*d*) δ 7.50 (d, *J* = 8.1 Hz, 2H), 7.45 – 7.39 (m, 3H), 7.26 (dd, *J* = 8.0, 6.6 Hz, 2H), 7.21 – 7.14 (m, 3H), 3.85 (s, 2H), 3.52 (s, 2H), 2.88 (dt, *J* = 11.1, 2.9 Hz, 2H), 2.64 (ddt, *J* = 11.9, 7.6, 4.0 Hz, 1H), 2.08 – 1.99 (m, 2H), 1.92 (qd, *J* = 12.3, 3.4 Hz, 2H), 1.79 – 1.69 (m, 2H).

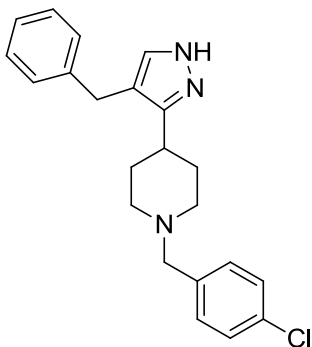
¹³C NMR (101 MHz, Chloroform-*d*) δ 148.30, 144.58, 141.16, 135.26, 132.05, 129.35, 128.30, 126.05, 119.00, 115.56, 110.64, 62.72, 54.12, 33.28, 31.77, 29.78.

HRMS calc'd for C₂₃H₂₅N₄ 357.20737; found [M+H] 357.20640

M.P. 164-166 °C

LCMS 25-95% 8 minutes MeOH:H₂O gradient >95% pure rt= 4.824

LCMS 75-95% 3 minutes MeOH:H₂O gradient >95% pure rt= .600

Compound 84

Prepared by general reductive amination procedure from **compound 74**. Purified on a 12 gram combiflash column with a gradient of 0-70% DCM:MeOH:NH₄OH 90:10:.5 in DCM to afford 4-(4-benzyl-1H-pyrazol-3-yl)-1-(4-chlorobenzyl)piperidine (170 mg, 35% yield over two steps).

¹H NMR (400 MHz, Chloroform-*d*) δ 7.34 (s, 1H), 7.29 – 7.23 (m, 4H), 7.21 – 7.14 (m, 5H), 3.82 (s, 2H), 3.45 (s, 2H), 2.91 (dd, *J* = 11.4, 3.5 Hz, 2H), 2.62 (tt, *J* = 11.7, 4.0 Hz, 1H), 1.98 (ddd, *J* = 12.8, 11.0, 2.0 Hz, 2H), 1.94 – 1.82 (m, 2H), 1.75 – 1.67 (m, 2H).

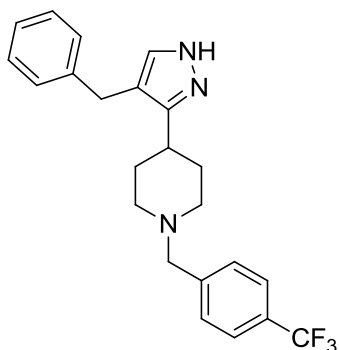
¹³C NMR (101 MHz, Chloroform-*d*) δ 141.43, 136.98, 132.92, 130.69, 128.61, 128.56, 126.22, 115.88, 62.79, 54.16, 33.58, 31.89, 30.05.

HRMS calc'd for C₂₂H₂₅N₃Cl 366.17315; found [M+H] 366.17210

M.P. 163-165 °C

LCMS 50-95% 5 minutes MeOH:H₂O gradient >95% pure rt= 3.221

LCMS 75-95% 3 minutes MeOH:H₂O gradient >95% pure rt= .676

Compound 85

Prepared by general reductive amination procedure from **compound 74**. Purified on a 12 gram combiflash column with a gradient of 0-70% DCM:MeOH:NH₄OH 90:10:.5 in DCM to afford 4-(4-benzyl-1H-pyrazol-3-yl)-1-(4-(trifluoromethyl)benzyl)piperidine (270 mg, 50 % yield over two steps).

¹H NMR (400 MHz, Chloroform-*d*) δ 7.55 – 7.48 (m, 2H), 7.42 (d, *J* = 8.1 Hz, 2H), 7.35 (d, *J* = 13.1 Hz, 1H), 7.29 – 7.22 (m, 2H), 7.16 (tt, *J* = 7.0, 1.9 Hz, 3H), 3.82 (s, 2H), 3.55 (s, 2H), 2.92 (dd, *J* = 11.5, 3.4 Hz, 2H), 2.63 (tq, *J* = 11.7, 3.9 Hz, 1H), 2.11 – 1.96 (m, 2H), 1.95 – 1.79 (m, 2H), 1.79 – 1.67 (m, 2H).

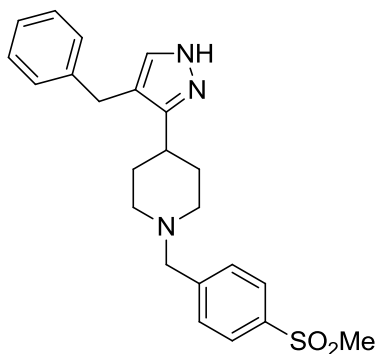
¹³C NMR (151 MHz, Chloroform-*d*) δ 141.45, 140.60, 129.12, 128.81, 128.46, 126.45, 126.10, 116.00, 61.07, 54.23, 33.85, 31.81, 30.12.

¹⁹F NMR (376 MHz, Chloroform-*d*) δ -62.76.

LCMS 25-95% 8 minutes MeOH:H₂O gradient >95% pure rt= 6.198

LCMS 75-95% 3 minutes MeOH:H₂O gradient >95% pure rt= .718

HRMS calc'd for C₂₃H₂₅N₃F₃ 400.19951; found [M+H] 400.19921

Compound 86

Prepared by general reductive amination procedure from **compound 74**. Purified on a 12 gram combiflash column with a gradient of 0-70% DCM:MeOH:NH₄OH 90:10:5 in DCM to afford 4-(4-benzyl-1H-pyrazol-3-yl)-1-(4-(methylsulfonyl)benzyl)piperidine (185 mg, 45% yield

over two steps).

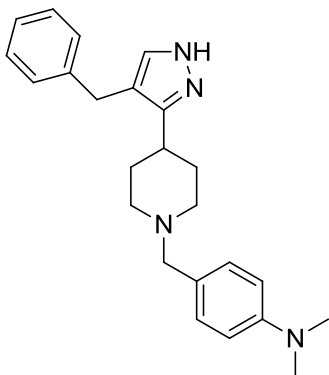
¹H NMR (400 MHz, Chloroform-*d*) δ 7.84 (dd, *J* = 8.3, 1.5 Hz, 2H), 7.51 (dd, *J* = 8.3, 1.6 Hz, 2H), 7.32 – 7.21 (m, 3H), 7.20 – 7.12 (m, 3H), 3.80 (s, 2H), 3.55 (s, 2H), 3.02 (s, 3H), 2.93 – 2.83 (m, 2H), 2.61 (tt, *J* = 12.0, 4.0 Hz, 1H), 2.10 – 1.98 (m, 2H), 1.90 – 1.78 (m, 2H), 1.76 – 1.68 (m, 2H).

¹³C NMR (101 MHz, Chloroform-*d*) δ 163.91, 151.86, 141.01, 139.54, 128.39, 128.32, 126.05, 122.77, 116.80, 115.92, 108.05, 64.45, 54.29, 33.24, 31.62, 29.78.

HRMS calc'd for C₂₃H₂₈O₂N₃S 410.18967; found [M+H] 410.18947

LCMS 25-95% 8 minutes MeOH:H₂O gradient >95% pure rt= 4.936

LCMS 75-95% 3 minutes MeOH:H₂O gradient >95% pure rt= .609

Compound 87

Prepared by general reductive amination procedure from **compound 74**. Purified on a 12 gram combiflash column with a gradient of 0-70% DCM:MeOH:NH₄OH 90:10:.5 in DCM to afford 4-((4-(4-benzyl-1H-pyrazol-3-yl)piperidin-1-yl)methyl)-N,N-dimethylaniline (110 mg, 44% yield over two steps).

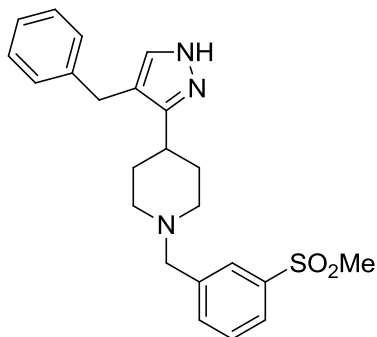
¹H NMR (400 MHz, Chloroform-*d*) δ 7.30 (s, 1H), 7.28 – 7.23 (m, 2H), 7.20 – 7.13 (m, 5H), 6.68 – 6.64 (m, 2H), 3.80 (s, 2H), 3.45 (s, 2H), 3.02 – 2.93 (m, 2H), 2.91 (s, 6H), 2.61 (tt, *J* = 11.8, 4.0 Hz, 1H), 2.03 – 1.79 (m, 4H), 1.74 – 1.68 (m, 2H).

¹³C NMR (101 MHz, Chloroform-*d*) δ 149.79, 141.21, 130.32, 128.35, 125.91, 125.57, 115.60, 112.30, 62.80, 40.69, 33.33, 31.61, 29.80.

HRMS calc'd for C₂₄H₃₁N₄ 375.25432; found [M+H] 375.25517

LCMS 75-95% 3 minutes MeOH:H₂O gradient >95% pure rt= .840

LCMS 25-95% 8 minutes MeOH:H₂O gradient >95% pure rt= 6.300

Compound 88

Prepared by general reductive amination procedure from **compound 74**. Purified on a 12 gram combiflash column with a gradient of 0-70% DCM:MeOH:NH₄OH 90:10:5 in DCM to afford 4-(4-benzyl-1H-pyrazol-3-yl)-1-(3-(methylsulfonyl)benzyl)piperidine (205 mg, 75% yield

over two steps).

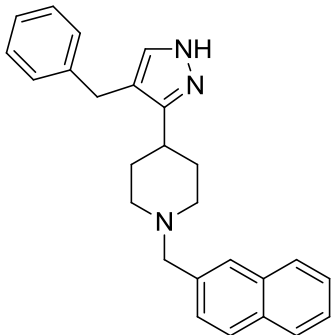
¹H NMR (400 MHz, Chloroform-*d*) δ 7.87 (t, *J* = 1.6 Hz, 1H), 7.79 (ddt, *J* = 7.8, 1.8, 0.9 Hz, 1H), 7.61 (dq, *J* = 7.8, 1.1 Hz, 1H), 7.46 (t, *J* = 7.7 Hz, 1H), 7.28 (d, *J* = 0.8 Hz, 1H), 7.26 – 7.20 (m, 2H), 7.18 – 7.11 (m, 3H), 3.79 (s, 2H), 3.55 (s, 2H), 3.02 (s, 3H), 2.88 (dt, *J* = 11.8, 3.0 Hz, 2H), 2.60 (tt, *J* = 12.0, 3.8 Hz, 1H), 2.08 – 1.97 (m, 2H), 1.83 (qd, *J* = 12.3, 3.7 Hz, 2H), 1.75 – 1.67 (m, 2H).

¹³C NMR (101 MHz, Chloroform-*d*) δ 148.42, 141.08, 140.64, 134.20, 129.27, 128.34, 127.50, 125.96, 115.88, 62.47, 53.97, 44.41, 33.36, 31.56, 29.77.

HRMS calc'd for C₂₃H₂₈O₂N₃S 410.18967; found [M+H] 410.18982

LCMS 75-95% 3 minutes MeOH:H₂O gradient >95% pure rt= .619

LCMS 25-95% 8 minutes MeOH:H₂O gradient >95% pure rt= 5.035

Compound 89

Prepared by general reductive amination procedure from **compound 74**. Purified on a 12 gram combiflash column with a gradient of 0-70% DCM:MeOH:NH₄OH 90:10:5 in DCM to afford 4-(4-benzyl-1H-pyrazol-3-yl)-1-(naphthalen-2-ylmethyl)piperidine (290 mg, 57% yield over two steps).

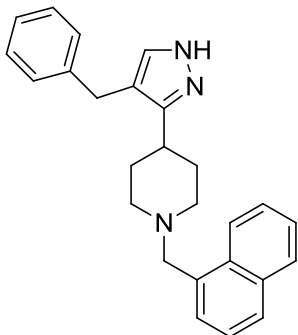
¹H NMR (400 MHz, Chloroform-*d*) δ 7.83 – 7.75 (m, 3H), 7.75 – 7.71 (m, 1H), 7.51 – 7.47 (m, 1H), 7.47 – 7.43 (m, 2H), 7.36 (s, 1H), 7.30 – 7.23 (m, 2H), 7.21 – 7.15 (m, 3H), 3.83 (s, 2H), 3.67 (s, 2H), 3.00 (dt, *J* = 11.2, 3.0 Hz, 2H), 2.65 (tt, *J* = 12.0, 3.9 Hz, 1H), 2.06 (td, *J* = 11.5, 11.1, 2.3 Hz, 2H), 1.93 (qd, *J* = 12.3, 3.5 Hz, 2H), 1.79 – 1.70 (m, 2H).

¹³C NMR (101 MHz, Chloroform-*d*) δ 141.49, 136.07, 133.50, 132.95, 128.61, 128.08, 127.96, 127.92, 127.88, 127.75, 126.19, 125.82, 115.91, 63.74, 54.30, 33.65, 31.94, 30.08.

HRMS calc'd for C₂₆H₂₈N₃ 382.22777; found [M+H] 382.22675

LCMS 50-95% 5 minutes MeOH:H₂O gradient >95% pure rt= 3.691

LCMS 75-95% 3 minutes MeOH:H₂O gradient >95% pure rt= .757

Compound 90

Prepared by general reductive amination procedure from **compound 74**. Purified on a 12 gram combiflash column with a gradient of 0-70% DCM:MeOH:NH₄OH 90:10:5 in DCM to afford 4-(4-benzyl-1H-pyrazol-3-yl)-1-(naphthalen-1-ylmethyl)piperidine (275 mg, 54% yield over two steps).

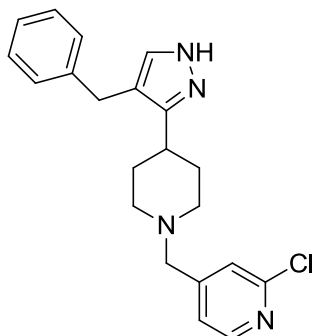
¹H NMR (400 MHz, Chloroform-*d*) δ 8.34 – 8.31 (m, 1H), 7.85 (dd, *J* = 7.8, 1.8 Hz, 1H), 7.78 (d, *J* = 7.9 Hz, 1H), 7.51 – 7.42 (m, 3H), 7.42 – 7.36 (m, 1H), 7.31 – 7.25 (m, 3H), 7.25 – 7.18 (m, 1H), 7.18 – 7.14 (m, 2H), 3.90 (s, 2H), 3.80 (s, 2H), 3.02 (dt, *J* = 11.4, 2.8 Hz, 2H), 2.67 (tt, *J* = 12.1, 3.9 Hz, 1H), 2.15 – 2.04 (m, 2H), 1.96 – 1.82 (m, 2H), 1.76 – 1.67 (m, 2H).

¹³C NMR (101 MHz, Chloroform-*d*) δ 141.61, 134.65, 134.08, 132.83, 128.63, 128.59, 128.07, 127.54, 126.16, 125.97, 125.84, 125.37, 125.03, 115.80, 61.66, 54.63, 33.86, 32.09, 30.06.

HRMS calc'd for C₂₆H₂₈N₃ 382.22777; found [M+H] 382.22833

LCMS 50-95% 8 minutes MeOH:H₂O gradient >95% pure rt= 3.078

LCMS 75-95% 3 minutes MeOH:H₂O gradient >95% pure rt= .848

Compound 91

Prepared by general reductive amination procedure from **compound 74**. Purified on a 12 gram combiflash column with a gradient of 0-70% DCM:MeOH:NH₄OH 90:10:.5 in DCM to afford 4-((4-(4-benzyl-1H-pyrazol-3-yl)piperidin-1-yl)methyl)-2-chloropyridine (145 mg, 60% yield over two steps).

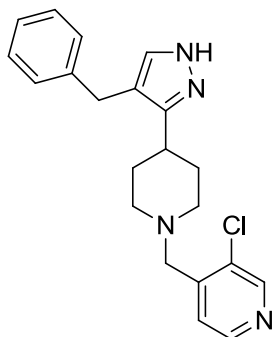
¹H NMR (400 MHz, Chloroform-*d*) δ 8.50 (s, 1H), 8.37 (d, *J* = 4.9 Hz, 1H), 7.48 – 7.42 (m, 1H), 7.35 (s, 1H), 7.24 (tt, *J* = 6.5, 1.1 Hz, 2H), 7.19 – 7.11 (m, 3H), 3.82 (s, 2H), 3.58 (s, 2H), 2.90 (dt, *J* = 11.7, 3.1 Hz, 2H), 2.64 (tt, *J* = 12.1, 3.9 Hz, 1H), 2.14 (td, *J* = 11.8, 2.4 Hz, 2H), 1.99 – 1.83 (m, 2H), 1.78 – 1.69 (m, 2H).

¹³C NMR (101 MHz, Chloroform-*d*) δ 149.10, 147.62, 145.69, 141.05, 131.76, 128.36, 128.33, 126.01, 124.23, 115.89, 58.50, 54.28, 33.28, 31.76, 29.81.

HRMS calc'd for C₂₁H₂₄N₄Cl 367.16840; found [M+H] 367.16865

LCMS 75-95% 3 minutes MeOH:H₂O gradient >95% pure rt= .665

LCMS 25-95% 8 minutes MeOH:H₂O gradient >95% pure rt= 5.457

Compound 92

Prepared by general reductive amination procedure from **compound 74**. Purified on a 12 gram combiflash column with a gradient of 0-70% DCM:MeOH:NH₄OH 90:10:.5 in DCM to afford 4-((4-(4-benzyl-1H-pyrazol-3-yl)piperidin-1-yl)methyl)-3-chloropyridine (155 mg, 64% yield over two steps).

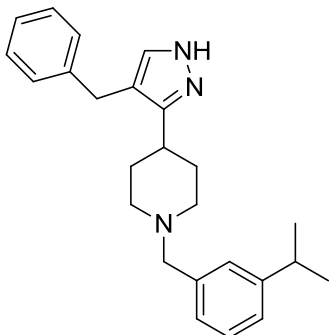
¹H NMR (400 MHz, Chloroform-*d*) δ 8.24 (d, *J* = 5.0 Hz, 1H), 7.35 (s, 1H), 7.28 (s, 1H), 7.28 – 7.21 (m, 2H), 7.19 – 7.12 (m, 4H), 3.82 (s, 2H), 3.45 (s, 2H), 2.85 (dt, *J* = 11.6, 3.0 Hz, 2H), 2.62 (tt, *J* = 11.9, 3.9 Hz, 1H), 2.04 (td, *J* = 11.7, 2.4 Hz, 2H), 1.88 (qd, *J* = 12.3, 3.6 Hz, 2H), 1.78 – 1.67 (m, 2H).

¹³C NMR (101 MHz, Chloroform-*d*) δ 151.83, 149.47, 148.59, 141.06, 134.61, 128.34, 126.00, 123.95, 122.44, 115.87, 61.45, 54.13, 33.31, 31.64, 29.82.

HRMS calc'd for C₂₁H₂₄N₄Cl 367.16840; found [M+H] 367.16849

LCMS 75-95% 3 minutes MeOH:H₂O gradient >95% pure rt= .680

LCMS 25-95% 8 minutes MeOH:H₂O gradient >95% pure rt= 5.672

Compound 93

Prepared by general reductive amination procedure from **compound 74**. Purified on a 12 gram combiflash column with a gradient of 0-70% DCM:MeOH:NH₄OH 90:10:.5 in DCM to afford 4-(4-benzyl-1H-pyrazol-3-yl)-1-(3-isopropylbenzyl)piperidine (215 mg, 58% yield over two

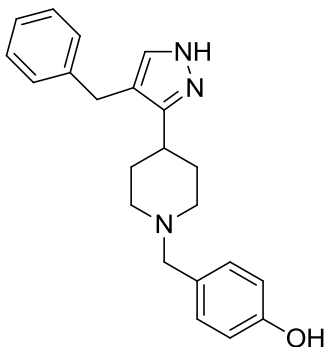
steps).

¹H NMR (400 MHz, Chloroform-*d*) δ 7.30 – 7.18 (m, 4H), 7.18 – 7.10 (m, 6H), 3.80 (s, 2H), 3.69 (d, *J* = 0.8 Hz, 1H), 3.53 (s, 2H), 2.98 (dt, *J* = 11.5, 3.2 Hz, 2H), 2.88 (p, *J* = 6.9 Hz, 1H), 2.62 (tt, *J* = 12.0, 3.9 Hz, 1H), 2.09 – 1.96 (m, 2H), 1.88 (qd, *J* = 11.7, 10.9, 3.0 Hz, 2H), 1.78 – 1.69 (m, 2H), 1.23 (d, *J* = 6.9, Hz, 6H).

¹³C NMR (101 MHz, Chloroform-*d*) δ 148.84, 141.11, 137.27, 128.35, 127.66, 126.91, 125.95, 125.20, 115.79, 63.28, 53.74, 34.00, 33.25, 31.35, 29.79, 24.03.

LCMS 25-95% 8 minutes MeOH:H₂O gradient >95% pure rt= 7.098

LCMS 75-95% 3 minutes MeOH:H₂O gradient >95% pure rt= .900

Compound 94

Prepared by general reductive amination procedure from **compound 74**. Purified on a 12 gram combiflash column with a gradient of 0-70% DCM:MeOH:NH₄OH 90:10:.5 in DCM to afford 4-((4-(4-benzyl-1H-pyrazol-3-yl)piperidin-1-yl)methyl)phenol (150 mg, 65% yield over two steps).

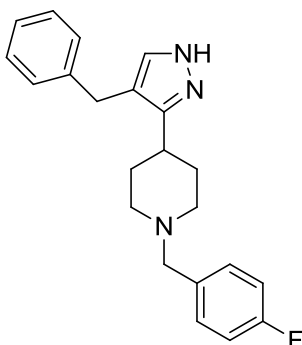
¹H NMR (400 MHz, Chloroform-*d*) δ 7.27 – 7.19 (m, 3H), 7.17 – 7.12 (m, 1H), 7.12 – 7.08 (m, 2H), 7.07 – 7.02 (m, 2H), 6.71 – 6.65 (m, 2H), 3.75 (s, 2H), 3.39 (s, 2H), 2.96 (dd, *J* = 8.9, 5.8 Hz, 2H), 2.61 (t, *J* = 7.2 Hz, 2H), 2.04 – 1.91 (m, 2H), 1.92 – 1.75 (m, 2H), 1.67 (dd, *J* = 11.9, 4.0 Hz, 2H).

¹³C NMR (101 MHz, Chloroform-*d*) δ 156.16, 147.34, 141.05, 135.92, 130.87, 128.32, 125.95, 115.65, 62.62, 45.84, 33.10, 31.11, 29.72.

HRMS calc'd for C₂₂H₂₆ON₃ 348.20704; found [M+H] 348.20736

LCMS 75-95% 3 minutes MeOH:H₂O gradient >95% pure rt= .613

LCMS 25-95% 8 minutes MeOH:H₂O gradient >95% pure rt= 5.255

Compound 95

Prepared by general reductive amination procedure from **compound 74**. Purified on a 12 gram combiflash column with a gradient of 0-70% DCM:MeOH:NH₄OH 90:10:.5 in DCM to afford 4-(4-benzyl-1H-pyrazol-3-yl)-1-(4-fluorobenzyl)piperidine (170 mg, 73% yield over two steps).

¹H NMR (400 MHz, Chloroform-*d*) δ 7.37 – 7.21 (m, 5H), 7.22 – 7.10 (m, 3H), 7.04 – 6.91 (m, 2H), 3.80 (s, 2H), 3.51 (s, 2H), 2.95 (dt, *J* = 11.9, 3.2 Hz, 2H), 2.62 (tt, *J* = 11.9, 4.0 Hz, 1H), 2.07 – 1.99 (m, 2H), 1.94 – 1.80 (m, 2H), 1.77 – 1.68 (m, 2H).

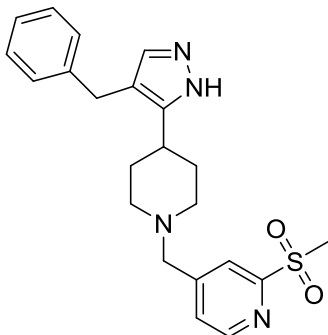
¹³C NMR (101 MHz, Chloroform-*d*) δ 163.25, 160.82, 148.10, 141.00, 134.84, 133.23, 130.76, 128.33, 126.01, 115.96, 114.92, 62.12, 53.53, 33.26, 31.21, 29.79.

¹⁹F NMR (376 MHz, Chloroform-*d*) δ -115.87.

HRMS calc'd for C₂₂H₂₂N₃F 350.20270; found [M+H] 350.20270

LCMS 75-95% 3 minutes MeOH:H₂O gradient >95% pure rt= .663

LCMS 25-95% 8 minutes MeOH:H₂O gradient >95% pure rt= 5.410

Compound 98

Prepared by general reductive amination procedure from **compound 74**. Purified on a 4 gram combiflash column with a gradient of 0-75% DCM:MeOH:NH₄OH 90:10:.5 in DCM to afford 4-((4-(4-benzyl-1H-pyrazol-3-yl)piperidin-1-yl)methyl)-2-(methylsulfonyl)pyridine (105 mg, 44% yield

over two steps).

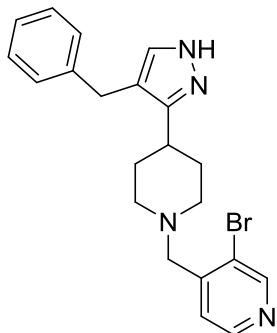
¹H NMR (400 MHz, Chloroform-*d*) δ 8.61 (dq, *J* = 4.9, 0.9 Hz, 1H), 8.05 (dt, *J* = 1.5, 0.7 Hz, 1H), 7.58 – 7.54 (m, 1H), 7.30 (s, 1H), 7.29 – 7.23 (m, 2H), 7.20 – 7.13 (m, 3H), 3.82 (s, 2H), 3.59 (s, 2H), 3.23 (s, 3H), 2.89 – 2.81 (m, 2H), 2.69 – 2.57 (m, 1H), 2.16 – 2.03 (m, 2H), 1.93 – 1.79 (m, 2H), 1.77 – 1.69 (m, 2H).

¹³C NMR (101 MHz, Chloroform-*d*) δ 157.98, 151.80, 150.01, 141.01, 128.39, 127.23, 126.03, 120.86, 116.09, 61.63, 54.14, 40.06, 33.36, 31.54, 29.82.

HRMS calc'd for C₂₂H₂₇O₂N₄S 411.18492; found [M+H] 411.18546

LCMS 75-95% 3 minutes MeOH:H₂O gradient >95% pure rt= .742

LCMS 25-95% 8 minutes MeOH:H₂O gradient >95% pure rt= 5.214

Compound 99

Prepared by general reductive amination procedure from **compound 74**. DMSO was added dropwise until the aldehyde dissolved. Purified on a 4 gram combiflash column with a gradient of 0-50% DCM:MeOH:NH₄OH 90:10:.5 in DCM to 4-((4-(4-benzyl-1H-pyrazol-3-yl)piperidin-1-yl)methyl)-3-bromopyridine

(27 mg, 25% yield over two steps).

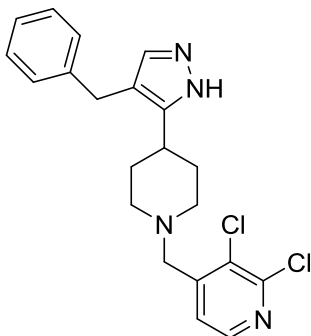
¹H NMR (400 MHz, Chloroform-*d*) δ 8.66 (s, 1H), 8.48 (s, 1H), 7.61 (d, *J* = 34.7 Hz, 1H), 7.31 – 7.21 (m, 4H), 7.23 – 7.01 (m, 2H), 3.90 – 3.54 (m, 4H), 3.07 (td, *J* = 12.7, 3.0 Hz, 2H), 2.65 (td, *J* = 12.5, 3.3 Hz, 1H), 2.26 (d, *J* = 16.8 Hz, 2H), 1.95 (s, 2H), 1.74 (dd, *J* = 30.5, 8.1 Hz, 1H).

¹³C NMR (101 MHz, Chloroform-*d*) δ 160.82, 151.90, 148.60, 132.16, 128.69, 128.43, 128.33, 126.12, 60.30, 46.14, 39.95, 30.68, 29.79.

HRMS calc'd for C₂₄H₂₇O₂N₃F₃S 478.17706; found [M+H] 478.17655

LCMS 75-95% 3 minutes MeOH:H₂O gradient >95% pure rt= 1.067

LCMS 50-95% 8 minutes MeOH:H₂O gradient >95% pure rt= 3.970

Compound 100

Prepared by general reductive amination procedure from **compound 74**. Purified on a 4 gram combiflash column with a gradient of 0-75% DCM:MeOH:NH₄OH 90:10:.5 in DCM to afford 4-((4-(4-benzyl-1H-pyrazol-3-yl)piperidin-1-yl)methyl)-2,3-dichloropyridine (133 mg, 57% yield over two steps).

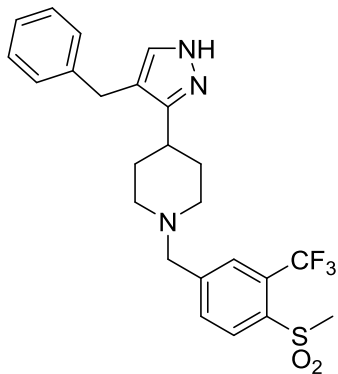
¹H NMR (400 MHz, Chloroform-*d*) δ 8.12 (dd, *J* = 4.9, 1.1 Hz, 1H), 7.46 – 7.39 (m, 2H), 7.28 – 7.21 (m, 2H), 7.19 – 7.12 (m, 3H), 3.84 (s, 2H), 3.58 (s, 2H), 2.89 (dt, *J* = 11.5, 3.2 Hz, 2H), 2.66 (tt, *J* = 12.2, 4.1 Hz, 1H), 2.21 – 2.11 (m, 2H), 1.94 (qd, *J* = 12.2, 3.4 Hz, 2H), 1.82 – 1.71 (m, 2H).

¹³C NMR (101 MHz, Chloroform-*d*) δ 149.38, 146.53, 141.05, 129.61, 128.38, 126.03, 123.10, 115.80, 59.50, 54.37, 33.21, 31.80, 29.80.

HRMS calc'd for C₂₁H₂₃ N₄Cl₂ 401.12943; found [M+H] 401.12950

LCMS 75-95% 3 minutes MeOH:H₂O gradient >95% pure rt= 1.154

LCMS 25-95% 8 minutes MeOH:H₂O gradient >95% pure rt= 7.372

Compound 101

Prepared by general reductive amination procedure from **compound 74**. DMSO was added dropwise until the aldehyde dissolved. Purified on a 4 gram combiflash column with a gradient of 0-50% DCM:MeOH:NH₄OH 90:10:.5 in DCM to afford 4-(4-benzyl-1H-pyrazol-3-yl)-1-(4-(methylsulfonyl)-3-(trifluoromethyl)benzyl)piperidine (74 mg, 59% yield over

two steps).

¹H NMR (400 MHz, Chloroform-*d*) δ 8.23 (d, *J* = 8.2 Hz, 1H), 7.93 – 7.89 (m, 1H), 7.82 – 7.75 (m, 1H), 7.33 – 7.23 (m, 3H), 7.21 – 7.12 (m, 3H), 3.82 (s, 2H), 3.66 (d, *J* = 10.7 Hz, 2H), 3.17 (s, 3H), 2.92 (d, *J* = 11.3 Hz, 2H), 2.73 – 2.63 (m, 1H), 2.14 (s, 2H), 1.89 (qd, *J* = 12.2, 11.7, 3.7 Hz, 2H), 1.77 (d, *J* = 12.5 Hz, 2H).

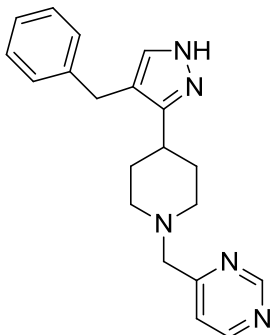
¹³C NMR (101 MHz, Chloroform-*d*) δ 140.92, 132.25, 128.64, 128.38, 128.33, 126.04, 124.03, 121.31, 116.12, 61.73, 54.00, 45.04, 40.90, 31.32, 29.78.

¹⁹F NMR (376 MHz, Chloroform-*d*) δ -53.53.

HRMS calc'd for C₂₄H₂₇O₂N₃F₃S 478.17706; found [M+H] 478.17655

LCMS 75-95% 3 minutes MeOH:H₂O gradient >95% pure rt= 1.084

LCMS 50-95% 8 minutes MeOH:H₂O gradient >95% pure rt= 4.007

Compound 102

Prepared by general reductive amination procedure from **compound 74**. Purified on a 12 gram combiflash column with a gradient of 0-70% DCM:MeOH:NH₄OH 90:10:.5 in DCM to afford 4-((4-(4-benzyl-1H-pyrazol-3-yl)piperidin-1-yl)methyl)pyrimidine (93 mg, 72% yield over two steps).

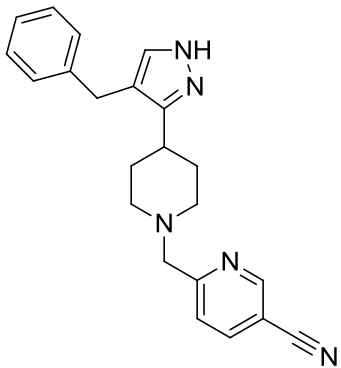
¹H NMR (400 MHz, Chloroform-*d*) δ 9.12 (d, *J* = 1.4 Hz, 1H), 8.64 (d, *J* = 5.2 Hz, 1H), 7.50 (dd, *J* = 5.1, 1.4 Hz, 1H), 7.34 – 7.21 (m, 3H), 7.21 – 7.10 (m, 3H), 3.81 (s, 2H), 3.63 (s, 2H), 2.91 (dt, *J* = 11.9, 3.2 Hz, 2H), 2.63 (tt, *J* = 12.1, 3.9 Hz, 1H), 2.15 (td, *J* = 11.8, 2.5 Hz, 2H), 1.96 – 1.81 (m, 2H), 1.75 (ddt, *J* = 12.5, 4.4, 2.3 Hz, 2H).

¹³C NMR (101 MHz, Chloroform-*d*) δ 168.02, 158.52, 157.04, 140.94, 128.36, 126.04, 120.13, 116.15, 63.80, 54.30, 33.27, 31.59, 29.80.

HRMS calc'd for C₂₀H₂₄N₅ 334.20262; found [M+H] 334.20242

LCMS 25-95% 8 minutes MeOH:H₂O gradient >95% pure rt= 4.692

LCMS 75-95% 3 minutes MeOH:H₂O gradient >95% pure rt= .616

Compound 103

Prepared by general reductive amination procedure from **compound 74**. Purified on a 12 gram combiflash column with a gradient of 0-70% DCM:MeOH:NH₄OH 90:10:.5 in DCM to afford 6-((4-(4-benzyl-1H-pyrazol-3-yl)piperidin-1-yl)methyl)nicotinonitrile (215 mg, 66% yield over two steps).

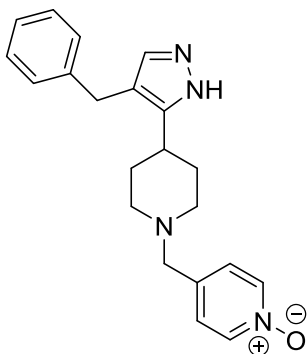
¹H NMR (400 MHz, Chloroform-*d*) δ 8.76 (d, *J* = 2.1 Hz, 1H), 7.80 (dd, *J* = 8.1, 2.2 Hz, 1H), 7.58 (d, *J* = 8.1 Hz, 1H), 7.30 (s, 1H), 7.24 (t, *J* = 7.4 Hz, 2H), 7.19 – 7.11 (m, 3H), 3.80 (s, 2H), 3.69 (s, 2H), 2.88 (dt, *J* = 11.8, 3.2 Hz, 2H), 2.63 (tt, *J* = 12.1, 3.8 Hz, 1H), 2.14 (td, *J* = 11.9, 2.5 Hz, 2H), 1.90 (qd, *J* = 12.4, 3.6 Hz, 2H), 1.73 (dd, *J* = 13.0, 4.1 Hz, 2H).

¹³C NMR (101 MHz, Chloroform-*d*) δ 163.91, 151.86, 141.01, 139.54, 128.39, 128.32, 126.05, 122.77, 116.80, 115.92, 108.05, 64.45, 54.29, 33.24, 31.62, 29.78.

HRMS calc'd for C₂₂H₂₄N₅ 358.20262; found [M+H] 358.20229

LCMS 25-95% 8 minutes MeOH:H₂O gradient >95% pure rt= 5.146

LCMS 75-95% 3 minutes MeOH:H₂O gradient >95% pure rt= .614

Compound 104

Prepared by general reductive amination procedure from **compound 74**. Purified on a 4 gram combiflash column with a gradient of 0-75% DCM:MeOH:NH₄OH 90:10:.5 in DCM to afford 4-((4-benzyl-1H-pyrazol-3-yl)methyl)piperidin-1-yl)methylpyridine 1-oxide (96 mg, 47% yield over two steps).

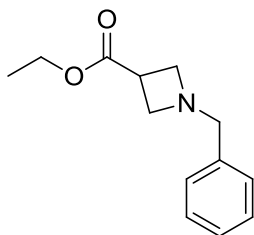
¹H NMR (400 MHz, Chloroform-*d*) δ 8.17 (d, *J* = 7.0 Hz, 2H), 7.29 – 7.24 (m, 3H), 7.22 (d, *J* = 7.0 Hz, 2H), 7.17 – 7.09 (m, 3H), 3.78 (s, 2H), 3.43 (s, 2H), 2.84 (dt, *J* = 11.8, 3.0 Hz, 2H), 2.59 (tt, *J* = 12.0, 3.9 Hz, 1H), 2.08 – 1.98 (m, 2H), 1.92 – 1.77 (m, 2H), 1.75 – 1.66 (m, 2H).

¹³C NMR (101 MHz, Chloroform-*d*) δ 141.11, 138.86, 128.34, 128.33, 126.01, 125.97, 115.78, 65.83, 54.07, 33.33, 31.55, 29.81.

HRMS calc'd for C₂₁H₂₅ON₄ 349.20229; found [M+H] 349.20172

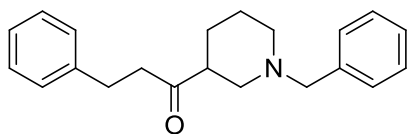
LCMS 75-95% 3 minutes MeOH:H₂O gradient >95% pure rt= .732

LCMS 25-95% 8 minutes MeOH:H₂O gradient >95% pure rt= 4.619

Compound 107

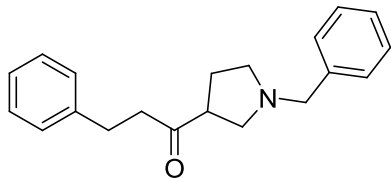
To a solution of azetidine-3-carboxylic acid (5.0 g, 50 mmol) in DCM (250 mL, .2 M) was added benzaldehyde (6.3 g, 59 mmol, 1.2 eq). The solution was allowed to stir for thirty minutes followed by addition of sodium triacetoxyborohydride (15.7 g, 74 mmol, 1.5 eq).

After stirring for an additional thirty minutes the reaction was checked by LCMS and determined to be complete. Thionyl chloride (49.2 g, 10 eq) was then added slowly with vigorous stirring. The reaction was then warmed to 50°C for two hours, checked by LCMS tracking the methyl ester as product with complete conversion. The solution was then chilled to 0°C and 200 proof ethanol (11.4 g, 247 mmol, 5 eq) was slowly added. The solution was then concentrated and partitioned between DCM and brine. The aqueous layer was basified with 10% NaOH. The layers were then separated and the aqueous layer was extracted with DCM (3 times). The organic layers were combined, dried over anhydrous sodium sulfate, filtered, and concentrated. The product was taken on to the next step crude.

Compound 108

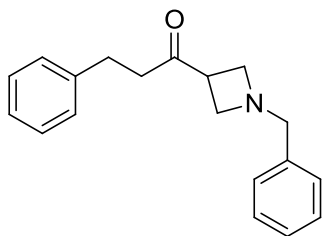
Ethyl 1-benzylpiperidine-3-carboxylate (2.50 g, 10.1 mmol) as a solution in THF (100 mL, .1 M) was added

to a flame dried 500 mL round bottom flask containing the Weinreb amine salt (1.09 g, 11.1 mmol, 1.1 eq) and stirred at -5°C . Phenethylmagnesium bromide (41 mL, 41 mmol, 4 eq) was then added dropwise and the reaction was allowed to stir until complete consumption of starting material at -5°C . After formation of the Weinreb amide the reaction was slowly warmed to room temperature and tracked by LCMS. After an additional 2 hours of stirring at room temperature the reaction was quenched with NH_4Cl (20 mL) and basified with 10% NaOH . The mixture was further partitioned with EtOAc and separated. The aqueous layer was extracted with DCM (3 times). The organic layers were combined, dried over anhydrous magnesium sulfate, filtered and concentrated to afford 1-(1-benzylpiperidin-3-yl)-3-phenylpropan-1-one which was taken on to the next step crude.

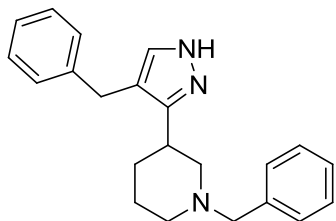
Compound 109

Ethyl 1-benzylpyrrolidine-3-carboxylate (2.50 g, 10.7 mmol) as a solution in THF (107 mL, .1 M) was added to a flame dried 500 mL round bottom flask containing the

Weinreb amine salt (1.15 g, 11.1 mmol, 1.1 eq) and stirred at -5°C . Phenethylmagnesium bromide (43 mL, 43 mmol, 4 eq) was then added dropwise and the reaction was allowed to stir until complete consumption of starting material at -5°C . After formation of the Weinreb amide the reaction was slowly warmed to room temperature and tracked by LCMS. After an additional 2 hours of stirring at room temperature the reaction was quenched with NH_4Cl (20 mL) and basified with 10% NaOH . The mixture was further partitioned with EtOAc and separated. The aqueous layer was extracted with DCM (3 times). The organic layers were combined, dried over anhydrous magnesium sulfate, filtered and concentrated to afford 1-(1-benzylpyrrolidin-3-yl)-3-phenylpropan-1-one which was taken on to the next step crude.

Compound 110

Ethyl 1-benzylazetidine-3-carboxylate (2.5 g, 11.4 mmol) as a solution in THF (110 mL, .1 M) was added to a flame dried 500 mL round bottom flask containing the Weinreb amine salt (1.22 g, 12.5 mmol, 1.1 eq) and stirred at -5°C . Phenethylmagnesium bromide (46 mL, 46 mmol, 4 eq) was then added dropwise and the reaction was allowed to stir until complete consumption of starting material at -5°C . After formation of the Weinreb amide the reaction was slowly warmed to room temperature and tracked by LCMS. After an additional 2 hours of stirring at room temperature the reaction was quenched with NH_4Cl (20 mL) and basified with 10% NaOH . The mixture was further partitioned with EtOAc and separated. The aqueous layer was extracted with DCM (3 times). The organic layers were combined, dried over anhydrous magnesium sulfate, filtered and concentrated to afford 1-(1-benzylazetidin-3-yl)-3-phenylpropan-1-one which was taken on to the next step crude.

Compound 111

To a solution of 1-(1-benzylpiperidin-3-yl)-3-phenylpropan-1-one **compound 108** (3.11 g, 10.1 mmol) in THF (100 mL, .1 M) in a flame dried 250 mL round bottom flask was added NaH (1.12 g, 30 mmol, 3 eq) and stirred at RT. Methyl formate (12.2 g, 200 mmol, 20 eq) was then added followed by 15-crown-5 (.56 g, .25 mmol, .25 eq). The reaction was tracked by LCMS and after 1 hour was quenched with 5 mL of H₂O dropwise. The reaction was then allowed to vent until no more hydrogen gas was evolved followed by the dropwise addition of hydrazine (1.62 g, 51 mmol, 5 eq) and tracked by LCMS. After an additional hour of stirring, the reaction was partitioned between water and EtOAc then basified with a 10% NaOH solution. The layers were separated and the aqueous layer was extracted with DCM (3 times). The organic layers were combined, dried over anhydrous sodium sulfate, filtered, and concentrated. The crude mixture was then purified on a 40 gram combiflash column with a gradient from 0-70% DCM:MeOH:NH₄OH (90:10:.5) in DCM to afford 1-benzyl-3-(4-benzyl-1H-pyrazol-3-yl)piperidine pyrazole (.998 g, 30% yield over two steps).

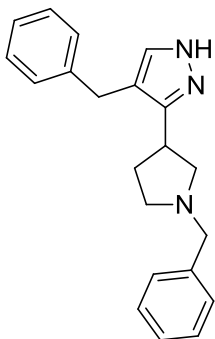
¹H NMR (400 MHz, Chloroform-*d*) δ 7.35 – 7.29 (m, 4H), 7.28 (s, 1H), 7.27 – 7.21 (m, 3H), 7.19 – 7.17 (m, 1H), 7.16 – 7.11 (m, 2H), 3.68 (s, 2H), 3.48 (s, 2H), 3.03 (p, *J* = 4.3 Hz, 1H), 2.80 – 2.60 (m, 2H), 2.58 – 2.43 (m, 1H), 2.40 – 2.17 (m, 1H), 1.73 – 1.55 (m, 2H), 1.55 – 1.42 (m, 2H).

¹³C NMR (101 MHz, Chloroform-*d*) δ 141.15, 137.68, 129.27, 128.44, 128.35, 127.29, 125.91, 115.22, 70.56, 63.72, 57.69, 53.95, 29.68, 29.39.

HRMS calc'd for C₂₂H₂₆N₃ 332.21212; found [M+H] 332.21169

LCMS 25-95% 8 minutes MeOH:H₂O gradient >95% pure rt= 5.933

LCMS 75-95% 3 minutes MeOH:H₂O gradient >95% pure rt= .724

Compound 112

To a solution of 1-(1-benzylpyrrolidin-3-yl)-3-phenylpropan-1-one **compound 109** (3.14 g, 10.7 mmol) in THF (107 mL, .1 M) in a flame dried 250 mL round bottom flask was added NaH (1.19 g, 32 mmol, 3 eq) and stirred at RT. Methyl formate (12.9 g, 214 mmol, 20 eq) was then added followed by 15-crown-5 (.59 g, .27 mmol, .25 eq). The reaction was tracked by LCMS and after 1 hour was quenched with 5 mL of H₂O dropwise. The reaction was then allowed to vent until no more hydrogen gas was evolved followed by the dropwise addition of hydrazine (1.72 g, 54 mmol, 5 eq) and tracked by LCMS. After an additional hour of stirring, the reaction was partitioned between water and EtOAc then basified with a 10% NaOH solution. The layers were separated and the aqueous layer was extracted with DCM (3 times). The organic layers were combined, dried over anhydrous sodium sulfate, filtered, and concentrated. The crude mixture was then purified on a 40 gram combiflash column with a gradient from 0-70% DCM:MeOH:NH₄OH (90:10:.5) in DCM to afford 4-benzyl-3-(1-benzylpyrrolidin-3-yl)-1H-pyrazole (1.150 g, 34% yield over two steps).

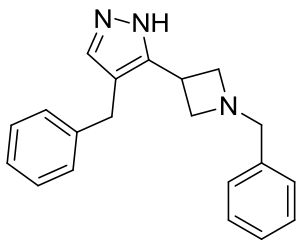
¹H NMR (400 MHz, Chloroform-*d*) δ 7.35 – 7.30 (m, 4H), 7.30 – 7.27 (m, 1H), 7.27 – 7.23 (m, 3H), 7.21 – 7.19 (m, 1H), 7.18 – 7.13 (m, 2H), 3.80 (s, 2H), 3.66 (s, 2H), 3.44 – 3.33 (m, 1H), 2.87 (td, *J* = 8.9, 4.7 Hz, 1H), 2.78 (dd, *J* = 9.3, 4.6 Hz, 1H), 2.66 (dt, *J* = 9.2, 6.2 Hz, 1H), 2.50 (dq, *J* = 15.2, 8.7, 7.5 Hz, 1H), 2.16 (dtd, *J* = 13.6, 9.1, 4.8 Hz, 1H), 1.93 – 1.77 (m, 1H).

¹³C NMR (101 MHz, Chloroform-*d*) δ 147.49, 141.25, 138.73, 136.57, 128.86, 128.41, 128.37, 127.15, 125.94, 115.31, 60.33, 59.78, 53.23, 33.35, 31.28, 29.75.

HRMS calc'd for $C_{21}H_{24}N_3$ 318.19647; found [M+H] 318.19544

LCMS 25-95% 8 minutes MeOH:H₂O gradient >95% pure rt= 5.926

LCMS 75-95% 3 minutes MeOH:H₂O gradient >95% pure rt= .728

Compound 113

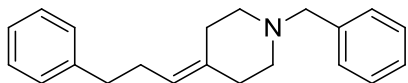
To a solution of 1-(1-benzylazetididin-3-yl)-3-phenylpropan-1-one **compound 110** (2 g, 7.2 mmol) in THF (71 mL, .1 M) in a flame dried 250 mL round bottom flask was added NaH (1.19 g, 32 mmol, 4.5 eq) and stirred at RT. Methyl formate (4.30 g, 72 mmol, 10 eq) was then added followed by 15-crown-5 (.16 g, .72 mmol, .1 eq). The reaction was tracked by LCMS and after 1 hour was quenched with 5 mL of H₂O dropwise. The reaction was then allowed to vent until no more hydrogen gas was evolved, followed by the dropwise addition of hydrazine hydrate (2.29 g, 36 mmol, 5 eq) and tracked by LCMS. After an additional hour of stirring, the reaction was partitioned between water and EtOAc then basified with a 10% NaOH solution. The layers were separated and the aqueous layer was extracted with DCM (3 times). The organic layers were combined, dried over anhydrous sodium sulfate, filtered, and concentrated. The crude mixture was then purified on a 40 gram combiflash column with a gradient from 0-70% DCM:MeOH:NH₄OH (90:10:.5) in DCM to afford 4-benzyl-3-(1-benzylazetididin-3-yl)-1H-pyrazole (.250 g, 12% yield over three steps).

¹H NMR (400 MHz, Chloroform-*d*) δ 7.32 – 7.21 (m, 8H), 7.20 – 7.14 (m, 1H), 7.12 – 7.08 (m, 2H), 3.74 (s, 2H), 3.70 – 3.66 (m, 1H), 3.64 (s, 2H), 3.60 – 3.52 (m, 2H), 3.33 (t, *J* = 7.0 Hz, 2H).

¹³C NMR (101 MHz, Chloroform-*d*) δ 140.83, 137.59, 128.59, 128.42, 128.41, 128.27, 127.19, 126.05, 116.84, 70.40, 63.37, 60.02, 29.71, 27.29.

LCMS 75-95% 3 minutes MeOH:H₂O gradient >95% pure rt= .749

LCMS 50-95% 8 minutes MeOH:H₂O gradient >95% pure rt= 2.648

Compound 114

Synthesized using the exact procedure from. Shen, D.-

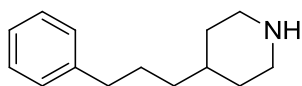
M., et al. (2004). "Antagonists of human CCR5 receptor

containing 4-(pyrazolyl)piperidine side chains. Part 1: Discovery and SAR study of 4-pyrazolylpiperidine side chains." Bioorganic & Medicinal Chemistry Letters **14**(4): 935-939.

^1H NMR (400 MHz, Chloroform-*d*) δ 7.56 – 7.01 (m, 10H), 5.22 – 5.12 (m, 1H), 2.74 (q, $J = 7.9, 6.9$ Hz, 1H), 2.64 (dd, $J = 8.5, 6.8$ Hz, 2H), 2.48 (dt, $J = 12.4, 6.6$ Hz, 2H), 2.40 (dd, $J = 6.4, 4.9$ Hz, 2H), 2.35 – 2.24 (m, 4H), 2.24 – 2.12 (m, 4H).

HRMS calc'd for $\text{C}_{15}\text{H}_{20}\text{O}_3\text{N}_1$ 262.14377; found [M+H]

Matched known material

Compound 115

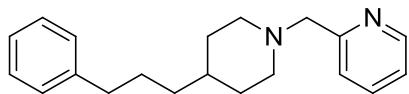
Prepared by general hydrogenation procedure A from **compound 114**, taken on to the next step crude.

^1H NMR (400 MHz, Chloroform-*d*) δ 7.24 (t, $J = 7.6$ Hz, 2H), 7.18 – 7.05 (m, 3H), 3.54 – 3.29 (m, 2H), 2.93 – 2.67 (m, 2H), 2.56 (t, $J = 7.6$ Hz, 2H), 1.95 – 1.73 (m, 2H), 1.66 – 1.40 (m, 4H), 1.40 – 1.21 (m, 2H).

^{13}C NMR (101 MHz, Chloroform-*d*) δ 142.24, 128.56, 128.53, 126.06, 44.27, 36.07, 35.47, 34.30, 28.92, 28.50.

HRMS calc'd for $\text{C}_{14}\text{H}_{22}\text{N}$ 204.17468; found $[\text{M}+\text{H}]$ 204.17433

M.P. 157-159 °C

Compound 116

Prepared by general reductive amination procedure from **compound 115**. Purified on 4 gram combiflash column

with a gradient of 0-10% 3.5N NH₃ MeOH solution in DCM (165 mg, 57% yield over two steps)

¹H NMR (400 MHz, Chloroform-*d*) δ 8.53 (dd, *J* = 5.0, 1.7 Hz, 1H), 7.61 (td, *J* = 7.7, 1.8 Hz, 1H), 7.38 (d, *J* = 7.8 Hz, 1H), 7.25 (dd, *J* = 8.6, 6.4 Hz, 2H), 7.18 – 7.10 (m, 4H), 3.60 (s, 2H), 2.92 – 2.80 (m, 2H), 2.56 (t, *J* = 7.8 Hz, 2H), 2.09 – 1.94 (m, 2H), 1.71 – 1.54 (m, 4H), 1.35 – 1.15 (m, 4H).

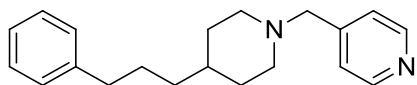
¹³C NMR (101 MHz, Chloroform-*d*) δ 159.29, 149.32, 142.97, 136.53, 128.57, 125.82, 123.43, 122.08, 65.31, 54.48, 36.38, 35.76, 32.57, 28.98.

HRMS calc'd for C₂₀H₂₇N₂ 295.21688; found [M+H] 295.21639

LCMS 75-95% 3 minutes MeOH:H₂O gradient >95% pure rt= .646

HIV-1_{BaL} inhibition in MAGI Cells- IC₅₀=73.5 μM IC₉₀= 227 μM

HIV-1_{IIB} inhibition in MAGI Cells- IC₅₀=137 μM IC₉₀= 256 μM

Compound 117

Prepared by general reductive amination procedure from **compound 115**. Purified on a 4 gram combiflash

column with a gradient of 0-40% DCM:MeOH:NH₄OH 90:10:.5 in DCM to afford 4-((4-(3-phenylpropyl)piperidin-1-yl)methyl)pyridine (45 mg, 62% yield).

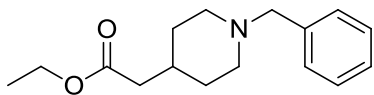
¹H NMR (400 MHz, Chloroform-*d*) δ 8.54 – 8.50 (m, 2H), 7.32 – 7.23 (m, 4H), 7.22 – 7.13 (m, 3H), 3.47 (s, 2H), 2.85 – 2.77 (m, 2H), 2.62 – 2.55 (m, 2H), 1.95 (t, *J* = 2.0 Hz, 2H), 1.71 – 1.57 (m, 4H), 1.33 – 1.18 (m, 5H).

¹³C NMR (101 MHz, Chloroform-*d*) δ 149.65, 148.10, 142.68, 128.34, 125.62, 123.89, 62.18, 54.11, 36.20, 36.14, 35.51, 32.32, 28.72.

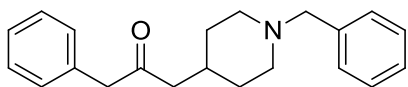
HRMS calc'd for C₇H₁₀ONS 295.21688; found [M+H] 295.21707

LCMS 75-95% 3 minutes MeOH:H₂O gradient >95% pure rt= .924

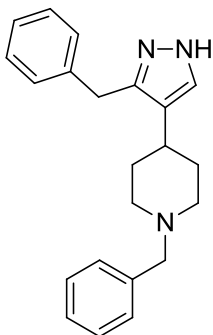
LCMS 25-95% 8 minutes MeOH:H₂O gradient >95% pure rt= 6.248

Compound 119

Prepared by general reductive amination procedure from the HCl salt of ethyl 2-(piperidin-4-yl)acetate (2.45 g, 14.3 mmol) . Taken on crude to the next step.

Compound 120

Ethyl 2-(1-benzylpiperidin-4-yl)acetate (3.08 g, 11.8 mmol) as a solution in THF (120 mL, .1 M) was added to a flame dried 500 mL round bottom flask containing the Weinreb amine salt (1.26 g, 13.0 mmol, 1.1 eq) and stirred at -5°C. Phenethylmagnesium bromide (47 mL, 47 mmol, 4 eq) was then added dropwise and the reaction was allowed to stir until complete consumption of starting material at -5°C. After formation of the Weinreb amide the reaction was slowly warmed to room temperature and tracked by LCMS. After an additional 2 hours of stirring at room temperature the reaction was quenched with NH₄Cl (20 mL) and basified with 10% NaOH. The mixture was further partitioned with EtOAc and separated. The aqueous layer was extracted with DCM (3 times). The organic layers were combined, dried over anhydrous magnesium sulfate, filtered and concentrated to afford 1-(1-benzylpiperidin-4-yl)-3-phenylpropan-2-one which was taken on to the next step crude.

Compound 121

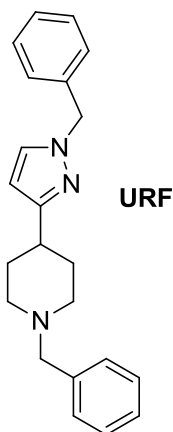
To a solution of 1-(1-benzylpiperidin-4-yl)-3-phenylpropan-2-one ARP5-129 (3.62 g, 11.8 mmol) in THF (120 mL, .1 M) in a flame dried 250 mL round bottom flask was added NaH (1.30 g, 35.3 mmol, 3 eq) and stirred at RT. Methyl formate (7.07 g, 118 mmol, 10 eq) was then added followed by 15-crown-5 (.26 g, .12 mmol, .1 eq). The reaction was tracked by LCMS and after 1 hour was quenched with 5 mL of H₂O dropwise. The reaction was then allowed to vent until no more hydrogen gas was evolved followed by the dropwise addition of hydrazine hydrate (3.02 g, 47 mmol, 4 eq) and tracked by LCMS. After an additional hour of stirring, the reaction was partitioned between water and EtOAc then basified with a 10% NaOH solution. The layers were separated and the aqueous layer was extracted with DCM (3 times). The organic layers were combined, dried over anhydrous sodium sulfate, filtered, and concentrated. The crude mixture was then purified on a 40 gram combiflash column with a gradient from 0-70% DCM:MeOH:NH₄OH (90:10:.5) in DCM to afford 1-benzyl-4-(3-benzyl-1H-pyrazol-4-yl)piperidine (.150 g, 4% yield over three steps).

¹H NMR (400 MHz, Chloroform-*d*) δ 7.62 (s, 1H), 7.41 – 7.33 (m, 4H), 7.32 – 7.21 (m, 6H), 3.69 (s, 2H), 3.48 (s, 2H), 2.83 (dt, *J* = 12.2, 3.0 Hz, 2H), 2.77 – 2.70 (m, 1H), 1.93 – 1.82 (m, 2H), 1.68 – 1.55 (m, 2H), 1.38 – 1.20 (m, 2H).

¹³C NMR (101 MHz, Chloroform-*d*) δ 133.52, 129.28, 128.60, 128.13, 127.92, 126.97, 126.35, 63.34, 53.55, 50.74, 36.23, 32.12.

LCMS 75-95% 3 minutes MeOH:H₂O gradient >95% pure rt= .785

LCMS 25-95% 8 minutes MeOH:H₂O gradient >95% pure rt= 6.197

Compound 123

To a solution of 1-(1-benzylpiperidin-4-yl)ethanone ARP5-49 (1.45 g, 6.67 mmol) in THF (66 mL, .1 M) in a flame dried 250 mL round bottom flask was added NaH (.492 g, 13.3 mmol, 2 eq) and stirred at RT. Methyl formate (8 g, 133 mmol, 20 eq) was then added followed by 15-crown-5 (.147 g, .667 mmol, .1 eq). The reaction was tracked by LCMS and after 1 hour was quenched with 1 mL of H₂O dropwise. The reaction was then diluted with MeOH (66 mL, .1 M) followed by the addition of benzyl hydrazine HCl (3.70 g, 23.3 mmol, 3.5 eq) and tracked by LCMS. After an additional hour of stirring the reaction was concentrated in vacuo to remove MeOH. The oily residue was partitioned between water and DCM and basified with 10% NaOH solution. The layers were separated and the aqueous layer was extracted with DCM (3 times). The organic layers were combined, dried over anhydrous magnesium sulfate, filtered and concentrated. The crude mixture was then purified on a 40 gram combiflash column with a gradient from 0-70% DCM:MeOH:NH₄OH (90:10:.5) in DCM to afford 1-benzyl-4-(1-benzyl-1H-pyrazol-3 or 5-yl)piperidine as two isomers (1.80 g, 86% combined yield over two steps).

URF: 540 mg pure regioisomer

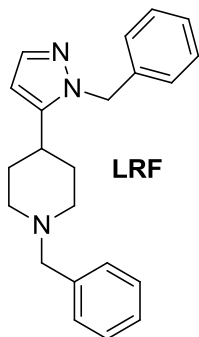
¹H NMR (400 MHz, Chloroform-*d*) δ 7.61 – 7.55 (m, 2H), 7.34 (qd, *J* = 4.0, 2.0 Hz, 3H), 7.27 – 7.20 (m, 4H), 7.11 – 7.06 (m, 2H), 6.04 (d, *J* = 2.1 Hz, 1H), 5.15 (d, *J* = 1.7 Hz, 2H), 4.03 (s, 2H), 3.33 – 3.17 (m, 2H), 2.95 – 2.74 (m, 3H), 2.28 – 2.12 (m, 4H).

^{13}C NMR (101 MHz, Chloroform- d) δ 154.02, 136.55, 131.19, 130.22, 129.56, 129.03, 128.70, 127.92, 127.49, 103.13, 70.39, 60.86, 55.70, 51.52, 28.67.

LCMS 10-95% 10 minutes MeOH:H₂O gradient >95% pure rt= 6.781

LCMS 75-95% 3 minutes MeOH:H₂O gradient >95% pure rt= .604

HRMS calc'd for C₂₂H₂₆N₃ 332.21212; found [M+H] 332.21188

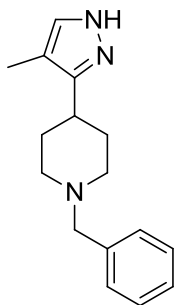
Compound 124

To a solution of 1-(1-benzylpiperidin-4-yl)ethanone ARP5-49 (1.45 g, 6.67 mmol) in THF (66 mL, .1 M) in a flame dried 250 mL round bottom flask was added NaH (.492 g, 13.3 mmol, 2 eq) and stirred at RT. Methyl formate (8 g, 133 mmol, 20 eq) was then added followed by 15-crown-5 (.147 g, .667 mmol, .1 eq). The reaction was tracked by LCMS and after 1 hour was quenched with 1 mL of H₂O dropwise. The reaction was then diluted with MeOH (66 mL, .1 M) followed by the addition of benzyl hydrazine HCl (3.70 g, 23.3 mmol, 3.5 eq) and tracked by LCMS. After an additional hour of stirring the reaction was concentrated in vacuo to remove MeOH. The oily residue was partitioned between water and DCM and basified with 10% NaOH solution. The layers were separated and the aqueous layer was extracted with DCM (3 times). The organic layers were combined, dried over anhydrous magnesium sulfate, filtered and concentrated. The crude mixture was then purified on a 40 gram combiflash column with a gradient from 0-70% DCM:MeOH:NH₄OH (90:10:.5) in DCM to afford 1-benzyl-4-(1-benzyl-1H-pyrazol-3 or 5-yl)piperidine as two isomers (1.80 g, 86% combined yield over two steps). LRF: 260 mg mixture of two regioisomer 1:2 LRF to URF ratio

LCMS 10-95% 10 minutes MeOH:H₂O gradient >95% pure rt= 6.340 , 6.784 1:2 ratio respectively

LCMS 75-95% 3 minutes MeOH:H₂O gradient >95% pure rt= .610

HRMS calc'd for C₂₂H₂₆N₃ 332.21212; found [M+H] 332.21188

Compound 125

To a solution of 1-(1-benzylpiperidin-4-yl)propan-1-one ARP5-28B (2.89 g, 12.5 mmol) in THF (125 mL, .1 M) in a flame dried 250 mL round bottom flask was added NaH (1.35 g, 56 mmol, 4.5 eq) and stirred at RT. Methyl formate (15 g, 250 mmol, 20 eq) was then added followed by 15-crown-5 (.69 g, .31 mmol, .25 eq). The reaction was tracked by LCMS and after 1 hour was quenched with 1 mL of H₂O dropwise. The reaction was then diluted with MeOH (125 mL, .1 M) followed by the dropwise addition of hydrazine (6.16 g, 125 mmol, 10 eq) and tracked by LCMS. After an additional hour of stirring the reaction was concentrated in vacuo to remove MeOH. The oily residue was partitioned between water and DCM and basified with 10% NaOH solution. The layers were separated and the aqueous layer was extracted with DCM (3 times). The organic layers were combined, dried over anhydrous magnesium sulfate, filtered and concentrated. The crude mixture was then purified on a 24 gram combiflash column with a gradient from 0-70% DCM:MeOH:NH₄OH (90:10:.5) in DCM to afford 1-benzyl-4-(4-methyl-1H-pyrazol-3-yl)piperidine (.5 g, 16% yield over two steps).

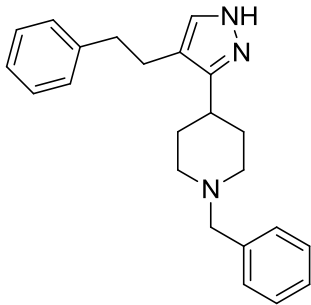
¹H NMR (600 MHz, Chloroform-*d*) δ 7.47 (s, 1H), 7.40 (d, *J* = 7.1 Hz, 2H), 7.35 (t, *J* = 7.5 Hz, 2H), 7.30 – 7.26 (m, 1H), 3.59 (s, 2H), 3.04 (dt, *J* = 12.1, 2.9 Hz, 2H), 2.73 (tt, *J* = 12.2, 3.9 Hz, 1H), 2.16 – 2.11 (m, 2H), 2.10 (s, 3H), 2.01 (qd, *J* = 12.5, 3.7 Hz, 2H), 1.89 – 1.83 (m, 2H).

¹³C NMR (151 MHz, cdcl₃) δ 158.77, 138.79, 129.59, 129.25, 128.63, 127.41, 111.63, 63.70, 54.44, 33.85, 31.77, 8.86.

HRMS calc'd for C₁₆H₂₂N₃ 256.18082; found [M+H] 256.18085

M.P. 93-97 °C

LCMS 50-95% 3 minutes MeOH:H₂O gradient >95% pure rt= .656

Compound 126

To a solution of 1-(1-benzylpiperidin-4-yl)-4-phenylbutan-1-one **compound 68** 1.43 g, 4.45 mmol) in THF (45 mL, .1 M) in a flame dried 250 mL round bottom flask was added NaH (.739 g, 20 mmol, 2 eq) and stirred at RT. Methyl formate (5.34 g, 89 mmol, 20 eq) was then added followed by 15-crown-5 (.098 g, .445 mmol, .1 eq). The reaction was tracked by LCMS and after 1 hour was quenched with 1 mL of H₂O dropwise. The reaction was then diluted with MeOH (45 mL, .1 M) followed by the dropwise addition of hydrazine (.5 g, 15.6 mmol, 3.5 eq) and tracked by LCMS. After an additional hour of stirring the reaction was concentrated in vacuo to remove MeOH. The oily residue was partitioned between water and DCM and basified with 10% NaOH solution. The layers were separated and the aqueous layer was extracted with DCM (3 times). The organic layers were combined, dried over anhydrous magnesium sulfate, filtered and concentrated. The crude mixture was then purified on a 40 gram combiflash column with a gradient from 0-70% DCM:MeOH:NH₄OH (90:10:.5) in DCM to afford 1-benzyl-4-(4-phenethyl-1H-pyrazol-3-yl)piperidine (.150 g, 10% yield over two steps).

¹H NMR (400 MHz, Chloroform-*d*) δ 7.33 – 7.26 (m, 5H), 7.26 – 7.22 (m, 2H), 7.19 – 7.12 (m, 3H), 3.68 (s, 2H), 2.94 (dq, *J* = 10.1, 3.7 Hz, 2H), 2.87 – 2.78 (m, 2H), 2.72 (dd, *J* = 8.5, 6.2 Hz, 2H), 2.48 (tt, *J* = 12.2, 3.9 Hz, 1H), 2.04 – 1.93 (m, 2H), 1.81 (qd, *J* = 12.6, 3.9 Hz, 2H), 1.71 – 1.60 (m, 2H).

¹³C NMR (101 MHz, Chloroform-*d*) δ 141.75, 138.18, 129.20, 128.52, 128.30, 128.17, 127.00, 125.94, 116.28, 70.50, 63.36, 53.93, 37.42, 31.71, 25.64.

HRMS calc'd for C₂₃H₂₈N₃ 346.22777; found [M+H] 346.22770

LCMS 25-95% 8 minutes MeOH:H₂O gradient >95% pure rt= 5.726

LCMS 75-95% 3 minutes MeOH:H₂O gradient >95% pure rt= .675